# Towards Fluorescence-Guided Head and Neck Cancer Surgery

Stijn Keereweer

ISBN: 978-94-6182-408-0
Layout and printing: Off Page (www.offpage.nl)
Cover illustration copyright of TSA Medien – www.tsamedien.de

# Towards Fluorescence-Guided Head and Neck Cancer Surgery

Op weg naar fluorescentiegeleide chirurgie van hoofd-hals tumoren

**Proefschrift**

**Ter verkrijging van de graad van doctor aan de**
**Erasmus Universiteit Rotterdam**
**op gezag van de**
**rector magnificus**

**prof. dr. H.A.P. Pols**

**En volgens besluit van het College voor Promoties.**
**De openbare verdediging zal plaatsvinden op**

vrijdag 7 maart 2014 om 13:30 uur

Stijn Keereweer
geboren te Hoorn

**Promotiecommissie**

| | |
|---|---|
| Promotores: | Prof.dr. R.J. Baatenburg de Jong |
| | Prof.dr. C.W.G.M. Löwik |
| Overige leden: | Prof.dr. A. Van der Lugt |
| | Prof.dr.ir. H.J.C.M. Sterenborg |
| | Prof.dr. C. Verhoef |
| Co-promotor: | Dr. J.D.F. Kerrebijn |

"God's first creature, which was light"

Francis Bacon

Aan Rinske,
"Light of my life, …"

# Table of contents

# 1 General introduction and outline of the thesis

# General introduction

## *Vision is a complex process*

Visual input and associative processing of images in the brain has been fundamental for animal evolution. Processing of images in the visual cortex and the ability to store images in memory over longer time periods is a paramount precondition for most strategies of survival. Moreover, the social and cultural achievements governing all kind of human interactions, including communication and emotion, rely heavily on our visual perception.

Even Charles Darwin himself experienced sincere difficulties in conceptualizing the mystery how natural selection could have resulted in such a complex process as vision. In his *Origin of Species (1859)*[1], he wrote that the evolution of the eye, one of the most elegant organs, at first glance seemed *"absurd in the highest possible degree"*. However, he went on to explain that despite the difficulty in imagining it, it would be feasible "…if numerous gradations from a perfect and complex eye to one very imperfect and simple, each grade being useful to its possessor, can be shown to exist; if further, the eye does vary ever so slightly, and the variations be inherited, which is certainly the case; and if any variation or modification in the organ be ever useful to an animal under changing conditions of life, then the difficulty of believing that a perfect and complex eye could be formed by natural selection, though insuperable by our imagination, can hardly be considered real."[1]

Parallel to development of sight, representational systems have evolved that permit the brain to model the world, to identify objects and events, to attach meaning and significance to them, and to establish their causal relations.[2] Standard accounts of vision assume that the purpose of the visual system is to construct an internal model of the world outside: to create a kind of *simulacrum* of the real thing, which can then serve as the perceptual foundation for all visually derived thought and action.

The concept of interpretation of the "objective world" poses many difficulties and has been a subject of intensive debate since the early onset of philosophy and observational science. In *Sophist*[3], Plato speaks of two kinds of image-making. The first is a faithful reproduction, directed towards producing an exact copy of the original. The second is distorted intentionally, in order to make the copy appear correct to observers. The example of Greek statuary is given, in which statues were crafted larger on top than on bottom so that viewers from the ground would see it correctly. If they could view it in scale, they would realize it was malformed.[3]

## *Observational science*

In the early days of biology research, observation of organisms to understand the underlying principles of life from birth to death was the only way to collect information. As always, these visual impressions are projected towards the knowledge that is concealed in memory. Images are interpreted by intuitive matching of the new to the known. The use of light to render an image began with discovery of the Camera Obscura around 1550, although the theoretical optical principle of a pinhole camera had first been described by Aristotle (384-322 BC). A simple lens was used which focused on a wall or a drawing board in order

to trace the image. In the first decade of the 1900's, radiology evolved as a medical subspecialty after the discovery of x-rays by Wilhelm Röntgen (1845-1923). The extensive use of x-ray imaging during the second world war, and the advent of the digital computer and new imaging modalities like ultrasound and magnetic resonance imaging have created a revolution of diagnostic imaging techniques in the past 25 years (Figure 1).

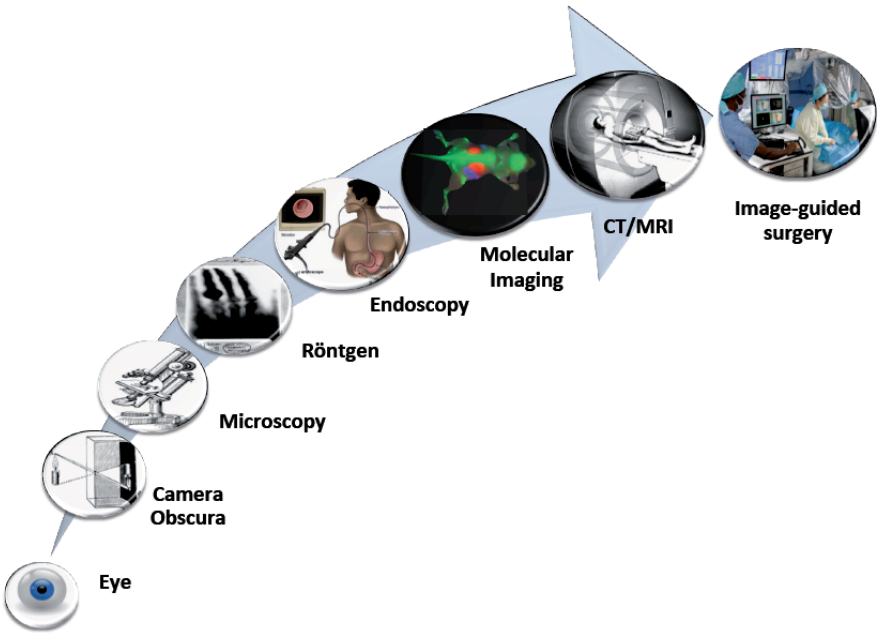


**Fig. 1.** The evolution of observational medical science.

## *Evolution of imaging towards the molecular level*

As we know now, the molecular level determines the properties of biological systems. For a long time, the mechanisms of causation from genotype to phenotype have remained obscure. Mendel was not yet aware of the molecules involved in heredity, although he could show a clear and causative relation between the phenotype of parents and offspring. The genome age has inversed our view to the biology: knowledge of the primary information encoded in the genome has guided the analysis of the molecular makeup of the cells.[4]

Over the past decades, molecular imaging has gained strong influence on medicine and biology, leading the way in exploiting molecular, biological and genetic information to develop precise *in vivo* diagnostic methods. These methods are increasingly precious for the follow-up and the evaluation of new treatments of many pathological states. A key paradigm towards further understanding of (patho-) physiological processes was established with the introduction of real-time imaging technologies: synchronous data capturing and

processing that results in a direct presentation of the fluorescent images. Using dynamic imaging modalities, the interaction of molecules in time, space, and condition could be followed in its natural environment.

### *Introducing image-guided surgery*

From the evolution of vision in the earliest stages of life, to the primitive forms of imaging in the medieval era, technologies have culminated into the high standards of state-of-the-art imaging modalities. Currently, we are on the verge of the next step of imaging, entering the realm of real-time image-guided surgery. This now allows us to introduce real-time imaging, up to the cellular level, into the operation room. In terms of Plato's *Sophist*, we are thereby trying to create an exact copy of the original. However, in spirit of the greatest philosophers of our time, we should be aware of the observer's reference frame and, consequently, the risk of unintentionally creating a simulacrum that has a different "objective reality" than the copy that is considered identical to the original by its observers. This must be bore in mind when exploring a relatively new field as optical image-guided surgery, and dictates thorough research in the preclinical phase.

### *Towards optical image-guided head and neck cancer surgery*

Although imaging of tumors in the head and neck region has made great progress over the last decades, translation of these images to the operation field sometimes remains a challenge for the surgeon. A critical aspect of oncologic surgery is to adequately discriminate between tumor and normal tissue and consequently determine the tumor-free margin, which is essential for the prognosis of the patient. Currently, the only way to do this during surgery is by visual appearance and palpation, which might in part explain the suboptimal survival rates after surgery. In oral cancer for instance, local recurrence rates of 21.9% have been reported when involved margins are found on histopathology, compared to 3.9% local recurrences in patients with tumor-free margins.[5] Involved surgical margins increase the risk of death at 5 years by 90%.[6] Nevertheless, in current clinical practice, involved surgical margins are found in 16-31% of the patients that were operated with the objective of achieving a macroscopic clearance of 1 cm.[7,8] If close resection margins (<5 mm) are included on top of that, a total of 85% positive or close resection margins has been reported.[8]

New intraoperative visualization techniques using near-infrared (NIR) fluorescence imaging are being developed that could help the surgeon to discriminate between healthy and cancer tissue.[9,10] The concept of using NIR light has proven a crucial step towards the application in intraoperative image-guided surgery. Absorption describes the phenomenon that electromagnetic energy of a photon is taken up by matter, typically the electrons of an atom. The combination of light absorption by hemoglobin in the visible light spectrum (<600 nm) and other components (e.g. water and lipids) in the infrared range (>900 nm), offers an optical imaging window from approximately 650 to 900 nm in which the absorption coefficient of tissue is at a minimum. Furthermore, light scattering (deflection of

the path that photons travel after contact with particles or irregularities in the propagation medium) and fluorescence of normal components of the tissue (i.e., autofluorescence) are decreased and tissue penetration is increased in this spectrum.

Introduction of real-time imaging technologies into the operating room has the potential to improve resection of diseased tissue with optimal preservation of healthy tissue, resulting in image-guided surgery. However, real-time imaging requires specific targeting to detect malignant cells or tissues, for which multiple strategies can be followed. Optical imaging is currently considered the optimal technique for intraoperative image-guided surgery. In optical imaging, the properties of light are exploited to image anatomic or chemical characteristics of tissue. Imaging of optical contrast can be performed using either the properties intrinsic to the tissue, or, analogous to many radiolabeled agents, using antibodies or ligands conjugated to an optically active reporter to target a recognized disease biomarker. These injectable substances are called fluorescence agents or probes.[9] Although a very promising technique, optical image-guided surgery has yet no place in head and neck oncology.

## Outline of the thesis

In **Part I**, the current modalities of optical imaging are introduced and reviewed. **Chapter 2** focuses on the various techniques, contrast agents, and camera systems that are currently used for image-guided cancer surgery. Furthermore, an overview is provided of the wide range of molecular contrast agents that each target specific hallmarks of cancer and the perspectives on its future use in cancer surgery is described.

In order to investigate the feasibility of these alternative optical imaging strategies for targeting of head and neck cancers, two different head and neck cancer animal models were introduced. Using these models, detection of head and neck cancer was performed *in vivo,* using various NIR fluorescence agents and subsequent optical imaging. These studies are described in **Part II**.

In **Chapter 3**, an orthotopical animal model of oral cancer and cervical lymph node metastasis was used. In order to gain optimal tumor-to-background ratios (TBR), activatable agents were used that contain a cleavage site specific to tumor specific enzymes.[11-13] These agents are injected in a quenched (i.e., non-fluorescent) state, minimizing fluorescence at the time of administration. After cleavage by the specific enzyme, the agent becomes dequenched (i.e., fluorescent) and emits a fluorescent signal of 700 nm. In this study, we used ProSense680 (PerkinElmer, Waltham, MA), which is activated by cathepsins (mostly cathepsin B), and MMPSense680 (PerkinElmer), which is activated by matrix metalloproteinases (MMPs). These proteolytic enzymes are involved in degradation of the extracellular matrix of the head and neck tumor,[14,15] and are therefore mainly found in the invasive tumor front. We aimed to assess the feasibility of protease-activatable optical imaging for detection of oral cancer and cervical lymph node metastasis.

In Chapter 2, NIR fluorescence agents were described that target the various hallmarks of cancer. One of these hallmarks, limitless replicative potential of tumor cells, contains an essential feature of carcinogenesis and is facilitated in part by increased expression of growth signaling receptors. In **Chapter 4**, the feasibility of targeted NIR fluorescence optical imaging was assessed in the aforementioned animal model of oral cancer and cervical lymph node metastasis. For tumor-specific targeting, agents were used that fluoresce in the 800 nm range and detect increased epidermal growth factor (EGF) receptor expression or increased tumor glucose metabolism.

In Chapter 3, NIR fluorescence agents were used that fluoresce at 700 nm. Subsequently, the use of agents that have emission peaks at 800 nm was described in Chapter 4. We hypothesized that tumor detection could be improved by targeting multiple tumor-specific characteristics simultaneously with fluorophores that emit light at different wavelengths. Therefore, in **Chapter 5**, dual wavelength targeting by NIR fluorescence technologies for *in vivo* cancer imaging was explored. In the 700 nm region, ProSense680 and MMPSense680 (PerkinElmer) were used that detect increased activity of cathepsins and MMPs, respectively. The use of these agents was combined with NIR fluorescence agents that emit at 800 nm, which included 2DG CW800 (LI-COR Biosciences), detecting tumor cells through uptake by the glucose transporter, and EGF CW800 (LI-COR Biosciences),

which is internalized by the EGF receptor of tumor cells. This study was performed in an animal model of hypopharyngeal cancer to demonstrate the extensive applicability of the used agents in head and neck cancers with variable molecular characteristics. Although an orthotopical tumor model is preferred in order to maintain optimal conditions of the natural surroundings of the tumor, the cells were injected subcutaneously because inoculation into the hypopharynx would lead to high risk of dyspnea or suffocation during the earliest stages of carcinogenesis.

The use of dual wavelength imaging was further exploited in **Chapter 6**, which focused on two important aspects of cancer: involvement of αvβ3 integrins[16] and the enhanced permeability and retention (EPR) effect.[17] Integrins are transmembrane cell surface receptors that are involved in cell migration, invasion and extravasation.[16] Because these are all key components in angiogenesis, tumorigenesis and metastasis, integrins have been distinguished as appealing targets for cancer imaging.[18] The EPR effect is a result of abnormal formation of newly formed tumor vessels. As a result, macromolecules selectively leak out from tumor vessels and accumulate in tumor interstitial tissues. Therefore, in Chapter 6, a combination of two NIR fluorescence agents was used that either target integrins or the EPR effect for clear demarcation of oral cancer in an orthotopical mouse model. Agents were used that fluoresce at different wavelengths, allowing for simultaneous, dual wavelength imaging of their signals.

Overall, optical imaging using NIR fluorescence light is a new imaging modality that has recently emerged in the field of cancer imaging. After extensive preclinical research, **Part III** focuses on the first steps of translation to the clinical practice that are currently being made. In **Chapter 7**, the preclinical and clinical results are discussed of NIR optical imaging for non-invasive detection and classification of tumors, therapy monitoring, sentinel lymph node procedures, and image-guided cancer surgery. An overview of the preclinical studies that have preceded the current essential steps of translational medicine is provided, as well as the future directions of optical imaging.

Finally, the fundamental aspects of optical imaging, its limitations and the challenges that lie ahead are the focus of **Part IV**: the General Discussion**.** In **Chapter 8**, the basic aspects of the technique are studied with special attention to its consequences for the clinical practice. It provides a complete overview of its possibilities and limitations and describes in detail how optical imaging can become a powerful intraoperative tool in guiding the future oncologic surgeon towards radical resection and optimal clinical results and will form the foundation of tomorrow's medicine. Next, the results of NIR fluorescence imaging of head and neck cancer in animal models are discussed in **Chapter 9**, followed by a discussion in **Chapter 10** on the future directions and hurdles that have yet to be overcome in order to establish a strong foundation on which the field can build the next generation of advances.

In this thesis, we have set the first steps towards detection of head and neck cancer within the relatively young revolutionary field of optical imaging. In the **Conclusion**, it is stated that although there are limitations to the intrinsic capacity of the technique, when practical and technical surgical possibilities are carefully considered, optical imaging can

be a very powerful intraoperative tool in guiding the future head and neck surgeon towards radical resection and optimal clinical results. All results are summarized in an **English** and **Dutch Summary**.

## References


1. Darwin, C. *On the origin of species by means of natural selection : or, The preservation of favoured races in the struggle for life*, (John Murray, Albemarle Street, London, 1859).
2. Milner, A.D. & Goodale, M.A. *The visual brain in action*, (Oxford University Press, Oxford ; New York, 2006).
3. Plato & White, N.P. *Sophist*, (Hackett Pub. Co., Indianapolis, 1993).
4. Wolkenhauer, O., Ullah, M., Wellstead, P. & Cho, K.H. The dynamic systems approach to control and regulation of intracellular networks. *FEBS letters* **579**, 1846-1853 (2005).
5. Slootweg, P.J., Hordijk, G.J., Schade, Y., van Es, R.J. & Koole, R. Treatment failure and margin status in head and neck cancer. A critical view on the potential value of molecular pathology. *Oral oncology* **38**, 500-503 (2002).
6. Binahmed, A., Nason, R.W. & Abdoh, A.A. The clinical significance of the positive surgical margin in oral cancer. *Oral oncology* **43**, 780-784 (2007).
7. McMahon, J., *et al.* Influence of condition of surgical margins on local recurrence and disease-specific survival in oral and oropharyngeal cancer. *The British journal of oral & maxillofacial surgery* **41**, 224-231 (2003).
8. Smits, R.W.H., Koljenovic, S., Puppels, G.J. & Baatenburg de Jong, R.J. Hoog percentage positieve en krappe snijranden bij mondholtetumor resecties. Presented at the *Dutch Head and Neck Oncology Cooperative Group* (Rotterdam, The Netherlands, 2013).
9. Frangioni, J.V. New technologies for human cancer imaging. *J Clin Oncol* **26**, 4012-4021 (2008).
10. Weissleder, R. & Pittet, M.J. Imaging in the era of molecular oncology. *Nature* **452**, 580-589 (2008).
11. Mahmood, U. & Weissleder, R. Near-infrared optical imaging of proteases in cancer. *Mol Cancer Ther* **2**, 489-496 (2003).
12. Wunderbaldinger, P., Turetschek, K. & Bremer, C. Near-infrared fluorescence imaging of lymph nodes using a new enzyme sensing activatable macromolecular optical probe. *European radiology* **13**, 2206-2211 (2003).
13. Weissleder, R., Tung, C.H., Mahmood, U. & Bogdanov, A., Jr. In vivo imaging of tumors with protease-activated near-infrared fluorescent probes. *Nat Biotechnol* **17**, 375-378 (1999).
14. Wickramasinghe, N.S., Nagaraj, N.S., Vigneswaran, N. & Zacharias, W. Cathepsin B promotes both motility and invasiveness of oral carcinoma cells. *Arch Biochem Biophys* **436**, 187-195 (2005).
15. Yang, X., *et al.* Increased expression of Cathepsin B in oral squamous cell carcinoma. *Int J Oral Maxillofac Surg* **39**, 174-181 (2010).
16. Hood, J.D. & Cheresh, D.A. Role of integrins in cell invasion and migration. *Nat Rev Cancer* **2**, 91-100 (2002).
17. Fang, J., Nakamura, H. & Maeda, H. The EPR effect: Unique features of tumor blood vessels for drug delivery, factors involved, and limitations and augmentation of the effect. *Adv Drug Deliv Rev* **63**, 136-151 (2011).
18. Desgrosellier, J.S. & Cheresh, D.A. Integrins in cancer: biological implications and therapeutic opportunities. *Nat Rev Cancer* **10**, 9-22 (2010).

# I CURRENT MODALITIES OF OPTICAL IMAGE-GUIDED SURGERY

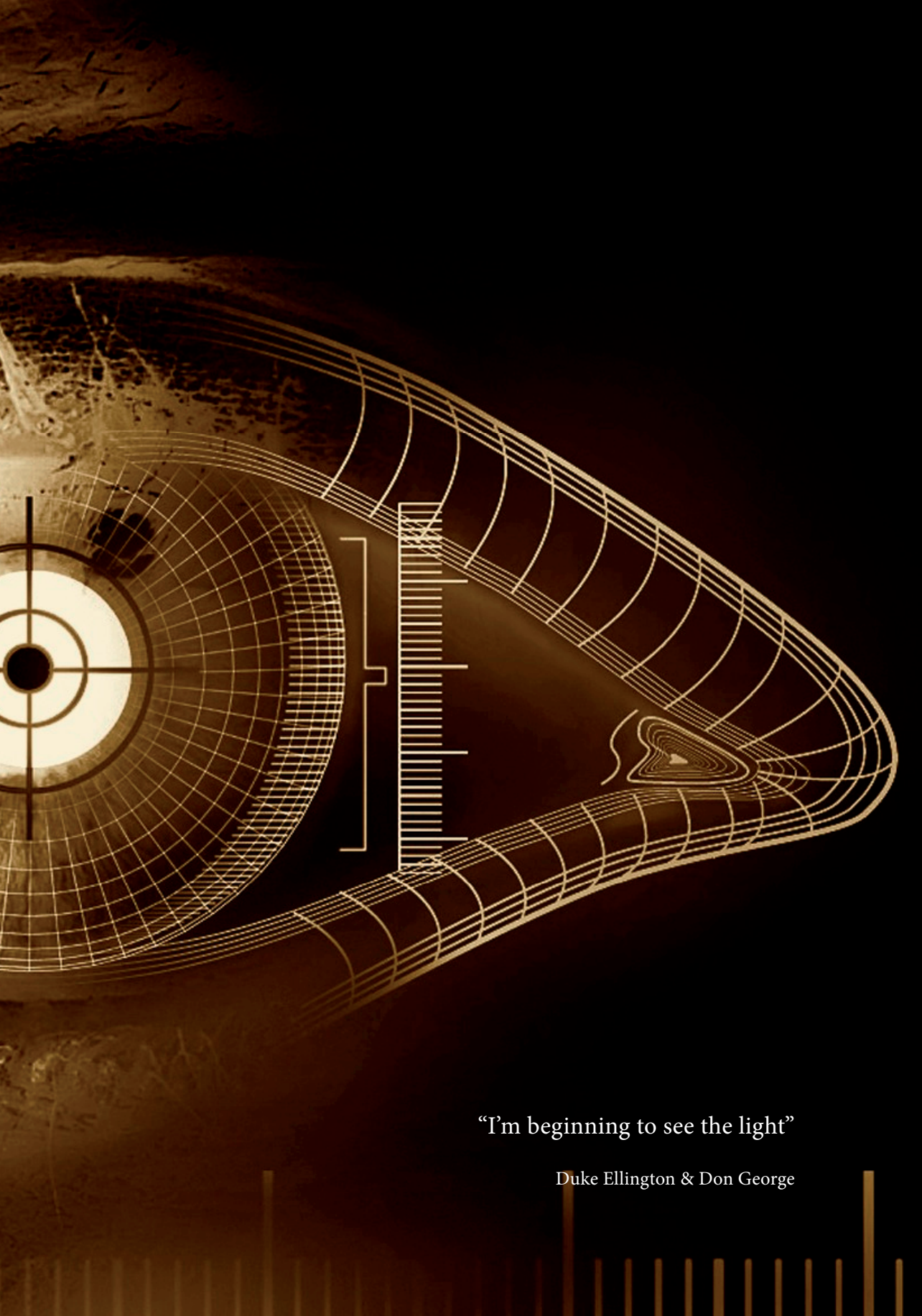

"I'm beginning to see the light"

Duke Ellington & Don George

# 2 Optical image-guided surgery – Where do we stand?

## Current practice and future directions

This Chapter was edited from the following articles:

"Image-Guided Surgery in Head and Neck Cancer: Current Practice and Future Directions of Optical Imaging"

Stijn Keereweer, Henricus J.C.M. Sterenborg, Jeroen D.F. Kerrebijn, Pieter B.A.A. Van Driel, Robert J. Baatenburg de Jong, Clemens W.G.M. Löwik

**Head Neck, 2012** vol. 34(1) pp. 120-6
DOI: 10.1002/hed.21625

"Optical Image-Guided Surgery – Where Do We Stand?"

Stijn Keereweer, Jeroen D.F. Kerrebijn, Pieter B.A.A. van Driel, Bangwen Xie, Eric L. Kaijzel, Thomas J.A. Snoeks, Ivo Que, Merlijn Hutteman, Joost R. van der Vorst, J. Sven D. Mieog, Alexander L. Vahrmeijer, Cornelis J.H. van de Velde, Robert J. Baatenburg de Jong, Clemens W.G.M. Löwik

**Molecular Imaging & Biology, 2011** vol. 13(2) pp. 199-20
DOI: 10.1007/s11307-010-0373-2

## Abstract

A key aspect for the postoperative prognosis of patients with head and neck cancer is complete tumor resection. In current practice, the intraoperative assessment of the tumor-free margin is dependent on visual appearance and palpation of the tumor. Optical imaging has the potential of traversing the gap between radiology and surgery by providing real-time visualization of the tumor, thereby allowing for image-guided surgery. The use of the near-infrared light spectrum offers two essential advantages: increased tissue penetration of light and an increased signal-to-background-ratio of contrast agents.

In this review, the current practice and limitations of image-guided surgery by optical imaging using intrinsic fluorescence or contrast agents are described. Furthermore, we provide an overview of the wide range of molecular contrast agents targeting specific hallmarks of cancer and we describe perspectives on its future use in cancer surgery.

## Introduction

Over the last decades, imaging technologies have made significant developments, resulting in their current perpetual role in clinical oncology. The field has expanded greatly and now comprises various modalities, including ultrasonography (US), computed tomography (CT), magnetic resonance imaging (MRI), positron emission tomography (PET) and single-photon-emission computed tomography (SPECT). Because each modality has its specific advantages and disadvantages, the combination of different techniques has become standard practice for tumor detection, staging and treatment evaluation.[1]

For the surgeon however, a major challenge remains in the translation of these images to the operation field. A critical aspect of oncologic surgery is to adequately discriminate between tumor and normal tissue and consequently determine the tumor-free margin which is essential for the prognosis of the patient. Nevertheless, currently, the only way to do this during surgery is by visual appearance and palpation.

Real-time imaging technologies (i.e., synchronous data capturing and processing that results in a direct presentation of the fluorescent images) could offer the possibility to put the images right under the hands of the surgeon, warranting intraoperative image-guided surgery. In order to detect malignant cells or tissues, the various hallmarks of cancer can be used as a target for imaging strategies: increased growth and growth factor signaling receptors, limitless replicative potential, sustained angiogenesis, and increased proteolytic activity resulting in tissue invasion and metastasis (Figure 1).[2]

The characteristic of increased metabolism is exploited in PET technology, using the glucose-mimetic 2-deoxy-2-[18F]fluoro-D-glucose (18FDG). Tumor cells most frequently use glycolysis for energy generation, resulting in an increased glucose metabolism and the overexpression of glucose transporters (GLUTs).[3] 18FDG is taken up by metabolically active cells, making it applicable in a wide range of tumors.[4] For intraoperative evaluation of tumor localization and margin status in breast cancer surgery, a hand-held PET-probe to detect the high-energy gamma rays during surgery has been developed.[5] This device was also used in the resection of head and neck cancer, and helped guiding diagnostic neck dissections.[6]

Although very useful for diagnostic applications, the PET imaging technology has several disadvantages for widely used intraoperative practice. Due to its limited spatial resolution, small tumors (<1 cm) have proven difficult to detect by this hand-held probe.[5] Furthermore, the use of PET technology is restricted to specialized centers for logistical, practical, and financial reasons. Radiochemists, a cyclotron, and specialized waste processing facilities are required in order to produce the radiopharmaceuticals. Although radiation exposure for the patient and operation personnel is minimized due to tracer amounts of the very short-lived agents, the short half-life time limits the time-frame in which the agents have to be administered. This requires careful planning with the risk of high expenses when an operation procedure is delayed.

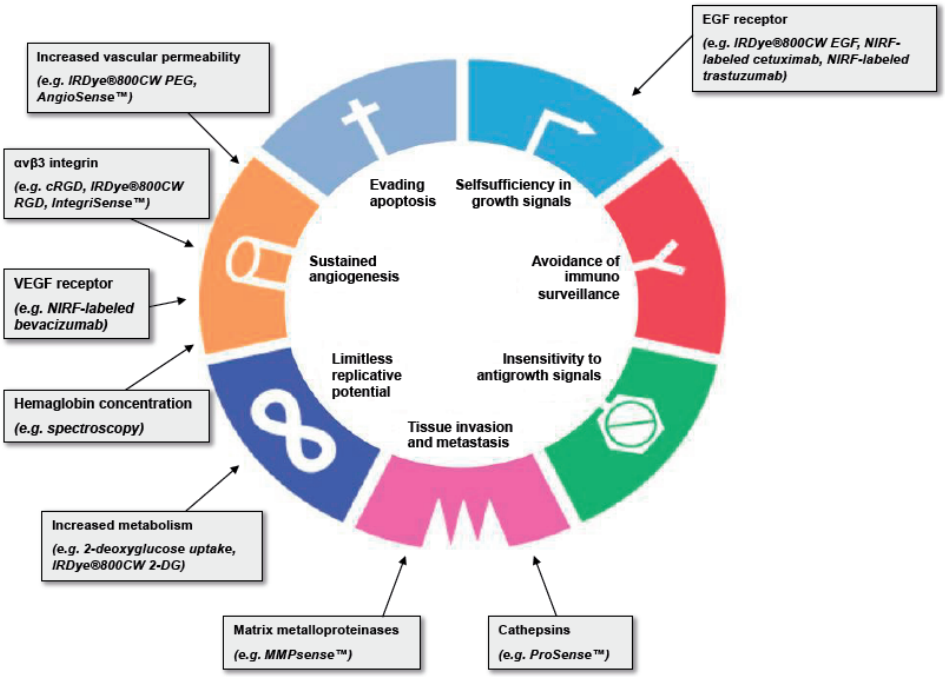


**Fig. 1.** Hallmarks of cancer and their targets for optical imaging. EGF, epidermal growth factor; cRGD, cyclic arginine-glycine-aspartate; VEGF, vascular endothelial growth factor; NIRF, near infrared fluorescence. Reprinted with kind permission from Kroemer, G & Pouyssegur, J; Tumor cell metabolism: cancer's Achilles' heel. Cancer Cell. 2008 Jun;13(6):472-82.

In neurosurgery, intraoperative magnetic resonance imaging (ioMRI)-guided surgery has been developed during the last two decades.[7] It allows the neurosurgeon to alter the surgical approach during the operation to compensate for shifting of the brain, which usually occurs due to tumor removal, development of brain edema, and loss of cerebrospinal fluid. However, the introduction of MRI technology into the operation room results into extended practical, logistical and financial difficulties that do not outweigh the benefits for general oncological surgery.

Interesting developments have been made in the last years using Raman spectroscopy. A Raman spectrum is generated by a shift in frequency in the incident excitation light of tissue, resulting in in-elastic scattering. The shift in frequency is caused by discrete changes in emergent light, above and below the wavelength of the incident photons, due to the vibrational frequencies of the bio-molecules that constitute the tissue. There are several characteristic features of spectroscopy which make it attractive for oncological applications. Specific lesions can be identified using optical fibers for *in vivo* measurements. Furthermore, they do not require the use of dyes, labels or other contrast-enhancing agents, implicating that tissues can be studied in their native states.

Various groups have performed Raman spectroscopic studies where spectral differences have been reported between normal and cancerous lesions. In this way, the detection of cancers and precancers has been described in skin, mucosal surfaces, and solid organs.[8-10]

These interesting results suggest its relevance to clinical oncological applications. However, several hurdles have yet to be overcome. The Raman effect comprises a very small fraction (~1 in $10^7$) of the incident photons, resulting in much weaker signals than autofluorescence. Hence, these signals can be easily masked by the broad-band fluorescence background, hampering interpretation of the spectra. Additionally, in most of these studies a fiber-optic Raman probe is required to access the tissues of interest *in vivo*. Although a necessary and important step towards a widespread clinical use, such fiber-based Raman technology using manageable probes with real-time translation software is yet to be developed.[11]

Optical imaging is currently considered the optimal technique for intraoperative image-guided surgery. In optical imaging, the properties of light are exploited to image anatomic or chemical characteristics of tissue. Imaging of optical contrast can be performed using either the properties intrinsic to the tissue, or, analogous to many radio-labeled agents, using antibodies or ligands conjugated to an optically active reporter to target a recognized disease biomarker.[1]

Over the last decade, a significant amount of work has been done in the field of optical imaging in oncology. In head and neck cancer, a substantial part of the reports have focused on the intrinsic fluorescence of malignant tissues. This review outlines the various techniques, contrast agents, and camera systems that are currently used for image-guided surgery. Furthermore, an overview of the wide range of molecular contrast agents that each target specific hallmarks of cancer is provided and the perspectives on its future use in cancer surgery is described.

## Tumor detection using intrinsic fluorescence

Autofluorescence refers to the intrinsic fluorescence of the tissue that is excited when activated by ultraviolet, visible, or near-infrared (NIR) radiation of suitable wavelength. Because cancerous transformation leads to morphologic and biochemical alterations which affect the optical properties of the tissue, in some cases the autofluorescence may actually illuminate the structures of interest and can serve as a useful diagnostic indicator.[12]

The preliminary results of detection of oral squamous cell carcinoma using intrinsic fluorescence have been described by Dhingra et al,[13] followed by the first prototype of a hand-held device in 2004.[14] These results have been promising, and more recently, high sensitivity and specificity scores have been reported in detecting oral neoplasia.[15, 16]

Muller et al[17] combined the intrinsic fluorescence spectroscopy with diffuse reflectance spectroscopy and light scattering spectroscopy in oral squamous cell carcinoma patients. Diffuse reflectance spectroscopy is a measurement technique based on detection of diffusely scattered light, specifically in reflection geometry. When incident light strikes a surface, the light that penetrates is reflected in all directions, a phenomenon that is called

diffuse reflectance. Diffusely reflected white light enters the tissue and scatters multiple times before it is collected at the tissue surface and its intensities can be estimated based on diffusion theory. The combined use of these techniques, "trimodal spectroscopy", resulted in a sensitivity and specificity of both 96 % in distinguishing cancerous and dysplastic lesions from normal tissue.[17]

The use of intrinsic fluorescence has also been explored for detection of laryngeal cancer and tumor precursor lesions.[18, 19] However, in these studies, not only normal, dysplastic, and cancerous lesions were compared, but it was also noted that scar formation (e.g. after surgery or radiotherapy), subepithelial hematoma, minimal amount of blood in the larynx or hypopharynx, simplex hyperplasia, papilloma without epithelial dysplasia, marked hyperkeratosis, bacterial colonization, and inflammation could all produce false-positive findings, thereby limiting the predictive value.[20] Therefore, it must be concluded that the current technique for endoscopic intrinsic fluorescence is not yet superior to the gold standard of microlaryngoscopy, but might provide significant added value.[21]

Several counter-arguments regarding the clinical application of intrinsic fluorescence have emerged over the last years. Determination of the various mechanisms that influence the signal and its relative contribution has proven to be a complex process.[22] Even though some preclinical studies may suggest a correlation between certain components in the intrinsic fluorescence and the stage of the disease, such correlations have shown to be difficult to exploit clinically. The measured intrinsic fluorescence signal does not only depend on the concentration of the fluorophore (i.e. the component of a molecule which causes a molecule to be fluorescent), but also on the optical properties of the tissue. The same optical properties influence the color of the tissue. Thus, when the spectroscopic device is positioned based on visual clues of the lesion, the correlation with malignancy is lost, resulting in a biased measurement. The work of De Veld et al[22] illustrated that the spectroscopy only confirmed the visibility of the lesion with a very high sensitivity, whereas it could not distinguish between benign and malignant visible lesions. To avoid this bias, one would either have to find a way to find an invisible lesion, or develop a method to untangle fluorescence information and the effects of optical properties on the signal. Such methods are currently under development, but have not yet reached successful clinical application.[23]

## Tumor detection using conventional fluorescence

As mentioned earlier, tumor cells or biomarkers can also be imaged using antibodies or ligands conjugated to an optically active reporter (i.e. fluorophore). The principle of optical imaging is based on the concept of signal-to-background ratio (SBR), which is equivalent to the tumor-to-background ratio (TBR) in cancer imaging. The intensity of the signal must be increased at least 2 folds in order to be discriminated from nonspecific surrounding signals. The conventional fluorescence imaging techniques use probes (i.e. an antibody or ligand conjugated to an optically active reporter that is designed to target a disease-specific biomarker) in the visible light spectrum (~ 400-600 nm), which results in low SBR due to the relatively high level of nonspecific background light. A second disadvantage of visible

light is its absorption by biological chromophores, in particular hemoglobin. Absorption is the phenomenon that describes how the electromagnetic energy of a photon is taken up by matter, typically the electrons of an atom. Absorption limits the depth penetration to a few millimeters. Biological chromophores can also increase the scattering of light. To gain the required sensitivity and specificity to make optical imaging a potentially useful technique for image-guided surgery, the light properties of this spectrum are not sufficient.

## Tumor detection using near-infrared fluorescence

A crucial step has been made by the introduction of near-infrared (NIR) imaging techniques, which has led to a revolution in optical imaging. The absorption coefficient of tissue is at a minimum when using light in the NIR region due to light absorption by hemoglobin in the visible light spectrum (<600 nm) and other components such as water and lipids in the infrared range (>950 nm). This results in an optical imaging window from approximately 650 to 950 nm that allows for minimal light absorption and nonspecific autofluorescence, resulting in an increase in tissue penetration. These features of NIR light provide crucial advantages for its application in intraoperative image-guided surgery and a wide variety of strategies can be chosen when targeting specific (tumor) cells.

### *Near-Infrared Spectroscopy*

The intrinsic optical absorption signals of blood, water, and lipid, correlated with increased hemoglobin concentration due to angiogenesis and decreased hemoglobin saturation due to hypermetabolism, can be utilized in NIR spectroscopy to detect and localize cancer.[24] Diffuse optical imaging is a measurement technique based on detection of diffusely scattered light. It is used to estimate the average optical properties of tissue at multiple wavelengths based on diffusion theory. The technology assumes that light propagation is dominated by multiple scattering and is modeled as a diffusive process where photons behave as stochastic particles. Semi-quantitative tissue measurements can be obtained by separating light absorption from scattering using spatially- or temporally-modulated photon migration technologies. Using diffuse optical tomography techniques[25] or time-domain optical mammography[26] (Softscan®, Advanced Research Technologies, Montreal, Canada) to measure photon migration through the breast, variations in the functional and structural NIR properties (e.g. scattering, oxy- and deoxy-hemoglobin concentrations) were observed, enabling differentiation between benign and malignant tumors.[26] However, these techniques are not directly suitable for intraoperative use.

### *Non-Targeted Exogenous Contrast Agents*

Various nonspecific agents have been developed that are currently available for research and clinical use (e.g. fluorescein, indocyanine green (ICG), cresyl violet acetate, toluidine blue, Lugol's iodine). ICG (emission peak: 830 nm) has optical properties that are suitable for NIR imaging, which have been exploited for imaging of angiogenesis and identification of hepatic segments for facilitation of hepatic resection.[27, 28] Moreover, promising results

have been reported in the field of sentinel lymph node mapping, which we will describe later. In principle, because these agents are not tumor-specific, they are not optimally suited for determination of the tumor-free margin. Very recently however, real-time demarcation of small and grossly unidentifiable liver cancers using ICG has been described due to the disordered biliary excretion of ICG in cancer tissues and noncancerous liver tissues compressed by the tumor.[29]

### *Non-Targeted Activatable Organic Fluorophores*

When focusing on the expansive character of the tumor resulting from upregulation of proteolytic enzymes, a different strategy can be followed by using activatable fluorophores. This method allows detection of proteases that are relatively abundant in malignant tissue, which can be associated with specific characteristics (e.g. invasive, aggressive or metastatic tendency) of the tumor. These agents are injected in a quenched (i.e. inactivated) state, resulting in minimal fluorescence at the time of administration. When cleaved by specific enzymes, the agent becomes dequenched (i.e. activated), and fluorescence can be measured. Due to the cleavability, these probes have higher SBR when compared to nonspecific probes.

Weissleder et al. have developed a series of such cleavable NIR probes that are activated by proteases such as cathepsins and matrix metalloproteinases[30, 31] that are currently commercially available (Visen Medical, Boston, MA). A different quencher mechanism, using an inhibitory domain made up of negatively charged residues fused to activatable polyarginine-based cell-penetrating peptides has been described by Tsien et al. for use in the detection of matrix metalloproteinases.[32] However, these agents are not targeting specific molecules in cancer cells only. Cathepsins and matrix metalloproteinases are also produced by macrophages and neutrophils, and hence are abundant in inflammatory tissue[33] and in cerebral ischemia.[34] Nonetheless, our preclinical results in rats[35] and the previously mentioned studies are very promising (Figure 2).

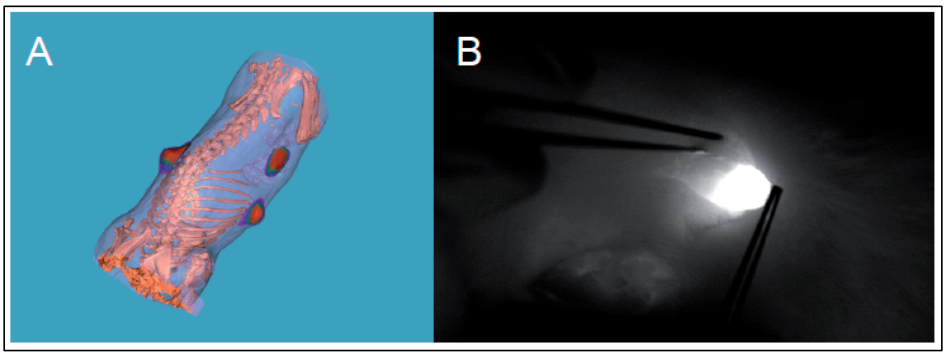


**Fig. 2.** Detection of breast cancer using the non-targeted activatable organic NIRF probe ProSense 680™ in a syngeneic rat model of primary breast cancer. A. 3-dimensional fusion of contrast-enhanced micro-CT and fluorescence imaging. In collaboration with J. Dijkstra, Division of Image Processing, LUMC. B. NIRF image-guided resection of one of the primary tumors using the Fluobeam™.

### *Targeted Organic Fluorophores*

Essential for the limitless replicative potential of tumor cells are the increased metabolism and expression of growth signaling receptors, combined with increased tumor angiogenesis to supply sufficient oxygen and nutrients. These characteristics have been exploited as a target for chemotherapeutics in head and neck cancer (e.g. cetuximab, bevacizumab), but can also be used for molecular-specific detection of cancer cells (Figure 1). In these agents, the NIR fluorophore has been conjugated to a specific targeting ligand or monoclonal antibody. Such agents have shown excellent SBR in whole animals and images can be collected over longer periods than the short-lived radiotracers labeled with fluorine-18 or carbon-11.

The epidermal growth factor receptor (EGFR) is expressed in the majority of head and neck squamous cell carcinomas.[36] The antibody has been coupled to a fluorophore Cy 5.5 (excitation 678 nm, emission 703 nm) and used to describe in vivo detection of the primary tumor,[37] identification of regional and distant metastasis,[38] evaluate chemoradiotherapeutic treatment,[39] detect residual disease, and guide surgical resections[40] in head and neck mouse tumor models (Figure 3). The conjugation of cetuximab to ICG, a nonspecific NIR fluorophore, has been reported to lack the sensitivity for use in a clinical setting.[41]

Production of the vascular endothelial growth factor (VEGF) is upregulated in tumor cells to promote angiogenesis. This provides a second target for chemotherapy, especially in recurrent or metastatic disease, as is illustrated by the use of bevacizumab, anti-VEGF antibody, for head and neck tumors.[42] Conjugation of Cy 5.5 to bevacizumab has also been described in the mouse model that was mentioned earlier, with a sensitivity and specificity of 80.9% and 91.7%, respectively.[41]

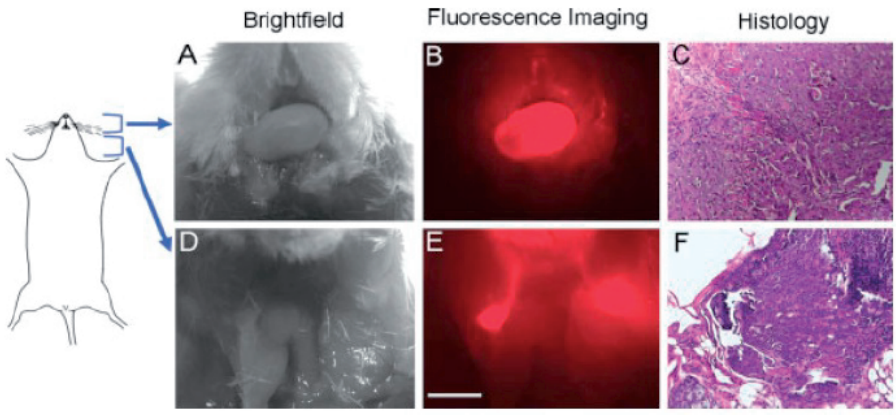


**Fig. 3.** Cervical metastases in an orthotopic murine model were detected with systemically injected cetuximab–Cy5.5 conjugate. The primary tongue tumor (A–C) was clearly visualized under fluorescent imaging after systemic injection of cetuximab–Cy5.5. After removal of cervical skin, bilateral draining lymph nodes could be identified and confirmed by pathology. Bar 5 2 mm. Reproduced with kind permission from Gleysteen JP, Newman JR, Chhieng D, Frost A, Zinn KR, Rosenthal EL. Fluorescent labeled anti-EGFR antibody for identification of regional and distant metastasis in a preclinical xenograft model. Head Neck 2008;30(6):782-9.

Instead of conjugation of the fluorophore to a monoclonal antibody, it can also be bound to a specific ligand, as was illustrated with VEGF and EGF.[43, 44] The latter was conjugated to the IRdye800CW (Li-Cor Bioscience, Lincoln, NE; excitation 785 nm, emission 810 nm). Due to the higher excitation frequency, IRdye800CW has much better penetration and SBR than Cy 5.5 as was illustrated by a comparative study of human breast cancer cell lines in subcutaneous xenograft models.[45] To image the expansive feature of cancer cells, the use of CD147 has been proposed as a third target in head and neck cancer imaging.[46] CD147 is a membrane spanning molecule highly expressed in tumor cells which stimulates the production of matrix metalloproteinases in neighboring fibroblasts. Analogous to the previously described studies, this molecule has been conjugated to Cy5.5 and in vivo fluorescent imaging was possible in a mouse head and neck tumor model.

A fourth tumor characteristic that has been explored for optical imaging is the transferrin receptor (TfR). This is a cell-membrane internalizing receptor that is largely responsible for iron sequestration. In normal squamous epithelium, TfR is expressed in only the parabasal and basal layers at a very low level and rarely in benign lesions; however it is overexpressed in many head and neck tumors.[47] Its use has been reported in imaging of a head and neck tumor mouse model by conjugation of a TfR antibody to Alexa-488 (excitation 494, emission 519), indicating a potential use for non-invasive imaging of head and neck tumors.[48]

An exciting new approach, similar to the non-targeted activatable organic fluorophores described earlier, is the use of quenched fluorophores conjugated to tumor targeting monoclonal antibodies. This approach was successfully explored by the group of Kobayashi et al.[49] They used avidin (targeting the d-galactose receptor) and trastuzumab (anti-HER2) labeled with the TAMRA (fluorophore)-QSY7 (quencher) pair. After internalization into the cell, the probe was cleaved, resulting in dequenching and target-specific fluorescence imaging with high SBR.

In strategies for imaging (tumor) angiogenesis, a crucial concept has been the targeting of alpha-v-beta-3 (αvβ3) integrin, a critically important adhesion molecule in the regulation of angiogenesis. This molecule can be found at the sprouting ends of newly formed blood vessels but also frequently on many epithelial tumor cells. High expression of adhesion receptors can be detected when targeting αvβ3 integrin by cyclic arginine-glycine-aspartate (cRGD) conjugated to Cy 5.5 or IRdye800CW.[50] The use of the quenching technique has been described in this respect as well, by means of a quenched cRGD molecule (RAFT-c(-RGDfK-)(4)-Cy5-SS-Q) which becomes activated during internalization into the cell.[51]

Increased αvβ3 expression can also be visualized by direct binding of a small peptidomimetic antagonist coupled to a NIR fluorescent dye (VivoTag-S680), known as IntegriSense (Visen Medical, Boston, MA). IntegriSense has a much higher specificity for $\alpha_v\beta_3$ integrin compared to RGD-based probes. It was shown to co-localize at the surface of both $\alpha_v\beta_3$ integrin positive endothelial and tumor cells. The signal is additionally enhanced by the internalization into $\alpha_v\beta_3$ integrin positive tumor cells, leading to a slower clearance of the probe from tumors compared to surrounding tissues.[52] This probe has successfully been

used to visualize liver metastasis from colon cancer in a rat model. It is important to note that most fluorescent dyes are related to high background signal in the liver, kidneys and bladder due to biodistribution and clearance of the agent, whereas in this study, the liver metastases could be clearly demarcated.[53]

Tumor cell metabolism is upregulated due to nearly all hallmarks of cancer,[54] leading to increased expression of membrane glucose transporter proteins (i.e. GLUT) and consequently increased glucose metabolism. Analogous to PET technology, this aspect can be targeted using a glucose analogue 2-deoxyglucose (2-DG) conjugated with IRDyeCW800. Very interesting results have recently been published revealing imaging glucose uptake in intracranial gliomas using the glucose analogue 2-deoxyglucose (2-DG) conjugated with IRDye800CW.[55]

### *Nanoparticles*

Nanoparticles hold an exceptional position in the discussion regarding the feasibility of fluorescent probes for optical imaging. Quantum dot nanoparticles are small crystals (2–10 nm diameter), made of inorganic semiconductor materials. They possess several physical properties that make them appealing for use as imaging reporters. The high quantum yields result in high signal intensity, enabling detection at lower expression levels compared to organic fluorophores. In addition, the fluorescence emission spectra can be tuned depending on their size, allowing for multiplexed imaging. Furthermore, quantum dot nanoparticles have proven to be photostable and have the possibility to target multiple biomarkers, due to its ability to contain multiple probe molecules. Finally, multimodal targeted quantum dot-based nanoparticles coated with a paramagnetic micellar shells have been described, allowing for both optical and magnetic resonance detection of tumor angiogenesis (Figure 4).[56]

However, the toxicity of quantum dot nanoparticles is a serious concern. The problem is that most quantum dots (albeit a very diverse group of substances) are based on heavy metal cores (e.g. Cd-Se, Cd-Te), which have been reported to be cytotoxic in their soluble form due to the release of toxic Cd(2+) ions and their surface chemistry and stability towards aggregation.[57, 58] These issues raise such significant hazards that, at present, clinical application of quantum dot nanoparticles does not seem feasible.

Silica nanoparticles have been developed as an alternative to quantum dots that combine the versatility and functionality of organic dyes with the stability and biocompatibility of the silica surface.[59] In a recent study, the biodistribution, including long-term quantitative tissue distribution, subcellular distribution, and the toxicity of silica nanoparticles were assessed in a mouse model. The results indicated that the small size of the silica nanoparticles resulted in high permeability and lengthy accumulation of the agent in lungs, liver and spleen, and could potentially cause liver injury when intravenously injected.[60] Because size, surface area, surface chemistry, solubility and shape are probably all key features that play a role in determining the harmful potential for engineered nanomaterials,[61] extensive research will have to be performed over the coming years in order to address these issues.

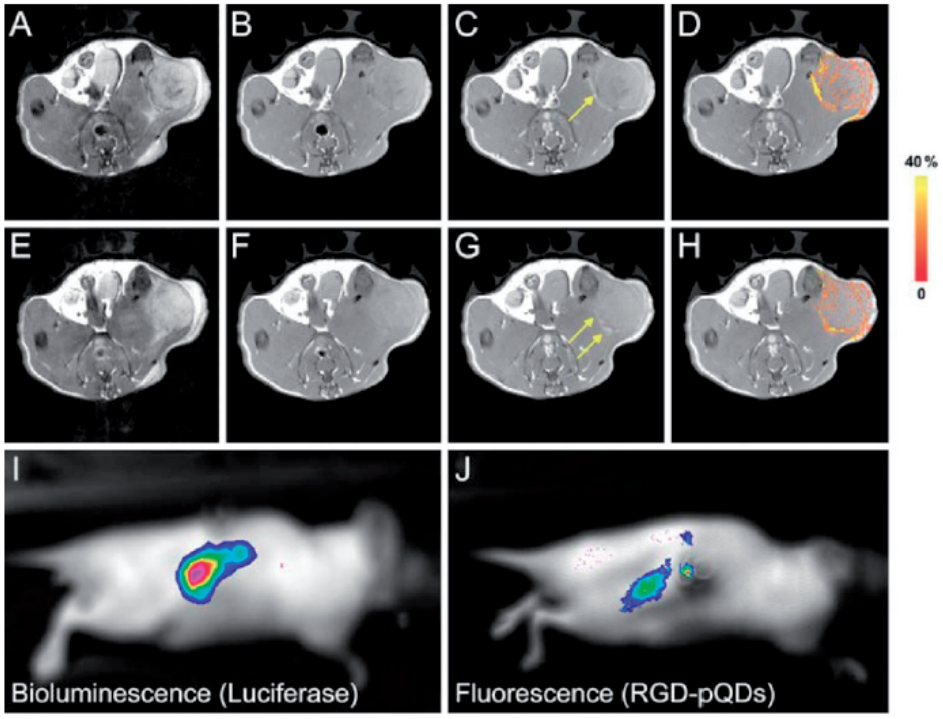


**Fig. 4.** Magnetic resonance and optical molecular imaging of tumor angiogenesis using alpha-v-beta-3 targeted multimodal quantum dot-based nanoparticles. T2-weighted images (A,E), collected before the nanoparticles were injected, show the contour of the tumor on the flank. T1-weighted images (B,C,F,G) with TR = 800 ms were measured before (B,F) and 45 min after (C,G) the injection of the nanoparticles. The arrows in (C,G) indicate bright (positive contrast) regions in the periphery of the tumor. In D,H, pixels in the tumor with signal enhancement of at least three times the noise level are color coded according to the pseudo-color scale on the right. I,J Bioluminescence imaging and fluorescence imaging of a Balb/c nude mouse with a luciferase-expressing renal carcinoma tumor after injection of luciferin (I). The strong bioluminescence signal is indicative of tumor growth in the right kidney. This signal colocalizes with a strong fluorescence signal (J) originating from intravenously administrated nanoparticles that are accumulated in the tumor.
Republished with kind permission from Mulder WJ, Castermans K, van Beijnum JR et al. Molecular imaging of tumor angiogenesis using alphavbeta3-integrin targeted multimodal quantum dots. *Angiogenesis*. 2009;12(1):17-24.

In conclusion, several strategies are at hand in the optical imaging field using NIR, with probes that can reach significant SBR and can be combined to increase the specificity and sensitivity of tumor detection (Figure 5). Because organic fluorophores are more biocompatible than inorganic agents, it is expected that when using the former agents, toxicity issues will play a minor role, as illustrated by ICG and fluorescein, which are already widely used in the clinic. However, for clinical translation of these results, pharmacokinetic studies are required for each fluorophore or fluorophore conjugate. Furthermore, in order

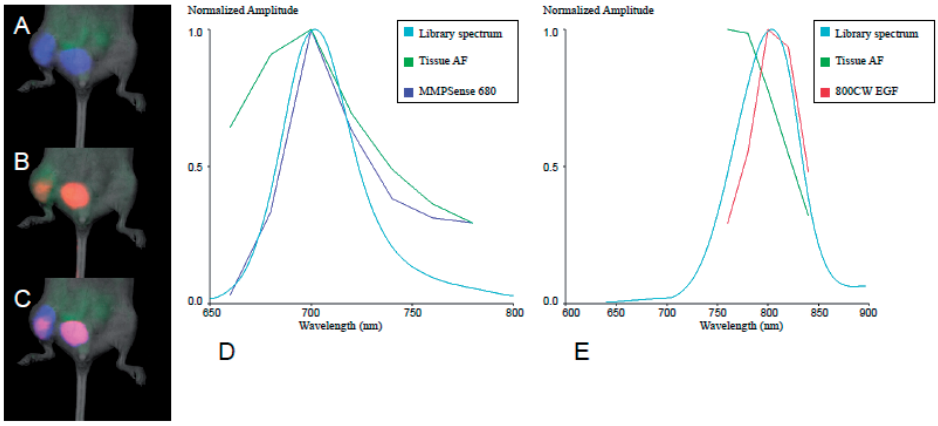


**Fig. 5.** Illustration of the use of two fluorescent agents with emission on different wavelenghts, showing the simultaneous detection of an MDA-MB231 breast cancer bone metastases in the right hind limb of a nude mouse. MDA-MB231 cells express relatively high levels of EGFR and are highly osteolytic. Nonspecific uptake of the probes in the bladder is also shown. A. Fluorescent image showing the blue signal of MMPSense™ 680; green is tissue autofluorescence. B. Fluorescent image showing the red signal of IRDye® 800CW EGF; green is tissue autofluorescence C. Fluorescent composite image showing both signals simultaneously (purple); green is tissue autofluorescence. D. Graphic showing peak signal intensity of MMPSense™ 680 at 700 nm (blue line), unmixed from autofluorescence (green line). E. Graphic showing peak signal intensity of IRDye® 800 CW EGF at 800 nm (red line), unmixed from autofluorescence (green line).
The MMPSense signal covers a larger area compared to the IRDye® 800CW EGF signal. This is most probably due to the fact that IRDye® 800CW EGF only detects the MDA-MB231 cells, whereas MMPSense also detects the highly increased osteoclastic bone resorption (ostelytic lesion) as a result of matrix metalloproteinase-9 expression of resorbing osteoclasts. AF; autofluorescence.

for these applications to be used intraoperatively, the development of suitable camera systems is required.

## Future directions

### *Intrinsic fluorescence imaging*

The use of intrinsic fluorescence in detection of head and neck cancer is expected to be limited to analyzing lesions that are already suspicious to the naked eye, as was illustrated by a case report of detection of an occult cancerous lesion during routine oral examination in a patient which had been treated for cervical lymph node metastasis of unknown primary tumor.[62] In this way, this technique could provide added value in the clinical setting in the years to come. However, for image-guided surgery, a clear demarcation of the tumor-free margin is required, necessitating the development of techniques that are capable of correcting the measured signal for scattering and absorption. In theory, this information could be provided by differential pathlength spectroscopy, which is currently being investigated in vivo.[63]

## *Optical image-guided surgery*

NIR optical imaging seems a good option for real-time image-guided surgery. If adequate imaging resolution can be achieved, intraoperative tumor visualization may improve complete tumor resection without unnecessary damage to healthy tissue and has the potential to more accurately assess tumor margins during surgery. Moreover, through biochemical changes involved in the earliest stages of neoplastic development, this technique promises to identify malignant lesions before they become visible to the naked eye or to currently available intraoperative imaging modalities.

Considering its wide range of applications, one could wonder why this technique has just recently emerged. Essentially, the development has been hampered by the lack of suitable NIR fluorescent probes and dedicated camera systems for the intraoperative visualization of these probes.

Conventional camera systems are limited to single-band NIR cameras, which have two drawbacks: they do not enable separation of autofluorescence from fluorescent probe signal, and it is not possible to correct for geometric and intensity distortions caused by photon-tissue interactions. Dedicated NIR camera systems that have been used for intraoperative optical image-guided surgery include the Photodynamic Eye (PDE; Hamamatsu Photonics, Hamamatsu City, Japan) and a self-build system, the Fluorescence-Assisted Resection and Exploration (FLARE™) from the Fragioni laboratory (Brookline, MA).[64] Currently, two smaller systems have been developed: the Mini-FLARE™ from the Frangioni laboratory and the Fluobeam from Fluoptics (Grenoble, France) (Figure 6).

Imaging over a range of NIR wavelengths enables correction for photon-tissue interaction and spectral unmixing of fluorescent signals. Spectral unmixing is the decomposition of the complete spectrum of a fluorescence signal into a collection of predefined spectra. This technique is used to determine the individual contribution of each fluorophore, i.e. linear unmixing. In preclinical studies, spectral unmixing has already proven to be superior to conventional fluorescence detection and was shown to greatly improve sensitivity and localization accuracy of NIR cameras.[65-67] However, these systems are not able to unmix the signals in real-time, which would be required for intraoperative image-guided surgery.

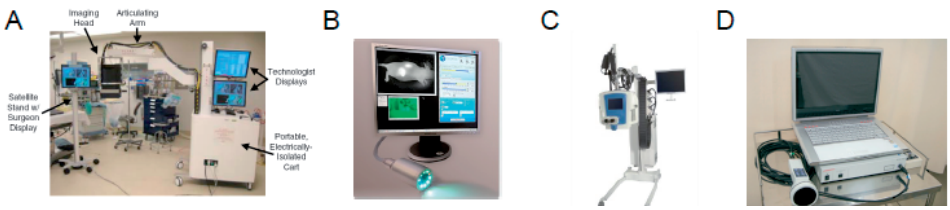


**Fig. 6.** Near-infrared intraoperative camera systems. A. FLARE™ camera system (www.frangionilab.org). B. Artist impression of Fluobeam™ (www.fluoptics.com). C. Artemis™ camera system (www.O2view.com) D. The Photodynamic Eye (Hamamatsu Photonics, Hamamatsu City, Japan).

Currently, two new camera systems have been developed that can detect and unmix NIR fluorescence in real-time. The first system has been developed by the group of Ntziachristos,[68] which implements a correction scheme that improves the accuracy of epi-illumination fluorescence images for light intensity variation in tissues. The implementation is based on the use of three cameras operating in parallel, utilizing a common main objective, which allows for the concurrent collection of color, fluorescence, and light attenuation images at the excitation wavelength from the same field of view. The correction is based on a ratio approach of fluorescence over light attenuation images. Color images and video are used for surgical guidance and for registration with the corrected fluorescence images. The second camera system is the Artemis, developed by O2view (Marken, The Netherlands). The Artemis is a real-time stereoscopic imaging system that combines visible light with NIR light images. It is equipped with a laser diode and the camera system allows additional 3D visualization of fluorescent molecules, superimposed on color stereoscopic vision. It has the potential to make multispectral images because it is using a 5-channel prism (covering the range from 400 – 1000 nm) enabling to capture images from 5 different CCD/CMOS sensors simultaneously with 5 different color bands.

### *Sentinel Lymph Node Mapping*

The first steps for translation of this technique to the clinic have been made in sentinel lymph node mapping. The sentinel lymph node is the first lymph node to which the lymphatic fluid coming from the tumor drains and in which tumor cells will first metastasize. Currently, lymphatic imaging is performed using dye-injection, nuclear imaging, CT and MRI,[69] which each have their specific limitations regarding sensitivity, resolution, exposure to radioactivity, or practical use. NIR fluorescence imaging allows for high spatial and temporal resolution without ionizing radiation, making it an easy-to-use and safe technique. With parallel imaging of visible and near-infrared light, the contrast agents can be traced to the sentinel lymph nodes in real-time, without affecting the visual appearance of the surgical field.

Considering the recent clinical results using intraoperative NIR fluorescence cameras[64, 70] or portable NIR imaging devices,[71] for now, sentinel lymph node mapping is one of the most promising clinical applications for NIR fluorescence imaging in the field of oncology.

### *Other Surgical Applications*

Intraoperative optical imaging camera systems are being developed resulting in the detection of a variety of tumors in preclinical studies during surgical procedures. In addition to intraoperative tumor detection, endoscopic systems are under development for diagnostic and surgical applications.[72]

In neurosurgery, the use of 5-aminolevulinic acid (5-ALA) for detection of malignant gliomas by optical imaging techniques has been recently studied. The intraoperative use for fluorescence guidance has been described in a phase II trial as an effective adjunct in the surgery of recurrent malignant gliomas.[73]

### *Clinical availability of fluorescent probes*

The use of NIR fluorescence optical imaging in the field of sentinel lymph node mapping is rapidly expanding in clinical oncology. ICG, approved by the Food and Drug Administration (FDA) for various other applications, will play a major role in this respect, potentially demonstrating the clinical advantage over current lymph node mapping protocols.

However, FDA approval of organic fluorophores is a necessary step towards clinical targeting of tumor specific signals. Once these agents are also found to be safe, it is anticipated that the initial steps will be taken in conjugating them to already FDA approved and clinically used monoclonal antibodies (e.g. cetuximab, bevacizumab). In the following years, FDA approval of the activatable agents is required to fully exploit the possibilities of optical imaging, and thereby enhance the specificity and sensitivity of this technique. Furthermore, if the toxicity issues of nanoparticles can be solved, interesting developments in that field can be expected due to the aforementioned advantages regarding multimodality and multitargeted imaging. All these developments will have to be accompanied by parallel development of adequate, manageable, intraoperative camera systems.

Very recently, intriguing research regarding undetectable fluorescence of non-fluorescent, light-absorbing molecules has been described by stimulating photon emission techniques.[74] Although yet far from practical applications, these studies hold promising possibilities for clinical or even intraoperative use in the years to come.

## Conclusion

It is clear that the properties of NIR optical imaging are well suited for real-time fluorescence imaging during surgery. The technique has the potential to identify malignant lesions through biochemical changes involved in the earliest stages of neoplastic development before becoming visible to the naked eye. To achieve this, a combination of the different strategies that each target specific hallmarks of cancer will most likely be required. Consequently, the oncologic surgeon will be able to assess tumor margins during surgery and will be guided toward optimal radical resection without unnecessary damage to the healthy tissues.

## References


1. Frangioni JV. New technologies for human cancer imaging. J Clin Oncol. 2008; 26(24): 4012-21.
2. Hanahan D, Weinberg RA. The hallmarks of cancer. Cell. 2000; 100(1): 57-70.
3. Semenza GL, Artemov D, Bedi A, Bhujwalla Z, Chiles K, Feldser D, et al. 'The metabolism of tumours': 70 years later. Novartis Found Symp. 2001; 240: 251-60; discussion 60-4.
4. Kelloff GJ, Hoffman JM, Johnson B, Scher HI, Siegel BA, Cheng EY, et al. Progress and promise of FDG-PET imaging for cancer patient management and oncologic drug development. Clinical cancer research : an official journal of the American Association for Cancer Research. 2005; 11(8): 2785-808.
5. Strong VE, Humm J, Russo P, Jungbluth A, Wong WD, Daghighian F, et al. A novel method to localize antibody-targeted cancer deposits intraoperatively using handheld PET beta and gamma probes. Surg Endosc. 2008; 22(2): 386-91.
6. Gulec SA, Hoenie E, Hostetter R, Schwartzentruber D. PET probe-guided surgery: applications and clinical protocol. World J Surg Oncol. 2007; 5: 65.
7. Hall WA, Truwit CL. Intraoperative MR-guided neurosurgery. J Magn Reson Imaging. 2008; 27(2): 368-75.
8. de Jong BW, Schut TC, Maquelin K, van der Kwast T, Bangma CH, Kok DJ, et al. Discrimination between nontumor bladder tissue and tumor by Raman spectroscopy. Analytical chemistry. 2006; 78(22): 7761-9.
9. Shetty G, Kendall C, Shepherd N, Stone N, Barr H. Raman spectroscopy: elucidation of biochemical changes in carcinogenesis of oesophagus. Br J Cancer. 2006; 94(10): 1460-4.
10. Stone N, Stavroulaki P, Kendall C, Birchall M, Barr H. Raman spectroscopy for early detection of laryngeal malignancy: preliminary results. The Laryngoscope. 2000; 110(10 Pt 1): 1756-63.
11. Nijssen A, Koljenovic S, Bakker Schut TC, Caspers PJ, Puppels GJ. Towards oncological application of Raman spectroscopy. J Biophotonics. 2009; 2(1-2): 29-36.
12. DaCosta RS, Andersson H, Wilson BC. Molecular fluorescence excitation-emission matrices relevant to tissue spectroscopy. Photochem Photobiol. 2003; 78(4): 384-92.
13. Dhingra JK, Perrault DF, Jr., McMillan K, Rebeiz EE, Kabani S, Manoharan R, et al. Early diagnosis of upper aerodigestive tract cancer by autofluorescence. Arch Otolaryngol Head Neck Surg. 1996; 122(11): 1181-6.
14. Svistun E, Alizadeh-Naderi R, El-Naggar A, Jacob R, Gillenwater A, Richards-Kortum R. Vision enhancement system for detection of oral cavity neoplasia based on autofluorescence. Head Neck. 2004; 26(3): 205-15.
15. Poh CF, Ng SP, Williams PM, Zhang L, Laronde DM, Lane P, et al. Direct fluorescence visualization of clinically occult high-risk oral premalignant disease using a simple hand-held device. Head Neck. 2007; 29(1): 71-6.
16. Roblyer D, Kurachi C, Stepanek V, Williams MD, El-Naggar AK, Lee JJ, et al. Objective detection and delineation of oral neoplasia using autofluorescence imaging. Cancer Prev Res (Phila Pa). 2009; 2(5): 423-31.
17. Muller MG, Valdez TA, Georgakoudi I, Backman V, Fuentes C, Kabani S, et al. Spectroscopic detection and evaluation of morphologic and biochemical changes in early human oral carcinoma. Cancer. 2003; 97(7): 1681-92.
18. Delank W, Khanavkar B, Nakhosteen JA, Stoll W. A pilot study of autofluorescent endoscopy for the in vivo detection of laryngeal cancer. Laryngoscope. 2000; 110(3 Pt 1): 368-73.
19. Malzahn K, Dreyer T, Glanz H, Arens C. Autofluorescence endoscopy in the diagnosis of early laryngeal cancer and its precursor lesions. Laryngoscope. 2002; 112(3): 488-93.
20. Baletic N, Malicevic H, Petrovic Z, Marinkovic-Eric J, Peric A. Advantages and limitations of the autofluorescent diagnostics of the laryngeal cancer and precancerosis. Eur Arch Otorhinolaryngol. 2009.
21. Kraft M, Glanz H, von Gerlach S, Wisweh H, Lubatschowski H, Arens C. Clinical value of optical coherence tomography in laryngology. Head Neck. 2008; 30(12): 1628-35.
22. De Veld DC, Witjes MJ, Sterenborg HJ, Roodenburg JL. The status of in vivo autofluorescence spectroscopy and imaging for oral oncology. Oral Oncol. 2005; 41(2): 117-31.
23. Amelink A, Kruijt B, Robinson DJ, Sterenborg HJ. Quantitative fluorescence spectroscopy in turbid media using fluorescence differential path length spectroscopy. J Biomed Opt. 2008; 13(5): 054051.

24. Nioka S, Chance B. NIR spectroscopic detection of breast cancer. Technology in cancer research & treatment. 2005; 4(5): 497-512.
25. Choe R, Konecky SD, Corlu A, Lee K, Durduran T, Busch DR, et al. Differentiation of benign and malignant breast tumors by in-vivo three-dimensional parallel-plate diffuse optical tomography. Journal of biomedical optics. 2009; 14(2): 024020.
26. Intes X. Time-domain optical mammography SoftScan: initial results. Acad Radiol. 2005; 12(8): 934-47.
27. Pierce MC, Javier DJ, Richards-Kortum R. Optical contrast agents and imaging systems for detection and diagnosis of cancer. Int J Cancer. 2008; 123(9): 1979-90.
28. Aoki T, Yasuda D, Shimizu Y, Odaira M, Niiya T, Kusano T, et al. Image-guided liver mapping using fluorescence navigation system with indocyanine green for anatomical hepatic resection. World J Surg. 2008; 32(8): 1763-7.
29. Ishizawa T, Fukushima N, Shibahara J, Masuda K, Tamura S, Aoki T, et al. Real-time identification of liver cancers by using indocyanine green fluorescent imaging. Cancer. 2009; 115(11): 2491-504.
30. Mahmood U, Weissleder R. Near-infrared optical imaging of proteases in cancer. Mol Cancer Ther. 2003; 2(5): 489-96.
31. Wunderbaldinger P, Turetschek K, Bremer C. Near-infrared fluorescence imaging of lymph nodes using a new enzyme sensing activatable macromolecular optical probe. European radiology. 2003; 13(9): 2206-11.
32. Jiang T, Olson ES, Nguyen QT, Roy M, Jennings PA, Tsien RY. Tumor imaging by means of proteolytic activation of cell-penetrating peptides. P Natl Acad Sci USA. 2004; 101(51): 17867-72.
33. Wunder A, Straub RH, Gay S, Funk J, Muller-Ladner U. Molecular imaging: novel tools in visualizing rheumatoid arthritis. Rheumatology (Oxford). 2005; 44(11): 1341-9.
34. Klohs J, Baeva N, Steinbrink J, Bourayou R, Boettcher C, Royl G, et al. In vivo near-infrared fluorescence imaging of matrix metalloproteinase activity after cerebral ischemia. J Cereb Blood Flow Metab. 2009; 29(7): 1284-92.
35. Mieog JS, Hutteman M, van der Vorst JR, Kuppen PJ, Que I, Dijkstra J, et al. Image-guided tumor resection using real-time near-infrared fluorescence in a syngeneic rat model of primary breast cancer. Breast cancer research and treatment. 2011; 128(3): 679-89.
36. Pomerantz RG, Grandis JR. The epidermal growth factor receptor signaling network in head and neck carcinogenesis and implications for targeted therapy. Semin Oncol. 2004; 31(6): 734-43.
37. Rosenthal EL, Kulbersh BD, Duncan RD, Zhang W, Magnuson JS, Carroll WR, et al. In vivo detection of head and neck cancer orthotopic xenografts by immunofluorescence. Laryngoscope. 2006; 116(9): 1636-41.
38. Gleysteen JP, Newman JR, Chhieng D, Frost A, Zinn KR, Rosenthal EL. Fluorescent labeled anti-EGFR antibody for identification of regional and distant metastasis in a preclinical xenograft model. Head Neck. 2008; 30(6): 782-9.
39. Gleysteen JP, Duncan RD, Magnuson JS, Skipper JB, Zinn K, Rosenthal EL. Fluorescently labeled cetuximab to evaluate head and neck cancer response to treatment. Cancer Biol Ther. 2007; 6(8): 1181-5.
40. Kulbersh BD, Duncan RD, Magnuson JS, Skipper JB, Zinn K, Rosenthal EL. Sensitivity and specificity of fluorescent immunoguided neoplasm detection in head and neck cancer xenografts. Arch Otolaryngol Head Neck Surg. 2007; 133(5): 511-5.
41. Withrow KP, Newman JR, Skipper JB, Gleysteen JP, Magnuson JS, Zinn K, et al. Assessment of bevacizumab conjugated to Cy5.5 for detection of head and neck cancer xenografts. Technology in cancer research & treatment. 2008; 7(1): 61-6.
42. Cohen EE, Davis DW, Karrison TG, Seiwert TY, Wong SJ, Nattam S, et al. Erlotinib and bevacizumab in patients with recurrent or metastatic squamous-cell carcinoma of the head and neck: a phase I/II study. Lancet Oncol. 2009; 10(3): 247-57.
43. Backer MV, Levashova Z, Patel V, Jehning BT, Claffey K, Blankenberg FG, et al. Molecular imaging of VEGF receptors in angiogenic vasculature with single-chain VEGF-based probes. Nat Med. 2007; 13(4): 504-9.
44. Kovar JL, Volcheck WM, Chen J, Simpson MA. Purification method directly influences effectiveness of an epidermal growth factor-coupled targeting agent for noninvasive tumor detection in mice. Anal Biochem. 2007; 361(1): 47-54.
45. Adams KE, Ke S, Kwon S, Liang F, Fan Z, Lu Y, et al. Comparison of visible and near-infrared wavelength-excitable fluorescent dyes for

molecular imaging of cancer. J Biomed Opt. 2007; 12(2): 024017.

46. Newman JR, Gleysteen JP, Baranano CF, Bremser JR, Zhang W, Zinn KR, et al. Stereomicroscopic fluorescence imaging of head and neck cancer xenografts targeting CD147. Cancer Biol Ther. 2008; 7(7): 1063-70.
47. Kearsley JH, Furlong KL, Cooke RA, Waters MJ. An immunohistochemical assessment of cellular proliferation markers in head and neck squamous cell cancers. Br J Cancer. 1990; 61(6): 821-7.
48. Shan L, Hao Y, Wang S, Korotcov A, Zhang R, Wang T, et al. Visualizing head and neck tumors in vivo using near-infrared fluorescent transferrin conjugate. Mol Imaging. 2008; 7(1): 42-9.
49. Ogawa M, Kosaka N, Longmire MR, Urano Y, Choyke PL, Kobayashi H. Fluorophore-quencher based activatable targeted optical probes for detecting in vivo cancer metastases. Mol Pharm. 2009; 6(2): 386-95.
50. Chen K, Xie J, Chen X. RGD-human serum albumin conjugates as efficient tumor targeting probes. Molecular imaging. 2009; 8(2): 65-73.
51. Jin ZH, Razkin J, Josserand V, Boturyn D, Grichine A, Texier I, et al. In vivo noninvasive optical imaging of receptor-mediated RGD internalization using self-quenched Cy5-labeled RAFT-c(-RGDfK-)(4). Molecular imaging. 2007; 6(1): 43-55.
52. Kossodo S, Pickarski M, Lin SA, Gleason A, Gaspar R, Buono C, et al. Dual in vivo quantification of integrin-targeted and protease-activated agents in cancer using fluorescence molecular tomography (FMT). Molecular imaging and biology : MIB : the official publication of the Academy of Molecular Imaging. 2010; 12(5): 488-99.
53. Hutteman M, Mieog JS, van der Vorst JR, Dijkstra J, Kuppen PJ, van der Laan AM, et al. Intraoperative near-infrared fluorescence imaging of colorectal metastases targeting integrin alpha(v)beta(3) expression in a syngeneic rat model. Eur J Surg Oncol. 2011; 37(3): 252-7.
54. Kroemer G, Pouyssegur J. Tumor cell metabolism: cancer's Achilles' heel. Cancer Cell. 2008; 13(6): 472-82.
55. Zhou H, Luby-Phelps K, Mickey BE, Habib AA, Mason RP, Zhao D. Dynamic near-infrared optical imaging of 2-deoxyglucose uptake by intracranial glioma of athymic mice. PLoS One. 2009; 4(11): e8051.
56. Mulder WJ, Castermans K, van Beijnum JR, Oude Egbrink MG, Chin PT, Fayad ZA, et al. Molecular imaging of tumor angiogenesis using alphavbeta3-integrin targeted multimodal quantum dots. Angiogenesis. 2009; 12(1): 17-24.
57. Kirchner C, Liedl T, Kudera S, Pellegrino T, Munoz Javier A, Gaub HE, et al. Cytotoxicity of colloidal CdSe and CdSe/ZnS nanoparticles. Nano Lett. 2005; 5(2): 331-8.
58. Lewinski N, Colvin V, Drezek R. Cytotoxicity of nanoparticles. Small. 2008; 4(1): 26-49.
59. Choi J, Burns AA, Williams RM, Zhou Z, Flesken-Nikitin A, Zipfel WR, et al. Core-shell silica nanoparticles as fluorescent labels for nanomedicine. Journal of biomedical optics. 2007; 12(6): 064007.
60. Xie G, Sun J, Zhong G, Shi L, Zhang D. Biodistribution and toxicity of intravenously administered silica nanoparticles in mice. Arch Toxicol. 2010; 84(3): 183-90.
61. Oberdorster G, Oberdorster E, Oberdorster J. Nanotoxicology: an emerging discipline evolving from studies of ultrafine particles. Environ Health Perspect. 2005; 113(7): 823-39.
62. Vigneswaran N, Koh S, Gillenwater A. Incidental detection of an occult oral malignancy with autofluorescence imaging: a case report. Head Neck Oncol. 2009; 1(1): 37.
63. Kruijt B, Kascakova S, de Bruijn HS, van der Ploeg-van den Heuvel A, Sterenborg HJ, Robinson DJ, et al. In vivo quantification of chromophore concentration using fluorescence differential path length spectroscopy. J Biomed Opt. 2009; 14(3): 034022.
64. De Grand AM, Frangioni JV. An operational near-infrared fluorescence imaging system prototype for large animal surgery. Technology in cancer research & treatment. 2003; 2(6): 553-62.
65. Mansfield JR, Hoyt C, Levenson RM. Visualization of microscopy-based spectral imaging data from multi-label tissue sections. Curr Protoc Mol Biol. 2008; Chapter 14: Unit 14 9.
66. Mayes P, Dicker D, Liu Y, El-Deiry W. Noninvasive vascular imaging in fluorescent tumors using multispectral unmixing. Biotechniques. 2008; 45(4): 459-60, 61-4.
67. Xu H, Rice BW. In-vivo fluorescence imaging with a multivariate curve resolution spectral unmixing technique. Journal of biomedical optics. 2009; 14(6): 064011.

68. Themelis G, Yoo JS, Soh KS, Schulz R, Ntziachristos V. Real-time intraoperative fluorescence imaging system using light-absorption correction. J Biomed Opt. 2009; 14(6): 064012.
69. Barrett T, Choyke PL, Kobayashi H. Imaging of the lymphatic system: new horizons. Contrast Media Mol Imaging. 2006; 1(6): 230-45.
70. Troyan SL, Kianzad V, Gibbs-Strauss SL, Gioux S, Matsui A, Oketokoun R, et al. The FLARE intraoperative near-infrared fluorescence imaging system: a first-in-human clinical trial in breast cancer sentinel lymph node mapping. Annals of surgical oncology. 2009; 16(10): 2943-52.
71. Tagaya N, Yamazaki R, Nakagawa A, Abe A, Hamada K, Kubota K, et al. Intraoperative identification of sentinel lymph nodes by near-infrared fluorescence imaging in patients with breast cancer. Am J Surg. 2008; 195(6): 850-3.
72. Figueiredo JL, Alencar H, Weissleder R, Mahmood U. Near infrared thoracoscopy of tumoral protease activity for improved detection of peripheral lung cancer. Int J Cancer. 2006; 118(11): 2672-7.
73. Nabavi A, Thurm H, Zountsas B, Pietsch T, Lanfermann H, Pichlmeier U, et al. Five-aminolevulinic acid for fluorescence-guided resection of recurrent malignant gliomas: a phase ii study. Neurosurgery. 2009; 65(6): 1070-6; discussion 6-7.
74. Min W, Lu S, Chong S, Roy R, Holtom GR, Xie XS. Imaging chromophores with undetectable fluorescence by stimulated emission microscopy. Nature. 2009; 461(7267): 1105-9.

# II OPTICAL IMAGING OF HEAD AND NECK CANCER IN ANIMAL MODELS

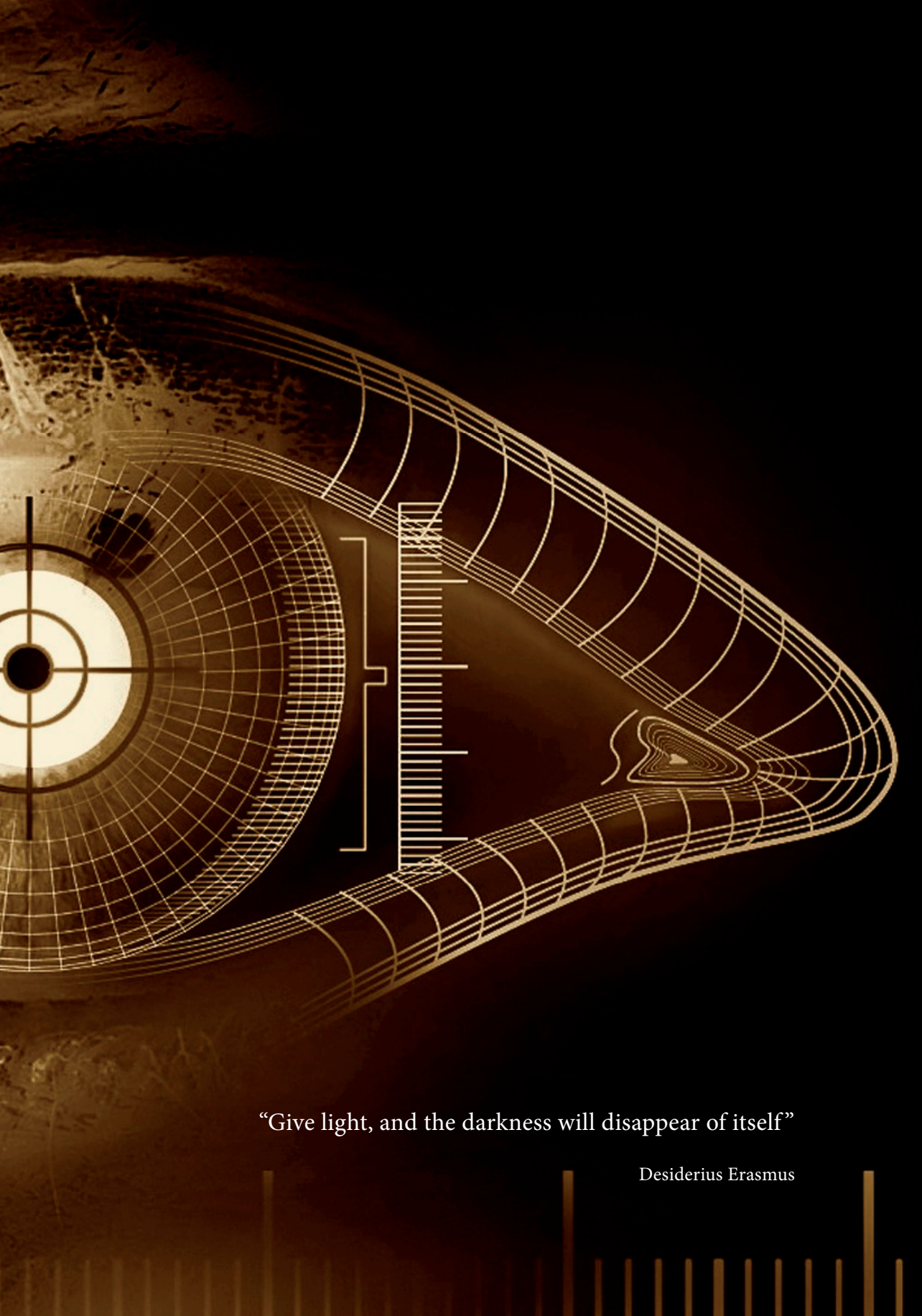

"Give light, and the darkness will disappear of itself"

Desiderius Erasmus

# 3 Detection of oral cancer and cervical lymph node metastasis using activatable near-infrared fluorescent agents targeting degradation of the extracellular matrix

Stijn Keereweer,[1,2] J.Sven D. Mieog,[3] Isabel M. Mol,[2]
Pieter B.A.A. Van Driel,[2] Thomas J.A. Snoeks,[2]
Robert J. Baatenburg de Jong,[1] Alexander L. Vahrmeijer,[3]
Jeroen D.F. Kerrebijn,[1] Clemens W.G.M. Löwik[2]

1. Erasmus Medical Center, Department of Otorhinolaryngology Head and Neck Surgery, Rotterdam, The Netherlands.
2. Leiden University Medical Center, Molecular Endocrinology and Molecular Imaging, Leiden, The Netherlands.
3. Leiden University Medical Center, Department of Surgery, Leiden, The Netherlands.

Published in **Archives of Otolaryngology Head and Neck Surgery, June 2011,** 137(6):609-15

## Abstract

### *Objective*

To assess the feasibility of optical imaging using activatable near-infrared fluorescence (NIRF) agents to detect oral cancer and cervical lymph node metastasis *in vivo*.

### *Design*

In vivo study.

### *Setting*

University medical center.

### *Subjects*

Female nude mice aged 4-6 weeks.

### *Intervention*

Luciferase-expressing OSC-19-luc cells were injected into the tongues of nude mice. A control group of nude mice was injected in the tongue with physiological saline. Tumor growth was followed by bioluminescence imaging. After 3 weeks, animals were randomly allocated to intravenous administration of 1 of 2 activatable NIRF agents: ProSense680 or MMPSense680. Fluorescence imaging was performed of the mice and tumor-to-background ratio (TBR) was determined on histological sections of the tongue and cervical lymph nodes after resection at necropsy.

### *Main outcome measure*

Fluorescence signals.

### *Results*

The fluorescence signals in tongue tumor and cervical lymph node metastases were significantly higher than those in control animals. Histological analysis demonstrated the highest proteolytic activity at the invasive tumor border where the extracellular matrix is degraded. The mean (SD) TBR of ProSense680 in the tongue was 15.8 (8.1) and in the lymph nodes was 11.8 (3.6). For MMPSense680, the mean (SD) TBR in the tongue was 18.6 (SD=9.4) and in the lymph nodes was 10.5 (4.0).

### *Conclusions*

Oral cancer and cervical lymph node metastases can be detected by targeting increased proteolytic activity at the tumor borders with NIRF optical imaging. These NIRF agents could be used for real-time image-guided surgery, which has the potential to improve the complete surgical resection of oral cancer.


Abbreviations used: BLI, bioluminescence imaging; ECM, extracellular matrix; FLI, fluorescence imaging; HE, hematoxylin-eosin; MMP, matrix metalloproteinase; NIRF, near-infrared fluorescence; OSCC, oral squamous cell carcinoma; PET, positron emission tomography; PBS, phosphate buffered saline; TBR, tumor-to-background ratio.

## Introduction

Intraoperative assessment of tumor-free margins in head and neck cancer surgery is critical to completely remove the primary tumor and improve prognosis while minimizing surgical morbidity.[1] Currently, preoperative assessment of tumor size and involvement of regional lymph nodes is performed using different imaging modalities. However, in the operating room, the surgeon is confined to visual appearance and palpation of the tumor and cervical lymph nodes.

As a result, involved surgical margins have been described in 16% of clinically radically resected oral and oropharyngeal squamous cell carcinoma (OSCC) specimens.[1] Postoperative radiotherapy is often administered in order to decrease local recurrence rate. However, local tumor recurrence for tongue carcinomas after curative intended surgery has been described in 22% of the patients.[2] Therefore, new intraoperative visualization techniques are required to assess tumor margins in real-time (i.e., synchronous data capturing and processing that results in a direct presentation of the fluorescent images) and to guide the subsequent surgical removal with adequate tumor-free margins. Optical imaging using near-infrared fluorescence (NIRF) light has recently emerged as a promising technique which has the potential to traverse the gap between preoperative radiology and surgery by providing real-time visualization of tumor tissue, warranting image-guided surgery.[3] The features of NIRF light provide crucial advantages for its application in image-guided surgery, due to light absorption (i.e. uptake of electromagnetic energy of a photon by the electrons of an atom) by hemoglobin in the visible light spectrum (<650 nm) and other components such as water and lipids in the infrared range (>900 nm). This results in an optical imaging window from approximately 650 to 900 nm in which the light scattering and nonspecific autofluorescence (i.e. fluorescence of normal components of the tissue) are minimal. Furthermore, the absorption coefficient is very low in this spectrum resulting in an increase of tissue penetration,[4] and interference of fluorescence with the surgical field is prevented due to the insensitivity of human eyes to near-infrared wavelengths.[3, 4]

When targeting specific cancer cells, a wide variety of strategies can be chosen that each target different tumor characteristics.[5] To gain optimal tumor-to-background ratios (TBR), new agents (i.e. antibodies or ligands conjugated to an optically active reporter that is designed to target a disease-specific biomarker) have been designed that contain a cleavage site specific to tumor specific enzymes.[6-8] These agents are injected in a quenched (i.e., non-fluorescent) state, minimizing fluorescence at the time of administration. After cleavage by the specific enzyme, the agent becomes dequenched (i.e., fluorescent). Next to increased TBR, the use of activatable agents has a second specific advantage, because they detect proteases that are associated with specific characteristics, for example the invasive, aggressive or metastatic tendency of the tumor.

The capability to degrade the extracellular matrix (ECM) surrounding the tumor to access blood vessels and lymphatic vessels is a prerequisite for tumors to invade and metastasize. In this process, the same mechanisms that normal cells use for migrating through tissue

barriers are exploited. Proteolytic enzymes, including matrix metalloproteinases (MMPs), and cathepsins (mostly cathepsin B) are involved in ECM degradation of OSCC.[9, 10] Increased production of these enzymes has been associated with the invasive and metastatic phenotype of the tumor.[9] Tumor-associated MMP expression and activity is the result of endogenous tumor cell-expression. However, in epithelial cancers, most of the upregulated MMPs are expressed by host stromal cells surrounding the tumor, especially in areas of active invasion.[11, 12] Cathepsin B is mostly upregulated in lysosomes of tumor cells that are located at the invasive tumor border, where ECM degradation takes place, and hence the proteolytic activity is increased.[9, 10] Furthermore, Cathepsin D has been described as a potential independent predictor of cervical lymph node metastasis in head and neck cancer.[13] Therefore, NIRF agents that are able to detect these proteases may be of use for intraoperative detection of OSCC[14].

We performed a study to assess the feasibility of protease-activatable optical imaging for detection of OSCC and cervical lymph node metastasis. To our knowledge, this is the first study that describes the use of activatable NIRF agents to detect OSCC in vivo.

## Materials and Methods

### *Reagents*

The NIRF agent ProSense680 (VisEn Medical, Woburn, MA) with peak excitation at 680 nm and emission at 700 nm was used for imaging of the tumor and involved margins. ProSense680 is conjugated to the fluorochrome VivoTag-S680 (VisEn Medical), and becomes activated after cleavage by proteolytic activation of lysosomal cysteine or serine proteases including cathepsin B. The second agent that was used was MMPSense680 (VisEn Medical) which is conjugated to the same fluorochrome and has the same fluorescence characteristics. This agent becomes activated after cleavage by MMPs.

### *Cell line*

For this study, the human OSCC cell line OSC-19-luc was used, which is known to metastasize to cervical lymph nodes. This cell line was established in Japan with cells from a patient with squamous cell carcinoma of the tongue that metastasized to a cervical lymph node.[15] The OSC-19-luc cells had been retrovirally infected before with the luciferase gene to allow bioluminescence imaging (BLI).[15] Bioluminescence is the process of light emission in living organisms. In contrast to fluorescence, bioluminescence does not require excitation by light, but is generated chemically. In bioluminescence imaging, the DNA of such an organism that encodes the luminescent protein is incorporated into a laboratory animal either via a viral vector or by creating a transgenic animal. Bioluminescence imaging is based on the detection of light produced during enzyme (luciferase)-mediated oxidation of a molecular substrate when the enzyme is expressed *in viv*o as a molecular reporter. The technique enables monitoring throughout the course of disease, allowing localization and serial quantification of biological processes without killing the laboratory animal. Cells were grown *in vitro* in Dulbecco modified Eagle medium supplemented with 10% fetal

bovine serum, L-glutamine, sodium pyruvate, nonessential amino acids, and a vitamin solution (Life Technologies Inc, Grand Island, NY).

### *Cell assays*

To test the sensitivity of in vitro detection of OSC-19-luc cells, 2 assays using ProSense680 and MMPSense680 were performed. An increasing amount of cells (range: 0 – 40 000) was seeded in two 96-wells plates. After 7 hours, ProSense680 (45 nM) was added in 100 µL per well in the first plate, which incubated on the cells during 24 hours. Medium without probe was added to other cells in the plate as a control. In addition, the cells were washed 3 times with phosphate buffered saline (PBS) to discard excess non-bound agent according to previous studies.[6] Finally, the wells were imaged using the Odyssey™ scanner (LI-COR Biosciences, Lincoln, NE; focus offset 3 mm, intensity 10, 700 nm channel). The same protocol was used for the assay of MMPSense680 in the second plate.

### *Animal model*

BALB/c nu/nu female mice, aged 4 to 6 weeks (Charles River Laboratories, L'Arbresle, France), were obtained and housed in accordance with the guidelines of the Animal Welfare Committee of the Leiden University Medical Center, which also approved the study. All experiments were conducted and the animals were humanely euthanized according to these guidelines. The animals were housed in the animal facility of the Leiden University Medical Center. Autoclaved pellet food and sterilized water were provided ad libitum. The weight of the animals was followed throughout the experiment to monitor their general health. Throughout tumor inoculation and the imaging procedures, the animals were anesthetized with 4% isoflurane for induction and 2% isoflurane for maintenance in oxygen with a flow of 0.8 L/min and placed on an animal bed with an integrated nose mask.

### *Study design*

To induce an OSCC model, 6 x $10^4$ OSC-19-luc cells, diluted in 30 µL PBS, were injected submucosally into the distal end of the tongue of 10 BALB/c nu/nu mice. Tumor growth was followed 2 times a week by BLI and visual inspection of the tongue.

At day 21, mice were randomly allocated to administration of 1 of the 2 activatable NIRF agents: ProSense680 or MMPSense680. For both ProSense680 and MMPSense680, a control group (each containing 5 BALB/c nu/nu mice without tumor) was treated with an injection of physiological saline in the tongue and later intravenously injected with either of the 2 activatable agents. The agents were injected intravenously (1.33 nmol, 100 µL per animal) into 1 of the tail veins. Fluorescence imaging (FLI) was performed 24 hours after injection, based on the blood pharmacokinetics of the agents (VisEn website: www.visenmedical.com), and the animals were humanely killed afterwards. Subsequently, the overlying skin of the cervical region was removed for gross examination. After whole animal FLI, the tongue and cervical lymph nodes were completely excised for additional ex vivo fluorescence measurements.

### *Bioluminescence and Fluorescence Imaging*

Currently, BLI is considered the most sensitive imaging technology available. A recent study[16] has shown the ability to pick up a single cancer cell in vitro using the same imaging systems and luciferase vectors that were used in the present study. Because BLI requires genetic modification of the cancer cells, this technique is not applicable for clinical use, and FLI is required to identify the tumor. However, in the experimental setting, BLI can be used as an internal control to assess co-localization with the fluorescence signal.

Non-invasive BLI was performed by anesthetizing the animals with 2% isoflurane before and during imaging. An aqueous solution of luciferin (Caliper LifeSciences, Hopkinton, MA) at 150 mg/kg in a volume of 50 µL was injected intraperitoneally 5 minutes prior to imaging, after which the animals were imaged using the IVIS 100 imaging system (Caliper LifeSciences, Hopkinton, MA). Quantification of the BLI signal was performed through standardized regions of interest using Living Image software (version 3.2, Caliper LifeSciences, Hopkinton, MA). The FLI of the mouse was performed using the Maestro™ (CRi, Woburn, MA), fitted with the yellow filter with acquisition range of 630-800 nm in 10 nm steps and variable acquisition time.

### *Histological analysis*

After FLI, tongues were surgically removed and snap frozen on dry ice. Subsequently, they were cut into slices (20 µm) and imaged using the Odyssey scanner, followed by imaging using the EVOS fl fluorescence microscope fitted with a Cy 5.5 filter (Advanced Microscopy Group, Bothell, WA). Then, tissue sections were air-dried and stained with standard hematoxylin-eosin.

Cervical lymph nodes were surgically removed and cut into 2 halves. One half was fixed in 3.7% formalin overnight and paraffin embedded, cut into slices (20 µm), imaged using the Odyssey scanner, and hematoxylin-eosin stained. The second half was snap frozen to allow for immunohistochemical analysis. Immunohistochemical staining was performed on 10-µm-thick fresh frozen tissue sections. Rabbit polyclonal antibodies against wide spectrum cytokeratin, diluted 1:100, were used (ab9377; Abcam, Cambridge, MA). The slides were then washed with phosphate-buffered saline and detected with biotinylated polyclonal goat anti-rabbit immunoglobulins, diluted at 1:600 (E0432; Dako, Heverlee, Belgium). Slides were counterstained with hematoxylin.

After merging of the fluorescence image with the microscopic image, co-localization of fluorescence signal with cancer tissue was determined and the TBR was calculated. To quantify the fluorescence signal regions of interest were drawn in the tumor region, as well as in the surrounding normal tissue at a range of 2 mm from the invasive tumor border as described previously.[17] This was repeated in 3 different slices of the same tissue specimen resulting in a mean TBR for each specimen, which was subsequently used for calculation of the overall TBR and standard deviation.

### *Statistical analysis*

Mean fluorescence intensity and associated standard deviations were assessed using the Living Image software (version 3.2, Caliper LifeSciences) for BLI data and the Maestro Software (version 2.10.0, CRi Inc.) for FLI data. Correlation was calculated using the Pearson correlation test for linear correlations and the Spearman correlation test for non-parametrical data. Unpaired or paired t-tests were used for testing differences of fluorescence intensity between groups. Statistical tests were two-tailed and $p < 0.05$ was considered significant. For statistical analysis, SPSS for Windows, version 16.0 was used. GraphPad Prism software (Version 5.01, La Jolla, CA) was used for generation of graphs and merging of fluorescence images with microscopic images was performed using Cyttron Visualization Platform (Version 1.3, Leiden University, The Netherlands).

## Results

### *In vitro*

The fluorescence intensity of ProSense680 was significantly correlated with the number of OSC-19-luc cells (correlation coefficient: 0.968, $p < 0.01$, Fig. 1). This finding suggests that ProSense680 is activated by OSC-19-luc cells, indicating its potential use for in vivo testing. No correlation was observed using MMPSense680, most likely because activity of matrix metalloproteinases is mainly increased in the surrounding tissue of cancer cells[11, 12] and, therefore, is not detectable in cell culture.

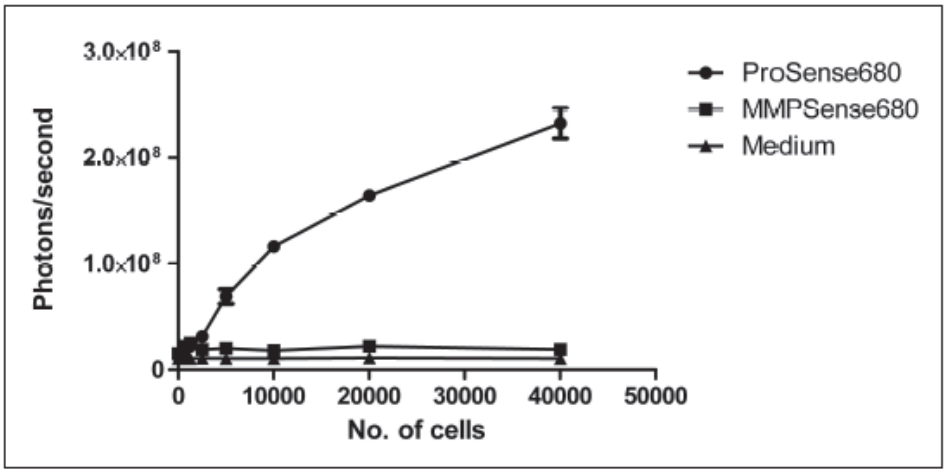


**Fig. 1.** Correlation of fluorescence and increased number of OSC-19-luc cells in vitro for ProSense680, MMPSense680 and medium (control). Data points represent the mean; error bars indicate the standard deviation.

*In vivo*

Seven days after inoculation of the OSC-19-luc cells, tongue tumors had developed in all 10 mice which could be followed by BLI signal (Fig. 2, A). After 11 days, BLI signal indicated uni- (n=1) or bilateral (n=9) cervical lymph node metastases in all animals (Fig. 2, B). Tumor growth as a function of time (including standard deviation) is illustrated in Fig. 2, C.

No BLI signal was found in the control animals. When FLI was performed after resection of the overlying skin in the control animals, a low-level background signal of both agents was observed in the tongue and cervical lymph nodes (Fig. 3, A+D). In the animals with OSCC, cervical lymph node metastases were not distinguishable by gross examination after resection of the overlying skin. However, the fluorescence images showed clear demarcation of tumor regions in both the tongue tumor and cervical lymph node metastases (Fig. 3, B+E). Furthermore, quantitative comparison between tumor and control animals (n = 5 per group) demonstrated significantly higher signals in malignant tissues for ProSense680

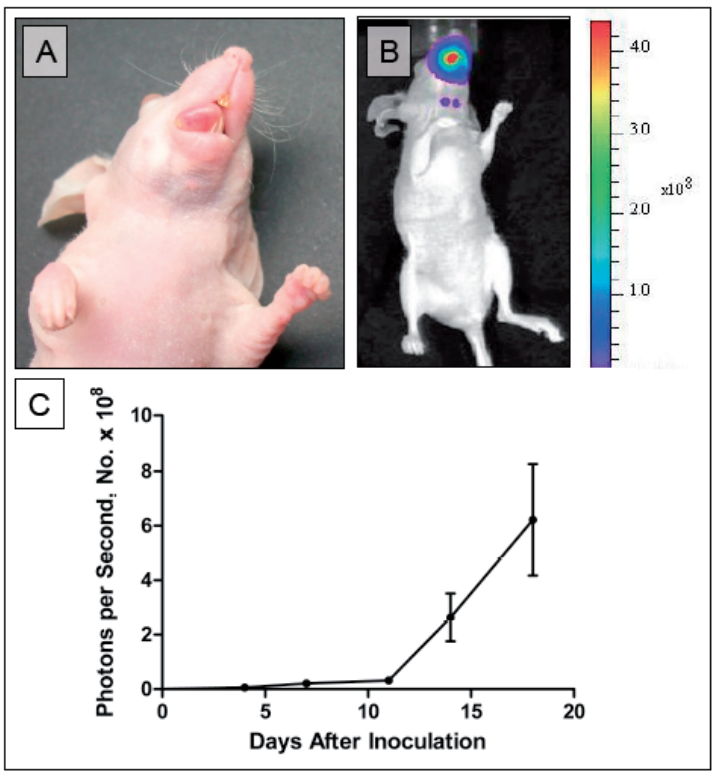


**Fig. 2.** Monitoring oropharyngeal squamous cell carcinoma (OSCC) tumor growth. A. Image of a mouse with OSCC tumor at day 14. B. Bioluminescence image (BLI) of a mouse with OSCC tumor at day 14 illustrating increased BLI signal in tongue and bilateral cervical lymph nodes. C. Increase in BLI signal as a function of time indicating tumor growth in all animals (n=10). Data points represent the mean; error bars indicate the standard deviation.

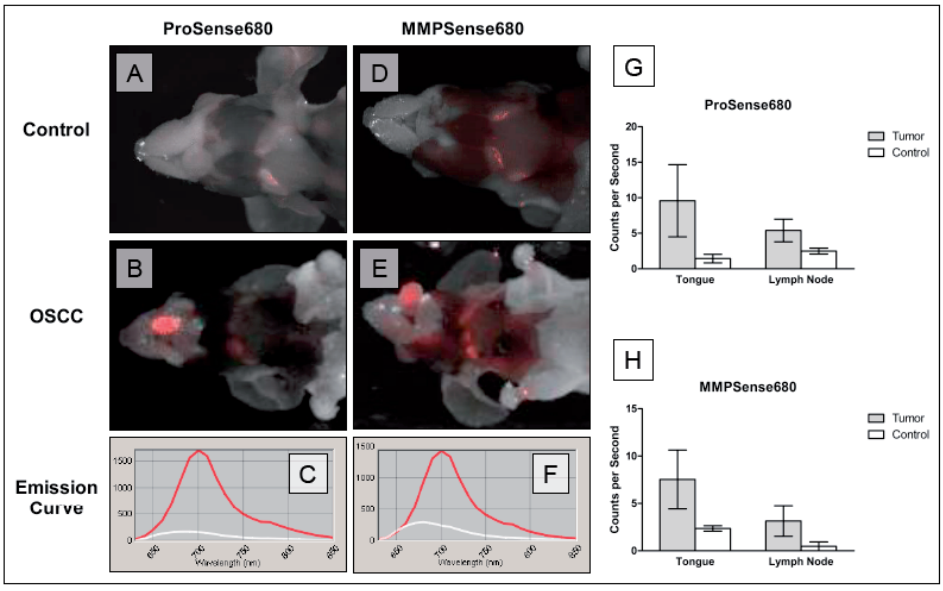


**Fig. 3.** Uptake of activatable near-infrared fluorescence agents ProSense680 and MMPSense680 in control animals and mice with oropharyngeal squamous cell carcinoma (OSCC). Pseudocolored fluorescence imaging (FLI) signal (red) of a control mouse and a mouse with OSCC is shown for ProSense680 (A, B) and MMPSense680 (D, E). The emission peaks of both agents at 700 nm are demonstrated (C, F). Differences in FLI signal intensity between tumor and control animals of ProSense680 and MMPSense680 are illustrated in (G) and (H). Error bars represent the standard deviation.

(tongue: $p = .02$; lymph nodes: $p < .001$) and MMPSense680 (tongue: $p = .02$; lymph nodes: $p = .01$) (Fig. 3, G+H).

### *Histologic analysis*

Histologic analysis of the tissues by a pathologist confirmed the presence of OSCC in the tongue specimens of all 10 mice that had been inoculated with the OSC-19-luc cells (Fig. 4 + 5). Furthermore, squamous cell carcinoma metastases were found in the lymph nodes that had an increased BLI signal (Fig. 6). No tumor was found on HE or immunohistochemical staining analysis in the lymph nodes without BLI signal.

High fluorescence signal of ProSense680 was found in the invasive border of the tongue tumor (Fig. 4, B+C), which is the region where cathepsin activity is increased to facilitate degradation of the ECM. As with cathepsins, MMPs are mainly active in the direct surrounding tissue of the tumor, corresponding with the region where the fluorescence signal of MMPSense680 was found (Fig. 5, B+C).

The mean (SD) TBR of ProSense680 in the tongue was 15.8 (8.1) and in the lymph nodes was 11.8 (3.6). For MMPSense680, the mean (SD) TBR in the tongue was 18.6 (9.4) and in the lymph nodes was 10.5 (4.0, Fig. 7). Subsequent imaging with brightfield microscopy with fluorescence overlay confirmed these findings (Fig. 8).

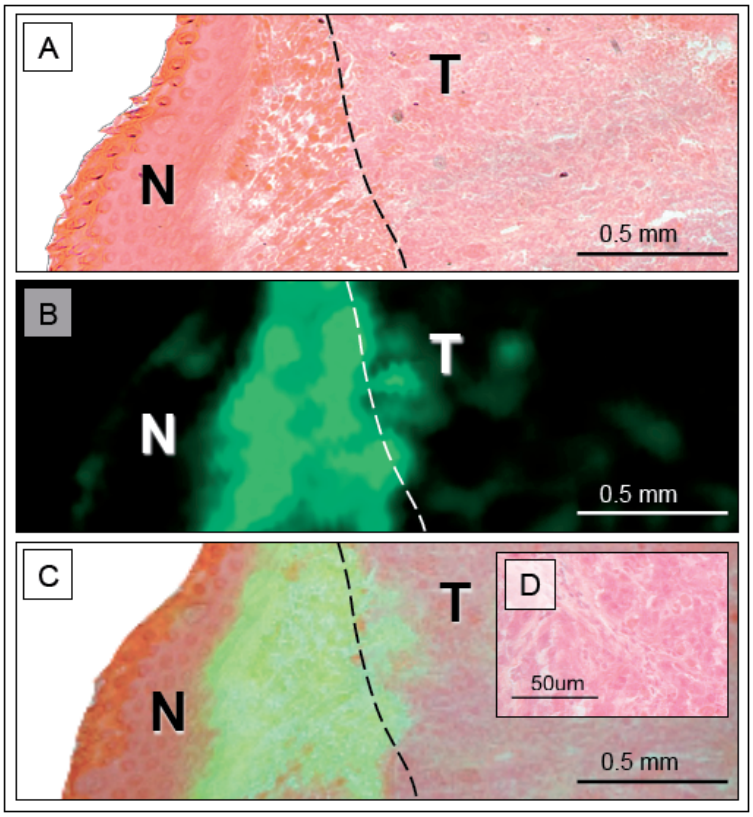


**Fig. 4.** Localization of ProSense680 in histologic sections of tongue tissue with oropharyngeal squamous cell carcinoma. A. Hematoxylin-eosin staining indicating tumor (T) and normal (N) tissue. Tumor border is indicated by a dotted line. B. Fluorescence signal (pseudocolored in green). C. Overlay image illustrates ProSense680 in the invasive front of the tumor.
is enhanced in the invasive border *(IB)* of the tumor *(T)* (A-C). FLI signal of MMPSense680 is found in the invasive tumor border as well as in the surrounding host stromal cells (D-F). N = normal tongue tissue, IB = invasive border, T = tumor.

## Discussion

In this study, OSCC with cervical lymph node metastasis was established in all the animals. Using optical imaging techniques to image the 2 activatable NIRF agents, ProSense680 and MMPSense680, we detected tongue tumor and cervical lymph node metastases. Histologic analysis demonstrated that proteolytic activity by cathepsins was highest at the invasive tumor border. This is explained by the upregulation of cathepsin B in lysosomes of tumor cells that are located at the invasive tumor border in order to degrade the ECM.[9,10] These findings are in accordance with a study by Mieog et al,[17] who demonstrated the use of ProSense680 for surgical removal of mammary cancer in a rat model. They demonstrated complete removal of the tumor under direct, real-time NIRF guidance using an intraoperative optical

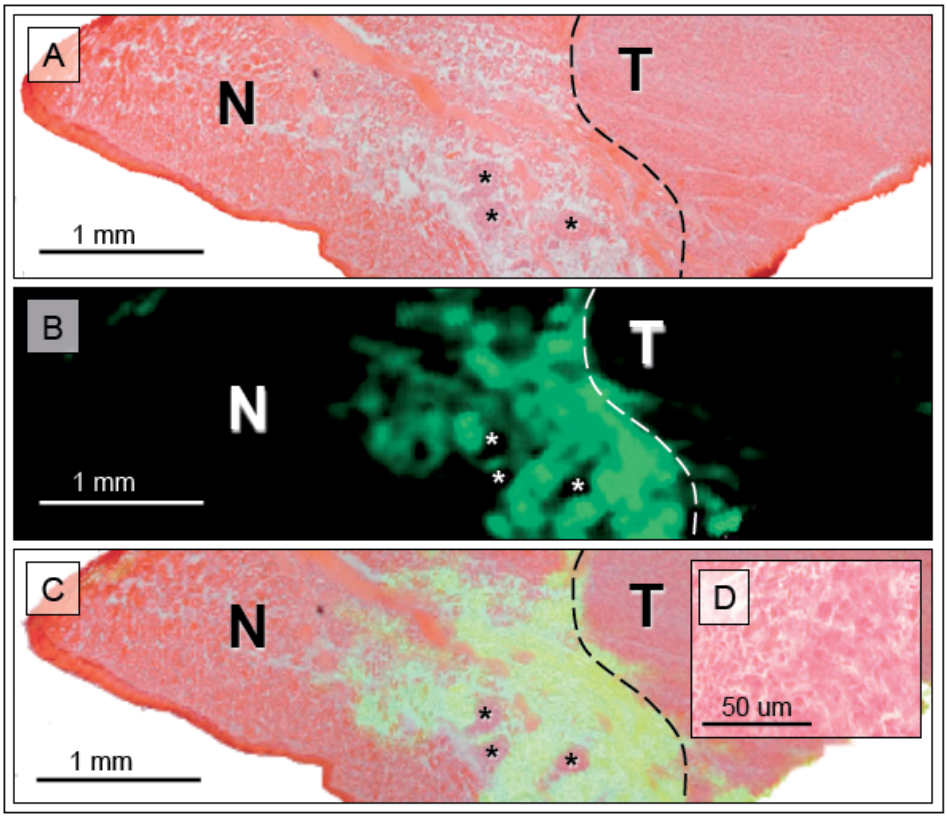


**Fig. 5.** Imaging of histological sections of cervical lymph nodes with OSCC metastasis. *In* vivo, these lymph node metastases had been indicated by BLI and FLI signal. A. Overview image of immunohistochemistry on a cervical lymph node; the dotted square indicates the area of magnification. B. Magnification (10x) illustrates immunohistochemical coloring of humane OSCC cells in the border (white arrows). C. Paraffin section of a different OSCC positive cervical lymph node (black arrow) in surrounding connective and adipose tissue. D. Pseudocolored (green) fluorescence signal of MMPSense680. E. Overlay image of C and D indicating fluorescence signal inside the tumor positive node.

imaging camera system. On histologic analysis, MMP activity was mainly increased at the invasive tumor border and tumor surrounding host stromal cells, which is a well-known feature of epithelial cancers.[11, 12]

In cancer surgery, detection of involved margins is essential for complete removal of the tumor. Therefore, it might be more important to show the border of the tumor, including the involved surrounding matrix, than the tumor mass itself. A high fluorescence signal of the tumor mass itself could potentially outshine the tumor resection margin, thereby prohibiting accurate determination of the tumor border.

A second interesting feature of MMPs is that increased activity can be used as a predictor for progression from oral dysplasia to cancer.[18] In this way, NIRF imaging using

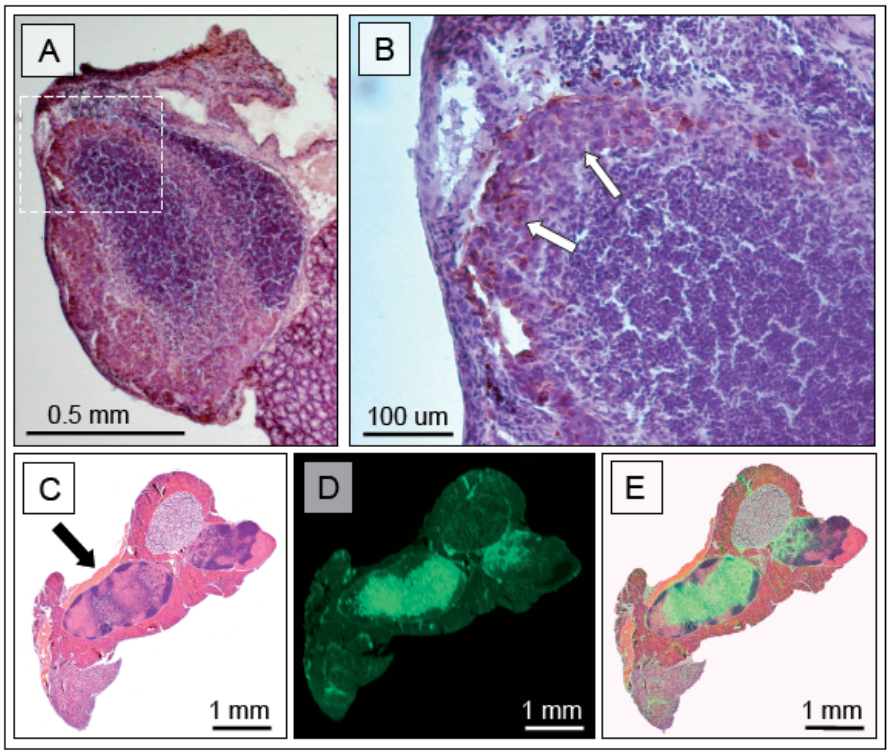


**Fig. 6.** Tumor-to-background ratio (TBR) of ProSense680 and MMPSense680 in histological sections of tongue tissue and cervical lymph nodes.

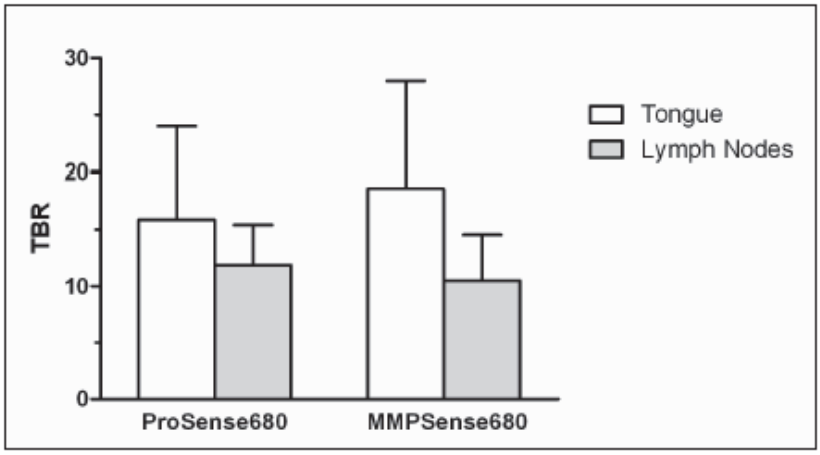


**Fig. 7.** Brightfield image with fluorescence overlay (emission ~ 700 nm) showing increased fluorescence signal (pseudocolored red) of ProSense680 (A) and MMPSense680 (C) at the invasive tumor front (10x magnification). Corresponding tissue samples with HE staining are shown in B and D.

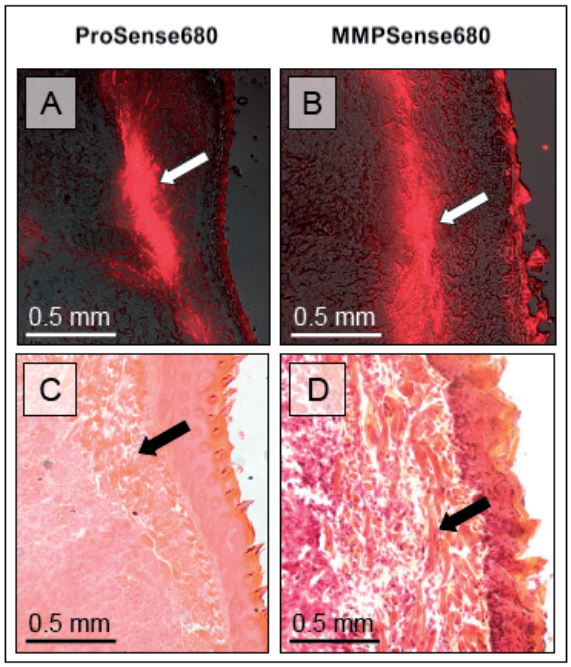


**Fig. 8.** Brightfield image with fluorescence overlay (emission ~ 700 nm) showing increased fluorescence signal *(pseudo-colored red)* of ProSense680 (A) and MMPSense680 (B) at the invasive tumor front *(indicated by white arrows)*. Corresponding tissue samples with HE staining are shown in C and D, demonstrating the tumor border *(black arrows)*.

MMPSense680 could potentially be used for tumor screening, follow-up of premalignant lesions, or tumor detection, which would be of great value for the current clinical practice. It is generally accepted that a TBR greater than 2 is sufficient to critically distinguish the fluorescence signal from the background during surgery.[3] In the present study, TBR was assessed on histology within 2 mm of the invasive border. Values ranged from 15.8 to 18.6 for tongue tissue, and 10.5 to 11.8 for lymph nodes. This strongly indicates the feasibility of the use of both agents for real-time image-guided surgery. Based on the present results, it is expected that these agents could be used for detection of cervical lymph node metastases in patients.

The ultimate goal of image-guided head and neck cancer surgery is complete removal of the tumor. However, further research is required to determine whether this technique will actually lead to more radical resections in clinical practice. Furthermore, before clinical studies can be performed, approval by the Food and Drug Administration to use these agents in patients is required.

## Conclusions

In conclusion, oral cancer and cervical lymph node metastases can be detected by targeting increased proteolytic activity at the tumor borders with NIRF optical imaging. This strategy could be used for real-time image-guided surgery, which can potentially improve the complete surgical resection rate in patients with oral cancer.

## Acknowledgements

Professor Hogendoorn, Ir, PhD, (Department of Pathology, Leiden University Medical Center) is gratefully acknowledged for his analysis of the tissue sections. The help of Prof. J.N. Myers, MD, PhD, (University of Texas, M.D. Anderson Cancer Center, Houston) in providing us with the OSC-19-luc cells is much appreciated. We thank J. Dijkstra, Ir, PhD, (Department of Radiology and Image Processing, Leiden University Medical Center) for his contribution to the overlay of histological images with fluorescence images and I. Que (Animal Experimentation Laboratory, Leiden University Medical Center) for his assistance in the animal experiments. The principal investigator had full access to all the data in the study and takes responsibility for the integrity of the data and the accuracy of the data analysis.

## References

1. McMahon J, O'Brien CJ, Pathak I et al. Influence of condition of surgical margins on local recurrence and disease-specific survival in oral and oropharyngeal cancer. Br J Oral Maxillofac Surg 2003;41(4):224-231.
2. Rusthoven KE, Raben D, Song JI, Kane M, Altoos TA, Chen C. Survival and patterns of relapse in patients with oral tongue cancer. J Oral Maxillofac Surg 2010;68(3):584-589.
3. Frangioni JV. New technologies for human cancer imaging. J Clin Oncol 2008;26(24):4012-4021.
4. Weissleder R, Pittet MJ. Imaging in the era of molecular oncology. Nature 2008;452(7187):580-589.
5. Keereweer S, Kerrebijn JD, van Driel PB et al. Optical Image-guided Surgery-Where Do We Stand? Mol Imaging Biol 2010.
6. Weissleder R, Tung CH, Mahmood U, Bogdanov A, Jr. In vivo imaging of tumors with protease-activated near-infrared fluorescent probes. Nat Biotechnol 1999;17(4):375-378.
7. Mahmood U, Weissleder R. Near-infrared optical imaging of proteases in cancer. Mol Cancer Ther 2003;2(5):489-496.
8. Wunderbaldinger P, Turetschek K, Bremer C. Near-infrared fluorescence imaging of lymph nodes using a new enzyme sensing activatable macromolecular optical probe. Eur Radiol 2003;13(9):2206-2211.
9. Wickramasinghe NS, Nagaraj NS, Vigneswaran N, Zacharias W. Cathepsin B promotes both motility and invasiveness of oral carcinoma cells. Arch Biochem Biophys 2005;436(1):187-195.
10. Yang X, Wei KJ, Zhang L et al. Increased expression of Cathepsin B in oral squamous cell carcinoma. Int J Oral Maxillofac Surg 2010;39(2):174-181.
11. Kessenbrock K, Plaks V, Werb Z. Matrix metalloproteinases: regulators of the tumor microenvironment. Cell 2010;141(1):52-67.
12. Scherer RL, McIntyre JO, Matrisian LM. Imaging matrix metalloproteinases in cancer. Cancer Metastasis Rev 2008;27(4):679-690.
13. Gandour-Edwards R, Trock B, Donald PJ. Predictive value of cathepsin-D for cervical lymph node metastasis in head and neck squamous cell carcinoma. Head Neck 1999;21(8):718-722.
14. Keereweer S, Sterenborg HJ, Kerrebijn JD, van Driel PB, de Jong RJ, Lowik CW. Image-guided surgery in head and neck cancer: Current practice and future directions of optical imaging. Head Neck 2011.

15. Sano D, Choi S, Milas ZL et al. The effect of combination anti-endothelial growth factor receptor and anti-vascular endothelial growth factor receptor 2 targeted therapy on lymph node metastasis: a study in an orthotopic nude mouse model of squamous cell carcinoma of the oral tongue. Arch Otolaryngol Head Neck Surg 2009;135(4):411-420.
16. Kim JB, Urban K, Cochran E et al. Non-invasive detection of a small number of bioluminescent cancer cells in vivo. PLoS One 2010;5(2):e9364.
17. Sven DM, Vahrmeijer AL, Hutteman M et al. Novel intraoperative near-infrared fluorescence camera system for optical image-guided cancer surgery. Mol Imaging 2010;9(4):223-231.
18. Smith J, Rattay T, McConkey C, Helliwell T, Mehanna H. Biomarkers in dysplasia of the oral cavity: a systematic review. Oral Oncol 2009;45(8):647-653.

# 4

# Detection of oral cancer and cervical lymph node metastasis targeting increased epidermal growth factor receptor expression or increased tumor glucose metabolism

Stijn Keereweer,[1,2] Jeroen D.F. Kerrebijn,[1] Isabel M. Mol,[2]
J. Sven D. Mieog,[3] Pieter B.A.A. Van Driel,[2]
Robert J. Baatenburg de Jong,[1] Alexander L. Vahrmeijer,[3]
Clemens W.G.M. Löwik[2]

1. Erasmus Medical Center, Department of Otorhinolaryngology Head and Neck Surgery, Rotterdam, The Netherlands.
2. Leiden University Medical Center, Molecular Endocrinology and Molecular Imaging, Leiden, The Netherlands.
3. Leiden University Medical Center, Department of Surgery, Leiden, The Netherlands.

Published in **Head & Neck, July 2012,** 34(7):1002-8

## Abstract

### *Background*

In oral cancer surgery, intraoperative optical imaging could help the surgeon to determine adequate tumor-free margins.

### *Methods*

Tumor-specific near-infrared fluorescence agents targeting epidermal growth factor receptor (CW800 EGF) or glucose transporter system (CW800 2-DG) were administered to mice with tongue carcinoma and cervical lymph node metastases. Tumor growth was followed by bioluminescence imaging. Fluorescence signals were compared to a control group of healthy animals.

### *Results*

Significantly higher fluorescence was found in tongue tumors and cervical lymph node metastases compared to control animals. Fluorescence correlated with histopathology. Tumor-to-background ratio of CW800 EGF in the tongue was 13.8 (SD = 6.1) and in the lymph nodes 15.7 (SD = 8.8). For CW800 2-DG, the tumor-to-background ratio in the tongue was 4.6 (SD = 2.1) and in the lymph nodes 33.9 (SD = 18.4).

### *Conclusions*

Optical imaging can be used to detect oral cancer and cervical lymph node metastases and could potentially improve complete surgical resection by real-time image-guided surgery.

Abbreviations used: ECM, extracellular matrix; GLUT, glucose transporter; HE, hematoxylin-eosin; MMP, matrix metalloproteinase; NIR, near-infrared; OSCC, oral squamous cell carcinoma; PET, positron emission tomography; PBS, phosphate buffered saline.

## Introduction

In daily practice of oral cancer surgery, intraoperative determination of adequate tumor-free margins is performed by palpation and visual inspection. However, involved surgical margins have been reported in 16% of the patients with oropharyngeal or oral squamous cell carcinoma (OSCC) that were operated with the primary objective of achieving a macroscopic clearance of 1 cm.[1] Furthermore, local recurrence rates of 22% have been reported in patients treated for tongue carcinomas with curative intended surgery.[2] New intraoperative visualization techniques using near-infrared (NIR) fluorescence optical imaging are being developed, that could help the surgeon to discriminate between healthy and cancer tissue.[3, 4] NIR fluorescence agents that target specific tumor characteristics provide the possibility of real-time image-guided surgery.[5]

The essence of optical image-guided cancer surgery revolves around a sufficient tumor-to-background ratio to accurately distinguish tumor from healthy tissue. Due to light absorption by hemoglobin in the visible light spectrum (<650 nm) and other components such as water and lipids in the infrared range (>900 nm), the near-infrared region offers optimal fluorescence characteristics to provide sufficient tumor-to-background ratios. Fluorophores that emit light at the 800 nm region have increased penetration depth and lower non-specific fluorescence due to lower absorption coefficients of tissues, compared to fluorophores that emit at lower wavelengths. These fluorescence characteristics result in better tumor-to-background ratios and sensitivity.[6, 7]

Many targeting strategies have been proposed to detect head and neck cancer by NIR fluorescence optical imaging.[8] Limitless replicative potential of tumor cells, an essential feature of carcinogenesis, is facilitated in part by increased expression of growth signaling receptors. In the majority of head and neck cancers, increased expression of the epidermal growth factor (EGF) receptor is found,[9] providing a potential target for tumor imaging. A second feature of tumor growth is exploited in positron emission tomography (PET) technology, by targeting the increased metabolism of cancer cells using the glucose-mimetic 2-deoxy-2-[18F]fluoro-D-glucose (18FDG).[10] Recently, two NIR fluorescence agents have been developed for optical imaging that target these characteristics. Increased EGF receptor expression can be targeted by a recombinant of human EGF which has been labeled to a fluorophore that fluoresces in the 800 nm region (CW800 EGF, LI-COR™ Biosciences, Lincoln, NE).[11] A fluorescent analogue to 18FDG (CW800 2-DG, LI-COR Biosciences), has been used to target increased glucose uptake in tumors.[12]

The purpose of this study was to assess the feasibility of targeted NIR fluorescence optical imaging of OSCC and cervical lymph node metastasis in an animal model. For tumor-specific targeting, agents were used that fluoresce in the 800 nm range and detect increased EGF receptor expression or increased tumor metabolism.

## Materials and Methods

### *Animal model*

The study protocol was approved by Animal Welfare Committee of the Leiden University Medical Center. Housing of the BALB/c nu/nu female mice (aged 4 to 6 weeks, Charles River Laboratories, L'Arbresle, France), conducting of the experiments, and euthanizing were performed in accordance with the guidelines of this Animal Welfare Committee. Autoclaved pellet food and sterilized water were provided without restriction. The weight of the animals was followed throughout the experiment to monitor their general health state.

To develop orthotopic oral cancer mouse models, OSC-19-luc cells were used that had been kindly received from the laboratory of Prof. J.N. Myers, MD, PhD, University of Texas, M.D. Anderson Cancer Center, Houston. This cell line was established with cells from a patient with OSCC of the tongue that metastasized to a cervical lymph node and has been described to have increased expression of EGF receptor.[13] To allow bioluminescence imaging, the OSC-19-luc cells had been retrovirally infected with the luciferase gene.[13] Cells were grown *in vitro* in Dulbecco modified Eagle medium (DMEM, Gibco, Invitrogen) supplemented with 10% fetal bovine serum, L-glutamine, sodium pyruvate, nonessential amino acids, and a 2-fold vitamin solution (Life Technologies Inc, Grand Island, New York).

The cells (6 x $10^4$ OSC-19-luc cells, diluted in 30 µL phosphate buffered saline (PBS)) were inoculated submucosally into the distal end of the tongue of the animals as described previously.[14] Throughout tumor inoculation and imaging procedures, the animals were anesthetized with 4% isoflurane for induction and 2% isoflurane for maintenance in oxygen with a flow of 0.8 L/min and placed on an animal bed with an integrated nose mask.

### *Bioluminescence and Fluorescence Imaging*

Bioluminescence imaging is currently considered the most sensitive imaging technology available. In contrast to fluorescence, bioluminescence does not require excitation by light, but is generated chemically. Bioluminescence imaging is based on the detection of light produced during enzyme (luciferase)-mediated oxidation of a molecular substrate when the enzyme is expressed *in viv*o as a molecular reporter. The technique enables monitoring throughout the course of disease, allowing localization and serial quantification of biological processes without killing the laboratory animal. Recent reports have shown the ability to pick up a single cancer cell in vivo, using the same imaging systems and luciferase-vectors that were used in our study.[15] However, because bioluminescence imaging requires genetic modification of the cancer cells, this technique is not applicable for clinical use and fluorescence imaging is required to identify the tumor. To follow tumor growth non-invasively, bioluminescence imaging was performed by intraperitoneal injection of an aqueous solution of luciferin (Caliper LifeSciences, Hopkinton, MA) at 150 mg/kg in a volume of 50 µL, 5 minutes prior to imaging, followed by imaging of the animals using the IVIS Spectrum imaging system (Caliper LifeSciences). Quantification of the bioluminescence signal was performed through standardized regions of interest using Living Image software (version 3.2, Caliper LifeSciences).

For fluorescence imaging, 2 NIR fluorescence agents were used that were coupled to the IRDye CW800 (excitation 774 nm, emission 789 nm). The first agent, CW800 2-DG (LI-COR Biosciences), has been described to detect increased glucose uptake, mainly by the glucose transporter (GLUT)-1.[12] Although the exact mechanism is yet unknown, blockage of uptake of the agent with either unlabeled 2-DG or glucose has been reported, as well as localization in the cytoplasm, indicating involvement of the GLUT system. Contrary to GLUT-4, which are mainly found in striated muscle tissue,[16] GLUT-1 are found in stratified squamous epithelia and are upregulated in OSCC[16]; association with poor prognosis in patients has been described.[17] The second agent was CW800 EGF (LI-COR Biosciences), a fluorophore labeled recombinant of human EGF.[11]

Whole-body fluorescence imaging was performed using the Maestro™ scanner (CRi, Woburn, MA), fitted with the deep-red filter with acquisition range of 700-950 nm in 10 nm steps and variable acquisition time. A mirror was placed along both sides of the animal to include anterolateral views. Imaging of histological sections of excised tongue tissue and cervical lymph nodes was performed using the 800 nm channel of the Odyssey scanner.

### *Study design*

The sensitivity of both agents for detection of OSC-19-luc cells was tested *in vitro* with a cell binding assay according to previous experiments.[11, 12] An increasing amount of cells (range: 0 – 40 000) was seeded in a 96-wells microtiter plate. As a control, an assay of medium only (i.e., autofluorescence) and an assay of non-specific IRDye CW800 carboxylate (LI-COR Biosciences) were included. The cells were starved for 2 hours in serum-free low-glucose DMEM and incubated with CW800 2-DG (5 μM in 100 μL) at 37°C during an additional hour. For CW800 EGF and IRDye CW800, starvation media were replaced with media containing IRDye CW800 only (50 nM in 100 μL) or CW800 EGF (50 nM in 100 μL), and incubated at room temperature (25°C) for 15 minutes. Specificity of the NIR fluorescence agents was evaluated by competition assays in which starvation media were replaced with media containing increasing concentrations of unlabeled EGF (4–2140 nM, AF-100-15, Peprotech, Rocky Hill, NJ) plus CW800 EGF (70 nM), or increasing concentrations of unlabeled D+ glucose (0.8–375 μM) plus CW800 2-DG (5 μM). The assays were stopped by fixation with 4% formaldehyde solution for 20 minutes and washed four times with PBS to get rid of excess non-bound agents. Finally, the wells were imaged using the 800 nm channel of the Odyssey scanner (LI-COR Biosciences; focus offset 3 mm, intensity 8).

In the animal experiment, OSC-19-luc cells were inoculated into the tongues of 14 BALB/c nu/nu mice. Tumor growth was followed twice a week by bioluminescence imaging and visual inspection of the tongue. Due to small tongue sizes, comparison of fluorescence signals between tumor and healthy surrounding tongue tissue was not possible. Therefore, we introduced a control group of 14 BALB/c nu/nu mice that were injected in the tongue with physiological saline. After 3 weeks, mice of both groups were randomly allocated to intravenous administration of CW800 2-DG or CW800 EGF in one of the tail veins (10 nmol for CW800 2-DG and 1.33 nmol for CW800 EGF, 100 μL per

animal). Based on the blood pharmacokinetics of the agents (LI-COR Biosciences website: www.licor.com), whole-body fluorescence imaging was performed 24 hours after injection. First, the animals were killed and the overlying skin of the cervical region was removed for gross examination. Subsequently, whole-body fluorescence imaging was performed, followed by complete excision of the tongue and cervical lymph nodes for additional *ex vivo* fluorescence measurements and histological analysis.

The excised tongues and cervical lymph nodes were frozen on dry ice or paraffin embedded and fixed in 3.7% formalin overnight. Next, tissues were cut into 3 slices (10-20 μm) and imaged using the Odyssey scanner. After imaging, histological sections were air-dried and stained with standard hematoxylin-eosin stain. Lymph nodes were also stained with anti-human wide spectrum cytokeratin staining (Abcam Inc, Cambridge, MA) to help to identify smaller cervical lymph node metastases.

On histologic sections, colocalization of fluorescence signal with cancer tissue was determined after merging of the fluorescence image with the microscopic image. Subsequently, the tumor-to-background ratio in the histological sections was determined. The fluorescence signal was quantified by drawing regions of interest in the tumor region, as well as in the surrounding normal tissue at a range of 2 mm from the tumor border as described previously.[18] For each separate tissue specimen, the mean tumor-to-background ratio of all 3 slices was calculated.

### *Statistical analysis*

Using the Living Image software (version 3.2, Caliper LifeSciences) for bioluminescence data and the Maestro Software (version 2.10.0, CRi Inc.) for fluorescence data, fluorescence signal was measured using standard regions of interest. Statistical analysis was performed using SPSS for Windows, version 16.0. For bioluminescence and fluorescence imaging, mean signal intensity and associated standard deviations (SD) were reported. Unpaired or paired t-tests were used for testing differences of fluorescence intensity between tongue tissue with and without tumor. To calculate linear correlations, the Pearson correlation test was used, and the Spearman correlation test was performed for non-parametrical data. Statistical tests were two-tailed and $p < 0.05$ was considered significant. Generation of graphs was performed using GraphPad Prism software (Version 5.01, La Jolla, CA). For merging of fluorescence images with microscopic images, Cyttron Visualization Platform (Version 1.3, Leiden, The Netherlands) was used.

## Results

In the in vitro cell assay, the increased number of OSC-19-luc cells correlated significantly with an increasing fluorescence signal for both NIR fluorescence agents (Figure 1, a). The correlation coefficient was 0.984 for CW800 EGF ($p=0.01$) and 0.997 for CW800 2-DG ($p=0.01$), indicating the potential use of these agents for further in vivo testing. Very low signals of the non-specific unconjugated IRDye CW800 carboxylate and medium were seen, independent from the increasing number of tumor cells. The specificity of the agents

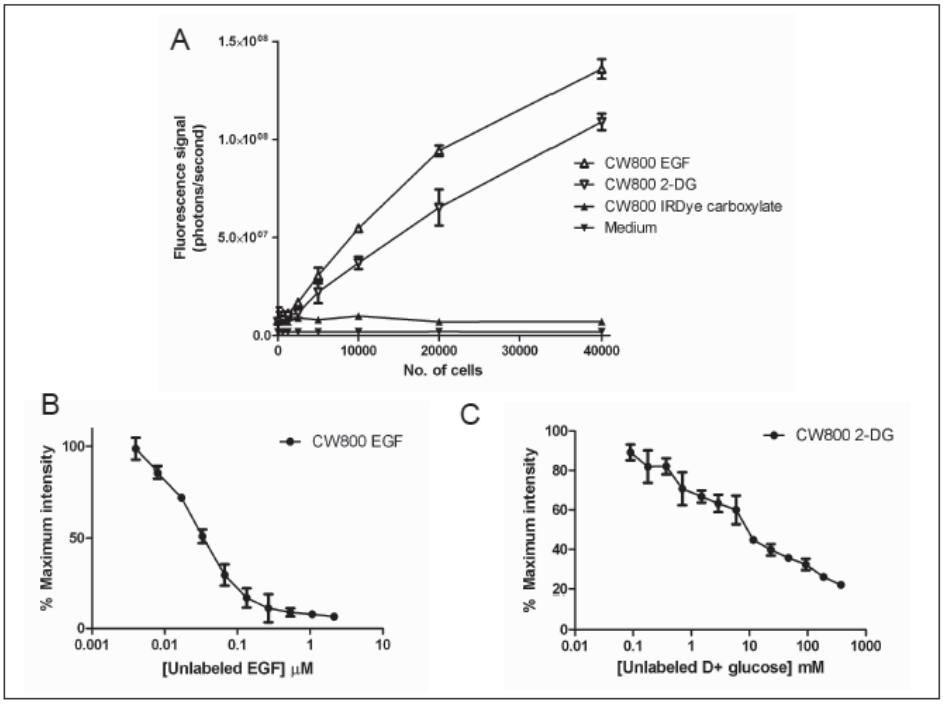


**Fig. 1.** Targeting specificity of CW800 EGF and CW800 2-DG to OSC-19-luc cells *in vitro*. A. Increasing numbers of cells correspond with increasing fluorescence signal of both agents, but not with fluorescence signals of non-specific CW800 IRDye carboxylate and medium. B. Competition experiments of CW800 EGF (70 nM) and increasing concentrations of free unlabeled EGF indicate high specificity. C. Competition experiments of CW800 2-DG (1 μM) and increasing concentrations of free unlabeled D+ glucose indicate high specificity. Data points represent the mean; error bars indicate the standard deviation.

for the EGF and GLUT-1 receptors on the tumor cells was evaluated by competitions with unlabeled EGF (Figure 1, b) and unlabeled D+ glucose (Figure 1, c). Both unlabeled EGF and D+ glucose reduced fluorescence in a concentration dependent manner.

In all 14 mice, tongue tumors had developed within 1 week after the inoculation with OSC-19-luc cells which could be detected as a bioluminescence signal. Four days later, all animals had uni- (n = 4) or bilateral (n = 10) cervical lymph node metastases in the neck, indicated by bioluminescence signals (Figure 2, a). Tumor growth as a function of time (including standard deviation) is illustrated in Figure 2, b.

In the 14 control animals, a low-level background fluorescence signal of both agents was observed in the tongue and cervical lymph nodes after resection of the overlying skin. However, in the animals with OSCC, fluorescence imaging showed clear demarcation of tumor regions in the tongue (Figure 3). Furthermore, although cervical lymph node metastases were not distinguishable by gross examination, fluorescence imaging revealed

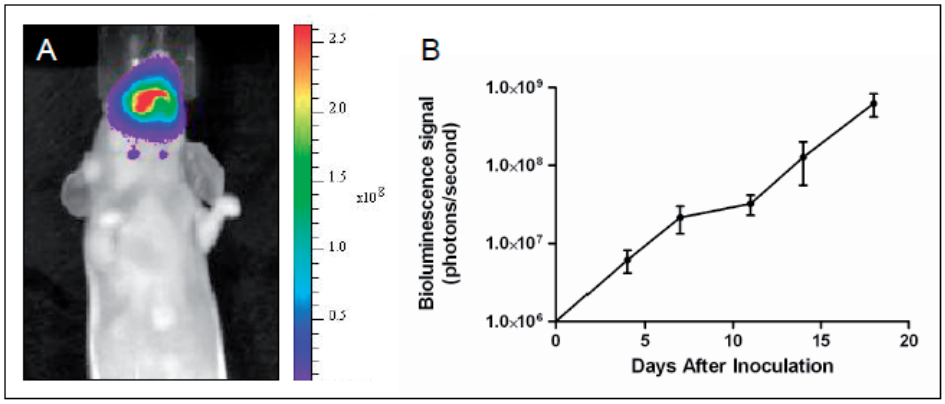


**Fig. 2.** Monitoring OSCC tumor growth. A. Image of a mouse with OSCC tumor at day 14. B. Bioluminescence image of a mouse with OSCC tumor at day 14 illustrating increased signal in tongue and bilateral cervical lymph nodes. C. Increase in bioluminescence signal as a function of time, indicating tumor growth in all animals (n=14). Data points represent the mean; error bars indicate the standard deviation.

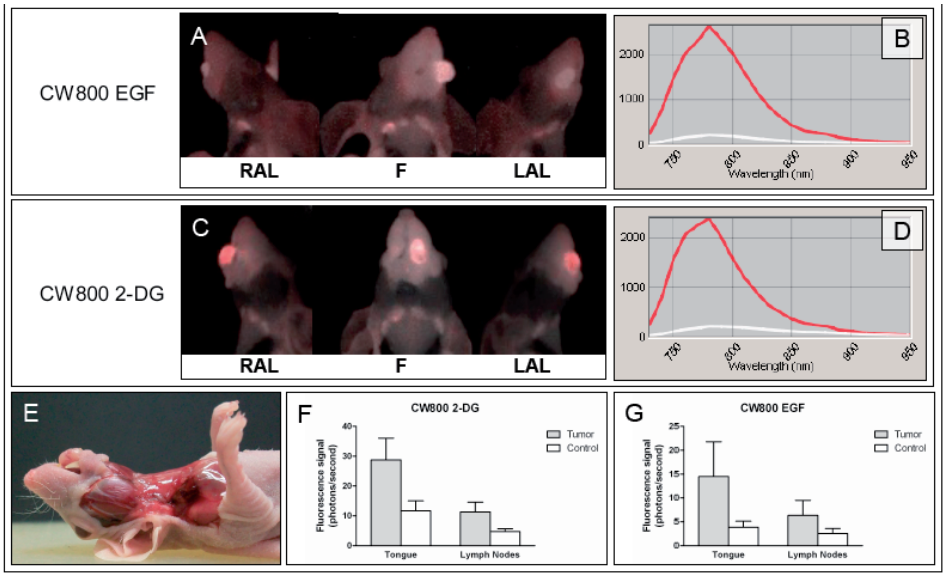


**Fig. 3.** Uptake of NIR fluorescence agents CW800 EGF and CW800 2-DG in animals with OSCC. Pseudocolored fluorescence signal (red) in the tongue and cervical lymph nodes with emission peaks at 785 nm is shown for CW800 EGF (A, B) and CW800 2-DG (C, D). Removed skin in an animal with OSCC and cervical lymph node metastasis is illustrated in E. Mean fluorescence signals of CW800 EGF (F) and CW800 2-DG (G) in the tongue and lymph nodes of mice with tumor and control mice are demonstrated. Error bars indicate the standard deviation. *RAL*; right antero-lateral view, *F*; frontal view, *LAL*; left antero-lateral view.

high signal intensity in cervical lymph node metastases that were also identified by bioluminescence (Figure 3).

When comparing the fluorescence signal in tongue and lymph nodes of tumor and control animals quantitatively, the signal intensity in malignant tissue was significantly higher for both CW800 EGF (tongue: $p = 0.020$, lymph nodes: $p = 0.005$) and CW800 2-DG (tongue: $p = 0.003$, lymph nodes: $p < 0.001$, Figure 3).

A pathologist confirmed the presence of OSCC in the tongue specimens of all 14 mice that had been inoculated with the OSC-19-luc cells. Colocalization of OSCC with fluorescence signal in the histological sections is demonstrated in Figure 4. As expected, lower fluorescence signals were found in the superficial layers of the tongue sections due to expression of EGF receptor and GLUT-1 in the normal squamous cell epithelium.[9, 16] Furthermore, OSCC metastases were found in all cervical lymph nodes that had shown increased bioluminescence signal, which also corresponded with fluorescence signal (Figure 5). On the histological sections, the tumor-to-background ratio of CW800 EGF in the tongue was 13.8 (SD = 6.1) and in the lymph nodes 15.7 (SD = 8.8). For CW800 2-DG, the tumor-to-background ratio in the tongue was 4.6 (SD = 2.1) and in the lymph nodes 33.9 (SD = 18.4, Figure 6). No tumor was found in the negative lymph nodes on hematoxylin-eosin or immunohistochemical staining analysis.



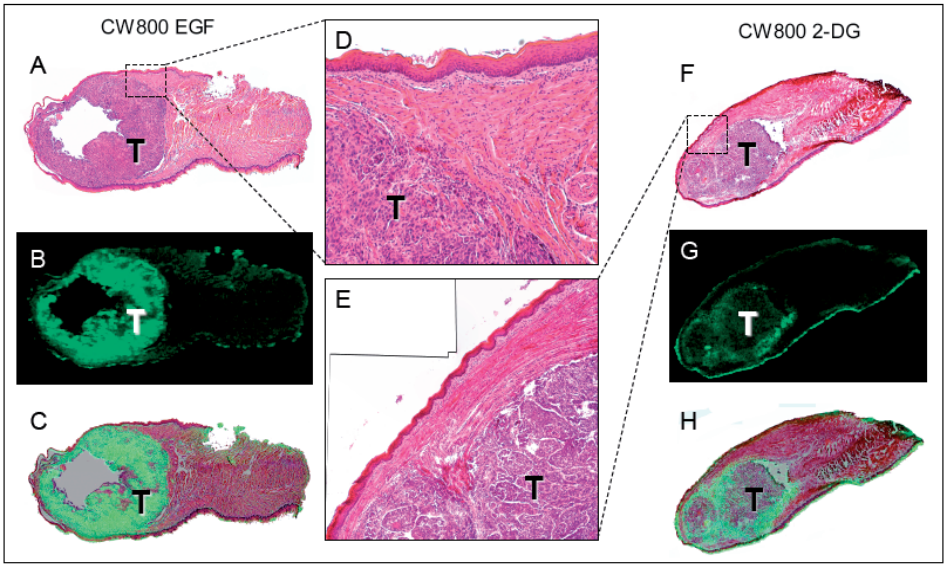


**Fig. 4.** Fluorescence signal (pseudocolored in green) corresponds to histolopathological prescence of OSCC in the tongue. A-C. Paraffin section of tongue with OSCC showing colocalization with CW800 EGF. D. A detail of (A) demonstrating tumor tissue (magnification 10x) F-H. Cryosection of tongue with OSCC showing colocalization with CW800 2-DG. A detail of (F) is shown in E (magnification 10x). *T;* Tumor.

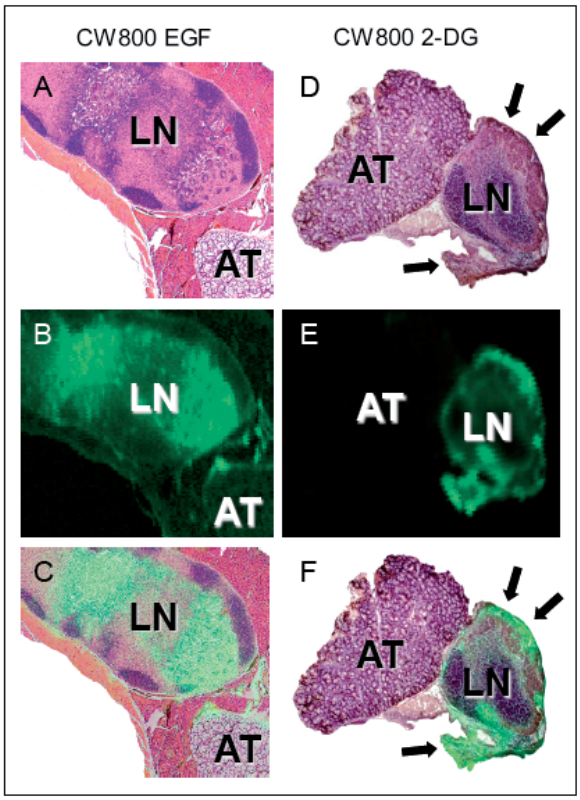


**Fig. 5.** Cervical lymph nodes with OSCC metastasis. A. Paraffin section of an OSCC positive cervical lymph node *(LN)* surrounded by connective tissue and adipose tissue *(AT)*. Pseudocolored (green) fluorescence signal of CW800 EGF (B) and overlay image (C) are shown. D. Cryosection of a cervical lymph node demonstrating immunohistochemical coloring of humane OSCC cells in the border (black arrows). E. Tumor positive areas correspond with pseudocolored (green) fluorescence signal of CW800 2-DG (E, F). All lymph node metastases had been indicated *in vivo* by bioluminescence and fluorescence signal.

## Discussion

Intraoperative detection of OSCC with sufficient sensitivity could lead to more adequate assessment of the tumor margin and consequently better survival and functionality after surgery. This study describes the establishment of OSCC with cervical lymph node metastases in an orthotopic animal model and the subsequent detection of the tumors using NIR fluorescence optical imaging.

Contrary to earlier studies describing detection of head and neck cancer using Cy 5.5 as a fluorophore (emitting at a wavelength of approximately 695 nm),[19-21] we used the IRDye CW800 which has better fluorescence characteristics for image-guided surgery purposes.[6] In vitro, tumor-specificity of both agents was demonstrated. In vivo, co-localization was

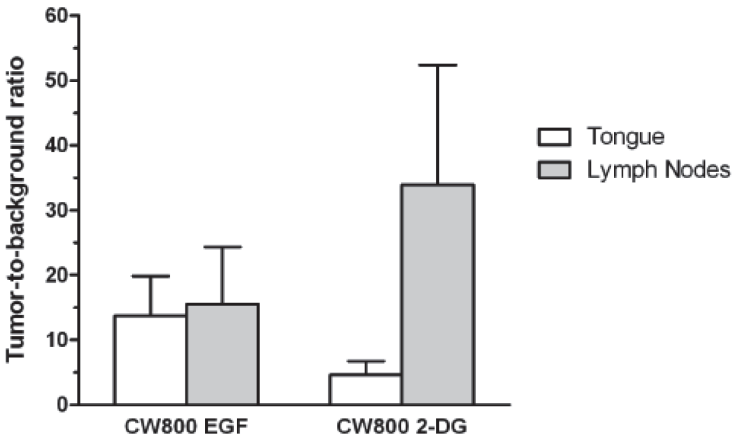


**Fig. 6.** Tumor-to-background ratio of both NIR fluorescence agents in histological sections of tongue and cervical lymph nodes.

found between the fluorescence and bioluminescence signal coming from luciferase-expressing OSCC cells. Further analysis on histological level confirmed the co-localization of fluorescence with histopathology and allowed determination of subsequent tumor-to-background ratios on histological sections (Figures 4-6). In previous experiments, we showed that no intratumoral fluorescence was seen after injection of non-specific polymers conjugated to the IRDye CW800, emphasizing tumor-specificity of the current agents (Supplementary Figure 1).[22]

Furthermore, since the first steps of optical imaging in head and neck cancer were made using fluorescently labeled cetuximab (targeting EGF receptor)[23] or bevacizumab (targeting vascular endothelial growth factor receptor),[24] many other strategies for tumor targeting have been described. Over the last years, this has led to an interesting range of possibilities for optical imaging of head and neck cancer.[8] The current study uses a fluorophore labeled recombinant of human EGF and a fluorescence agent analogous to 18FDG, 2 new targeting agents suitable for optical imaging of head and neck cancer. In the histologic sections, fluorescence signal of both agents was also found at the squamous cell epithelium of the tongue, indicating a positive control for the targeted receptors that are prevalent in normal tongue epithelium.[9, 16]

Sufficient tumor-to-background ratio is the core principle of image-guided cancer surgery. Within 2 mm from the tumor border, we report tumor-to-background ratios of the agents varying between 4.6 and 33.9 depending on the agent and imaged tissue. These results suggest the potential use of these agents for improved resection of tumor margins by optical image-guided surgery.

Furthermore, the use of optical imaging for detection of cervical lymph node metastases seems feasible. Currently, important research is focusing on detection of sentinel lymph

nodes in T1-2 oral cancers using non-tumor-specific radiotracers.[25] However, optical imaging of cervical lymph nodes using tumor-specific agents could eventually prevent the time-consuming step of intraoperative pathological analysis of fresh frozen tissue sections. NIR fluorescence agents could be used for staging of the neck, but because penetration depth is limited, adequate wide-field camera systems are required to reach sufficient sensitivity. Fluorescence microscopes could be used for microlaryngoscopy, but these intraoperative microscopes are not suited for open head and neck cancer surgery because these systems do not provide the wide-field epiluminscence imaging which is required to image the whole tumor and its surroundings. Therefore, various intraoperative camera systems are currently being developed that each have different sensitivity and resolution properties than the Maestro system that was used in this study. These systems include the Photodynamic Eye (PDE; Hamamatsu Photonics, Hamamatsu City, Japan), the SPY Imaging System (Novadaq, Bonita Springs, Florida), the Fluobeam (Fluoptics, Grenoble, France),[18] and the Fluorescence-Assisted Resection and Exploration (FLARE™) which has the extra advantage of merging fluorescence with bright-light images in real-time.[26] Although direct extrapolation of our results could be hindered because the properties of different camera systems may be different from the Maestro, the FLARE system already demonstrated high affinity for the IRDye CW800 in humans.[27]

Both CW800 EGF and CW800 2-DG are agents that could be used for real-time image-guided surgery of oral cancer. However, several limitations of the current study have to be noted. When using agents that target the EGF receptor or glucose metabolism, the sensitivity of tumor detection might be dependent on the metabolic rate of the tumor. Thus, in theory, tumors with lower metabolic rate might prove more difficult to detect by these agents. In addition, further research is required to show if this technique will actually lead to more radical resections in clinical practice. A preliminary study on optical image-guided surgery in a breast cancer animal model has shown promising results.[28] Finally, before clinical studies can be performed, approval by the U.S. Food and Drug Administration to use the agents in patients is required. Critical steps have recently been made by a toxicology study of IRDye CW800 in rats, which reported no evidence of toxicity or adverse effects.[29] Furthermore, no tumor promoting properties of EGF CW800 were shown in a longitudinal animal study of prostate cancer,[30] although no data on OSCC are yet available. Clinical trials are planned in the near future, which is of great importance for the field of surgical oncology.[29]

## Conclusions

NIR fluorescence optical imaging can be used to detect oral cancer and cervical lymph node metastases in an animal model. The fluorescence properties of agents that emit light in the 800 nm region result in significant tumor-to-background ratios, which is essential in intraoperative cancer detection. When these agents are approved for clinical practice, optical imaging has the potential to improve complete surgical resection of oral cancer and cervical lymph node metastases by real-time image-guided surgery.

## Acknowledgements

The authors thank Professor P.C.W. Hogendoorn, Ir, PhD (Department of Pathology, Leiden University Medical Center) for his analysis of the tissue sections; J. Dijkstra, Ir, PhD (Department of Radiology and Image Processing, Leiden University Medical Center) for his contribution to the overlay of histologic images with fluorescence images; and I. Que (Animal Experimentation Laboratory, Leiden University Medical Center) for his assistance in the animal experiments.



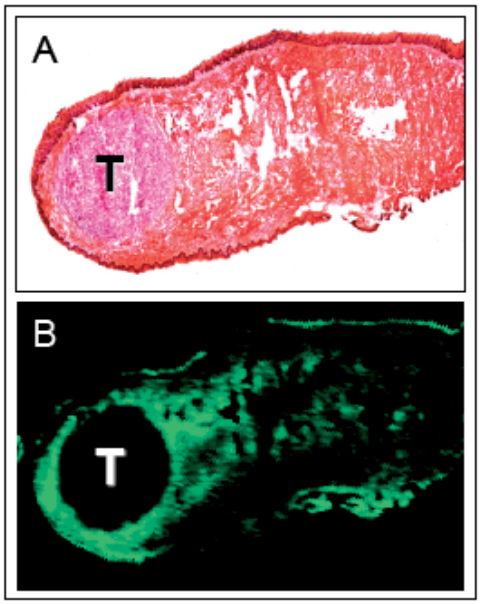


**Supplementary Fig. 1.** Injection of non-specific proteins of similar molecular weight conjugated to the IRDye 800CW shows fluorescence signal around the tumor as a result of enhanced permeability and retention effect. This indicates that the intratumoral fluorescence in figures 4-6 is specific for the tumor rather than just an indication of alterations in hydrostatic pressure or vascular permeability. A. H-E staining of 20 μm section indicating tumor in the tongue. B. Fluorescence image at 800 nm wavelength. T; tumor.

# References


1. McMahon J, O'Brien CJ, Pathak I et al. Influence of condition of surgical margins on local recurrence and disease-specific survival in oral and oropharyngeal cancer. Br J Oral Maxillofac Surg 2003;41(4):224-231.
2. Rusthoven KE, Raben D, Song JI, Kane M, Altoos TA, Chen C. Survival and patterns of relapse in patients with oral tongue cancer. J Oral Maxillofac Surg 2010;68(3):584-589.
3. Frangioni JV. New technologies for human cancer imaging. J Clin Oncol 2008;26(24):4012-4021.
4. Weissleder R, Pittet MJ. Imaging in the era of molecular oncology. Nature 2008;452(7187):580-589.
5. Keereweer S, Kerrebijn JD, van Driel PB et al. Optical Image-guided Surgery-Where Do We Stand? Mol Imaging Biol 2010.
6. Adams KE, Ke S, Kwon S et al. Comparison of visible and near-infrared wavelength-excitable fluorescent dyes for molecular imaging of cancer. J Biomed Opt 2007;12(2):024017.
7. Keereweer S, Mol IM, Vahrmeijer AL et al. Dual wavelength tumor targeting for detection of hypopharyngeal cancer using near-infrared optical imaging in an animal model. Int J Cancer 2012;131(7):1633-1640.
8. Keereweer S, Sterenborg HJ, Kerrebijn JD, van Driel PB, de Jong RJ, Lowik CW. Image-guided surgery in head and neck cancer: Current practice and future directions of optical imaging. Head Neck 2011.
9. Pomerantz RG, Grandis JR. The epidermal growth factor receptor signaling network in head and neck carcinogenesis and implications for targeted therapy. Semin Oncol 2004;31(6):734-743.
10. Kelloff GJ, Hoffman JM, Johnson B et al. Progress and promise of FDG-PET imaging for cancer patient management and oncologic drug development. Clin Cancer Res 2005;11(8):2785-2808.
11. Kovar JL, Volcheck WM, Chen J, Simpson MA. Purification method directly influences effectiveness of an epidermal growth factor-coupled targeting agent for noninvasive tumor detection in mice. Anal Biochem 2007;361(1):47-54.
12. Kovar JL, Volcheck W, Sevick-Muraca E, Simpson MA, Olive DM. Characterization and performance of a near-infrared 2-deoxyglucose optical imaging agent for mouse cancer models. Anal Biochem 2009;384(2):254-262.
13. Sano D, Choi S, Milas ZL et al. The effect of combination anti-endothelial growth factor receptor and anti-vascular endothelial growth factor receptor 2 targeted therapy on lymph node metastasis: a study in an orthotopic nude mouse model of squamous cell carcinoma of the oral tongue. Arch Otolaryngol Head Neck Surg 2009;135(4):411-420.
14. Keereweer S, Mieog JS, Mol IM et al. Detection of oral squamous cell carcinoma and cervical lymph node metastasis using activatable near-infrared fluorescence agents. Arch Otolaryngol Head Neck Surg 2011;137(6):609-615.
15. Kim JB, Urban K, Cochran E et al. Non-invasive detection of a small number of bioluminescent cancer cells in vivo. PLoS One 2010;5(2):e9364.
16. Voldstedlund M, Dabelsteen E. Expression of GLUT1 in stratified squamous epithelia and oral carcinoma from humans and rats. APMIS 1997;105(7):537-545.
17. Kunkel M, Reichert TE, Benz P et al. Overexpression of Glut-1 and increased glucose metabolism in tumors are associated with a poor prognosis in patients with oral squamous cell carcinoma. Cancer 2003;97(4):1015-1024.
18. Sven DM, Vahrmeijer AL, Hutteman M et al. Novel intraoperative near-infrared fluorescence camera system for optical image-guided cancer surgery. Mol Imaging 2010;9(4):223-231.
19. Gleysteen JP, Newman JR, Chhieng D, Frost A, Zinn KR, Rosenthal EL. Fluorescent labeled anti-EGFR antibody for identification of regional and distant metastasis in a preclinical xenograft model. Head Neck 2008;30(6):782-789.
20. Kulbersh BD, Duncan RD, Magnuson JS, Skipper JB, Zinn K, Rosenthal EL. Sensitivity and specificity of fluorescent immunoguided neoplasm detection in head and neck cancer xenografts. Arch Otolaryngol Head Neck Surg 2007;133(5):511-515.
21. Newman JR, Gleysteen JP, Baranano CF et al. Stereomicroscopic fluorescence imaging of head and neck cancer xenografts targeting CD147. Cancer Biol Ther 2008;7(7):1063-1070.
22. Keereweer S, Mol IM, Kerrebijn JD et al. Targeting integrins and enhanced permeability and retention (EPR) effect for optical imaging of oral cancer. J Surg Oncol 2012;105(7):714-718.

23. Rosenthal EL, Kulbersh BD, Duncan RD et al. In vivo detection of head and neck cancer orthotopic xenografts by immunofluorescence. Laryngoscope 2006;116(9):1636-1641.
24. Withrow KP, Newman JR, Skipper JB et al. Assessment of bevacizumab conjugated to Cy5.5 for detection of head and neck cancer xenografts. Technol Cancer Res Treat 2008;7(1):61-66.
25. Civantos FJ, Zitsch RP, Schuller DE et al. Sentinel lymph node biopsy accurately stages the regional lymph nodes for T1-T2 oral squamous cell carcinomas: results of a prospective multi-institutional trial. J Clin Oncol 2010;28(8):1395-1400.
26. Troyan SL, Kianzad V, Gibbs-Strauss SL et al. The FLARE intraoperative near-infrared fluorescence imaging system: a first-in-human clinical trial in breast cancer sentinel lymph node mapping. Ann Surg Oncol 2009;16(10):2943-2952.
27. Tanaka E, Ohnishi S, Laurence RG, Choi HS, Humblet V, Frangioni JV. Real-time intraoperative ureteral guidance using invisible near-infrared fluorescence. J Urol 2007;178(5):2197-2202.
28. Mieog JS, Hutteman M, van der Vorst JR et al. Image-guided tumor resection using real-time near-infrared fluorescence in a syngeneic rat model of primary breast cancer. Breast Cancer Res Treat 2010.
29. Marshall MV, Draney D, Sevick-Muraca EM, Olive DM. Single-Dose Intravenous Toxicity Study of IRDye 800CW in Sprague-Dawley Rats. Mol Imaging Biol 2010.
30. Kovar JL, Johnson MA, Volcheck WM, Chen J, Simpson MA. Hyaluronidase expression induces prostate tumor metastasis in an orthotopic mouse model. Am J Pathol 2006;169(4):1415-1426.

# 5

# Dual-wavelength detection of head and neck cancer simultaneously targeting increased degradation of the extracellular matrix and increased epidermal growth factor receptor expression or increased tumor glucose metabolism

Stijn Keereweer,[1,2] Isabel M. Mol,[2] Alexander L. Vahrmeijer,[3] Pieter B.A.A. Van Driel,[2] Robert J. Baatenburg de Jong,[1] Jeroen D.F. Kerrebijn,[1] Clemens W.G.M. Löwik,[2]

1. Erasmus Medical Center, Department of Otorhinolaryngology Head and Neck Surgery, Rotterdam, The Netherlands.
2. Leiden University Medical Center, Molecular Endocrinology and Molecular Imaging, Leiden, The Netherlands.
3. Leiden University Medical Center, Department of Surgery, Leiden, The Netherlands.


Published as: "Dual Wavelength Tumor Targeting for Detection of Hypopharyngeal Cancer Using Near-Infrared Optical Imaging in an Animal Model," in the **International Journal of Cancer, October 2012**, 131, 1633-1640 (2012)

## Abstract

Optical imaging is a promising technique to visualize cancer tissue during surgery. In this study, we explored the use of combinations of near-infrared fluorescence agents that emit fluorescence signal at different wavelengths and each target specific tumor characteristics. Two combinations of agents (ProSense680 combined with 2DG CW800 and MMPSense680 combined with EGF CW800) were used to detect hypopharyngeal cancer in an animal model. ProSense680 and MMPSense680 detect increased activity of cathepsins and matrix metalloproteinases, respectively. These enzymes are mainly found in the invasive tumor border due to degradation of the extracellular matrix. 2DG CW800 detects tumor cells with high glucose metabolism and EGF CW800 is internalized by the epidermal growth factor receptor of tumor cells. Whole-body imaging revealed clear demarcation of tumor tissue using all 4 agents. The tumor-to-background ratio (standard deviation, p-value) was 3.69 (0.72, $p<0.001$) for ProSense680; 4.26 (1.33, $p<0.001$) for MMPSense680; 5.81 (3.59, $p=0.02$) for 2DG CW800; and 4.84 (1.56, $p<0.001$) for EGF CW800. Fluorescence signal corresponded with histopathology and immunohistochemistry, demonstrating signal of ProSense680 and MMPSense680 in the invasive tumor border, and signal of 2DG CW800 and EGF CW800 in the tumor tissue. In conclusion, we demonstrated the feasibility of dual wavelength tumor detection using different targeting strategies simultaneously in an animal model. Combined targeting at different wavelengths allowed simultaneous imaging of different tumor characteristics. Near-infrared fluorescence optical imaging has the potential to be translated into the clinic in order to improve the complete removal of tumors by real-time image-guided surgery.

Abbreviations used: BLI, bioluminescence imaging; EGF, epidermal growth factor; EPR, enhanced permeability and retention; FLI, fluorescence imaging; H-E, hematoxylin-eosin; NIR, near-infrared; PET, positron emission tomography; PBS, phosphate buffered saline; TBR, tumor-to-background ratio.

## Introduction

In oncologic surgery, involvement of the surgical margins is a critical prognostic factor for survival. In current clinical practice, surgeons rely on palpation and visual inspection to discriminate between tumor and normal tissue and consequently determine an adequate tumor-free margin. However, incomplete tumor resections and surgical morbidity as a result of damage to vital structures are not uncommon. Better postoperative results (e.g., survival, functionality) could be achieved by imaging techniques that help the surgeon discriminate between healthy and diseased tissues (e.g., cancer) and identify vital structures during surgery. Near-infrared (NIR) fluorescence imaging is a promising technique that can be used to visualize cancer tissue during surgery.[1]



In NIR fluorescence imaging, fluorophores are used that emit signal between 650–900 nm, a range in which absorption coefficients of tissues are relatively low, and non-specific intrinsic fluorescence is minimized. Due to the reduced background signal in this spectrum, sensitivity and depth of penetration are increased, which is directly reflected in improved image quality.[1] By the use of new NIR fluorescence agents and special camera systems, direct tumor imaging can be incorporated into the operation field, allowing for real-time image-guided surgery.

In order to detect the tumor during surgery, a wide range of NIR fluorescence agents has been described that each have their specific targeting strategy.[2] Tumor detection can be improved by targeting multiple tumor-specific characteristics simultaneously with fluorophores that emit light at different wavelengths.[2] Dual-wavelength imaging has been used to correct for biodistribution parameters in vivo by separating true molecular target signals from biodistribution[3] and to improve tumor observation accuracy by simultaneous imaging of more than one target.[4] In the 700 nm region, ProSense680 and MMPSense680 (PerkinElmer, Waltham, MA) are NIR fluorescence agents that detect increased activity of cathepsins and matrix metalloproteinases (MMPs), respectively. These enzymes are mainly found in the invasive tumor border due to degradation of the extracellular matrix (ECM) directly surrounding the tumor. NIR fluorescence agents that emit at 800 nm are 2DG CW800 (LI-COR Biosciences, Lincoln, NE), which detects tumor cells through uptake by the glucose transporter, and EGF CW800 (LI-COR Biosciences), which is internalized by the epidermal growth factor (EGF) receptor of tumor cells. The combined use of agents that each have their specific targeting strategy and specific wavelength will result in different localizations of signals during imaging. This provides the surgeon with a complete view of the tumor and its invasive border, allowing better determination of the tumor margin and the extent to which the invasive tumor front should be resected. In this study, dual wavelength targeting by NIR fluorescence technologies for *in vivo* cancer imaging is explored. We describe the use of two combinations of NIR fluorescence agents that each target specific tumor characteristics at different wavelengths for detection of hypopharyngeal cancer in an animal model.

## Materials and Methods

### *Cell line and generation of luciferase-2-expressing FaDu cells*

The human hypopharyngeal squamous cell carcinoma line FaDu was obtained from the American Type Culture Collection (Manassas, VA), which was grown in Minimum Essential Medium (Gibco, Invitrogen) supplemented with 10% fetal bovine serum, 2mM Glutamax I (Gibco, Invitrogen), 50 units/ml of penicillin and 50 μg/ml streptomycin.

In order to image tumor cells in nude mice by bioluminescence imaging (BLI), FaDu cells were transfected with a luciferase-expressing vector (pCAGGS- Luc-2), using FuGene HD (Roche, Woerden, The Netherlands). Transfected cells were selected with 800 ug/mL G418 (Gibco, Invitrogen), and individual clones were analyzed for luciferase expression by plating in a 24-well plate, adding luciferin (50ug/ml) and measuring BLI in the IVIS Spectrum imaging system (Caliper LifeSciences, Hopkinton, MA). The selected FaDu-luc2 clone was the one that expressed the highest level of active luciferase.

### *Imaging agents*

Two combinations of NIR fluorescence agents (out of four possible combinations) were used in this study, based on their target localization. Each combination included an agent that provides an intratumoral signal combined with an agent that detects the invasive tumor front at a different wavelength. The first combination was ProSense680 (PerkinElmer) and 2DG CW800 (LI-COR Biosciences). ProSense680 (excitation: 680 nm, emission: 700 nm) is conjugated to the fluorochrome VivoTag®-S680 (PerkinElmer) in a quenched, non-fluorescent state. After cleavage by proteolytic activity of lysosomal cysteine or serine proteases such as cathepsin B, the agent becomes "activated" and fluorescent. 2DG CW800 (excitation: 774 nm, emission: 789 nm) has been described to detect increased glucose uptake, analogous to 2-deoxy-2-[18F] fluoro-D-glucose (18FDG) detection in positron emission tomography (PET) technology. Although the exact mechanism is yet unknown, it has been shown that uptake of the agent can be effectively blocked with either unlabeled 2DG or glucose, and confocal microscopy demonstrated that the agent is taken up by the cell and localized in the cytoplasm, indicating involvement of the GLUT transporter system.[5]

The second combination of agents was MMPSense680 (PerkinElmer) and EGF CW800 (LI-COR Biosciences). MMPSense680 is conjugated to the same fluorochrome as ProSense680 and therefore has the same fluorescence characteristics. This agent is also injected in a quenched, non-fluorescent state and becomes "activated" after cleavage by MMPs. EGF CW800 (excitation: 774 nm, emission: 789 nm) is a recombinant of human EGF labeled to a fluorophore. In vivo testing and specificity of the conjugate for the EGF receptor has previously been evaluated by competition with a monoclonal antibody.[6]

### *Optical Imaging Techniques*

Non-invasive BLI was performed by anesthetizing the animals with 2% isoflurane before and during imaging. An aqueous solution of luciferin (Caliper LifeSciences) at 150 mg/kg in a volume of 50 μL was injected intraperitoneally 5 minutes prior to imaging, after which

the animals were imaged using the IVIS Spectrum imaging system (Caliper LifeSciences). Quantification of the BLI signal was performed through standardized regions of interest using Living Image software (version 3.2, Caliper LifeSciences).

Fluorescence imaging (FLI) of the mouse was performed using the Pearl Impulse imaging system (LI-COR Biosciences), fitted with lasers that scan in the 700 nm and 800 nm channel with standard acquisition time. Microscopic images were acquired using the confocal laser scanning microscope (Carl Zeiss LSM 510, Germany).

### *Cell assays*



Before *in vivo* tests were performed, the sensitivity of *in vitro* detection of FaDu-luc2 cells was assessed by cell assays using ProSense680, MMPSense680, 2DG CW800 and EGF CW800. An increasing amount of cells (range: 0 – 40,000) was seeded in four 96-wells plates. A control was included using medium without a NIR fluorescence agent (i.e., autofluorescence). Different protocols were used for each agent. After 7 hours, ProSense680 (45 nM) was added in 100 µL per well in the first plate, which incubated on the cells during 24 hours. In addition, the cells were washed three times with phosphate buffered saline (PBS) to discard excess non-bound agent according to previous studies.[7] Finally, the wells were imaged using the Odyssey scanner (LI-COR Biosciences; focus offset 3 mm, intensity 10, 700 nm channel). The same protocol was used for the assay of MMPSense680.

In order to test the sensitivity of 2DG CW800 and EGF CW800, the protocol was adjusted according to previous experiments.[5] The cells were starved for 2 hours in serum-free low-glucose Minimum Essential Medium (Gibco, Invitrogen) and incubation with 2DG CW800 (5 µM in 100 µL) was performed at 37°C during an additional 2 hours. In another plate, the cells were starved for 2 hours in serum-free media. Starvation media were replaced with media containing EGF CW800 (50 nM in 100 µL), and incubated at room temperature (25°C) for 15 minutes. Both assays were stopped by fixation with 4% formaldehyde solution for 20 minutes and washed four times with PBS to get rid of excess non-bound agent. Next, the wells were imaged using the 800 nm channel of the Odyssey scanner (focus offset 3 mm, intensity 8).

### *Animal experiments*

Experiments were performed in BALB/c nu/nu female mice, aged 4 to 6 weeks, obtained from Charles River Laboratories, L'Arbresle, France. They were cared for according to our institution's animal facility standards and the Animal Welfare Committee of the Leiden University Medical Center approved the protocol. Conduction of the experiments and euthanasia of the animals were performed according to these guidelines. Autoclaved pellet food and sterilized water were provided *ad libitum*. The weight of the animals was followed during the experiment to monitor their general health state. Throughout tumor inoculation and imaging procedures, the animals were anesthetized with 4% isoflurane for induction and 2% isoflurane for maintenance in oxygen with a flow of 0.8 L/min and placed on an animal bed with an integrated nose mask.

In order to induce a hypopharyngeal squamous cell carcinoma model, 2 x $10^5$ FaDu-luc2 cells, diluted in 20 µL PBS, were inoculated subcutaneously at two spots at the back of 20 BALB/c nu/nu mice. Cranial injection sites at the back were chosen to prevent interference from non-specific FLI signal due to uptake of agents in the liver and kidneys. Tumor growth was followed two times a week by BLI and visual inspection.

At day 20-24, tumors had reached a mean BLI signal intensity of 5.6 x $10^8$ and mice were randomly allocated to administration of one of the two combinations of NIR fluorescence agents: ProSense680 and 2DG CW800 or MMPSense680 and EGF CW800. The agents were injected intravenously (1.33 nmol for EGF CW800, ProSense680 and MMPSense680 and 10 nmol for 2DG CW800, 100 µL per animal) into one of the tail veins. FLI was performed 24 hours after injection, based on the blood pharmacokinetics of the agents (PerkinElmer, LI-COR Biosciences), followed by injection of luciferin and subsequent BLI. Then, the maximum diameter of the tumor was measured manually using a calliper. Finally, the animals were injected with luciferin for the second time, sacrificed, and the tumors and lungs were surgically removed for histological analysis. Within 5 minutes after the second injection of luciferin, separate BLI of the lungs was performed to screen for pulmonary metastases.

After surgical removal of the tumors, the tissues were cut in two and each half was either fresh frozen on dry ice or fixed in 3.7% formalin overnight and paraffin embedded, then cut into slices (20 µm) and imaged using the Odyssey scanner. After imaging, tissue sections were air-dried and stained with immunohistochemistry or standard hematoxylin-eosin (H-E).

Immunohistochemical staining was done on 4-µm thick paraffin tissue sections. Rabbit polyclonal antibodies (Abcam, Cambridge, MA) were used against cathepsin B (ab33538, diluted at 1:40), the glucose transporter (GLUT-1, ab15309, diluted at 1:200), and the EGF receptor (ab2430, diluted at 1:50). The slides were then washed with PBS and detected with biotinylated polyclonal goat anti-rabbit immunoglobulins (E0432, diluted at 1:600, Dako, Heverlee, Belgium). For staining of MMPs, MMP-9 antibody was used (sc-6840, diluted at 1:100, Santa Cruz Biotechnology, Inc, Heidelberg, Germany) which was detected with biotinylated polyclonal rabbit anti-goat immunoglobulins (E0466, diluted at 1:400, Dako). All slides were counterstained with hematoxylin.

### *Data analysis*

Fluorescence signal was measured using standard regions of interest and data processing was performed using Pearl Impulse Software (Version 2.0.16, LI-COR Biosciences). Mean signal intensity and associated standard deviations (SD) were reported.

For statistical analysis, SPSS for Windows, version 16.0 was used. Unpaired or paired t-tests were performed for testing differences of fluorescence intensity between tissue with and without tumor. To calculate linear correlations, the Pearson correlation test was used, and the Spearman correlation test was performed for non-parametrical data. $R^2$ was determined for linear regression. Statistical tests were two-tailed and $p < 0.05$

was considered significant. Generation of graphs was performed using GraphPad Prism software (Version 5.01, La Jolla, CA).

## Results

### *Cell assays*

The number of FaDu-luc2 cells significantly correlated with fluorescence intensity for ProSense680, 2DG CW800, and EGF CW800 (correlation coefficients: 0.968, 0.997, and 0.984, respectively, $p < 0.01$ for all tests), as illustrated in Fig. 1. This suggests that these agents are taken up by FaDu-luc2 cells, indicating their potential use for *in vivo* testing. No correlation between an increasing number of cells and MMPSense680 was found in cell culture.



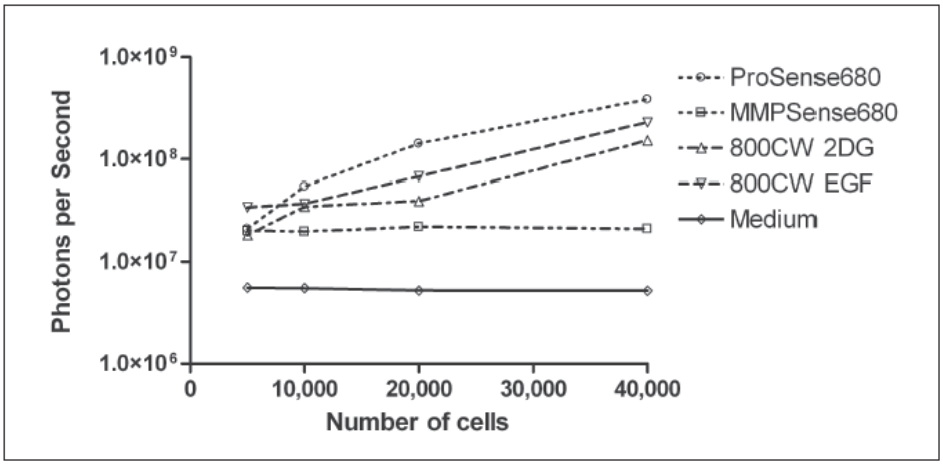


**Fig. 1.** Sensitivity of various NIR fluorescence agents for FaDu-luc2 cells *in vitro*. Increased signal intensity corresponding to increased number of FaDu-luc2 cells is shown for ProSense680, 2DG CW800, and EGF CW800. No signal increase is seen when medium of MMPSense680 was added to the cells.

### *Animal experiments*

Subcutaneous tumors were established 4 days after inoculation of the FaDu-luc2 cells in all mice, leading to a total of 40 tumors in 20 mice. The increase in BLI signal as a function of time showed a correlation coefficient of 0.905 ($p < 0.01$, Supplementary Data). After FLI measurements at day 20 or 24, the mean tumor diameter was 4.5 mm (SD=2.3). The correlation of tumor diameter with BLI signal was statistically significant ($R^2$=0.7292, $p<0.001$, Supplementary Data). No BLI signal was found in the resected lungs, indicating that no pulmonary metastasis of the primary tumors had occurred.

Using FLI, high signal intensities of all 4 NIR fluorescence agents were found in the tumor, while a low-level background signal was observed in the surrounding healthy tissue, indicating a clear demarcation of tumor regions (Fig. 2). Both ProSense680 and MMPSense680 were mainly located in a ring-like region around the tumor where the

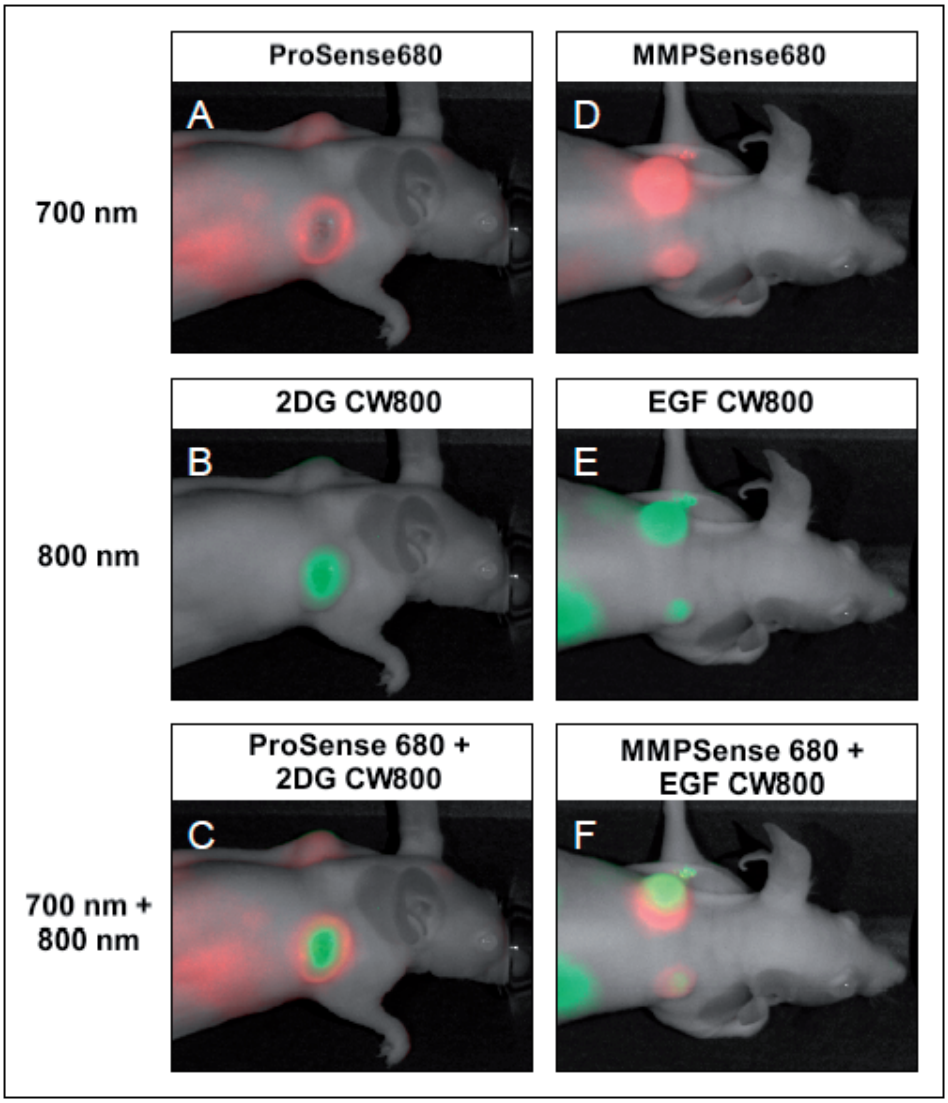


**Fig. 2.** Multi-targeted tumor detection. Detection of xenograft hypopharyngeal squamous cell cancer injected in two sites at the back of nude mice. Signal of agents that are imaged in the 700 nm channel *(red, pseudo colored)* is shown in A (ProSense680) and D (MMPSense680). Signals imaged in the 800 nm channel *(green, pseudo colored)* are shown in B (2DG CW800) and E (EGF CW800). Overlay images of both combinations of probes are demonstrated in C and F.

targeted enzymes are found (Fig. 2A and 2D), whereas 2DG CW800 and EGF CW800 were predominantly found at the core of the tumor (Fig. 2B and 2E). Merged images of both agents are shown in Fig. 2C and 2F, demonstrating the different localizations of the agents.

By comparing the quantitative FLI signal in the tumor region and in healthy surrounding tissue (except from the liver and kidney areas due to clearance of the agents), the tumor-to-background ratio (TBR) of each agent was calculated. The mean TBRs (standard deviation, p-value) were: ProSense680; 3.69 (0.72, $p<0.001$), MMPSense680; 4.26 (1.33, $p<0.001$), 2DG CW800; 5.81 (3.59, $p=0.02$) and EGF CW800; 4.84 (1.56, $p<0.001$, Fig. 3). TBRs of fluorescence agents with emission peaks at 800 nm were significantly higher than of agents with emission peaks at 700 nm ($p=0.02$).



The presence of hypopharyngeal squamous cell cancer was found in all 40 tumor specimens by histological analysis of the tissues by a pathologist. Analysis of the fluorescence signal in the tissue sections demonstrated high signal at 700 nm of ProSense680 in the tumor border (Fig. 4A), which is the region of the tumor where cathepsin activity is increased to facilitate degradation of the extracellular matrix (ECM). Immunohistochemical analysis illustrated co-localization of ProSense680 with cathepsin staining (Fig. 4D and 4G). In the 800 nm spectrum, 2DG CW800 was found in the tumor tissue (Fig. 4B), corresponding with localization of GLUT-1 staining (Fig 4E and 4H). Difference in localization between these agents is illustrated by dual wavelength imaging (Fig. 4C). H-E staining demonstrates presence of hypopharyngeal tumor in these sections in 4F and 4I.

Furthermore, histology showed that MMPSense680 signal at 700 nm was found in the direct surrounding tissue of the tumor, within a margin of 1-2 mm (Fig. 5A). The MMPs, which are involved in degradation of the ECM, were stained with immunohistochemistry in this same invasive tumor border (Fig. 5D and 5G). Both fluorescence signal of EGF CW800 and staining of the EGF receptor were found in the tumor tissue (Fig. 5B, 5E and 5H). Merged images of both wavelengths (Fig. 5C) and corresponding H-E images (Fig. 5F and

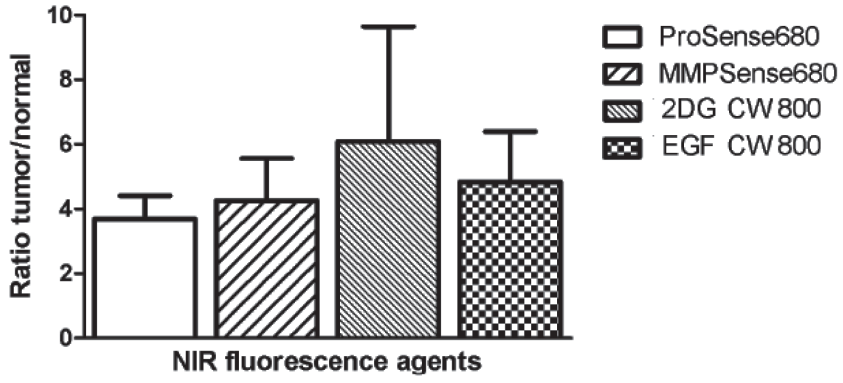


**Fig. 3.** Tumor-to-background ratio of each individual NIR fluorescence agent. Mean value and standard deviations are shown. *NIR: near-infrared.*

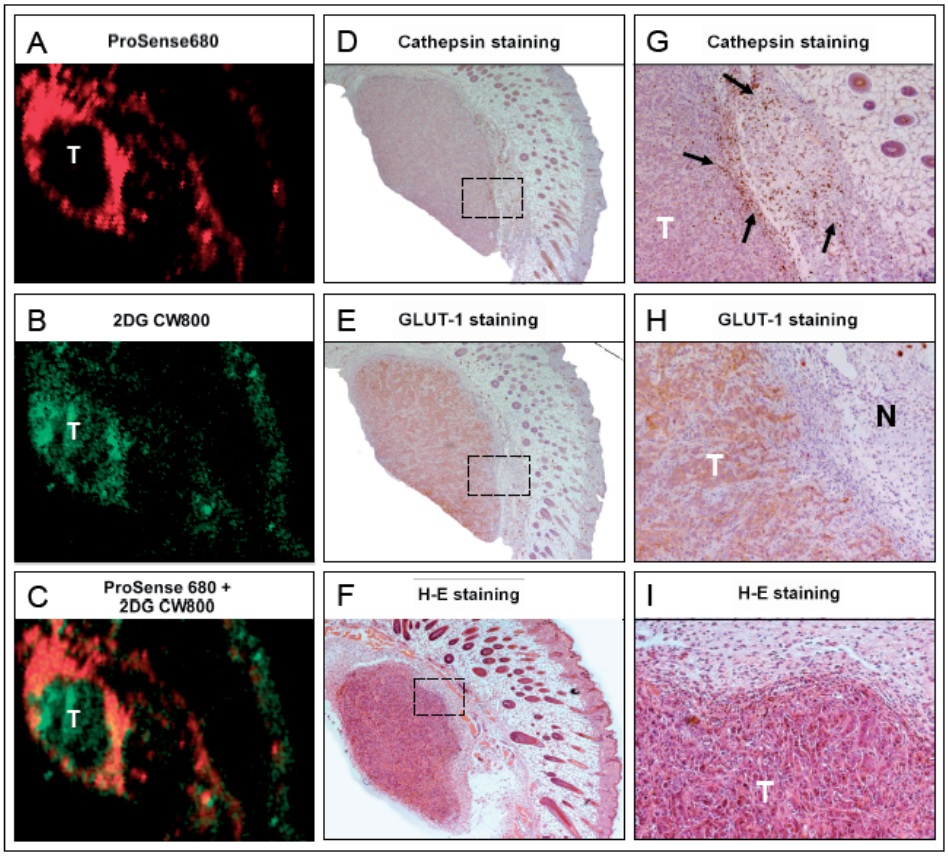


**Fig. 4.** Histological analysis showing co-localization of fluorescence signals of ProSense680 and 2DG CW800 with immunohistochemistry. A. ProSense680 is found in the invasive border (black arrows) of the tumor where cathepsins are stained (D, G) B. Fluorescence signal of 2DG CW800 is found in the primary tumor (T) corresponding with GLUT-1 staining (E, H). C. Different localizations of both agents are illustrated by dual wavelength imaging. Hypopharyngeal tumor is identified by H-E staining (F). Details of D, E, and F (indicated by the dashed squares) are shown in G, H, and I, respectively.

5I) are shown. To a lesser extent, fluorescence signals and immunohistochemical staining of both MMP-activity and EGF receptors were found in the normal epithelium of the skin, where these targets are normally situated (Fig. 5).

## Discussion

Surgical treatment of advanced hypopharyngeal cancer is associated with poor survival rates and significant morbidity, even when combined with postoperative radiotherapy.[8] Chemoradiation is an alternative treatment option for advanced hypopharyngeal cancer, but is also associated with significant morbidity and reduced quality of life.[9] Intraoperative techniques that can accurately determine microscopical tumor margins during surgery

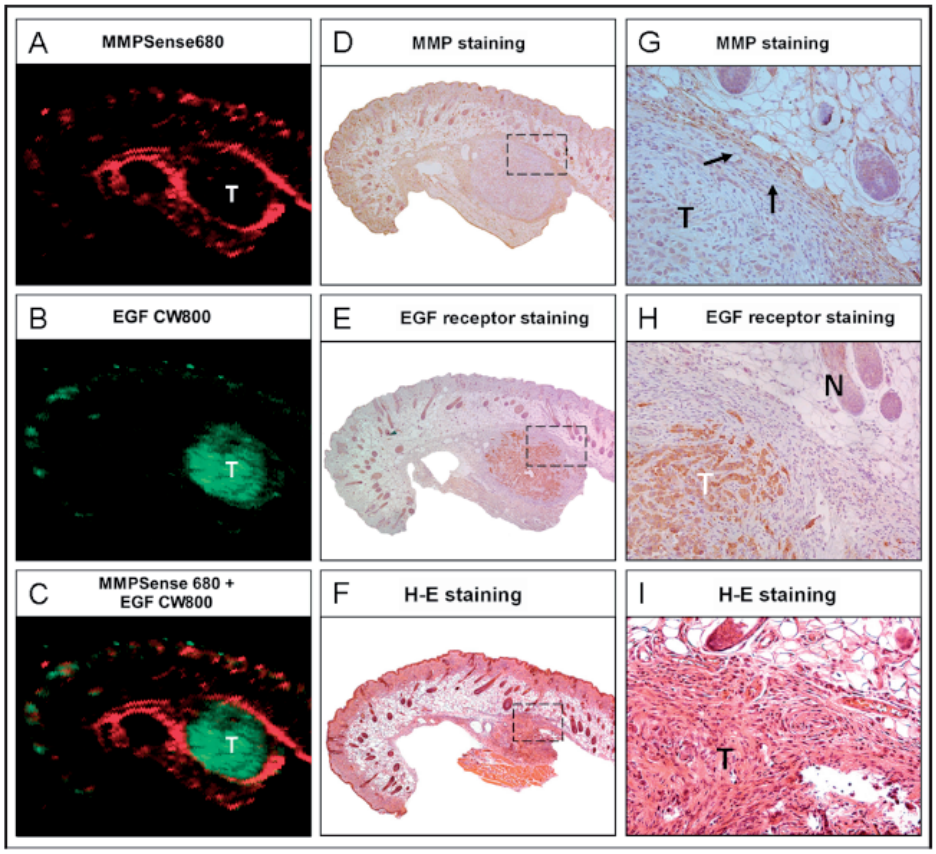


**Fig. 5.** Histological analysis showing co-localization of fluorescence signals of MMPSense680 and EGF CW800 with immunohistochemistry. A. MMPSense680 is found in the invasive tumor border (black arrows) where MMPs are stained (D, G). B. Fluorescence signal of EGF CW800 is found in the primary tumor (T) corresponding with staining of the EGF receptor (E, H). C. Different localizations of both agents are illustrated by dual wavelength imaging. Hypopharyngeal tumor is identified by H-E staining (F). Details of D, E, and F (indicated by the dashed squares) are shown in G, H, and I, respectively.

are likely to improve disease specific survival and reduce unnecessary loss of functionality after surgery.

Each agent that was used in this study had its specific targeting strategy, resulting in different localizations of signal during imaging. A combination of different fluorescence agents targeting several tumor characteristics is necessary to provide the surgeon with a complete view of the tumor and its invasive border. On FLI and histological analysis, ProSense680 and MMPSense680 were mainly found in the invasive tumor borders (Fig. 4 and 5). These agents become fluorescent by proteolytic activity of cathepsins (mostly cathepsin B) and MMPs respectively, which are both involved in tumor invasion by degradation of the ECM surrounding the tumor.[10, 11] Cathepsin B is mostly upregulated

in lysosomes of tumor cells that are located at the invasive tumor border. However, in epithelial cancers, most of the upregulated MMPs are expressed by the host stromal cells, especially in areas of active invasion.[12, 13] Microscopical analysis of the stroma surrounding the tumor illustrated the abundance of (myo-) fibroblasts (Fig. 4 and 5), which are well-known drivers for invasive cancer growth.[14] Furthermore, it has been previously shown that FaDu cells themselves express no MMPs.[15] This probably explains why, contrary to all other agents, no correlation was found between FLI signal intensity of MMPSense680 and increased amounts FaDu-luc2 cells *in vitro*, for the fibroblast are absent in cell cultures.

Targeting the EGF receptor by EGF CW800 resulted in specific imaging of the tumor *in vivo*. In head and neck cancer, 80-90% of the tumors are EGF receptor positive, which underlines its importance as a target for detection.[16, 17] Apart from the relevance for delineation of tumors in case of head and neck cancer, the potential use of these agents is much wider. The use of ProSense680 has also been portrayed in breast and colon cancers, emphasizing the widespread detection capacity of these agents.[18] Furthermore, the EGF receptor is upregulated in approximately one third of all epithelial cancers.[19] Moreover, increased glucose uptake is in part a result of increased tumor metabolism, one of the hallmarks of cancer,[2] a feature that is exploited by 2DG CW800.[5] The widespread potential of this targeting strategy is emphasized by 18FDG PET technology, which is already widely used in clinical practice for detection of many different cancers.[20] Next to the strategies that are used in this study, other targets have been proposed to detect head and neck cancer by NIR fluorescence optical imaging.[21] These mainly focus on detection of tumor vasculature by NIR fluorescence dyes labeled to agents that target αvβ3 integrins, vascular endothelial growth factor, or cyclic arginine-glycineaspartate. The current study shows the feasibility of dual wavelength targeting of hypopharyngeal cancer by NIR fluorescence imaging *in vivo*. A sufficient TBR is essential for real-time image-guided cancer surgery. The essence is to help the surgeon distinguish malignancy from normal tissue, which can be provided by sufficient contrast of the FLI signal compared to the healthy surroundings. In our experience, TBR > 2 is sufficient to critically distinguish the fluorescence signal from the background during surgery. In this study, TBRs ranged from 3.69 to 5.81 (Fig. 3), depending on the used NIR fluorescence agent, indicating the feasibility for image-guided surgery. Furthermore, significantly higher TBRs were found in the 800 nm spectrum compared to the 700 nm. This difference could be explained by different specificity of the imaged agents. However, intrinsic tissue fluorescence is lower at 800 nm as a result of lower absorption of hemoglobin, which may also contribute to higher TBRs.[2] In conclusion, we demonstrate that multiple tumor-specific targets can be visualized simultaneously with sufficient TBRs, which could improve the sensitivity of tumor detection using NIR optical imaging, especially in heterogeneous tumors.

Next to NIR fluorescence agents, parallel development of dedicated, manageable, intraoperative camera systems is required for optimal image-guided surgery. At this moment, various intraoperative optical imaging camera systems have been developed, including the Fluorescence-assisted Resection and Exploration (FLARE™, Frangioni laboratory, Boston,

MA), the Photodynamic Eye (PDE; Hamamatsu Photonics, Hamamatsu, Japan), the Fluobeam® (Fluoptics, Grenoble, France), the Spy imaging system (Novadaq, Canada) and a system build by the group of Ntziachristos. A new camera system is being developed which allows real-time multispectral imaging (Artemis; O2view, Marken, The Netherlands).

However, several limitations of the current study have to be noted. NIR fluorescent agents were used that target the expansive characteristics or increased metabolism of the tumor. In patients, this might result in interpersonal variability of sensitivity of tumor detection caused by differences in invasiveness and metabolic rate of the individual tumor. Consequently, tumors with lower invasive or metabolic rate might, in theory, prove more difficult to be detected by these agents. The possible influence of these intertumoral and interpersonal differences on fluorescence intensity should be taken into account when these agents are introduced into the clinic. Consequently, these differences make multiple wavelength imaging of tumors using different probes favorable over imaging using a single probe. Furthermore, contribution of the enhanced permeability and retention effect remains subject to debate. Tumor specificity could be a result of macromolecules larger than 40 kDa that selectively leak out from tumor vessels and accumulate in tumor tissues.[22] Finally, specificity of the targeting mechanism of 2DG has been reviewed extensively. As mentioned previously, the exact uptake mechanism of this conjugated remains unknown. Specificity for the GLUT transporter system could not be shown for a 2DG-Cy5.5 conjugate.[23] Therefore, competition experiments with the 2DG-CW800 dye using increasing concentrations of free unlabeled D+ glucose were performed in a previous study, demonstrating high specificity of the agent.[24] Taken together, we believe that 2-DG CW800 can be used as a tumor-specific imaging agent for near-infrared fluorescent imaging but that tumor specificity should be interpreted with caution as long as the exact uptake mechanism remains obscure. However, the ability to distinguish tumor tissue from healthy surrounding tissue is of primary importance for image-guided surgery, independent of the targeting mechanism.

For clinical applicability, detection thresholds of fluorescence agents contain essential information for assessment of complete surgical resection of tumors. Optical imaging provides sufficient contrast to visualize tumor margins and detect tumor deposits 3-5 mm deep.[25] However, further studies are required to determine the minimal detectable amount of tumor cells. Moreover, the combination with other therapeutic modalities has to be taken in account. In head and neck cancer, various therapeutic modalities are available for advanced (i.e. stage III-IV) tumors. In most cases, there is a choice between primary chemoradiation and primary surgery. In case of tumor recurrence or residual disease after chemoradiotherapy, salvage surgery is the only therapeutic option. The applicability of optical imaging in these specific cases is an interesting question for future research.

Finally, approval by the Food and Drug Administration to use the agents in patients is yet to be obtained. Although important steps have been made in a recent toxicology study of IRDye CW800 in rats that reports the absence of toxic or adverse effects,[26] the approval for combined use of different fluorescent agents might take longer. Clinical trials that will be planned in the near future will be imperative for the field of surgical oncology. Once

these agents are approved for clinical practice, optical imaging has the potential to improve complete surgical resection of tumor tissue by real-time image-guided surgery.

## Conclusions

In conclusion, we demonstrated the feasibility of combined tumor detection using different targeting strategies simultaneously in an animal model. Dual wavelength targeting allowed for simultaneous imaging of different tumor characteristics. In combination with the current rapid development of adequate camera systems, near-infrared fluorescence optical imaging has the potential to be translated into the clinic in order to improve the complete removal of a wide range of tumors by real-time image-guided surgery.

## Acknowledgements

Professor P.C.W. Hogendoorn, Ir, PhD, (Department of Pathology, Leiden University Medical Center) is gratefully acknowledged for his analysis of the tissue sections. We thank I. Que (Animal Experimentation Laboratory, Leiden University Medical Center) for his assistance in the animal experiments. R.H. Thoene and A. Van Wingerden are thankfully acknowledged for caring of the Animals. We thank I.H. Briaire - De Bruyn, Ir, for her assistance in laboratory analysis.

## References

1. Frangioni JV. New technologies for human cancer imaging. J Clin Oncol 2008;26:4012-21.
2. Keereweer S, Kerrebijn JD, van Driel PB, Xie B, Kaijzel EL, Snoeks TJ, Que I, Hutteman M, van der Vorst JR, Mieog JS, Vahrmeijer AL, van de Velde CJ, et al. Optical image-guided surgery--where do we stand? Mol Imaging Biol 2011;13:199-207.
3. Baeten J, Haller J, Shih H, Ntziachristos V. In vivo investigation of breast cancer progression by use of an internal control. Neoplasia 2009;11:220-7.
4. Keereweer S, Mol IM, Kerrebijn JD, Van Driel PB, Xie B, Baatenburg de Jong RJ, Vahrmeijer AL, Lowik CW. Targeting integrins and enhanced permeability and retention (EPR) effect for optical imaging of oral cancer. J Surg Oncol 2011.
5. Kovar JL, Volcheck W, Sevick-Muraca E, Simpson MA, Olive DM. Characterization and performance of a near-infrared 2-deoxyglucose optical imaging agent for mouse cancer models. Analytical biochemistry 2009;384:254-62.
6. Kovar JL, Johnson MA, Volcheck WM, Chen J, Simpson MA. Hyaluronidase expression induces prostate tumor metastasis in an orthotopic mouse model. The American journal of pathology 2006;169:1415-26.
7. Weissleder R, Tung CH, Mahmood U, Bogdanov A, Jr. In vivo imaging of tumors with protease-activated near-infrared fluorescent probes. Nat Biotechnol 1999;17:375-8.
8. Keereweer S, de Wilt JH, Sewnaik A, Meeuwis CA, Tilanus HW, Kerrebijn JD. Early and long-term morbidity after total laryngopharyngectomy. Eur Arch Otorhinolaryngol 2010;267:1437-44.
9. Keereweer S, Kerrebijn JD, Al-Mamgani A, Sewnaik A, de Jong RJ, van Meerten E. Chemoradiation for advanced hypopharyngeal carcinoma: a retrospective study on efficacy, morbidity and quality of life. Eur Arch Otorhinolaryngol 2011.
10. Wickramasinghe NS, Nagaraj NS, Vigneswaran N, Zacharias W. Cathepsin B promotes both motility and invasiveness of oral carcinoma cells. Arch Biochem Biophys 2005;436:187-95.
11. Yang X, Wei KJ, Zhang L, Pan HY, Li J, Chen WT, Zhong LP, Zhang ZY. Increased expression of Cathepsin B in oral squamous cell carcinoma. Int J Oral Maxillofac Surg 2010;39:174-81.

12. Kessenbrock K, Plaks V, Werb Z. Matrix metalloproteinases: regulators of the tumor microenvironment. Cell 2010;141:52-67.
13. Scherer RL, McIntyre JO, Matrisian LM. Imaging matrix metalloproteinases in cancer. Cancer Metastasis Rev 2008;27:679-90.
14. De Wever O, Demetter P, Mareel M, Bracke M. Stromal myofibroblasts are drivers of invasive cancer growth. Int J Cancer 2008;123:2229-38.
15. 15. Zhang W, Matrisian LM, Holmbeck K, Vick CC, Rosenthal EL. Fibroblast-derived MT1-MMP promotes tumor progression in vitro and in vivo. BMC Cancer 2006;6:52.
16. Leemans CR, Braakhuis BJ, Brakenhoff RH. The molecular biology of head and neck cancer. Nat Rev Cancer 2011;11:9-22.
17. Zimmermann M, Zouhair A, Azria D, Ozsahin M. The epidermal growth factor receptor (EGFR) in head and neck cancer: its role and treatment implications. Radiat Oncol 2006;1:11.
18. Mieog JS, Hutteman M, van der Vorst JR, Kuppen PJ, Que I, Dijkstra J, Kaijzel EL, Prins F, Lowik CW, Smit VT, van de Velde CJ, Vahrmeijer AL. Image-guided tumor resection using real-time near-infrared fluorescence in a syngeneic rat model of primary breast cancer. Breast Cancer Res Treat.
19. Mendelsohn J, Baselga J. Status of epidermal growth factor receptor antagonists in the biology and treatment of cancer. Journal of clinical oncology : official journal of the American Society of Clinical Oncology 2003;21:2787-99.
20. Gambhir SS. Molecular imaging of cancer with positron emission tomography. Nat Rev Cancer 2002;2:683-93.
21. Keereweer S, Sterenborg HJ, Kerrebijn JD, Van Driel PB, de Jong RJ, Lowik CW. Image-guided surgery in head and neck cancer: Current practice and future directions of optical imaging. Head Neck 2011.
22. Fang J, Nakamura H, Maeda H. The EPR effect: Unique features of tumor blood vessels for drug delivery, factors involved, and limitations and augmentation of the effect. Adv Drug Deliv Rev 2011;63:136-51.
23. Cheng Z, Levi J, Xiong Z, Gheysens O, Keren S, Chen X, Gambhir SS. Near-infrared fluorescent deoxyglucose analogue for tumor optical imaging in cell culture and living mice. Bioconjugate chemistry 2006;17:662-9.
24. Keereweer S, Kerrebijn JD, Mol IM, Mieog JS, Van Driel PB, Baatenburg de Jong RJ, Vahrmeijer AL, Lowik CW. Optical imaging of oral squamous cell carcinoma and cervical lymph node metastasis. Head Neck 2011.
25. Thurber GM, Figueiredo JL, Weissleder R. Detection limits of intraoperative near infrared imaging for tumor resection. J Surg Oncol 2010;102:758-64.
26. Marshall MV, Draney D, Sevick-Muraca EM, Olive DM. Single-dose intravenous toxicity study of IRDye 800CW in Sprague-Dawley rats. Molecular imaging and biology : MIB : the official publication of the Academy of Molecular Imaging 2010;12:583-94.

# 6 Dual-wavelength detection of oral cancer simultaneously targeting integrins and enhanced permeability and retention effect

Stijn Keereweer,[1] Isabel M. Mol,[2] Jeroen D.F. Kerrebijn,[1]
Pieter B.A.A. Van Driel,[2] Bangwen Xie,[2] Robert J. Baatenburg de Jong,[1]
Alexander L. Vahrmeijer,[3] Clemens W.G.M. Löwik[2]

1. Erasmus Medical Center, Department of Otorhinolaryngology Head and Neck Surgery, Rotterdam, The Netherlands.
2. Leiden University Medical Center, Endocrinology and Molecular Imaging, Leiden, The Netherlands.
3. Leiden University Medical Center, Department of Surgery, Leiden, The Netherlands.

Published as "Targeting Integrins and Enhanced Permeability and Retention (EPR) Effect for Optical Imaging of Oral Cancer" in **Journal of Surgical Oncology, June 2012** 1;105(7):714-8.
DOI: 10.1002/jso.22102

## Abstract

### *Objectives*

Near-infrared (NIR) fluorescence optical imaging is a promising technique to assess the tumor margins during oral cancer surgery. This technique requires targeting by specific fluorescence agents to differentiate tumor from normal surrounding tissue. We assessed the feasibility of cancer detection using NIR fluorescence agents that target either αvβ3 integrins or the enhanced permeability and retention (EPR) effect in an orthotopic mouse model of oral cancer.

### *Materials and Methods*

Binding of the integrin-targeted agent to tumor cells was assessed in vitro. Oral cancer was induced in 6 BALB/c nu/nu mice by submucosal inoculation of human OSC19-luc cells into the tongue. Tumor growth was followed with bioluminescence imaging. A combination of agents targeting integrins or EPR effect was injected followed by fluorescence imaging in vivo and ex vivo after resection of the tongues.

### *Results*

Oral cancer was clearly demarcated in vitro, in vivo, and on histological analysis. For the integrin-targeted agent, the mean tumor-to-background ratio (TBR) was 67.6 ± 24.8 ($p<0.001$) and intratumoral fluorescence signal was found both on histological analysis and in vitro. The agent targeting the EPR effect had a TBR of 13.4 ± 10.6 ($p=0.006$) and was located directly around the tumor within a margin of 3 mm.

### *Conclusion*

This study demonstrates the feasibility of optical imaging of oral cancer based on targeting of αvβ3 integrins and the EPR effect. Once these NIR fluorescence agents become available for clinical testing, optical image-guided surgery could reduce residual disease after oral cancer surgery.

## Introduction

A clean surgical margin is the quintessence of oral cancer surgery. When involved margins are found on histopathology, local recurrence rates of 21.9% have been reported, compared to 3.9% local recurrences in patients with tumor-free histological margins.[1] Involved surgical margins increase the risk of death at 5 years by 90%.[2] Nevertheless, in current clinical practice, involved surgical margins are found in 16% of the patients that were operated with the objective of achieving a macroscopic clearance of 1 cm.[3]

Optical image-guided surgery can help the surgeon to accurately assess tumor-free margins during an operation.[4] In optical imaging, fluorescence agents are used that emit signal in the near-infrared (NIR) range (650–900 nm), resulting in lower absorption coefficients of tissues, light scattering and non-specific intrinsic fluorescence. In addition, sensitivity and depth of penetration are increased, improving image quality.[4,5]



In order to image oral squamous cell carcinoma (OSCC) during surgery, preoperative injection of NIR fluorescence agents that target the tumor is required. Various targeting strategies are available,[5] but attention is increasingly focusing on two important aspects of cancer: involvement of αvβ3 integrins[6] and the enhanced permeability and retention (EPR) effect,[7] which we will discuss separately.

Integrins are transmembrane cell surface receptors that are involved in signal transduction, cell-cell interaction and adhesion to the extracellular matrix.[6] Hence, their activity is essential for cell migration, invasion and extravasation.[6] Because these are key components in tumorigenesis, angiogenesis, and metastasis, integrins have been distinguished as clinically relevant biomarkers of tumor progression. A fortiori, integrins, and specifically integrin αvβ3, are upregulated in activated endothelial cells as well as in tumor cells, including head and neck cancer,[7,9–11] which makes them appealing targets for cancer imaging and therapy.[8] For imaging, targeting of integrins has been used in positron emission and single-photon emission computed tomography.[9, 10] Chemotherapeutic targeting of integrins is reported in a Phase II clinical trial of patients with glioblastoma.[11] Consequently, we believe that expression of integrins in tumor cells provides an interesting target for optical imaging of OSCC.

A second important aspect of cancer that can be used for optical imaging is tumor targeting based on the EPR effect. In order to provide the tumor with a sufficient supply of nutrients and oxygen for rapid growth, angiogenesis is promoted in the earliest stages of cancerogenesis. However, these newly formed tumor vessels are usually abnormal in form and have defective architecture, leading to enhanced vascular permeability.[7, 12] Furthermore, tumor tissues usually lack effective lymphatic drainage resulting in abnormal molecular and fluid transport dynamics.[7, 13] As a result, macromolecules selectively leak out from tumor vessels and accumulate in tumor interstitial tissues. This unique pathophysiological nature of tumor blood vessels is considered a landmark principle in anticancer drug development[7] and could be exploited in optical cancer imaging.[13]

In optical imaging, NIR fluorescence agents are used to target and subsequently image the tissue of interest. Bioluminescence imaging (BLI) is a different imaging technique that

can be used for highly sensitive in vivo tumor localization.[14] Genetic modification of the cancer cells is required and BLI is thus not applicable for clinical use. However, it can be used in animal experiments to non-invasively follow tumor growth and as an internal control for co-localization with the fluorescence signal.

The aim of this study was to use a combination of two NIR fluorescence agents that either target integrins or the EPR effect for clear demarcation of OSCC in a mouse model. NIR-fluorescence agents were used that fluoresce at different wavelengths, allowing for simultaneous, dual wavelength imaging of their signals.[15] Fluorescence signal was correlated to BLI signal and histopathology.

## Materials and Methods

### *NIR fluorescence agents*

IntegriSense680 (PerkinElmer, Waltham, MA) is a targeted fluorescence imaging agent comprising a selective non-peptide small molecule integrin αvβ3 antagonist and a NIR fluorochrome with peak excitation at 675 nm and emission at 693 nm. Specific binding of the agent to tumor cells has been demonstrated in previous experiments.[16] The IRDye 800CW PEG (LI-COR Biosciences, Lincoln, NE) is a non-specific imaging agent intended to exploit the EPR effect in tumor biology. Surface of the fluorochrome (excitation; 774 nm, emission; 789 nm) has been conjugated to PEG to extend blood circulation time.[7, 13]

### *Tumor model*

Human OSCC cell line OSC-19-luc was cultured in Dulbecco Modified Eagle Medium supplemented with 10% fetal bovine serum, L-glutamine, sodium pyruvate, nonessential amino acids, and a vitamin solution (Life Technologies Inc, Grand Island, NY). These cells are retrovirally infected with the luciferase gene to allow BLI.[17] In accordance with previous studies,[18] 6 x $10^4$ OSC-19-luc cells, diluted in 30 µL phosphate buffered saline (PBS), were inoculated submucosally into the distal end of the tongue of 6 BALB/c nu/nu mice, aged 4 to 6 weeks (Charles River Laboratories, L'Arbresle, France). Tumor growth was followed by BLI and visual inspection of the tongue two times a week.[18] Sterilized water and autoclaved pellet food were provided ad libitum and weight of the animals was followed during the experiments to follow general health state. Animals were housed according to our institution's animal facility standards and the Animal Welfare Committee of the Leiden University Medical Center approved the experiments. Throughout tumor inoculation and imaging procedures, the animals were placed on an animal bed with an integrated nose mask and anesthetized with 4% isoflurane for induction and 2% isoflurane for maintenance in oxygen with a flow of 0.8 L/min.

### *Experimental design*

Contrary to 800CW PEG, IntegriSense680 specifically binds to tumor cells next to targeting tumor vascularisation.[16] Therefore, tumor-specific targeting by IntegriSense680 was imaged in vitro. OSC19-luc cells were plated onto poly-L-lysine coated 35mm glass

bottom dishes (MatTek Corporation, Ashland, MA). Twenty-four hours after plating, cells were incubated with nucleus staining (1 μg/ml, Hoechst 33342, Invitrogen, Carlsbad, CA) for 8 min. Next, cells were washed with warmed growth medium, followed by membrane staining (DiI, 5 μg/ml, v-22889, Invitrogen), for 10 min. Subsequently, cells were washed 3x with medium and incubated with IntegriSense (200 nM in medium) at 37°C for 30 min. To prevent non-specific fluorescence of the medium, cells were washed with PBS, directly followed by confocal microscopy on a Leica SP5 confocal system (Leica, Wetzlar, Germany).

For the in vivo experiment, tumor growth was followed using BLI. During BLI, animals were anesthetized with 2% isoflurane, followed by intraperitoneal injection of an aqueous solution of luciferin (Caliper LifeSciences, Hopkinton, MA) at 150 mg/kg in a volume of 50 μL 10 minutes prior to imaging. Next, the animals were imaged using the IVIS 100 imaging system (Caliper LifeSciences). Quantification of the BLI signal was performed through standardized regions of interest using Living Image software (version 3.2, Caliper LifeSciences).



In accordance with our previous studies,[18] a high BLI signal was found at day 11, indicating that OSCC had developed. Next, the animals with OSCC (N = 6) were systemically injected with a combination of IntegriSense680 and 800CW PEG (1.33 nmol, 100 μL per probe) into one of the tail veins. One control mouse was injected with physiological saline in the tongue and later intravenously injected with the same combination of agents. Whole-body fluorescence imaging (FLI) was performed at various time points: 15 min, 45 min, 90 min, 3 hrs, 6 hrs, and 24 hrs after injection, and the animals were sacrificed afterwards. Subsequently, the tongue was removed in total for gross examination and additional ex vivo fluorescence measurements. Whole-body FLI of the mouse and subsequent FLI of the surgically removed tongues was performed using the Maestro™ (CRi, Woburn, MA), fitted with the yellow filter with acquisition range of 630-800 nm in 10 nm steps and variable acquisition time followed by scanning using the deep-red filter with acquisition range of 700-950 nm. Spectral unmixing of the fluorescence signals was performed to reduce the effects of native tissue autofluorescence and separating multiple fluorescence agents.

To identify tumor tissue with FLI, higher fluorescence signal in the tumor compared to healthy surrounding tissue is required, which is generally reported by the tumor-to-background ratio (TBR).[4] In order to calculate the TBR, fluorescence signal of the tumor was quantified by drawing 2 regions of interest in the tumor region of which the mean value was used. The mean background value was calculated from 3 regions of interest in the surrounding normal tissue at a range of 2 mm from the tumor border. After imaging, the excised tongues were frozen on dry ice, cut into slices (20 μm) and FLI was performed of the histological sections by simultaneous scanning of the 700 and 800 nm channels using the Odyssey scanner (LI-COR Biosciences; focus offset 1 mm, intensity 5 for both channels). Subsequently, tissue sections were air-dried and stained with standard hematoxylin-eosin (H-E), followed by microscopical analysis by a pathologist. In this way, correspondence between fluorescence signal and histopathology could be determined in detail.

*Data analysis*

Merged NIR fluorescence light images of separate scans of the Maestro were created using Adobe Photoshop CS3 Software (Version 10.0.1, Adobe Systems Inc., San Jose, CA). GraphPad Prism software (Version 5.01, La Jolla, CA) was used for generation of graphs. Mean fluorescence intensity and associated standard deviations were assessed using the Living Image software (version 3.2, Caliper LifeSciences) for BLI data and the Maestro Software (version 2.10.0, CRi Inc.) for FLI data. Continuous variables were analyzed using the (paired) t-test for comparison of two groups. Statistical tests were two-tailed and $p < 0.05$ was considered significant. For statistical analysis, SPSS for Windows, version 16.0 was used.

## Results

The in vitro experiments demonstrated binding of IntegriSense680 to the OSC19-luc cells (Fig. 1). Co-localization of IntegriSense680 with the membrane staining is illustrated by the yellow signal in Fig. 1C. Next to binding to receptors at the surface of the cells, internalization into the cells was found. According to previous experiments[18], tumor growth was followed

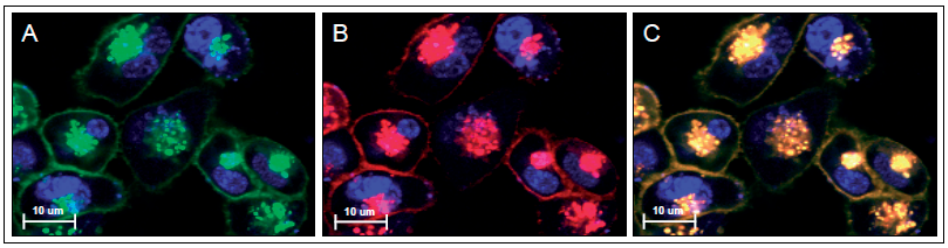


**Figure 1. Binding of Integrisense680 to OSC19-luc oral cancer cells.** A. Membrane staining (green signal) with nuclear staining (blue signal). B. IntegriSense680 (red signal) with nuclear staining (blue signal). C. Co-localization of IntegriSense680 with the membrane staining and intracellular uptake (yellow signal).

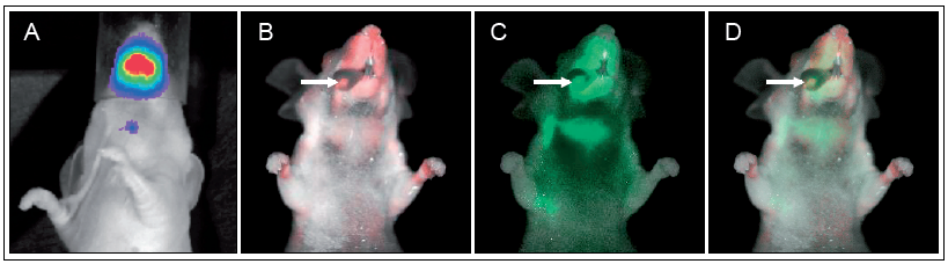


**Fig. 2.** In vivo imaging of oral cancer. Arrows indicate the tumor in the tip of the tongue. A. Bioluminescence image OSCC in the tongue and cervical lymph nodes after 11 days. B. Fluorescence image at 700 nm, 24 hrs after injection of IntegriSense680 (pseudo-colored red). C. Fluorescence image at 800 nm, 24 hrs after injection of 800CW PEG (pseudo-colored green). D. Merged image of Fig. 2B and 2C, demonstrating different localizations of the agents.

by whole-body BLI (data not shown). An example of the BLI signal is shown in Fig. 2A. After injection of both NIR fluorescence agents, whole-body dual wavelength FLI was performed at different time points and images were spectrally unmixed to allow separate subtraction of the 700 and 800 nm wavelengths. These images demonstrated background signal of both agents around the mouth and in the cervical and axillary regions at all time points. Demarcation of the tumor in the tip of the tongue by IntegriSense680 was only seen after 24 hrs (Fig. 2B). Similarly, increased fluorescence of 800CW PEG in the distal tongue was not seen until 24 hrs after injection (Fig. 2C). Compared with IntegriSense680, the signal of 800CW PEG was found over a larger area in the distal tongue (Fig. 2D). FLI of the control mouse without tumor showed no signal in the tongue for both agents. However,



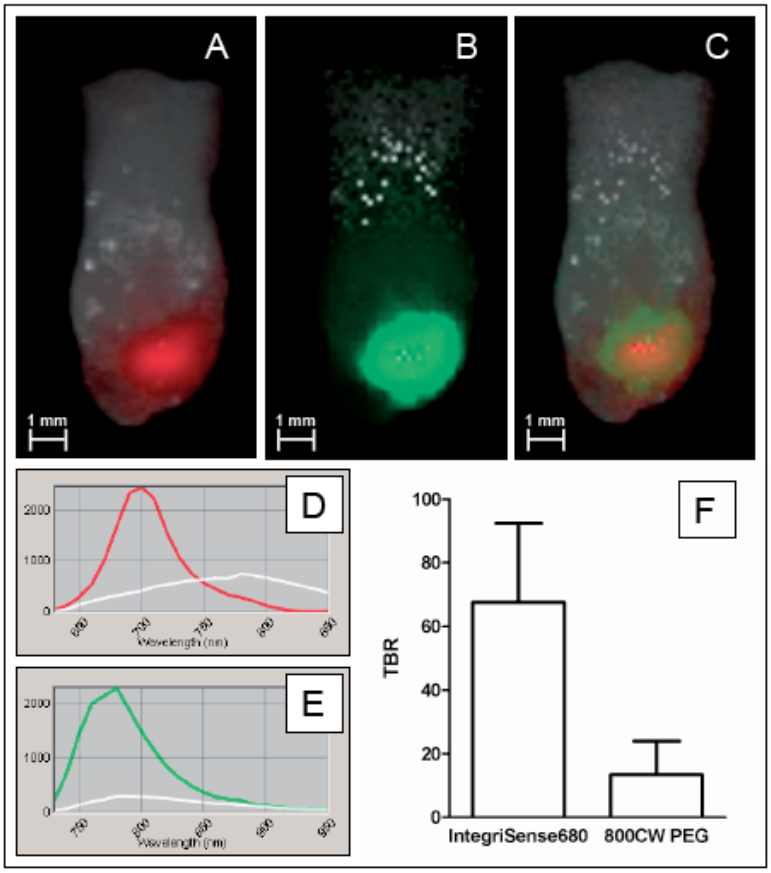


**Fig. 3.** Dual wavelength fluorescence imaging of tongue tumor and surrounding normal tissue. A. IntegriSense680 (pseudo-colored red), with corresponding light spectrum (D). B. 800CW PEG (pseudo-colored green) with corresponding light spectrum (E). C. Merged image of Fig. 3A and 3B, demonstrating different localizations of the agents. F. Tumor-to-background ratios *(TBR)* were calculated on these images.

the same background signal around the mouth and in the cervical and axillary regions was found (data not shown).

For image-guided surgery, higher fluorescence signal of the tumor related to its direct surrounding tissue is required, which is reflected in the TBR. In order to accurately determine the TBR of both agents, the tongue was removed and FLI was performed ex vivo. Spectral unmixing resulted in the image of IntegriSense680 (Fig. 3A) and its emission peak at 700 nm (Fig. 3D). The image and corresponding 800 nm spectrum of 800CW PEG are shown in Fig. 3B and 3E, respectively. Both NIR fluorescence agents demonstrated a clear demarcation of the tongue tumor compared to the surrounding healthy tongue tissue. The highest signal of IntegriSense680 was found in the center of the demarcated region, whereas 800CW PEG indicated a slightly wider region (Fig. 3C). The TBRs of both agents were calculated on the resected tongues. For IntegriSense680, the mean TBR was 67.6 ± 24.8 ($p<0.001$, Fig. 3F). The mean TBR of 800CW PEG was 13.4 ± 10.6 ($p=0.006$, Fig. 3F).

Histological analysis of unfixed 20 µm frozen tissue sections confirmed co-localization of IntegriSense680 with OSCC in the tongue (Fig. 4A and 4B). A low-level fluorescence signal of IntegriSense680 was also found in the healthy mucosal layer of the tongue (Fig. 4B). Presence of 800CW PEG was predominantly found in the tissue directly surrounding the tumor within a margin of 3 mm (Fig. 4C).

## Discussion

Optical image-guided surgery could be a very valuable tool to determine tumor margins during surgery. For imaging of head and neck cancer, various strategies are at hand to target

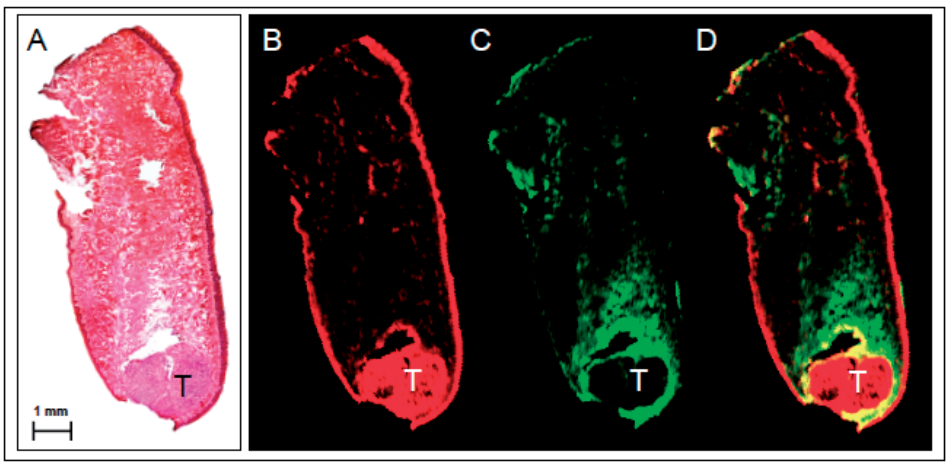


**Fig. 4.** Histological analysis of tongue with tumor. A. OSCC was identified on H-E staining analysis. B. IntegriSense680 (pseudo-colored red) clearly co-localizes with the tumor. C. 800CW PEG (pseudo-colored green) was found in the region directly surrounding the primary tumor. D. Difference in localization is illustrated by dual wavelength imaging. *T = Tumor*

the tumor using NIR fluorescence agents.[19] In this study, in vivo detection of OSCC by simultaneous imaging of IntegriSense680 and 800CW PEG is reported.

By targeting αvβ3 integrins using IntegriSense680, we demonstrated detailed demarcation of OSCC in vivo that was confirmed by histopathology, and found a mean TBR of 67.6. In larger tumors, TBRs typically range from 3 to 12 depending on the used NIR fluorescence agent.[20] Small tumors often have better uptake of imaging agents due to more efficient diffusion from the surface,[20] which could explain the high TBR found in this study. A second important factor is the camera system used, as lower TBRs of IntegriSense680 were recently reported using an intraoperative camera system for detection of colorectal metastases in the liver.[21] In normal oral mucosa, low levels of integrins are expressed.[22, 23] This explains the delineation of the squamous cell epithelium by low-level signals of IntegriSense680 on the histological sections (Fig. 4B), which further indicates specificity of the agent.



Macroscopic clearance of 1 cm is generally considered sufficient in oral cancer surgery.[3] Hence, the high TBRs, combined with the intratumoral signal of IntegriSense680 and signal of 800CW PEG within a margin of 3 mm indicate that both are powerful agents for detection of OSCC and delineation of tumor margins in vivo.

There are limitations to the use of these agents for detection of OSCC. Because 800CW PEG is merely a PEGylated fluorophore, it does not detect tumor-specific targets and FLI is completely based on the EPR effect. While EPR effect is used as a rationale for many applications, the exact mechanism is complicated and depends on the characteristics of both particle and vasculature [7, 12, 13] resulting in variations in vascular permeability within a tumor over time and between different tumors.[12] Furthermore, increased permeability is also found in inflammatory processes, although to a lesser extent than in tumor tissues, which could hamper specificity in the initial phase of the EPR effect.[24, 25] However, contrary to inflammatory tissues, retention of agents is highly increased in tumors due to defective architecture of lymphatic drainage.[24]

In addition, activation of αvβ3 integrins is not limited to tumor growth but is also associated with infection, thrombosis and autoimmune disorders.[8] These effects are important to consider when further clinical testing is performed, because they could potentially influence tumor-specific targeting.

In conclusion, this study demonstrates the feasibility of dual wavelength optical imaging of OSCC based on targeting of αvβ3 integrins and the EPR effect. These results warrant clinical validation of the technique, because once these NIR fluorescence agents become available for clinical testing, optical image-guided surgery could reduce residual disease after oral cancer surgery.

## Acknowledgements

Professor Hogendoorn, Ir, PhD, (Department of Pathology, Leiden University Medical Center) is gratefully acknowledged for his analysis of the tissue sections. The help of Prof. J.N. Myers, MD, PhD, (University of Texas, M.D. Anderson Cancer Center, Houston) in providing us with the OSC-19-luc cells is much appreciated. We thank I. Que (Animal

Experimentation Laboratory, Leiden University Medical Center) for his assistance in the animal experiments. The principal investigator had full access to all the data in the study and takes responsibility for the integrity of the data and the accuracy of the data analysis.

## References


1. Slootweg PJ, Hordijk GJ, Schade Y, van Es RJ, Koole R. Treatment failure and margin status in head and neck cancer. A critical view on the potential value of molecular pathology. Oral Oncol 2002;38(5):500-503.
2. Binahmed A, Nason RW, Abdoh AA. The clinical significance of the positive surgical margin in oral cancer. Oral Oncol 2007;43(8):780-784.
3. McMahon J, O'Brien CJ, Pathak I et al. Influence of condition of surgical margins on local recurrence and disease-specific survival in oral and oropharyngeal cancer. Br J Oral Maxillofac Surg 2003;41(4):224-231.
4. Frangioni JV. New technologies for human cancer imaging. J Clin Oncol 2008;26(24):4012-4021.
5. Keereweer S, Kerrebijn JD, van Driel PB et al. Optical Image-guided Surgery-Where Do We Stand? Mol Imaging Biol 2010.
6. Hood JD, Cheresh DA. Role of integrins in cell invasion and migration. Nat Rev Cancer 2002;2(2):91-100.
7. Fang J, Nakamura H, Maeda H. The EPR effect: Unique features of tumor blood vessels for drug delivery, factors involved, and limitations and augmentation of the effect. Adv Drug Deliv Rev 2010.
8. Desgrosellier JS, Cheresh DA. Integrins in cancer: biological implications and therapeutic opportunities. Nat Rev Cancer 2010;10(1):9-22.
9. Dijkgraaf I, Beer AJ, Wester HJ. Application of RGD-containing peptides as imaging probes for alphavbeta3 expression. Front Biosci 2009;14:887-899.
10. Haubner R, Wester HJ, Weber WA et al. Noninvasive imaging of alpha(v)beta3 integrin expression using 18F-labeled RGD-containing glycopeptide and positron emission tomography. Cancer Res 2001;61(5):1781-1785.
11. Reardon DA, Fink KL, Mikkelsen T et al. Randomized phase II study of cilengitide, an integrin-targeting arginine-glycine-aspartic acid peptide, in recurrent glioblastoma multiforme. J Clin Oncol 2008;26(34):5610-5617.
12. Jain RK, Stylianopoulos T. Delivering nanomedicine to solid tumors. Nat Rev Clin Oncol 2010;7(11):653-664.
13. Torchilin V. Tumor delivery of macromolecular drugs based on the EPR effect. Adv Drug Deliv Rev 2010.
14. Kim JB, Urban K, Cochran E et al. Non-invasive detection of a small number of bioluminescent cancer cells in vivo. PLoS One 2010;5(2):e9364.
15. Keereweer S, Mol IM, Vahrmeijer AL et al. Dual wavelength tumor targeting for detection of hypopharyngeal cancer using near-infrared optical imaging in an animal model. Int J Cancer 2012;131(7):1633-1640.
16. Kossodo S, Pickarski M, Lin SA et al. Dual In Vivo Quantification of Integrin-targeted and Protease-activated Agents in Cancer Using Fluorescence Molecular Tomography (FMT). Mol Imaging Biol 2009.
17. Sano D, Choi S, Milas ZL et al. The effect of combination anti-endothelial growth factor receptor and anti-vascular endothelial growth factor receptor 2 targeted therapy on lymph node metastasis: a study in an orthotopic nude mouse model of squamous cell carcinoma of the oral tongue. Arch Otolaryngol Head Neck Surg 2009;135(4):411-420.
18. Keereweer S, Kerrebijn JD, Mol IM et al. Optical imaging of oral squamous cell carcinoma and cervical lymph node metastasis. Head Neck 2012;34(7):1002-1008.
19. Keereweer S, Sterenborg HJ, Kerrebijn JD, van Driel PB, de Jong RJ, Lowik CW. Image-guided surgery in head and neck cancer: Current practice and future directions of optical imaging. Head Neck 2011.
20. Thurber GM, Figueiredo JL, Weissleder R. Detection limits of intraoperative near infrared imaging for tumor resection. J Surg Oncol 2010.
21. Hutteman M, Mieog JS, van der Vorst JR et al. Intraoperative near-infrared fluorescence imaging of colorectal metastases targeting integrin alpha(v)beta(3) expression in a syngeneic rat model. Eur J Surg Oncol 2011.

22. Gilcrease MZ. Integrin signaling in epithelial cells. Cancer Lett 2007;247(1):1-25.
23. Jones J, Watt FM, Speight PM. Changes in the expression of alpha v integrins in oral squamous cell carcinomas. J Oral Pathol Med 1997;26(2):63-68.
24. Sandanaraj BS, Gremlich HU, Kneuer R, Dawson J, Wacha S. Fluorescent nanoprobes as a biomarker for increased vascular permeability: implications in diagnosis and treatment of cancer and inflammation. Bioconjug Chem 2010;21(1):93-101.
25. Maeda H. Tumor-selective delivery of macromolecular drugs via the EPR effect: background and future prospects. Bioconjug Chem 2010;21(5):797-802.

# III

# CURRENT STATUS OF OPTICAL IMAGING IN DIAGNOSIS AND TREATMENT OF CANCER

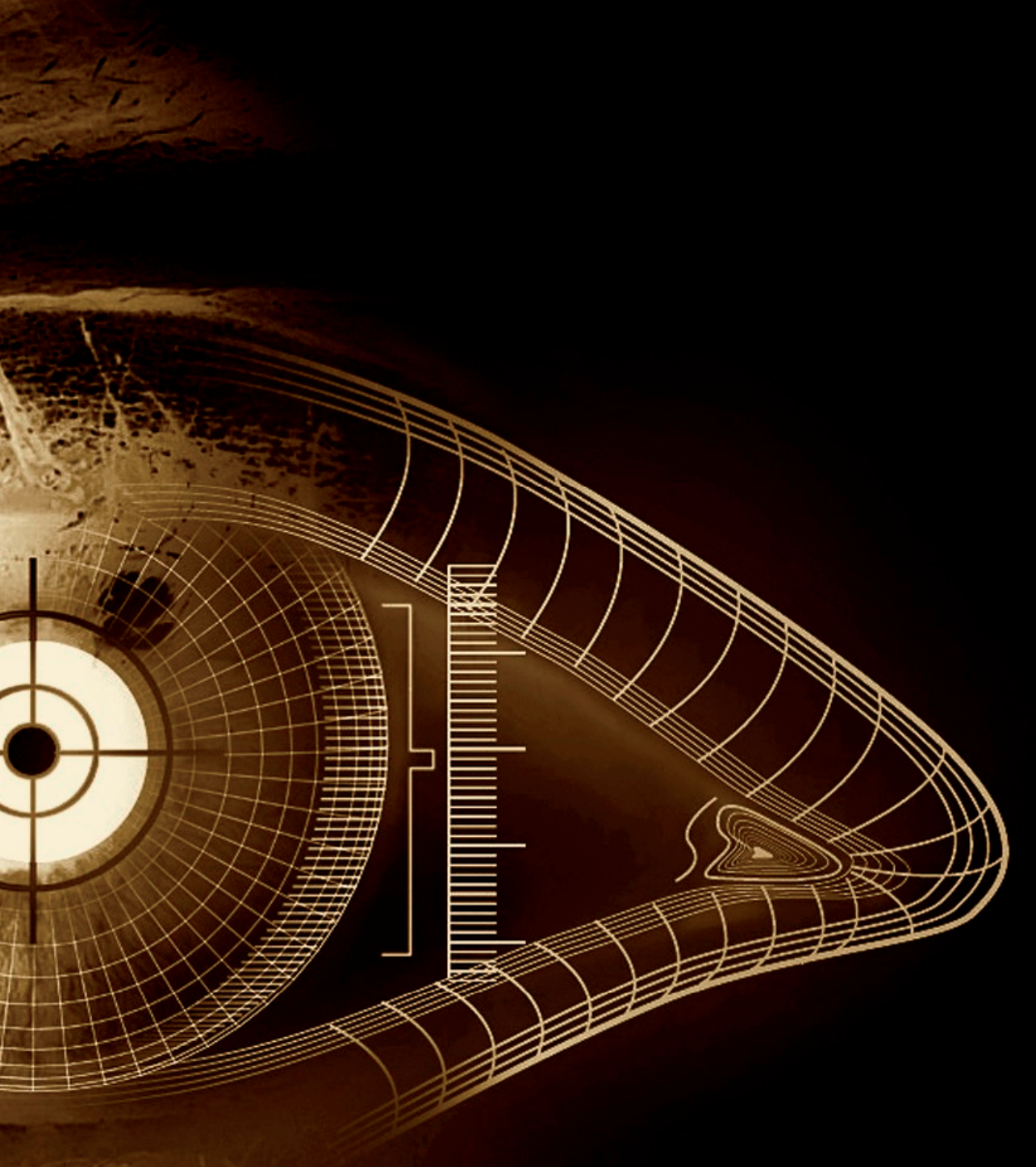

"Scientia vincere tenebras"
*"To conquer darkness through science"*

Free University of Brussel
Spreuk van de Vrije Universiteit Brussel

# 7 Developments in preclinical, translational, and clinical fluorescence cancer imaging

Stijn Keereweer[1,2*] & Merlijn Hutteman,[3*] Jeroen D.F. Kerrebijn,[1] Cornelis J.H. van de Velde,[3] Alexander L. Vahrmeijer,[3] Clemens W.G.M. Löwik[2]

1. Erasmus Medical Center, Department of Otorhinolaryngology Head and Neck Surgery, Rotterdam, The Netherlands.
2. Leiden University Medical Center, Molecular Endocrinology and Molecular Imaging, Leiden, The Netherlands.
3. Leiden University Medical Center, Department of Surgery, Leiden, The Netherlands.

* Stijn Keereweer and Merlijn Hutteman contributed equally to this manuscript.

Published as "Invited review: Translational Optical Imaging in Diagnosis and Treatment of Cancer" in **Current Pharmaceutical Biotechnology, March 2012**, 13(4):498-503

## Abstract

In cancer imaging, many different modalities are used that each have their specific features, leading to the combined use of different techniques for the detection, staging and treatment evaluation of cancer. Optical imaging using near-infrared fluorescence light is a new imaging modality that has recently emerged in the field of cancer imaging. After extensive preclinical research, the first steps of translation to the clinical practice are currently being made.

In this article, we discuss the preclinical and clinical results of near-infrared optical imaging for non-invasive detection and classification of tumors, therapy monitoring, sentinel lymph node procedures, and image-guided cancer surgery. Widespread availability of imaging systems and optical contrast agents will enable larger studies on their clinical benefit and can help establish a definitive role in clinical practice.

## Introduction

Ever since Wilhelm Röntgen discovered X-rays in 1895, clinical imaging has been used increasingly to aid caregivers in visualizing anatomy, physiological processes and disease beyond the capacity of their senses. Over the last decades, significant developments in imaging technologies have resulted in their established role in current clinical practice. Next to X-ray technology, the field of clinical imaging now includes ultrasonography (US), computed tomography (CT), magnetic resonance imaging (MRI), positron emission tomography (PET) and single-photon-emission computed tomography (SPECT). Each of these modalities has specific features, leading to the combined use of different techniques for the detection, staging and treatment evaluation of cancer [1].

The use of imaging modalities for guidance during surgical interventions has been limited to incidental use of intraoperative ultrasonography and X-ray fluoroscopy [2, 3]. Therefore, surgeons still mainly have to rely on palpation and visual inspection to discriminate between tumor and normal tissue and consequently determine an adequate tumor-free margin during surgery. Imaging techniques that can help the surgeon discriminate between healthy and diseased tissues (e.g., cancer) and identify vital structures (e.g., nerves, ureters, bile ducts) could be of great benefit.



Real-time imaging technologies offer a direct translation of preoperative images into the operation field, warranting image-guided surgery. A technique that has recently emerged as a potential candidate is optical imaging using near-infrared (NIR) fluorescence light.

## Clinical translation of optical imaging

Optical imaging uses specific properties of light to image anatomical or chemical characteristics of tissue. Analogous to many radiolabeled agents, imaging of optical contrast can be performed using ligands conjugated to an optically active reporter to target a recognized disease biomarker [1].

In the visible light spectrum (<650 nm), light is in part absorbed by hemoglobin, whereas water and lipids largely absorb light in the infrared range (>900 nm). The combination of these light characteristics offers an optical imaging window in the NIR spectrum (approximately 650 to 900 nm) in which the absorption coefficient, autofluorescence and light scattering of tissue are at a minimum (Figure 1). Consequently, tissue penetration is increased in this spectrum, leading to development of probes (i.e. antibodies or ligands conjugated to an optically active reporter that is designed to target a disease-specific biomarker) that provide high signal-to-background ratios (SBR) [1, 4]. These advantages can be used in tumor detection, tumor staging, image-guided surgery and follow-up after treatment.

## Non-invasive detection and classification of tumors and therapy monitoring

### *Preclinical results*

The intrinsic optical absorption signals of blood, water, and lipid, correlated with increased hemoglobin concentration due to angiogenesis and decreased hemoglobin saturation

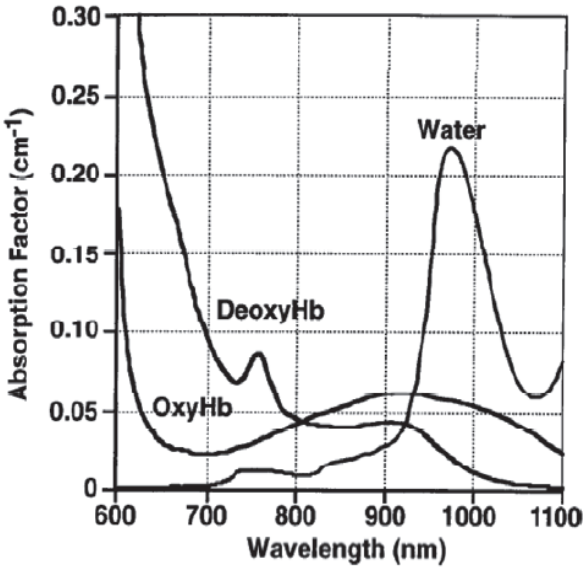


**Fig. 1.** Absorption of light by various components varies over the wavelength spectrum, resulting in an optimal window for fluorescence imaging in the NIR light region between 650 and 900 nm. OxyHb, oxygenated hemoglobin; DeoxyHb, deoxygenated hemoglobin. Figure reprinted from Chance, B.[46] With permission, Copyright Clearance Center Rightslink.

due to hypermetabolism, have been used in NIR spectroscopy to detect and localize cancer [5]. Furthermore, the use of exogenous contrast agents to detect and monitor tumor growth has been described. Planar fluorescence imaging has been used to register and quantify fluorescence signal on a two-dimensional image [6]. Planar fluorescence imaging is a conventional imaging technique that uses illumination of tissues with a plane wave (i.e. an expanded light beam), with subsequent collection of fluorescence signals that are emitted toward the camera. This can be applied in epi-illumination (i.e. photographic or reflectance imaging) or transillumination (collection of data on the opposite side) mode. More recently developed techniques have been used to generate three-dimensional images, in order to do volumetric assessments of fluorescence signal and to localize the signal. These techniques include fluorescence tomography imaging [7] (Figure 2a) and fluorescence lifetime imaging [8, 9], which have shown promising results in preclinical validation studies on tumor therapy monitoring. Fluorescence tomography is an imaging technology that is capable of spatially resolving the concentration of fluorescent agents located deep in soft tissue *in vivo*. Because of the possibility of co-registration with other imaging modalities such as MRI, PET, SPECT, and CT, it determines the position and quantity of a fluorescent source in a three-dimensional image.

For example, Choi and colleagues have used the FMT fluorescence tomography system (VisEn Medical, Bedford, MA) to monitor photodynamic therapy response [10]. Whole-body


**Fig. 2.** A. VisEn FMT 2500 NIR fluorescence tomography imaging system, for preclinical imaging applications B. Time-domain optical mammography (Softscan®), used for detection of breast cancer.

fluorescence tomography imaging is presently not available for clinical applications, as penetration depth of signal through tissue is limited to several centimeters. Fluorescence tomography does have potential application in selected areas, for example in breast, where the tissue volume that needs to be penetrated is relatively small. Lifetime imaging is an imaging technique that distinguishes individual fluorophores by their specific temporal decay (i.e. time domain) after excitation [8, 9].

## *Clinical results*

Diffuse optical imaging is a measurement technique based on detection of diffusely scattered light. It is used to estimate the average optical properties of tissue at multiple wavelengths based on diffusion theory. The technology assumes that light propagation is dominated by multiple scattering and is modeled as a diffusive process where photons behave as stochastic particles. Semi-quantitative tissue measurements can be obtained by separating light absorption from scattering using spatially- or temporally-modulated photon migration technologies.

Three-dimensional parallel-plate diffuse optical tomography [11] or time-domain optical mammography [12] (Figure 2b) have been used to measure photon migration through the breast and variations in the functional and structural NIR properties (e.g. scattering, oxy- and deoxy-hemoglobin concentrations), enabling differentiation between benign and

malignant tumors. Potential benefit of these techniques lies in the ability to non-invasively classify tumors and monitor therapy response. Clinical studies are currently being performed to assess patient benefit [12]. However, three-dimensional parallel-plate diffuse optical tomography and time-domain optical mammography require post-processing and therefore do not provide real-time imaging.

## Sentinel Lymph Node Detection

The sentinel lymph node (SLN) is the lymph node that directly drains from the tumor site and to which tumor cells will first metastasize. Currently, sentinel lymph node imaging is performed using dye-injection, nuclear imaging, CT and MRI [13], which each have their specific limitations regarding sensitivity, resolution, exposure to radioactivity, or practical use.

As in tumor detection applications, NIR fluorescence imaging of the SLN allows for high spatial and temporal resolution. Recent camera systems are able to detect sub millimeter spots with more than 30 frames-per-second, thereby providing real-time visualization [14, 15]. When camera systems are used with parallel imaging of visible and near-infrared light, the contrast agents can be traced to the SLNs in real-time, without affecting the visual appearance of the surgical field [16]. Furthermore, the lack of ionizing radiation makes it an easy-to-use and safe technique [1, 16].

### *Preclinical results*

Preclinical validation of SLN mapping using NIR fluorescence light has been performed using NIR fluorescence imaging systems (Maestro In-Vivo Imaging System, CRI Inc., Woburn, MA) [17], intraoperative imaging systems (FLARE, Frangioni Lab, Boston, MA) [16, 18, 19] and experimental laparoscopic camera systems [20]. In both small animal and large animal models, SLN mapping using NIR fluorescence light was found to be fast and feasible. Indocyanine green (ICG) is currently the only Food and Drug Administration (FDA) approved NIR fluorescent contrast agent and has been used intensively in SLN studies. Other compounds are being developed that have advantageous properties for SLN imaging. These agents can roughly be divided in organic fluorophores, organic nanoparticles and inorganic nanoparticles. Ohnishi and colleagues showed that several of those newly developed contrast agents showed superior results in comparison with ICG [18]. Novel organic fluorophores and organic nanoparticles based on currently clinically available compounds are more likely to be introduced in the clinic in a short timeframe, as the suspected toxicity is relatively low.

### *Clinical results*

At this moment, SLN mapping is one of the most promising clinical applications for NIR fluorescence imaging in the field of oncology. Recent clinical results reported the use of intraoperative NIR fluorescence cameras [14, 21] or portable NIR imaging devices [22-25] for SLN mapping. NIR fluorescence imaging using ICG has been shown to visualize the lymphatic channels transcutaneously. Multiple studies, containing in total more than 500 patients,

have been published using ICG as lymphatic tracer in SLN procedures in breast, skin, or gastro-intestinal cancer [14, 21-24, 26-28]. An example of SLN mapping in breast cancer is shown in Figure 3. At this moment, availability of camera systems is limited to a small number of research hospitals, limiting the introduction of these techniques into general clinical practice.

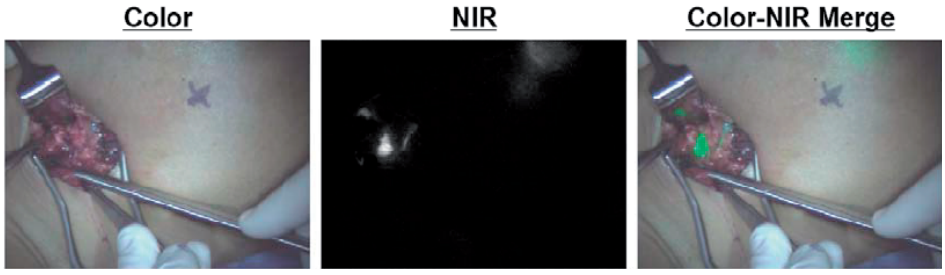


**Fig. 3.** Intraoperative detection of an axillary SLN in a patient with breast cancer.



## Tumor margin detection and image-guided resection

During cancer surgery, complete removal of all tumor tissue is pivotal for a patient's prognosis [4, 29]. Currently, surgeons can only rely on visual inspection and palpation to discriminate between healthy tissue and tumor tissue. Therefore, there is a need for imaging modalities that can visualize this distinction. If this can be achieved, tumor margins can be assessed more accurately during surgery which may improve radical resection without unnecessary damage to healthy tissue [1, 4]. Furthermore, it is anticipated that identification of malignant lesions will be possible before they become visible to the naked eye, through detection of biochemical changes involved in the earliest stages of neoplastic development.

### *Preclinical results*

Different strategies can be followed to detect malignant cells or tissues intraoperatively. The various hallmarks of cancer can be used as a target for imaging strategies: increased growth and growth factor signaling receptors, limitless replicative potential, sustained angiogenesis, and increased proteolytic activity resulting in tissue invasion and metastasis [4]. Enzyme activatable probes allow detection of proteases that are relatively abundant in malignant tissue, which can be associated with specific characteristics of the tumor, e.g. invasive, aggressive or metastatic tendency. These agents are injected in a quenched (i.e. non-fluorescent) state, resulting in minimal fluorescence at the time of administration. After cleavage by the specific enzyme, the agent becomes dequenched (i.e., fluorescent), resulting in a high SBR. Examples of activatable agents that have been used in animal cancer models are activatable polyarginine-based cell-penetrating peptides that detect matrix metalloproteinases [30], activity-based probes that target cysteine

cathepsins [31], and several commercially available probes that have been developed by Weissleder et al., which are activated by cathepsins or matrix metalloproteinases (VisEn Medical, Bedford, MA) [32, 33].

Instead of detection of tumor-associated proteases, molecular-specific detection of cancer cells can be performed using a specific targeting ligand or monoclonal antibody conjugated to a fluorophore. Tumor detection by exploiting the increased growth factor receptor expression of tumors has been described in all kinds of different tumors. In these studies, fluorophores that were coupled to monoclonal antibodies targeting the epidermal growth factor receptor, Her2/neu receptor, or vascular endothelial growth factor receptor were used [34-37]. For imaging of tumor angiogenesis, targeting of alpha-v-beta-3 (αvβ3) integrin, a critically important adhesion molecule in the regulation of angiogenesis, is a widely used strategy. Targeting of αvβ3 integrin by cyclic arginine-glycine-aspartate conjugated to various non-quenched or quenched fluorophores has been reported [7, 38, 39]. Finally, in analogy with PET technology, increased glucose metabolism due to increased expression of membrane glucose transporter proteins in intracranial gliomas has been reported [40]. An example of tumor detection using a protease sensing NIR fluorescent agent (ProSense, VisEn Medical, Bedford, MA) is shown in Figure 4.

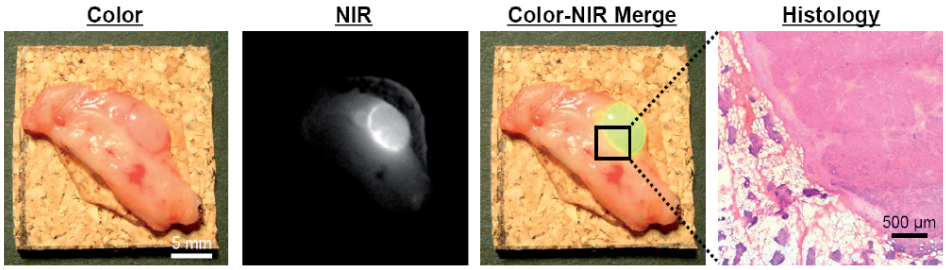


**Fig. 4.** NIR fluorescence imaging of excised primary breast cancer in a rat model using the ProSense680 and the Fluobeam camera system. A color image (first panel) a NIR fluorescence image (second panel), and a pseudocolored green merge of the two images (third panel) of a sectioned 4 mm EMR86 breast tumor with surrounding mammary fat pad is shown. A detail of the square region in the third panel is shown in the fourth panel (325 original magnification) with hematoxylin-eosin histologic staining.

## *Clinical results*

Over the last years, intraoperative optical imaging camera systems are being developed resulting in the detection of a variety of tumors during surgical procedures. These include the Fluorescence-assisted Resection and Exploration (FLARE™, Frangioni laboratory, Boston, MA), the Photodynamic Eye (PDE; Hamamatsu Photonics, Hamamatsu, Japan), and a system build by the group of Ntziachristos [16, 41, 42]. Furthermore, the use of endoscopic fluorescence systems has been reported for diagnostic and surgical applications [43].

In neurosurgery, the use of 5-aminolevulinic acid for detection of malignant gliomas by optical imaging techniques has been studied over the last years. The intraoperative use of fluorescence guidance has been described in a phase II trial as an effective adjunct in the surgery of recurrent malignant gliomas [44].

To date, three Japanese studies have reported the use of ICG in NIR fluorescence imaging of liver tumors. Ishizawa et al. [41] injected ICG in 37 patients with hepatocellular carcinoma and 12 patients with colorectal carcinoma liver metastases before surgery as part of a routine liver function test. Both during and after resection, the liver and liver specimens were imaged with the Photodynamic Eye imaging system (Hamamatsu Photonics, Hamamatsu, Japan). All pathologically confirmed hepatocellular carcinomas and colorectal metastases were identified in the excised surgical specimens using ICG (example shown in Figure 5).



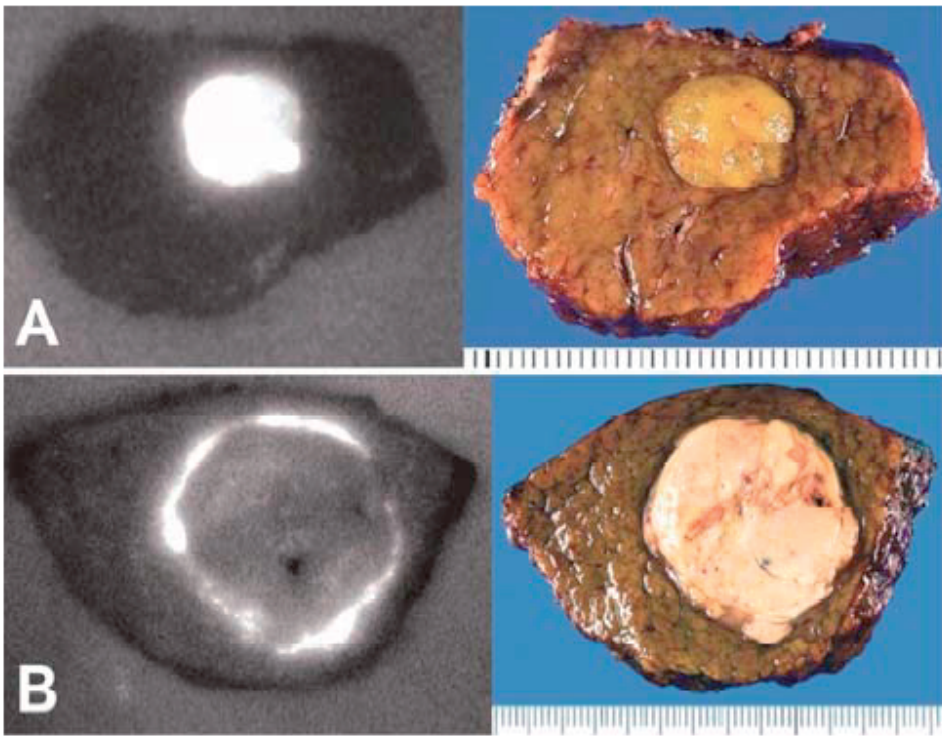


**Fig. 5.** Fluorescent patterns of liver cancers on NIR fluorescence image-guided surgical specimens (left) and their gross appearances (right). (A) Total fluorescent type; well-differentiated hepatocellular carcinoma (HCC), 7 mm in diameter. (B) Rim fluorescent type; poorly differentiated HCC, 30 mm in diameter. Reprinted from Ishizawa et al.[41] With permission, Copyright Clearance Center Rightslink.

## Future directions

The use of NIR fluorescence optical imaging in the field of SLN mapping is rapidly expanding in clinical oncology. ICG, approved by the FDA for various other applications, will play a major role in this respect, potentially demonstrating the clinical advantage over current lymph node mapping protocols.

### *Probe development and regulatory approval*

Preclinical trials have clearly demonstrated the large potential of targeting strategies for tumor detection using NIR fluorescence techniques. However, FDA approval of organic fluorophores is a necessary step towards clinical targeting of tumor specific signals. In the following years, FDA approval of the activatable agents is required to fully exploit the possibilities of optical imaging, and thereby enhancing the specificity and sensitivity of this technique. Once these agents are found to be safe, it is anticipated that the initial steps will be taken in their conjugation to already FDA approved and clinically used monoclonal antibodies (e.g. cetuximab, bevacizumab).

### *Development of imaging devices*

All these developments will have to be accompanied by parallel development of adequate, manageable, intraoperative camera systems. In order to guide the surgeon to perform a tumor resection with tumor-free margins, the development of camera systems that provide adequate imaging resolutions is essential. NIR fluorescence laparoscopic camera systems are currently being developed, which will allow NIR fluorescence image-guided surgery in a minimally invasive setting. Various techniques are being evaluated to correct for photon scattering and thereby enhance the depth at which NIR fluorescence signal can be detected [9, 42, 45]. When these probes and improved NIR fluorescence camera systems become clinically available, applications of NIR fluorescence image-guided cancer surgery will be greatly expanded.

Tumor detection and therapy monitoring using whole body optical imaging will be limited to preclinical applications in the foreseeable future due to lack of required penetration depth of NIR light. However, in selected indications (i.e. breast cancer) optical imaging is applicable using specialized devices.

## Conclusions

Recent developments in optical imaging have shown promising clinical applications for this technique. The current review describes its applications in oncology in particular. Preclinically, optical imaging has been employed in tumor identification, image-guided resection, therapy monitoring and SLN detection. Each of these indications is currently being translated into the clinic. Widespread availability of imaging systems and optical contrast agents will enable larger studies on its clinical benefit and can help establish a definitive role in clinical practice.

## List of abbreviations

CT = computed tomography
FDA = Food and Drug Administration
ICG = Indocyanine Green
MRI = magnetic resonance imaging
NIR = Near-Infrared
PET = positron emission tomography
SBR = Signal-to-Background Ratio
SLN = Sentinel Lymph Node
SPECT = single-photon-emission computed tomography
US = ultrasonography



## References


1. Frangioni JV. New technologies for human cancer imaging. J Clin Oncol 2008;26(24):4012-4021.
2. Leen E, Ceccotti P, Moug SJ et al. Potential value of contrast-enhanced intraoperative ultrasonography during partial hepatectomy for metastases: an essential investigation before resection? Ann Surg 2006;243(2):236-240.
3. Flum DR, Dellinger EP, Cheadle A, Chan L, Koepsell T. Intraoperative cholangiography and risk of common bile duct injury during cholecystectomy. JAMA 2003;289(13):1639-1644.
4. Keereweer S, Kerrebijn JD, van Driel PB et al. Optical Image-guided Surgery-Where Do We Stand? Mol Imaging Biol 2010.
5. Nioka S, Chance B. NIR spectroscopic detection of breast cancer. Technol Cancer Res Treat 2005;4(5):497-512.
6. Kaijzel EL, van der Pluijm G, Lowik CW. Whole-body optical imaging in animal models to assess cancer development and progression. Clin Cancer Res 2007;13(12):3490-3497.
7. Kossodo S, Pickarski M, Lin SA et al. Dual In Vivo Quantification of Integrin-targeted and Protease-activated Agents in Cancer Using Fluorescence Molecular Tomography (FMT). Mol Imaging Biol 2009.
8. Biffi S, Garrovo C, Macor P et al. In vivo biodistribution and lifetime analysis of cy5.5-conjugated rituximab in mice bearing lymphoid tumor xenograft using time-domain near-infrared optical imaging. Mol Imaging 2008;7(6):272-282.
9. Kumar AT, Raymond SB, Bacskai BJ, Boas DA. Comparison of frequency-domain and time-domain fluorescence lifetime tomography. Opt Lett 2008;33(5):470-472.
10. Choi Y, Weissleder R, Tung CH. Selective antitumor effect of novel protease-mediated photodynamic agent. Cancer Res 2006;66(14):7225-7229.
11. Choe R, Konecky SD, Corlu A et al. Differentiation of benign and malignant breast tumors by in-vivo three-dimensional parallel-plate diffuse optical tomography. J Biomed Opt 2009;14(2):024020.
12. Intes X. Time-domain optical mammography SoftScan: initial results. Acad Radiol 2005;12(8):934-947.
13. Barrett T, Choyke PL, Kobayashi H. Imaging of the lymphatic system: new horizons. Contrast Media Mol Imaging 2006;1(6):230-245.
14. Troyan SL, Kianzad V, Gibbs-Strauss SL et al. The FLARE intraoperative near-infrared fluorescence imaging system: a first-in-human clinical trial in breast cancer sentinel lymph node mapping. Ann Surg Oncol 2009;16(10):2943-2952.
15. Thurber GM, Figueiredo JL, Weissleder R. Detection limits of intraoperative near infrared imaging for tumor resection. J Surg Oncol 2010.
16. Tanaka E, Choi HS, Fujii H, Bawendi MG, Frangioni JV. Image-guided oncologic surgery using invisible light: completed pre-clinical development for sentinel lymph node mapping. Ann Surg Oncol 2006;13(12):1671-1681.

17. Hama Y, Koyama Y, Urano Y, Choyke PL, Kobayashi H. Simultaneous two-color spectral fluorescence lymphangiography with near infrared quantum dots to map two lymphatic flows from the breast and the upper extremity. Breast Cancer Res Treat 2007;103(1):23-28.
18. Ohnishi S, Lomnes SJ, Laurence RG, Gogbashian A, Mariani G, Frangioni JV. Organic alternatives to quantum dots for intraoperative near-infrared fluorescent sentinel lymph node mapping. Mol Imaging 2005;4(3):172-181.
19. Frangioni JV, Kim SW, Ohnishi S, Kim S, Bawendi MG. Sentinel lymph node mapping with type-II quantum dots. Methods Mol Biol 2007;374:147-159.
20. Koyama T, Tsubota A, Nariai K, Mitsunaga M, Yanaga K, Takahashi H. Novel biomedical imaging approach for detection of sentinel nodes in an experimental model of gastric cancer. Br J Surg 2007;94(8):996-1001.
21. Sevick-Muraca EM, Sharma R, Rasmussen JC et al. Imaging of lymph flow in breast cancer patients after microdose administration of a near-infrared fluorophore: feasibility study. Radiology 2008;246(3):734-741.
22. Fujiwara M, Mizukami T, Suzuki A, Fukamizu H. Sentinel lymph node detection in skin cancer patients using real-time fluorescence navigation with indocyanine green: preliminary experience. J Plast Reconstr Aesthet Surg 2009;62(10):e373-e378.
23. Tagaya N, Yamazaki R, Nakagawa A et al. Intraoperative identification of sentinel lymph nodes by near-infrared fluorescence imaging in patients with breast cancer. Am J Surg 2008;195(6):850-853.
24. Kitai T, Inomoto T, Miwa M, Shikayama T. Fluorescence navigation with indocyanine green for detecting sentinel lymph nodes in breast cancer. Breast Cancer 2005;12(3):211-215.
25. Murawa D, Hirche C, Dresel S, Hunerbein M. Sentinel lymph node biopsy in breast cancer guided by indocyanine green fluorescence. Br J Surg 2009;96(11):1289-1294.
26. Hirche C, Murawa D, Mohr Z, Kneif S, Hunerbein M. ICG fluorescence-guided sentinel node biopsy for axillary nodal staging in breast cancer. Breast Cancer Res Treat 2010.
27. Hojo T, Nagao T, Kikuyama M, Akashi S, Kinoshita T. Evaluation of sentinel node biopsy by combined fluorescent and dye method and lymph flow for breast cancer. Breast 2010.
28. Noura S, Ohue M, Seki Y et al. Feasibility of a Lateral Region Sentinel Node Biopsy of Lower Rectal Cancer Guided by Indocyanine Green Using a Near-Infrared Camera System. Ann Surg Oncol 2009.
29. Mieog JS, Vahrmeijer AL, Hutteman M et al. Novel Intraoperative Near-infrared Fluorescence Camera System For Optical Image-guided Cancer Surgery. Mol Imaging 2010;9(4):223-231.
30. Jiang T, Olson ES, Nguyen QT, Roy M, Jennings PA, Tsien RY. Tumor imaging by means of proteolytic activation of cell-penetrating peptides. Proc Natl Acad Sci U S A 2004;101(51):17867-17872.
31. Blum G, von DG, Merchant MJ, Blau HM, Bogyo M. Noninvasive optical imaging of cysteine protease activity using fluorescently quenched activity-based probes. Nat Chem Biol 2007;3(10):668-677.
32. Mahmood U, Weissleder R. Near-infrared optical imaging of proteases in cancer. Mol Cancer Ther 2003;2(5):489-496.
33. Wunderbaldinger P, Turetschek K, Bremer C. Near-infrared fluorescence imaging of lymph nodes using a new enzyme sensing activatable macromolecular optical probe. Eur Radiol 2003;13(9):2206-2211.
34. Gleysteen JP, Duncan RD, Magnuson JS, Skipper JB, Zinn K, Rosenthal EL. Fluorescently labeled cetuximab to evaluate head and neck cancer response to treatment. Cancer Biol Ther 2007;6(8):1181-1185.
35. Lee SB, Hassan M, Fisher R et al. Affibody molecules for in vivo characterization of HER2-positive tumors by near-infrared imaging. Clin Cancer Res 2008;14(12):3840-3849.
36. Withrow KP, Newman JR, Skipper JB et al. Assessment of bevacizumab conjugated to Cy5.5 for detection of head and neck cancer xenografts. Technol Cancer Res Treat 2008;7(1):61-66.
37. Ogawa M, Kosaka N, Longmire MR, Urano Y, Choyke PL, Kobayashi H. Fluorophore-Quencher Based Activatable Targeted Optical Probes for Detecting in Vivo Cancer Metastases. Mol Pharm 2009.
38. Chen K, Xie J, Chen X. RGD-human serum albumin conjugates as efficient tumor targeting probes. Mol Imaging 2009;8(2):65-73.
39. Jin ZH, Razkin J, Josserand V et al. In vivo noninvasive optical imaging of receptor-mediated RGD internalization using self-

quenched Cy5-labeled RAFT-c(-RGDfK-)(4). Mol Imaging 2007;6(1):43-55.

40. Zhou H, Luby-Phelps K, Mickey BE, Habib AA, Mason RP, Zhao D. Dynamic near-infrared optical imaging of 2-deoxyglucose uptake by intracranial glioma of athymic mice. PLoS One 2009;4(11):e8051.
41. Ishizawa T, Fukushima N, Shibahara J et al. Real-time identification of liver cancers by using indocyanine green fluorescent imaging. Cancer 2009;115(11):2491-2504.
42. Themelis G, Yoo JS, Soh KS, Schulz R, Ntziachristos V. Real-time intraoperative fluorescence imaging system using light-absorption correction. J Biomed Opt 2009;14(6):064012.
43. Figueiredo JL, Alencar H, Weissleder R, Mahmood U. Near infrared thoracoscopy of tumoral protease activity for improved detection of peripheral lung cancer. Int J Cancer 2006;118(11):2672-2677.
44. Nabavi A, Thurm H, Zountsas B et al. Five-aminolevulinic acid for fluorescence-guided resection of recurrent malignant gliomas: a phase ii study. Neurosurgery 2009;65(6):1070-1076.
45. Gioux S, Mazhar A, Cuccia DJ, Durkin AJ, Tromberg BJ, Frangioni JV. Three-dimensional surface profile intensity correction for spatially modulated imaging. J Biomed Opt 2009;14(3):034045.
46. Chance B. Near-infrared images using continuous, phase-modulated, and pulsed light with quantitation of blood and blood oxygenation. Ann N Y Acad Sci 1998;838:29-45.

# IV GENERAL DISCUSSION

"When you know a thing, to hold that you know it
And when you do not know a thing, to allow that you do not know it
- This is knowledge"

Confucius

# 8 Fundamental aspects, challenges, and limitations

Stijn Keereweer,[1] Pieter B.A.A. Van Driel,[2] Thomas J.A. Snoeks,[2] Jeroen D.F. Kerrebijn,[1] Robert J. Baatenburg de Jong,[1] Alexander L. Vahrmeijer,[3] Henricus J.C.M. Sterenborg,[4] Clemens W.G.M. Löwik[2]

1. Department of Otorhinolaryngology Head and Neck Surgery, Erasmus Medical Center, Rotterdam, The Netherlands.
2. Endocrinology and Molecular Imaging, Leiden University Medical Center, Leiden, The Netherlands.
3. Department of Surgery, Leiden University Medical Center, Leiden, The Netherlands.
4. Center of Optical Diagnostics and Therapy, Erasmus Medical Center, Rotterdam, The Netherlands.

Edited from: "Optical Image-Guided Cancer Surgery: Challenges and Limitations"
Published in **Clinical Cancer Research, July 2013**, 19(14):3745–54

## Abstract

### *Purpose*

To provide a clear overview of the various components that play an essential role in the conundrum of optical imaging for application in cancer surgery.

### *Background*

Optical image-guided cancer surgery is a promising technique to adequately determine tumor margins by tumor-specific targeting, potentially resulting in complete resection of tumor tissue with improved survival. However, identification of the photons coming from the fluorescent contrast agent is complicated by autofluorescence, optical tissue properties, and accurate fluorescent targeting agents and imaging systems. These factors all have an important influence on the image that is presented to the surgeon.

### *Results*

Considering the clinical consequences at stake, it is a prerequisite to answer the questions that are essential for the surgeon. What is optical image-guided surgery and how can it improve patient care? What should the oncologic surgeon know about the fundamental principles of optical imaging to understand which conclusions can be drawn from the images? And how do the limitations influence the clinical decision-making? This manuscript discusses these questions and provides a clear overview of the basic principles and practical applications.

### *Conclusion*

Although there are limitations to the intrinsic capacity of the technique, when practical and technical surgical possibilities are considered, optical imaging can be a very powerful intraoperative tool in guiding the future oncologic surgeon towards radical resection and optimal clinical results.

## Introduction

For cancer surgery with curative intentions, radical resection (i.e., removal of all cancer cells) is a sine qua non. In order to achieve this, the surgeon has to adequately assess the tumor resection margin during the operation. Optical molecular imaging using near-infrared (NIR) fluorescence introduces a revolutionary new approach to address this basic challenge in surgical oncology.(1-3)

The field of optical imaging emerged in the early 20$^{th}$ century with the observation of porphyrin fluorescence in certain tumors, but a lack of fundamental knowledge and suitable optical equipment prevented further development at the time.(4) The finding that photons in the NIR range (650-900 nm) travel through tissue much deeper than photons in the visible light range(5) was essential for the advancement of optical imaging towards clinical practice, and further development gained momentum over the last decade.(1, 6) In order to use optical imaging for visualization of cancer, fluorescent agents are injected that emit light in the NIR range and are tumor-specific using a variety of targeting strategies.(2) Because the human eye is not sensitive for light in the NIR region, dedicated camera systems are required to detect the fluorescence emission from these molecules.(2) By real-time intraoperative fluorescence imaging of tumor margins, the technique promises to guide the oncologic surgeon towards optimal radical resection and clinical results.



Preclinically, optical imaging has been employed in tumor identification; image-guided resection; therapy monitoring; and detection of sentinel lymph nodes. Because tumor-specific agents were not yet approved for clinical use, the first clinical studies were performed using non-specific fluorescent agents that had long been approved for different applications and could therefore be used for sentinel lymph node mapping.(6, 7) Clinical trials of tumor imaging using indocyanine green have been reported in hepatobiliary and colorectal cancer.(8) Recently, a milestone step was completed when the first in-human trial was reported using tumor-specific targeting,(9) marking the beginning of a new phase of optical image-guided surgery.

However, although it is very likely that the technique will deliver an important contribution to surgical oncology, there are fundamental limitations to this approach that influence the ability to differentiate the targeted tissue from its surroundings. Now that the first clinical trial has been reported, the group of oncologic surgeons that gets acquainted with the flourishing field of optical image-guided surgery is increasing day by day, with clinical consequences at stake. As we will show, it is essential for the clinician to understand which phenomena occur when photons travel through tissues and how these phenomena influence the optical image that is acquired. We therefore believe that it is now, more than ever, of paramount importance to provide the surgical oncologist a clear overview of the basic principles of optical image-guided surgery in order to be able to understand how these limitations influence the sensitivity of this technique. Awareness of these limitations and focusing research on solving these challenges is of utmost importance for proper implementation and evaluation of the clinical value of this new technology.

## The basic principle of fluorescence imaging

The geometrical principle of fluorescence imaging is illustrated in Figure 1a. A light source is required that sends out a bundle of light with a specific wavelength that is able to excite the fluorophore (i.e., excitation photons). Because the targeted fluorophore is located under the tissue surface, this excitation light has to enter and travel through tissue to reach the fluorophore. Light entering the tissue is partly influenced by reflection and refraction at the tissue surface. The direction of photons that travel through the tissue can be changed due to scattering. In addition, photons can be absorbed by various components in the tissue. Only when such a component is a fluorophore, which can be either an intrinsic tissue component (i.e., autofluorescence) or an injected external fluorescent agent, absorption of a photon results in a gain in energy of the fluorophore which then enters an excited state (Figure 1b). The electrons remain in this state for about $10^{-8}$ seconds depending on the molecule, which is called the lifetime of the fluorophore. After this phase, the system returns to its ground state and emits the photon, which could be heading into all directions (Figure 1b). The change in energy between the absorbed and the emitted photon results in a change in wavelength. This shift of shorter wavelengths (higher energy) of the absorption spectrum to longer wavelengths (lower energy) of the emitted fluorophores is called the Stokes shift. After excitation of the fluorophore, emission photons will also be influenced by scattering

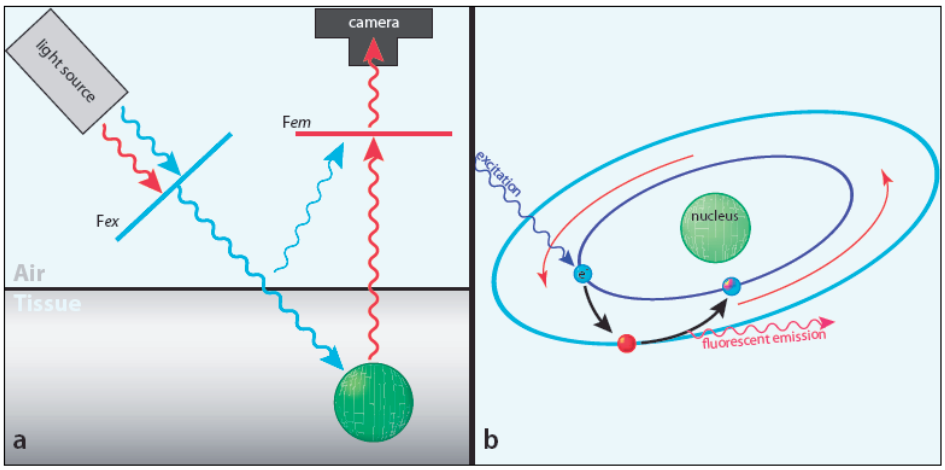


**Fig. 1.** Geometrical and basic principle of fluorescence imaging. (a) Light of the appropriate excitation wavelength is selected using a filter (F*ex*), which is located between a light source and the tissue. The excitation light travels through the tissue and is absorbed by a fluorophore, which subsequently emits light of a different wavelength. A small portion of this emitted light will exit the tissue and can be detected with a camera. A filter (F*em*) is placed in front of the camera, which allows only the emitted light to pass into the camera. (b) Absorbed light by the fluorophore instigates an electron (e) in the ground state towards an electronically excited state. Upon return to the ground state, the fluorophore emits a photon. The wavelength of this emitted photon is specific for the fluorophore. Fex, excitation filter; Fem, emission filter; e, electron

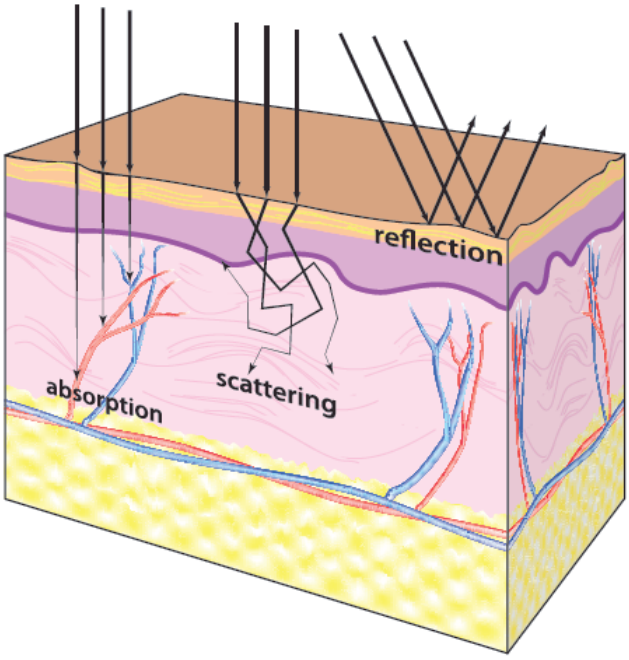


**Fig. 2.** Light propagation through tissue. Light travelling through tissue is subject to reflection, scattering and absorption.



and absorption, and the photons that reach the tissue surface will subsequently be influenced again by reflection and refraction at the surface. Finally, in a clinical geometry, only part of these photons can eventually be detected by the camera system. Although optical imaging is based on the detection of photons, Figure 2 illustrates that the path that photons travel through the imaged tissue is influenced by optical properties of the components in the tissue (i.e., absorption and scattering). As a result, fluorescence images will display intensities that are strongly influenced by varying absorption properties of the tissue and the images may be blurred due to scattering of light. The following paragraphs explain in detail how these phenomena influence the acquired image.

## What happens when light travels through tissue?

### *Absorption*

All tissues contain components that can absorb photons that travel through them. The composition of these components varies between different tissue types and organs, but also within these tissues, and may vary in time.(10) In general, the most relevant absorbers of photons are water, lipids, oxyhemoglobin and deoxyhemoglobin (Figure 3a).(11) Blood is the main absorber in the visible region, and the absorption of light by blood is the highest in the blue-green region. This fact can be illustrated by illuminating the human skin with white light.

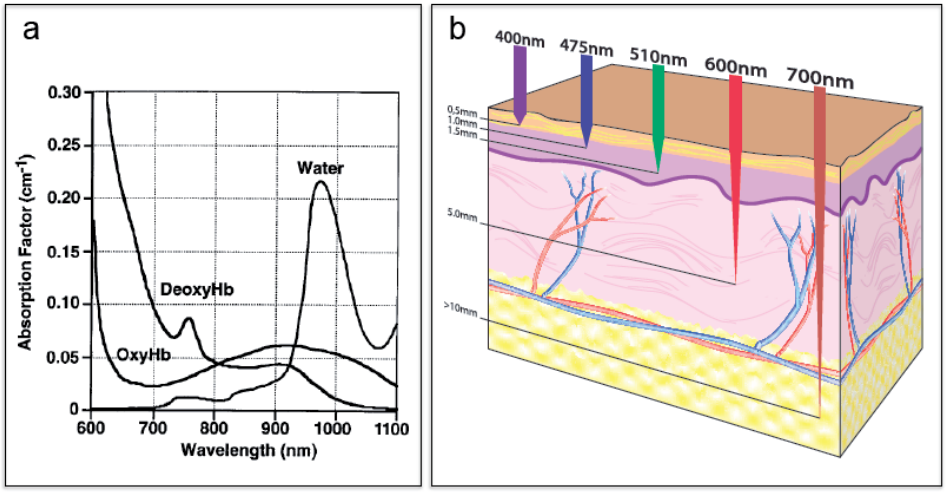


**Fig. 3.** Absorption of light. (a) Absorption of light by various components varies over the wavelength spectrum, resulting in an optimal window for fluorescence imaging in the NIR light region between 650 and 900 nm. Figure reprinted from Chance, B.[43] with permission, copyright clearance center rightslink. (b) Penetration of light range from 0.5 mm to >10 mm contingent to the wavelength. OxyHb, oxygenated hemoglobin; DeoxyHb, deoxygenated hemoglobin.

Due to absorption of photons with shorter wavelengths, a reddish reflection returns from the skin. In this way, absorbers influence the color of the light that exits imaged tissues. In the NIR range, the absorbance per volume of these components is much lower than in other parts of the spectrum, allowing for deeper penetration of photons into the tissue (Figure 3).

### *Scattering*

Next to absorption of the photon, a change in photon direction can occur, an effect known as scattering (Figure 4). In most part of the visible and NIR region, scattering events occur much more frequently than absorption events. Even though a forward direction of scattering photons is most likely to occur in tissues, the accumulation of multiple consecutive scatter events will result in a gradual randomization of the propagation direction (i.e., diffuse light, Figure 4).(12) Randomization of the direction of light reduces the signal strength as well as the accuracy of determination of the source localization. However, scattering can also have a positive effect on the fluorescence signal intensity because of its effect on the excitation light. The photons that excite the fluorophore follow a similar contorted light path as the emission light. In highly scattering tissue, the contorted light path causes retention of photons in that specific area. In other words, in a highly scattering medium, the photons bounce around locally for a longer time, increasing the chance for a fluorescence event. Consequently, there can be increased fluorescence intensity in tissues with more scattering compared to tissues with less scattering.(13) The net effect of scattering on fluorescence imaging depends on the exact optical properties of the tissue at hand.

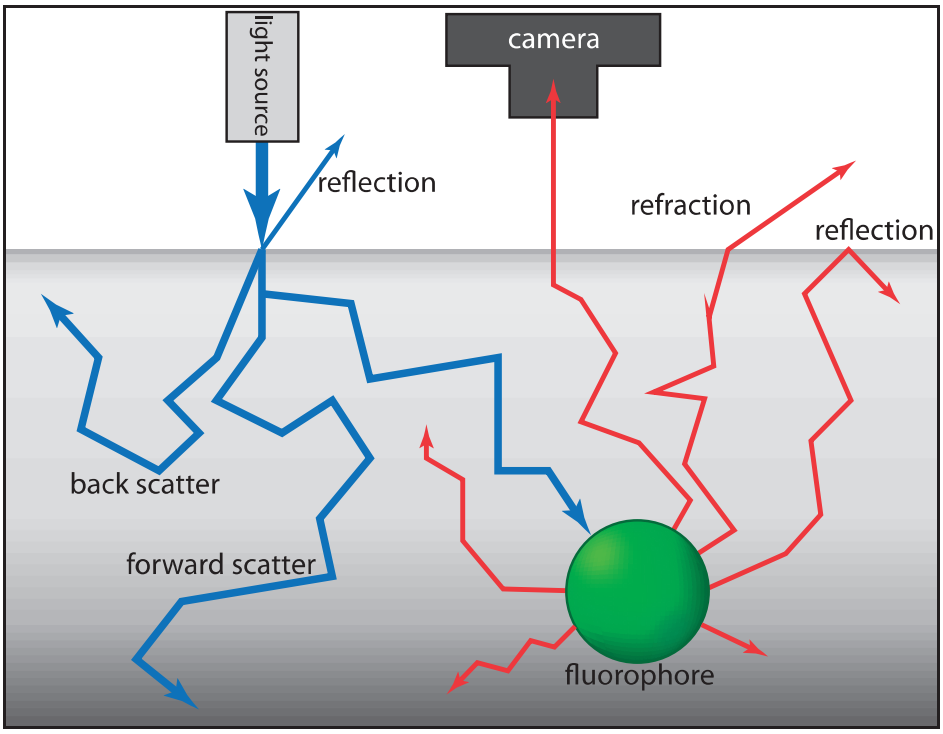


**Fig. 4.** Photons change direction multiple times when traveling through tissue. In the case of *forward scatter*, a photon travels more or less in the same direction before and after the scattering event, in the case of *backscatter* the photon will end up traveling in the opposite direction after the scattering event. During fluorescence imaging, the direction of both the excitation light as well as the emitted light is randomized due to scattering. Only a small portion of the excitation light will reach a fluorophore, and only the camera will capture a small portion of the emitted light. As a result, it is often difficult to pinpoint the exact origin of the detected fluorescent signal.



### *Influence of optical properties on light penetration depth*

Scattering and absorption coefficients vary between locations and tissues due to the different components within the heterogeneous tissue. Importantly, the influence of these phenomena on the fluorescence signal will be higher when fluorescent light has to emerge from larger tissue depths and consequently has to pass more absorbers and scattering events. In the visible light region, absorption by biological chromophores limits the penetration depth to a few millimeters with a maximum of 10 millimeter. Due to less absorption and scattering, penetration depth is increased to more than a centimeter in the NIR region,(14, 15) however strongly depending on the type of tissue.(1, 3, 16) The consequences of these effects are essential for understanding the limitations of optical image-guided surgery: at the surface, fluorescent agents will appear as a bright and sharply delineated spot. However, the target will always be surrounded by a halo of fluorescent light that was directed into

the tissue after emission, scattered around locally, and emitted from the surface at some distance from the target location. Moreover, due to absorption and scattering, an identical fluorescent agent that is located deeper within the tissue will have lower signal intensity and will be imaged as an indistinct blob (Figure 5).

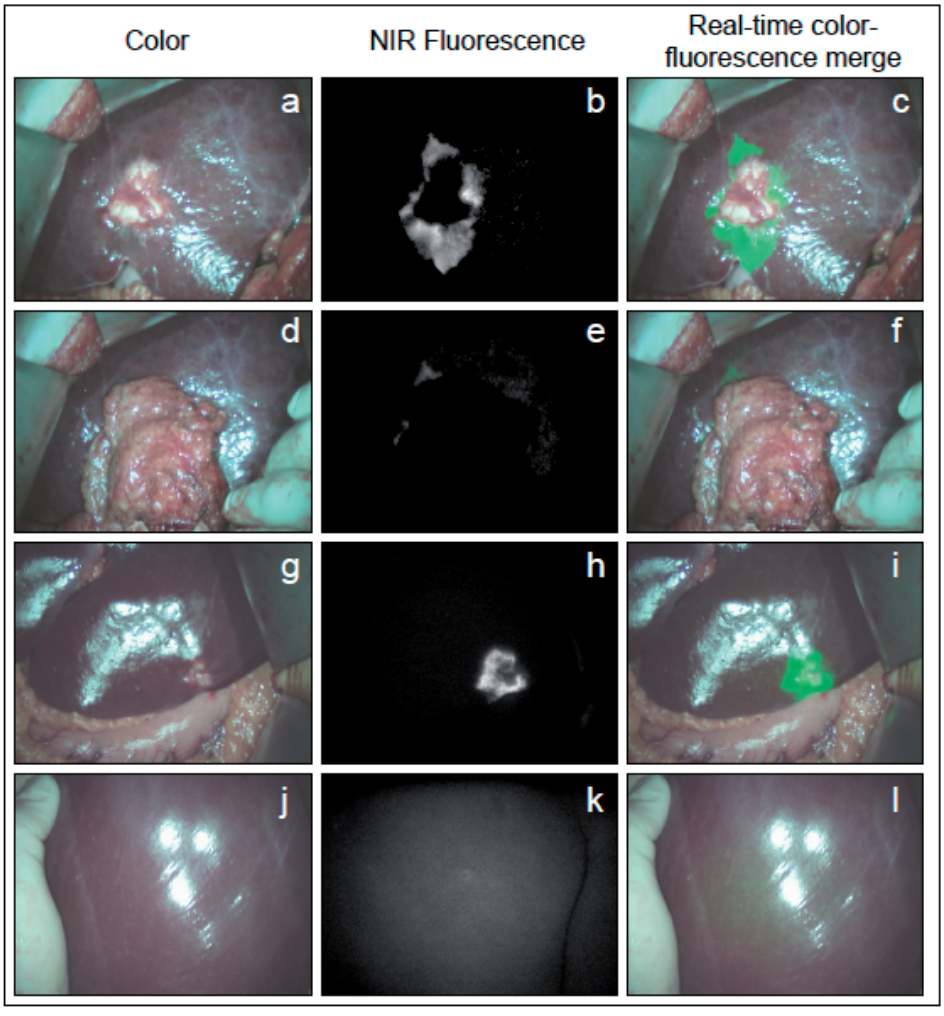


**Fig. 5.** Effect of optical tissue properties during real-time intraoperative optical imaging of liver metastases in humans. A liver metastasis is delineated by fluorescence signal (a-c). When a thick layer of greater omentum covers the area of interest, fluorescence signal is not detected (d-f).
A second liver metastasis is indicated in (g-i) in a different patient. However, when the liver is flipped around and the opposite side is imaged, high absorption of the liver that is saturated with blood results in an indistinct fluorescent blob (j-l).

### *Reflection and refraction*

As imaging during surgery always focuses on a surface, the mismatch between the indices of refraction of tissue and air is unavoidable, resulting in a change in direction of the photons. This mismatch in index of refraction causes reflections to occur at the surface. The excitation light will be partially reflected from the surface, like the sun on a water surface. When the light is nearly perpendicular to the surface of the tissue, the surface reflection is not more than a few percent. However, emitted fluorescent light that is generated inside the tissue is diffuse, and partly reaches the surface under large angles resulting in complete reflection within the tissue. This internal diffuse reflection coefficient at the surface can be in the order of 50%. Consequently, the emitted fluorescent light is even more diffuse and the amount of light that escapes the surface and can be detected by the fluorescence camera is further decreased.

## Fluorescence imaging and autofluorescence



The goal of fluorescence imaging is to detect a target by its specific fluorescence signal. Detection of the fluorescent signal of the targeted fluorophore is hampered because all cells contain various endogenous fluorophores that become fluorescent when excited by ultraviolet, visible, or NIR radiation of suitable wavelength. This intrinsic fluorescence of the tissue induces a non-specific background signal. The number of endogenous fluorophores varies strongly between tissue types. Moreover, the autofluorescence can change in time because of bleaching of the endogenous fluorophores, and because some of the endogenous fluorophores are related to metabolism (e.g., NADH, NAD, FAD, and FADH).

Because we can see cancerous lesions with our eyes, the optical properties of these lesions are changed by definition, and a difference in autofluorescence signal compared to the surroundings can be detected. This effect has been used for autofluorescence-guided surgery.(17) However, due to the aforementioned effects, "tumor-specific" autofluorescence signals can vary over time, making it an unreliable target. Furthermore, other benign visible changes (e.g. scar formation) also result in a change in autofluorescence, limiting the specificity of this technique.(18) But most importantly, despite positive correlations that have been reported in a number of studies that use autofluorescence to detect and remove the tumor,(17) it is not clear which biological aspects are responsible for the change in autofluorescence signal in the imaged lesions. Studies to assess these aspects are compromised because of artefacts as a result of color changes in cancer tissue.(18) The surgeon should therefore approach changes in autofluorescence with the same level of uncertainty as visible clues of cancerous tissue. If high correlation of autofluorescence and tumor tissue are consistently reported, they can be used to aid the surgeon in assessing the tumor margins, but should not be considered as tumor-specific proof of tumor margins.

As a good alternative, a target-specific agent that contains a fluorophore is usually injected intravenously. Now that we understand how optical properties can influence the optical path of the photon, we are confronted with a second challenge: how can we

determine if the photon that we detect has been excited by the targeted fluorophore, and not by its surrounding autofluorescent components?

For the targeted cancer cells to be detected, the signal of the target-specific fluorescence agent must be significantly higher than the non-specific autofluorescence. Although autofluorescence is much lower when NIR light is used, the signal-to-background ratio (SBR) must be sufficient in order to distinguish the photons of the target-specific fluorescent agent from the autofluorescence signal.

## What are the consequences of these effects for fluorescence imaging of cancer?

We have now set the stage for optical imaging in tissues and gained a clear picture of the problems that we face when we aim to detect a minimal amount of tumor-specific fluorescence agent within this diffuse heterogeneous medium containing absorbers, scatter events and endogenous fluorophores. Firstly, the fluorescence intensity is not only influenced by the concentration and fluorescence quantum yield of the fluorescent agent, but also by the tissue optical properties that are involved. For example, as a result of absorption by blood, fluorescence signals in organs with high blood volumes such as the liver,(19) highly vascularized tumors, or in tumor cells that co-opt host vessels(20) may appear lower than surrounding less-absorbing tissue, even if they contain larger amounts of contrast agent compared to the surrounding tissue.(21) Similarly, less-absorbing lesions (e.g., cysts, lymph nodes) may appear brighter in a heterogeneous environment. The variability in absorption and scattering between different tissues or even tissue components should be taken into account during the process of image-guided surgery. Secondly, intraoperative camera systems will not only detect the fluorescence signal of the fluorescent agent, but also the autofluorescence in the scanned region and therefore a sufficient SBR is required. At present, various strategies are being evaluated that attempt to improve adequate identification and quantification of the targeted photons.

## Strategies to reduce the influence of absorption and scattering on the image

With the state of the art technological advancements, it remains impossible to determine all absorbers and scatter events within a diffuse, inhomogeneous medium. However, calculation methods have been developed that try to estimate the perturbation caused by optical tissue properties and improve the image by partly correcting for these properties.(14) An intraoperative fluorescence imaging system has been developed that implements such a correction scheme for light intensity variation in tissues.(21) Improved accuracy was demonstrated within phantoms and tissues postmortem, independently of optical property variation in tissues. At a five-fold change of absorption variation within the fluorescent lesions, quantification errors were reduced from 25% in uncorrected images to 8% using the correction scheme.(21)

A second new technology that is investigated in this field is fluorescence differential path length spectroscopy, which determines fluorophore concentration based on the fluorescence intensity corrected for absorption.(22) This facilitates quantitative concentration measurements even for strong variations in either background absorption or scattering. However, this method can currently only be performed using fiberoptic measurement at a single point. An imaging version and subsequent intraoperative applications have not been developed yet. Finally, tomographic reconstruction techniques (23) Raman spectroscopy (24) and photoacoustic imaging (12, 25) may play important future roles, although currently not suited for real-time imaging in the surgical theatre. Raman spectroscopy is based on inelastic scattering: the effect on the frequency of excitation photons that changes upon interaction with tissue, which is independent of optical tissue properties or autofluorescence. (24, 26) In surface-enhanced Raman spectroscopy (SERS), tumor-specific nanobodies are injected that are able to increase the intrinsically very low Raman effect, thereby improving detectability. Promising preclinical results of brain tumor resection guided by SERS have been reported.(27) In photoacoustic imaging (also referred to as optoacoustic imaging), thermoelastic expansion of molecules resulting from laser pulse irradiation causes emission of acoustic waves that can be measured by photoacoustic spectroscopy. The resolution in photoacoustic imaging is not limited by tissue scattering but by the attenuation of acoustic frequencies by tissue.(12, 25) This technique improves deep-tissue imaging, but is less suitable for image-guided surgery.



## Strategies to distinguish the target-specific fluorescence signal from autofluorescence

There are currently two methods under investigation that attempt to separate the target-specific fluorescence signal from the non-specific autofluorescence (i.e., fluorescence of normal components of the tissue). The first is based on differences in the fluorescence spectrum between photons from these two fluorescent sources (i.e., spectral unmixing), and the second method exploits differences in fluorescence lifetime of the fluorophores (i.e., lifetime imaging).

The concept of spectral unmixing is based on the "signature" emission intensity that each fluorophore has at certain wavelengths, providing the fluorophore with its own specific emission spectrum.(28) Using spectral unmixing, the signal is decomposed into a collection of predefined spectra that is used to determine the individual contribution of each fluorophore. Using calculation models combined with the fluorophore specific emission spectrum as reference (i.e., linear unmixing), the contribution of each fluorophore in a total fluorescent signal can be extracted.(29) When spectral signatures of the fluorophore of interest and the autofluorescence are known, unmixing these specific fluorescence spectra may result in a more accurate SBR. The first in-human trial on intraoperative tumor-specific fluorescence imaging was performed using a camera system that was based on spectral unmixing technology.(9, 21) There are however fundamental problems with

this approach. Linear unmixing is based on the assumption that the measured spectrum consists of the sum of the fluorescence spectra of all the components in the tissue, i.e., linear mixing. As mentioned earlier, inhomogeneous optical properties influence the path that photons travel through the imaged tissue and therefore not only put their own signatures on the fluorescence spectrum, but may also do so non-linearly because of the inhomogeneous nature of tissue. Furthermore, the unmixing procedure is a very complex process that requires that all components that contribute to the spectrum are known, as well as all of their specific "signature" spectra, which also need to be sufficiently distinctive from one another.

The second method, fluorescence lifetime imaging, distinguishes individual fluorophores by their specific temporal decay after excitation. This fluorescence decay (i.e., lifetime) is a fluorophore-specific characteristic that is not influenced by the local concentration of fluorophores, the optical path, the local excitation intensity, or the local fluorescence detection efficiency. To acquire the characteristic decay curves, a picosecond laser pulse is used for excitation and fluorescence is measured as a function of time. Based on the specific lifetime of the fluorophores, the target-specific fluorescence signal can be distinguished from the non-specific autofluorescence. In addition, the temporal response at which photons emerge from the tissue can be measured (i.e., time-domain imaging), which is used to estimate the concentration and depth of the fluorescent source. Lifetime imaging requires specific conditions in terms of pulsed excitation and data capturing with complex data processing, which currently makes it a time-consuming technique. Although intraoperative lifetime based techniques are being developed at a strong pace and hold promising advantages, it will take some time before they can be used in a real-time intraoperative setting where mobility of the equipment and speed of data processing and interpretation are of the essence.(30)

## What is required for a target-specific fluorescence image?

So far, we have assumed that the fluorescent agent has been able to specifically target the tissue of interest with subsequent co-localization between the fluorescent signal and tumor cells. However, in order to gain a complete insight into the different phenomena that can influence the optical image, it is necessary to understand the challenges of tumor-specific targeting.

Based on the hallmarks of cancer,(31) a growing variety of tumor-specific targets are available for imaging of cancer.(2) The efficiency of target-specific agents to reach their intended target is defined by many variables, including affinity of the agent and abundance of the target receptors or epitopes.(16) In order to achieve target-specific fluorescence imaging, the contrast agent has to be delivered to the target, requires adequate contact time with the target for binding to occur, and has to be retained by the target while non-bound agents are cleared from the circulation.(10) It has been reported that at saturating doses of the agent, high affinity antibody uptake is dependent on antigen expression levels. However, at subsaturating doses, the signal is generally limited by delivery of the agent.(32)

For the agent to be effectively delivered to the target, many barriers in the human body have to be passed. Next to inhibitor proteins present in plasma that can non-specifically

bind to the agent,(1) walls of blood vessels provide a first barrier for drug delivery to targeted tumor tissues. In most cases, abnormal neovascularization of the tumor occurs (i.e., enhanced permeability and retention (EPR) effect) resulting in leaky tumor blood vessels.(33) As a result, macromolecular drugs can traverse the endothelium of these leaky blood vessels and passively accumulate in the interstitium of tumor tissues.(33) However, the EPR effect is largely dependent on the size of the agent; larger agents are less efficient in crossing the endothelial barrier.(34)

Tumor growth beyond the size of approximately 1 mm is dependent on oxygen and supply of nutrients, and therefore requires angiogenesis.(35) However, in smaller lesions, the angiogenic switch may not have occurred and drug delivery could be hampered due to the lack of adequate vascularization. In other cases, tumor cells may grow alongside preexistent host vasculature, a process known as vessel co-option.(20) In these cases where angiogenesis-directed targeting may not yet be possible, indirect indicators of tumor growth could be useful for tumor detection, even in the earliest stages of carcinogenesis. For example, NIR fluorescence agents that detect proteases that are involved in migration of tumor cells and degradation of the extracellular matrix can allow for imaging of the invasive tumor front(36-38) and preneoplastic lesions in Barrett's esophagus can be identified by targeting changed patterns of lectin binding.(39)



Once extravascular, two barriers for adequate binding of the agent remain. First the agent has to cross extracellular matrix tissue surrounding the target cells.(33) At this point, diffusion into the tumor is sometimes impeded by high hydrostatic pressure of many solid tumors, preventing homogeneous infiltration of the agent.(1) Next, binding of the agent to specific epitopes of the cancer cell has to occur, and internalization of the agent can further amplify the fluorescence signal.(23, 40, 41) Therefore, the cellular basement membrane is the third barrier, which can be passed using the transporter system of the cell by receptor-mediated endocytosis.(33) Finally, clearance of non-bound agent from the circulation is required to provide sufficient SBRs. This occurs through the liver (i.e., excretion into bile and feces) and/or the kidney (i.e., excretion into urine). Both the route of clearance and the clearance rate are important determinants for the blood half-life time and consequently the background signal and optimal imaging time of contrast agents.(40)

## How relevant is all this for the clinical practice of surgical oncology?

Optical imaging is a complicated process. In order to adequately interpret the intraoperative fluorescent image of the tumor that is presented, the surgeon should comprehend that the target-specific fluorescent agent had to get to and stay at the tumor, that part of the signal was reduced and distorted by absorbers and scatter events, and that the signal had to be subtracted from its autofluorescent surroundings. Considering all these influences that could hamper detection of cancer cells that are located under the surface, the additional value of NIR fluorescence imaging over conventional surgery could be questioned. After all, after a mere three decades of extensive research, the fundamental principles of optical

imaging still leave room for error and it currently seems that this approach will never be unambiguous.

In order to determine the additional value of intraoperative optical imaging, we need to ask ourselves what the fundamental purpose of this tool should be for surgical oncology. In essence, the goal of surgery is to remove all cancer cells while minimizing damage to surrounding healthy tissues. Considering the small size of a single cancer cell or group of cells, the limited target epitopes available for the fluorescent agent and the optical tissue properties and autofluorescence, detection of the last cancer cells under a surface will not always be possible. Nevertheless, it is very likely that the current technique of optical imaging, with its limitations, will offer improvement of the conventional surgical practice to successfully treat the patient and could provide a final solution to the conundrum of irradical resection.

The most obvious reason is that, although there are limitations when considering the cellular level, optical imaging allows for a more detailed delineation of the tumor margins than the conventional practice of assessment by palpation and visual aspects of the tumor. It was repeatedly shown in animal models that tumor margins can be clearly demarcated by optical imaging.(10, 38, 42) Consequently, the surgeon can resect the tumor based on these images with the required tumor-free margin outside the fluorescent tissue. Moreover, in some cases that have thin tumor strands that are invisible to the naked eye, a tumor-free margin of up to several centimeters is required for local control using conventional surgical practice. Although effects of scattering could result in a fluorescent halo of up to several millimeters under certain conditions, detection of these tumor strands using optical imaging would still largely reduce the need of these large tumor-free margins, resulting in improved postoperative functionality. Although yet to be proven in large clinical trials, it is anticipated that this will already lead to a decrease in local recurrence rate and improved patient survival and functionality.

Secondly, it has been suggested that penetration depth limitations might not be relevant for surgical practice because the surgeon will, by definition, bring the area of interest closer to the surface during the surgical procedure.(34, 43) When, after resection of the tumor mass, an area is found with persisting fluorescence signal indicating irradical margins, this could be resected subsequently until no more signal is found in a "cut the light-procedure", similar to the technique of Mohs surgery. Although a similar procedure, optical imaging will be much more efficient than Mohs surgery due to real-time acquisition and the fact that intraoperative pathological evaluation is not required. At the surface, the influence of optical properties will be minimized, improving the sensitivity even in cases of perineural or perivascular growth, as long as the photons from the contrast agent can be differentiated from autofluorescence.

Finally, although it is currently impossible to completely correct for an unknown variability in optical properties of the tissue, we should not forget that there is a very advanced system available that is highly capable of identifying distinct tissue components (e.g. blood vessels) during the surgical process: the surgeon itself. The true additional

value of this technique will become clear once the surgical expertise to distinguish tissue components becomes incorporated into the interpretation of the images. For example, the surgeon would preferable reinvestigate a suspicious region that has no fluorescence signal if it is covered by a blood vessel as long as the surgeon realizes that vessels can be highly absorbent. Using the knowledge about the tissues at hand, optical image-guided surgery will result in a dynamic and flexible process providing the surgeon with valuable additional information during the entire operation. This will likely require a learning curve that would follow the encouraging example of pioneer work in resection of malignant gliomas using 5-aminolevulinic acid. Preliminary intraoperative studies in this field provide detailed reports on these learning processes.(44, 45) These showed that photons are highly absorbed by blood or cauterized tissue debris after monopolar cautery resection and that suction of these layers or rinsing the surface with saline is required for unperturbed assessment of tissue fluorescence. Furthermore, necrotic tumor centers accumulated little fluorescence, which was not a problem because necrosis could easily be distinguished under white light and therefore did not impair fluorescence-guided tumor resection. Tissues were not falsely labeled by fluorescence from blood contaminating the tumor cavity, which might have been expected if plasma had contained substantial amounts of fluorescent agent. Photobleaching after overexposure was minimized with improved development of fluorophores. Finally, the fluorescent source could be located by manipulation of the tissues as illustrated in Figure 5. The success of this approach has led to a randomized controlled multicenter phase-III trial demonstrating improved progression-free survival in patients with malignant glioma using fluorescence-guided surgery.(46)



## What level of accuracy is required for the routine of surgical practice?

Considering the intraoperative flexibility of a trained surgeon and the practice of exploration of the area of interest during surgery, we believe that optical image-guided surgery has the potential to largely reduce the tumor-free safety-margin. If a tumor-free margin around the tumor could be minimized, postoperative functional outcome could be drastically improved in many cases where the tumor is surrounded by important anatomical structures. This would require tumor imaging with optimal sensitivity and specificity of the tumor-specific agent, followed by resection of the fluorescent tissue without any excess margin of healthy tissue. It is anticipated that sensitivity and specificity of the target-specific agent will be optimized by simultaneously targeting multiple tumor characteristics at different wavelengths.(42, 47) In order to adequately assess the fluorescent border, high accuracy of the imaging technique is demanded. This would require high-resolution images that can be acquired at higher magnifications than the regular macroscopic field of view. Although not suitable for intraoperative use, a system that incorporates both macroscopic and microscopic imaging has been tested in an experimental setting of cancer detection.(23) In the macroscopic field of view, the smallest lesion detectable with a highly expressed antigen

(e.g., several million antigens/cell) was approximately 600 μm, a volume that approaches pixel resolution of the macroscopic images (110 μm/pixel). Higher magnification of this tumor revealed images down to the single cell level due to higher resolution.(23) An example of improved resolution using this system is shown in Figure 6.

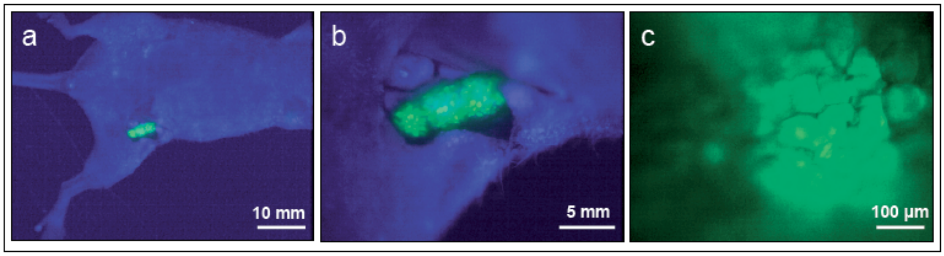


**Fig. 6.** Real-time magnification. RFP-GFP-transfected rhabdomyosarcoma cells were injected into the mammary fat pad of a mouse. Increased real-time magnification from a to c results in improved resolution.

These results suggest that incorporation of zoom-function into the intraoperative camera system would improve surgical accuracy by using a combination of macroscopic imaging (to survey the tissue and guide tumor resection) and microscopic imaging (to verify clean resection margins).(40) However, scattering generally determines the sharpness of the in vivo fluorescence image, especially for deeply located fluorescent sources, and not the imaging equipment. Furthermore, microsurgical or robotic camera systems are only used in some oncological surgical specialties (e.g. neurosurgery). Therefore, in daily routine and logistics of surgical practice in most other cases, the tremor of the surgical hand will limit removal of the tumor with accuracy smaller than 0.5 mm. As a result, the accuracy of removing the fluorescent tissue will not only be limited by the resolution of optical imaging, but also by the practical limitations of the surgical hand. As long as microscopic or robotic surgery is no routine practice, the discussion on the level of resolution will therefore lie within the margin of technical surgical possibilities. In analogy to highly accurate stereotactic radiotherapy using Cyberknife® that has a technical error-margin of 0.5-2 mm,(48) it is very likely that this level of accuracy will be sufficient to adequately treat the patient with minimal unnecessary loss of functionality.

## Challenges for clinical translation

Although a rapidly increasing amount of data is supporting the additional value of optical image-guided surgery for cancer therapy, challenges remain in translation of the preclinical experimental setup into routinely clinical practice.(2, 6) The technique requires development of tumor-specific fluorescence agents and dedicated intraoperative camera systems. Important progress has been made over the last years in both fields, but it is essential to identify the hurdles that are still impeding successful clinical translation.

An intrinsic limitation of development of fluorescence tumor-specific agents is the fact that such drugs are used as diagnostic tools instead of therapeutic drugs that require administration over a longer period of time. Development of diagnostic drugs is therefore subject to lower financial incentives for pharmaceutical companies. The first obvious steps were taken by conjugation of already clinically available tumor-specific agents (e.g. Cetuximab) to fluorophores.(2, 49) Until the technique will become available at a large scale, further development of these agents will have to be performed by non-profit (i.e. academic) organizations. Furthermore, dedicated imaging systems will have to become easily available for a large group of surgeons to stimulate adoption of the technique. Currently, the most advanced systems are still only available in the research setting of clinical trials,(7, 9) while other systems are already commercially available. (50, 51) These economic and implementation issues are critical for successful adoption of surgical optical imaging.



## Conclusion

Optical imaging has the potential to revolutionize cancer surgery by real-time fluorescence guidance in discriminating between healthy and diseased tissues and identifying vital structures. However, absorption, scattering and autofluorescence are fundamental optical tissue properties that influence the images and limit the ability to differentiate the targeted tissue from its surroundings. In pursuit of removing all cancer cells by resection of the total tumor-specific fluorescence signal, the oncologic surgeon should carefully consider these limitations during the process of image-guided cancer surgery. Although there are limitations to the intrinsic capacity of the technique, when practical and technical surgical possibilities are considered, optical imaging can be a very powerful intraoperative tool in guiding the future oncologic surgeon towards radical resection and optimal clinical results.

## Acknowledgements

We thank R.H. Thoene for her technical support and valuable contributions to this work. Figure 6 was produced by I. Que (Leiden University Medical Center), G. Bouw (Olympus Netherlands), Werner Kammerloher (former employee Olympus) and E.L. Kaijzel (Leiden University Medical Center).

## References

1. Frangioni JV. New technologies for human cancer imaging. J Clin Oncol. 2008;26:4012-21.
2. Keereweer S, Kerrebijn JD, van Driel PB, Xie B, Kaijzel EL, Snoeks TJ, et al. Optical image-guided surgery--where do we stand? Mol Imaging Biol. 2011;13:199-207.
3. Weissleder R, Pittet MJ. Imaging in the era of molecular oncology. Nature. 2008;452:580-9.
4. Rassmussen-Taxdal DS, Ward GE, Figge FH. Fluorescence of human lymphatic and cancer tissues following high doses of intravenous hematoporphyrin. Cancer. 1955;8:78-81.
5. Patterson MS, Chance B, Wilson BC. Time resolved reflectance and transmittance for the non-invasive measurement of tissue optical properties. Appl Opt. 1989;28:2331-6.

6. Keereweer S, Hutteman M, Kerrebijn JD, van de Velde CJ, Vahrmeijer AL, Lowik CW. Translational Optical Imaging in Diagnosis and Treatment of Cancer. Current pharmaceutical biotechnology. 2012.
7. Mieog JS, Troyan SL, Hutteman M, Donohoe KJ, van der Vorst JR, Stockdale A, et al. Toward optimization of imaging system and lymphatic tracer for near-infrared fluorescent sentinel lymph node mapping in breast cancer. Annals of surgical oncology. 2011;18:2483-91.
8. Schaafsma BE, Mieog JS, Hutteman M, van der Vorst JR, Kuppen PJ, Lowik CW, et al. The clinical use of indocyanine green as a near-infrared fluorescent contrast agent for image-guided oncologic surgery. Journal of surgical oncology. 2011;104:323-32.
9. van Dam GM, Themelis G, Crane LM, Harlaar NJ, Pleijhuis RG, Kelder W, et al. Intraoperative tumor-specific fluorescence imaging in ovarian cancer by folate receptor-alpha targeting: first in-human results. Nature medicine. 2011;17:1315-9.
10. Frangioni JV. In vivo near-infrared fluorescence imaging. Curr Opin Chem Biol. 2003;7:626-34.
11. Chance B. Near-infrared images using continuous, phase-modulated, and pulsed light with quantitation of blood and blood oxygenation. Ann N Y Acad Sci. 1998;838:29-45.
12. Ntziachristos V. Going deeper than microscopy: the optical imaging frontier in biology. Nat Methods. 2010;7:603-14.
13. Star WM. Light dosimetry in vivo. Phys Med Biol. 1997;42:763-87.
14. Bogaards A, Sterenborg HJCM, Wilson BC. In vivo quantification of fluorescent molecular markers in real-time: A review to evaluate the performance of five existing methods. Photodiagnosis and Photodynamic Therapy 2007;4:170-78.
15. Farrell TJ, Patterson MS. Diffusion modeling of fluorescence in tissue. In: Mycek M, Pogue BW, editors. Handbook of biomedical fluorescence. New York; 2003. p. 29-60.
16. Hilderbrand SA, Weissleder R. Near-infrared fluorescence: application to in vivo molecular imaging. Curr Opin Chem Biol. 2010;14:71-9.
17. Poh CF, Zhang L, Anderson DW, Durham JS, Williams PM, Priddy RW, et al. Fluorescence visualization detection of field alterations in tumor margins of oral cancer patients. Clinical cancer research : an official journal of the American Association for Cancer Research. 2006;12:6716-22.
18. De Veld DC, Witjes MJ, Sterenborg HJ, Roodenburg JL. The status of in vivo autofluorescence spectroscopy and imaging for oral oncology. Oral oncology. 2005;41:117-31.
19. Hutteman M, Mieog JS, van der Vorst JR, Dijkstra J, Kuppen PJ, van der Laan AM, et al. Intraoperative near-infrared fluorescence imaging of colorectal metastases targeting integrin alpha(v)beta(3) expression in a syngeneic rat model. Eur J Surg Oncol. 2011;37:252-7.
20. Holash J, Maisonpierre PC, Compton D, Boland P, Alexander CR, Zagzag D, et al. Vessel cooption, regression, and growth in tumors mediated by angiopoietins and VEGF. Science. 1999;284:1994-8.
21. Themelis G, Yoo JS, Soh KS, Schulz R, Ntziachristos V. Real-time intraoperative fluorescence imaging system using light-absorption correction. J Biomed Opt. 2009;14:064012.
22. Kruijt B, Kascakova S, de Bruijn HS, van der Ploeg-van den Heuvel A, Sterenborg HJ, Robinson DJ, et al. In vivo quantification of chromophore concentration using fluorescence differential path length spectroscopy. J Biomed Opt. 2009;14:034022.
23. Thurber GM, Figueiredo JL, Weissleder R. Detection limits of intraoperative near infrared imaging for tumor resection. J Surg Oncol. 2010;102:758-64.
24. Nijssen A, Koljenovic S, Bakker Schut TC, Caspers PJ, Puppels GJ. Towards oncological application of Raman spectroscopy. J Biophotonics. 2009;2:29-36.
25. Ntziachristos V, Ripoll J, Wang LV, Weissleder R. Looking and listening to light: the evolution of whole-body photonic imaging. Nature biotechnology. 2005;23:313-20.
26. Zavaleta CL, Kircher MF, Gambhir SS. Raman's "effect" on molecular imaging. J Nucl Med. 2011;52:1839-44.
27. Kircher MF, de la Zerda A, Jokerst JV, Zavaleta CL, Kempen PJ, Mittra E, et al. A brain tumor molecular imaging strategy using a new triple-modality MRI-photoacoustic-Raman nanoparticle. Nature medicine. 2012;18:829-34.
28. Mansfield JR. Distinguished photons: a review of in vivo spectral fluorescence imaging in small animals. Curr Pharm Biotechnol. 2010;11:628-38.

29. Zimmermann T. Spectral imaging and linear unmixing in light microscopy. Adv Biochem Eng Biotechnol. 2005;95:245-65.
30. Sun Y, Hatami N, Yee M, Phipps J, Elson DS, Gorin F, et al. Fluorescence lifetime imaging microscopy for brain tumor image-guided surgery. Journal of biomedical optics. 2010;15:056022.
31. Hanahan D, Weinberg RA. The hallmarks of cancer. Cell. 2000;100:57-70.
32. Thurber GM, Weissleder R. Quantitating antibody uptake in vivo: conditional dependence on antigen expression levels. Molecular imaging and biology : MIB : the official publication of the Academy of Molecular Imaging. 2011;13:623-32.
33. Fang J, Nakamura H, Maeda H. The EPR effect: Unique features of tumor blood vessels for drug delivery, factors involved, and limitations and augmentation of the effect. Adv Drug Deliv Rev. 2011;63:136-51.
34. Olafsen T, Wu AM. Antibody vectors for imaging. Semin Nucl Med. 2010;40:167-81.
35. Naumov GN, Akslen LA, Folkman J. Role of angiogenesis in human tumor dormancy: animal models of the angiogenic switch. Cell Cycle. 2006;5:1779-87.
36. Blum G, von Degenfeld G, Merchant MJ, Blau HM, Bogyo M. Noninvasive optical imaging of cysteine protease activity using fluorescently quenched activity-based probes. Nat Chem Biol. 2007;3:668-77.
37. Keereweer S, Mieog JS, Mol IM, Van Driel PB, Snoeks TJ, Baatenburg de Jong RJ, et al. Detection of oral squamous cell carcinoma and cervical lymph node metastasis using activatable near-infrared fluorescence agents. Arch Otolaryngol Head Neck Surg. 2011;137:609-15.
38. Weissleder R, Tung CH, Mahmood U, Bogdanov A, Jr. In vivo imaging of tumors with protease-activated near-infrared fluorescent probes. Nat Biotechnol. 1999;17:375-8.
39. Bird-Lieberman EL, Neves AA, Lao-Sirieix P, O'Donovan M, Novelli M, Lovat LB, et al. Molecular imaging using fluorescent lectins permits rapid endoscopic identification of dysplasia in Barrett's esophagus. Nature medicine. 2012;18:315-21.
40. Gioux S, Choi HS, Frangioni JV. Image-guided surgery using invisible near-infrared light: fundamentals of clinical translation. Mol Imaging. 2010;9:237-55.
41. Kovar JL, Volcheck W, Sevick-Muraca E, Simpson MA, Olive DM. Characterization and performance of a near-infrared 2-deoxyglucose optical imaging agent for mouse cancer models. Analytical biochemistry. 2009;384:254-62.
42. Keereweer S, Mol IM, Vahrmeijer AL, Van Driel PB, Baatenburg de Jong RJ, Kerrebijn JD, et al. Dual wavelength tumor targeting for detection of hypopharyngeal cancer using near-infrared optical imaging in an animal model. Int J Cancer. 2012.
43. Pleijhuis RG, Langhout GC, Helfrich W, Themelis G, Sarantopoulos A, Crane LM, et al. Near-infrared fluorescence (NIRF) imaging in breast-conserving surgery: assessing intraoperative techniques in tissue-simulating breast phantoms. Eur J Surg Oncol. 2011;37:32-9.
44. Stummer W, Stepp H, Moller G, Ehrhardt A, Leonhard M, Reulen HJ. Technical principles for protoporphyrin-IX-fluorescence guided microsurgical resection of malignant glioma tissue. Acta Neurochir (Wien). 1998;140:995-1000.
45. Stummer W, Stocker S, Wagner S, Stepp H, Fritsch C, Goetz C, et al. Intraoperative detection of malignant gliomas by 5-aminolevulinic acid-induced porphyrin fluorescence. Neurosurgery. 1998;42:518-25; discussion 25-6.
46. Stummer W, Pichlmeier U, Meinel T, Wiestler OD, Zanella F, Reulen HJ. Fluorescence-guided surgery with 5-aminolevulinic acid for resection of malignant glioma: a randomised controlled multicentre phase III trial. Lancet Oncol. 2006;7:392-401.
47. Xie BW, Mol IM, Keereweer S, van Beek ER, Que I, Snoeks TJ, et al. Dual-wavelength imaging of tumor progression by activatable and targeting near-infrared fluorescent probes in a bioluminescent breast cancer model. PLoS One. 2012;7:e31875.
48. Kilby W, Dooley JR, Kuduvalli G, Sayeh S, Maurer CR, Jr. The CyberKnife Robotic Radiosurgery System in 2010. Technology in cancer research & treatment. 2010;9:433-52.
49. Rosenthal EL, Kulbersh BD, King T, Chaudhuri TR, Zinn KR. Use of fluorescent labeled anti-epidermal growth factor receptor antibody to image head and neck squamous cell carcinoma xenografts. Mol Cancer Ther. 2007;6:1230-8.
50. Noura S, Ohue M, Seki Y, Tanaka K, Motoori M, Kishi K, et al. Feasibility of a lateral region sentinel node biopsy of lower rectal cancer guided by indocyanine green using a near-infrared camera system. Annals of surgical oncology. 2010;17:144-51.

51. Heath CH, Deep NL, Sweeny L, Zinn KR, Rosenthal EL. Use of panitumumab-IRDye800 to image microscopic head and neck cancer in an orthotopic surgical model. Annals of surgical oncology. 2012;19:3879-87.

52. Chance B. Near-infrared images using continuous, phase-modulated, and pulsed light with quantitation of blood and blood oxygenation. Annals of the New York Academy of Sciences. 1998;838:29-45.

# 9 Experimental aspects and limitations

When considering the history of other imaging modalities (e.g. CT, MRI, ultrasound and PET), one finds that the mean time-interval between first-in-human studies and routine clinical practice is 23 years.[1] The field of optical imaging in its current form has emerged since the start of the new millennium. As professor John V. Frangioni (Beth Israel Deaconess Medical Center, Boston, MA) has stated repeatedly, we are halfway the developmental stages of this technique and the next decade will determine if optical image-guided cancer surgery will establish a definite role in clinical practice.[1] The prosperity for image-guided head and neck cancer surgery is largely dependent on the evolution of clinically available NIR fluorescence agents and intraoperative camera systems that will be developed in other, larger-scaled, fields of oncologic surgery, including breast cancer and colon cancer. The absolute additional value of this technique can only be assessed in clinical trials. Therefore, it is of great importance that Van Dam et al. have recently reported the first in-human trial, marking the beginning of a new phase of optical image-guided surgery.[2] The following section discusses important aspects of the experiments as the were performed in this Thesis, as well as important issues that should be addressed in order to improve introduction of optical imaging into clinical trials.



## The immunodeficient animal model

Acceptance of biological differences between species is a prerequisite for experimental animal research. Ethics generally restrict scientists to animal models that are genetically and physiologically very different from the model for which most of the research is intended: the human species. However, animal models are not optimal and one should be very careful not to irrefutably extrapolate results from animal studies into human conditions with corresponding clinical premises. Therefore, the animal model should be carefully chosen, and its differences with the conditions for which the applications are intended should be considered meticulously.

In this thesis, we have chosen to use oral or hypopharyngeal squamous carcinoma cells that had been isolated from a human tumor. This is mandatory when investigating tumor-specific markers for detection of the tumor. In order to prevent rejection of the cancer cells by the immune system after inoculation, immunodeficient animals were used. The main advantage is that specificity of the targeting agents in this animal model will more likely be applicable for human tumor cells. However, the major disadvantage is that the tumor is growing in an immunodeficient environment. The tumor and its surrounding host tissue have extensive reciprocal effects that can have an important impact on the pathophysiology. These effects may also have significant influence on the use of NIR fluorescence agents, especially for the non-targeted group of agents.

An example was shown in Chapter 3, where non-targeted agents were used that are activated by proteolytic activity of cathepsins or matrix metalloproteinases. As explained in this chapter, these enzymes are also involved in inflammatory processes, which could interfere with the interpretation of the tumor margin. In theory, this could also hamper differentiation between reactive cervical lymph nodes and cervical lymph node metastases.

Furthermore, the EPR effect as described in Chapter 6 could in some cases be found in inflammatory tissues,[3] although it has been reported that the permeability and especially retention duration are much lower in infections.[4] In conclusion, for specific research regarding the influence of the immune system onto the detection of primary tumors and lymph node metastases, the effects could best be investigated in an immunocompetent animal model.

The effect of the immune system on the specificity of non-targeted NIR fluorophores should be clarified before these agents are used in the clinical setting. In order to test this in a mouse model, two different strategies could be used. The first strategy uses a syngeneic oral squamous carcinoma cell line. In this way, oral cancer cells derived from a mouse could be inoculated into the tongue of an immunocompetent mouse with the same genetic background resulting in a low risk of rejection, and the effect of the immune system could be studied carefully. The second setup would involve induction of the tumor in the animal model using carcinogenic agents. For example, the carcinogenic 4-nitroquinoline-1-oxide (4NQO) can be applied 3 times a week during 16 weeks resulting in mouse oral tumors that show strong similarities with human oral tumors.[5] This strategy has two important advantages. First, it does not require inoculation of allograft cells, which is always associated with a risk of rejection. But more importantly, treatment with 4NQO results in development of all precancerous stadia during the application process (mild dysplasia after 24 weeks, moderate dysplasia after 28 weeks, severe dysplasia after 28 weeks, and invasive squamous cell carcinoma after 32 weeks). Such a model could introduce the first steps of screening experiments using NIR fluorescence imaging for high-risk precancerous lesions.

## Assessment of clear surgical margins

In Chapters 3-6, NIR fluorescence agents were identified that are able to specifically target head and neck squamous cell carcinoma (HNSCC) in vivo. It was shown that these targets corresponded with histopathology. However, it has yet to be assessed whether a surgical procedure guided by the image of these agents will indeed result in a complete tumor resection with clear surgical margins. In other words, the clinical benefit of optical imaging over current surgical protocols still needs to be determined.

In an experimental setting, optical image-guided surgery could be followed by bioluminescence imaging to monitor residual disease or tumor recurrence. In a clinical setting, radicality can be determined by histologic analysis of the removed tissue specimen and by cryosections of the healthy remaining tissues, although this always includes a risk of sampling errors.

However, histologic complete surgical resection does not necessarily imply better treatment. Disease-free and overall survival scores determine the treatment efficacy and long-term follow-up is therefore required to irrefutably assess the advantages of optical image-guided surgery. Furthermore, stage III or IV tumors are usually followed by radiotherapy to irradiate the potentially remaining cancer cells which will make it even more difficult to determine the beneficial effects.

## The ideal imaging agent

After extensive preclinical research, the obvious question would consider which agent would be preferred for optical image-guided surgery in a patient with tongue cancer. However, based on the contemporary data, we are not yet able to answer this question. The ideal imaging agent would have an optimal TBR, as well as optimal pharmacokinetic and pharmacodynamic properties. These factors can influence each other significantly: after clearance of the agent from the circulation, the fluorescence signal from a tumor is often reduced but the TBR will usually be increased as a result of lower background signal. All agents that were tested in our studies had sufficient TBRs and could therefore be eligible for clinical use.

However, as mentioned previously, data from these preclinical studies should be interpreted with caution. For example, differences in TBRs between various agents could not only indicate a difference in efficacy of the agent, but could also illustrate differences in optical properties of the targeted tissue, concentration of the agent, or targeted receptor expression. Furthermore, the pharmacological properties of these agents in an animal model could be different in humans, potentially influencing the TBR. Hence, although the preclinical work demonstrates the feasibility of optical image-guided surgery and provides direction for further research, the quest for the preferred imaging agent can only be completed in a clinical setting.



## Sentinel lymph node mapping in HNSCC

Currently, the first steps for translation of optical image-guided surgery to the clinic are being made in sentinel lymph node (SLN) mapping. The SLN is the first lymph node that receives lymphatic drainage from a tumor, and identification of the SLN and analysis for tumor involvement may predict the status of the remaining lymph nodes. The use of NIR fluorescence optical imaging in the field of SLN mapping is recently introduced in clinical oncology.[6-9] Indocyanine green (ICG) is a dye that has already been used over the last fifty years for other clinical applications and is therefore approved by the FDA for use in humans. However not tumor-specific, this dye has now been extensively used off label in the looming field of NIR fluorescence SLN imaging, demonstrating the potential clinical advantage over current lymph node mapping protocols.[7] Currently, lymphatic imaging is performed using dye-injection, nuclear imaging, CT and MRI, which each have their specific limitations regarding sensitivity, resolution, exposure to radioactivity, or practical use. NIR fluorescence imaging allows for high spatial and temporal resolution without ionizing radiation, making it an easy-to-use and safe technique. With parallel imaging of visible and near-infrared light, the contrast agents can be traced to the SLN in real-time, without affecting the visual appearance of the surgical field.[7]

Despite extensive effort, the SLN procedure has not gained a definite place within surgical protocols of HNSCC. However, introduction of NIR optical imaging may shine new light onto this field because more accurate detection can be achieved due to higher

resolution. A recent study demonstrated the feasibility of sentinel cervical lymph node detection using optical imaging in an animal model although transcutaneous detection was not always possible due to limited penetration depth.[10] The first proof-of-principle clinical trial of SLN detection in patients with oral cavity carcinoma using optical imaging is has recently been finished in collaboration with the Leiden University Medical Center.[11] This study demonstrated feasibility to detect the SLN in head and neck cancer patients. However, a false-negative node was found, illustrating that the discussion on the role of SLN mapping in HNSCC is still relevant. Additional research is needed to determine if optical imaging is able to provide definitive answers to these questions.

## Field cancerization

An interesting problem for optical image-guided cancer surgery is introduced with the concept of field cancerization.[12] Head and neck carcinomas develop within preneoplastic fields of mucosal epithelium made up of genetically altered cells. However, these precursor changes in the oral mucosa may have a macroscopically normal appearance. Therefore, preneoplastic lesions can be found in parts of the surrounding mucosal epithelium of oral and oropharyngeal tumors[12] and can extend into the surgical margins when tumors are excised[13] causing local recurrences and second primary tumors. The relation between dysplastic changes surrounding tumors and the rate of local recurrences and multiple primary tumors in oral cancer has been reviewed extensively.[12, 13]

The paradigm of field cancerization poses a problem for identification of tumor-free margins using optical imaging. Considering the surrounding preneoplastic lesions and their relevance for local recurrence rates, it might not be sufficient to completely remove all cancer cells by image-guided surgery. The additional advantage of optical imaging techniques in the operation room would thereby be limited to more accurate assessment of the tumor margin than can be obtained with conventional surgery. However, in order to cure the patient without a chance of local recurrence, NIR fluorescence agents that are able to target the molecular markers that identify precancerous lesions could overcome the problem of preneoplastic lesions.

An important aspect of the genetic basis of multi-step progression from normal mucosa to HNSCC is found in the role of p53[14] and loss of heterozygosity of specific chromosomes.[12, 13, 15] Although the cancerization process can be clearly identified genetically, no specific targeting agents have thus far been found for identification of preneoplastic lesions. Very recently, the first indirect detection of dysplasia in Barrett's esophagus has been described using a cathepsin activatable agents similar to the ProSense agent that was used in Chapters 3 and 5.[16] An important reason is that preneoplastic fields have much more biological similarities with normal mucosa than with tumor, making array and proteomic studies very difficult. Furthermore, investigation of tissue that appears abnormal or is identified by a change in autofluorescence (i.e., fluorescence of normal components of the tissue) does not provide information about the macroscopically normal mucosa.[17] However, if these molecular markers would be found, the field of optical imaging could not only improve

postoperative survival rates, but could eventually be expanded and play an essential role in screening of high-risk patient populations and post-treatment follow-up.

## Multimodality imaging

Over the last century, evolution of imaging modalities in medicine has resulted in a wide range of diagnostic options. However, each specific imaging modality has its own advantages and disadvantages resulting in adjuvant use of various techniques for many diagnostic indications. The rapid development of molecular imaging in the last decades has opened new possibilities for incorporation of these different techniques into new multimodality imaging. As soon as the intraoperative optical imaging has proven a definite beneficial role for surgical oncology, new promising possibilities emerge to combine preoperative imaging modalities with intraoperative applications of image-guided surgery. For example, coupling of a fluorescent dye to tumor-specific radioactive tracers could result in preoperatively detection by PET or SPECT with subsequent intraoperative identification using optical imaging.

A second possible application of multimodality imaging could be found in a combination of navigation surgery and tumor-specific optical imaging. For many surgical applications, intraoperative navigation systems can be used to help guide the surgeon to localize the operative target within the anatomical structures. These systems are extensively being used in neurosurgery[18] and for instance in endoscopic sinus surgery.[19] The essence of this procedure is found in an accurate model of the patient, which is usually generated using preoperative CT or MRI imaging with subsequent creation of a three-dimensional data set. Next, synchronization of the radiologic data set with the position of the patient inside the operation room is required. During surgery, the surgeon can now be informed on his exact position using a sensing probe that corresponds with the preoperative image.

Computer-assisted navigation techniques could play an important role in optical image-guided surgery. For this application, fluorophores could be conjugated to particles that can be imaged using MRI, such as iron oxide. This strategy is currently used in magnetic iron oxide nanoparticles that are being developed for various tumor targeting therapies.[20] A third possibility for multimodal application is the use of agents that allow both detection and therapy of the targeted tumor, a field known as theranostics. An example is described in Chapter 10, by the combination of optical imaging technologies with photodynamic therapy. Finally, combined use of (wide-field) fluorescence imaging and Raman spectroscopy[21] could result in intraoperative histopathological determination of clear surgical margins. In this way, the tumor could be resected guided by the fluorescence signal, followed by Raman spectroscopic analysis of (suspect parts) of the ablative wound bed to confirm clear surgical margins.



## Acknowledgements

We would like to thank Prof. dr. Ruud H. Brakenhoff (VU Medical Center, Amsterdam, The Netherlands) for his valuable comments regarding the conundrum of field cancerization.

## References


1. Gioux S, Choi HS, Frangioni JV. Image-guided surgery using invisible near-infrared light: fundamentals of clinical translation. Mol Imaging. 2010; 9(5): 237-55.
2. van Dam GM, Themelis G, Crane LM, Harlaar NJ, Pleijhuis RG, Kelder W, et al. Intraoperative tumor-specific fluorescence imaging in ovarian cancer by folate receptor-alpha targeting: first in-human results. Nature medicine. 2011; 17(10): 1315-9.
3. Maeda H. Tumor-selective delivery of macromolecular drugs via the EPR effect: background and future prospects. Bioconjugate chemistry. 2010; 21(5): 797-802.
4. Sandanaraj BS, Gremlich HU, Kneuer R, Dawson J, Wacha S. Fluorescent nanoprobes as a biomarker for increased vascular permeability: implications in diagnosis and treatment of cancer and inflammation. Bioconjugate chemistry. 2010; 21(1): 93-101.
5. Schoop RA, Noteborn MH, Baatenburg de Jong RJ. A mouse model for oral squamous cell carcinoma. J Mol Histol. 2009; 40(3): 177-81.
6. Hutteman M, Choi HS, Mieog JS, van der Vorst JR, Ashitate Y, Kuppen PJ, et al. Clinical translation of ex vivo sentinel lymph node mapping for colorectal cancer using invisible near-infrared fluorescence light. Annals of surgical oncology. 2011; 18(4): 1006-14.
7. Hutteman M, Mieog JS, van der Vorst JR, Liefers GJ, Putter H, Lowik CW, et al. Randomized, double-blind comparison of indocyanine green with or without albumin premixing for near-infrared fluorescence imaging of sentinel lymph nodes in breast cancer patients. Breast Cancer Res Treat. 2011; 127(1): 163-70.
8. Hutteman M, van der Vorst JR, Gaarenstroom KN, Peters AA, Mieog JS, Schaafsma BE, et al. Optimization of near-infrared fluorescent sentinel lymph node mapping for vulvar cancer. American journal of obstetrics and gynecology. 2011.
9. van der Vorst JR, Hutteman M, Gaarenstroom KN, Peters AA, Mieog JS, Schaafsma BE, et al. Optimization of near-infrared fluorescent sentinel lymph node mapping in cervical cancer patients. Int J Gynecol Cancer. 2011; 21(8): 1472-8.
10. Yamauchi K, Nagafuji H, Nakamura T, Sato T, Kohno N. Feasibility of ICG fluorescence-guided sentinel node biopsy in animal models using the HyperEye Medical System. Annals of surgical oncology. 2011; 18(7): 2042-7.
11. van der Vorst JR, Schaafsma BE, Verbeek FP, Keereweer S, Jansen JC, van der Velden LA, et al. Near-infrared fluorescence sentinel lymph node mapping of the oral cavity in head and neck cancer patients. Oral oncology. 2013; 49(1): 15-9.
12. Braakhuis BJ, Tabor MP, Kummer JA, Leemans CR, Brakenhoff RH. A genetic explanation of Slaughter's concept of field cancerization: evidence and clinical implications. Cancer Res. 2003; 63(8): 1727-30.
13. Graveland AP, Golusinski PJ, Buijze M, Douma R, Sons N, Kuik DJ, et al. Loss of heterozygosity at 9p and p53 immunopositivity in surgical margins predict local relapse in head and neck squamous cell carcinoma. Int J Cancer. 2011; 128(8): 1852-9.
14. Califano J, van der Riet P, Westra W, Nawroz H, Clayman G, Piantadosi S, et al. Genetic progression model for head and neck cancer: implications for field cancerization. Cancer Res. 1996; 56(11): 2488-92.
15. Leemans CR, Braakhuis BJ, Brakenhoff RH. The molecular biology of head and neck cancer. Nat Rev Cancer. 2011; 11(1): 9-22.
16. Bird-Lieberman EL, Neves AA, Lao-Sirieix P, O'Donovan M, Novelli M, Lovat LB, et al. Molecular imaging using fluorescent lectins permits rapid endoscopic identification of dysplasia in Barrett's esophagus. Nature medicine. 2012; 18(2): 315-21.
17. De Veld DC, Witjes MJ, Sterenborg HJ, Roodenburg JL. The status of in vivo autofluorescence spectroscopy and imaging for oral oncology. Oral oncology. 2005; 41(2): 117-31.
18. Omay SB, Barnett GH. Surgical navigation for meningioma surgery. J Neurooncol. 2010; 99(3): 357-64.
19. Virgin FW, Bleier BS, Woodworth BA. Evolving materials and techniques for endoscopic sinus surgery. Otolaryngol Clin North Am. 2010; 43(3): 653-72, xi.
20. Chen B, Wu W, Wang X. Magnetic iron oxide nanoparticles for tumor-targeted therapy. Curr Cancer Drug Targets. 2011; 11(2): 184-9.
21. Nijssen A, Koljenovic S, Bakker Schut TC, Caspers PJ, Puppels GJ. Towards oncological application of Raman spectroscopy. J Biophotonics. 2009; 2(1-2): 29-36.

# 10 Future directions

Stijn Keereweer,[1,2] Pieter B.A.A. Van Driel,[1] Dominic J. Robinson,[3] Clemens W.G.M. Lowik[1]

1. Department of Molecular Imaging, Leiden University Medical Center, Leiden, The Netherlands
2. Department of Otorhinolaryngology-Head and Neck Surgery, Erasmus Medical Center, Rotterdam, The Netherlands
3. Center for Optical Diagnostics and Therapy, Postgraduate School of Molecular Medicine, Department of Dermatology, Erasmus MC, Rotterdam, The Netherlands

Adapted from "Shifting Focus in Optical Image-Guided Cancer Therapy"
Published in **Molecular Imaging & Biology**, **2013 Sept 14**. PMID: 24037176

## Abstract

Cancer patients could benefit from a surgical procedure that helps the surgeon to determine adequate tumor resection margins. Systemic injection of tumor-specific fluorescence agents with subsequent intraoperative optical imaging can guide the surgeon in this process. However, tumor heterogeneity hampers tumor-specific targeting. In addition, determination of adequate resection margins can be very challenging due to invasive tumor strands that are difficult to resolve and because of the confounding effect of variations in tissue optical properties in the surgical margin. We provide an overview of the "classic approach" of imaging tumor-specific targets or tumor-associated pathophysiological processes, and explain the limitations of these targeting strategies. It is proposed that problems of tumor heterogeneity can theoretically be circumvented by shifting focus of tumor targeting towards the follicle-stimulating hormone receptor (FSHR). Furthermore, we discuss why objective determination of resection margins is required to improve resection of the invasive strands, a goal that may be achieved by targeting the FSHR. When invasive strands would nevertheless extend beyond such a standardized resection margin, we suggest that adjuvant photodynamic therapy would be a very suitable therapeutic regimen. Finally, we describe how point optical spectroscopy can be used to scrutinize suspect tissue that is difficult to differentiate from normal tissue by measuring the local tissue optical properties to recover a local intrinsic fluorescence measurement.

## Introduction

Despite the technological advancements of preoperative imaging techniques, clinical outcome of cancer surgery for most cancer types has only gradually improved over the last three decades. Introduction of real-time optical imaging could revolutionize the intraoperative approach to cure cancer by providing the surgeon with direct feedback on histopathologic markers. This intraoperative tissue characterization could improve surgical outcome, local control, and disease-free survival. In addition, it enables better preservation of healthy tissue, which is critical to postoperative functionality and quality of life. In optical imaging, tumor-specific fluorescent agents can be systemically injected to guide the surgeon in adequately determining resection margins.

Although feasibility of intraoperative tumor-specific near-infrared (NIR) fluorescence imaging was demonstrated in humans[1], cancer targeting with high sensitivity and specificity remains challenging. The continuous quest for a universal tumor-specific target has not yet been successful and the growing insight in cancer invasion is increasingly pointing toward multifactorial processes[2-3]. There are many general aspects involved in making a tumor-specific targeting agent suitable for in vivo use, including high affinity of the agent with low non-specific binding, abundance of the target receptors or epitopes,[4] biodistribution of the agent to the target, sufficient contact time with the target for binding to occur, retaining of the agent while non-bound agents are cleared from the circulation, and toxicity issues.[5] These aspects have been extensively reviewed elsewhere.[5-8] Although an extensive amount of work is still needed to consider these issues, we anticipate that the next generations of fluorescent agent design will continue to improve these aspects. However, we have identified the 3 fundamental challenges that will remain to contribute to the conundrum of optical image-guided cancer surgery: dealing with tumor heterogeneity; obtaining adequate resection margins that include invasive tumor strands; and managing the confounding effects of differences and variations in optical tissue properties (Fig. 1). This review aims to explain the limitations of the "classic approach" of (combined) imaging of tumor-specific cell-surface receptors and tumor-associated pathophysiological processes. Next, we suggest that shifting focus to the follicle-stimulating hormone receptor (FSHR) could theoretically circumvent the problems of tumor heterogeneity. Furthermore, we advocate the need for objective intraoperative determination of resection margins to improve resection of the invasive strands and explain how this may be achieved by targeting the FSHR. If invasive strands would extend beyond the resection margin, we propose that photodynamic therapy (PDT) is the ideal adjuvant therapeutic regimen that is likely to play an increasingly important role in optical image-guided cancer therapy. Finally, the confounding effects of differences in tissue optical properties impede the ability to differentiate between areas of healthy and tumor tissue, particularly in the surgical margin where fluorescent signals can be lower. We describe how point reflectance and fluorescence spectroscopy using fiber optic probes can be used to overcome these effects.

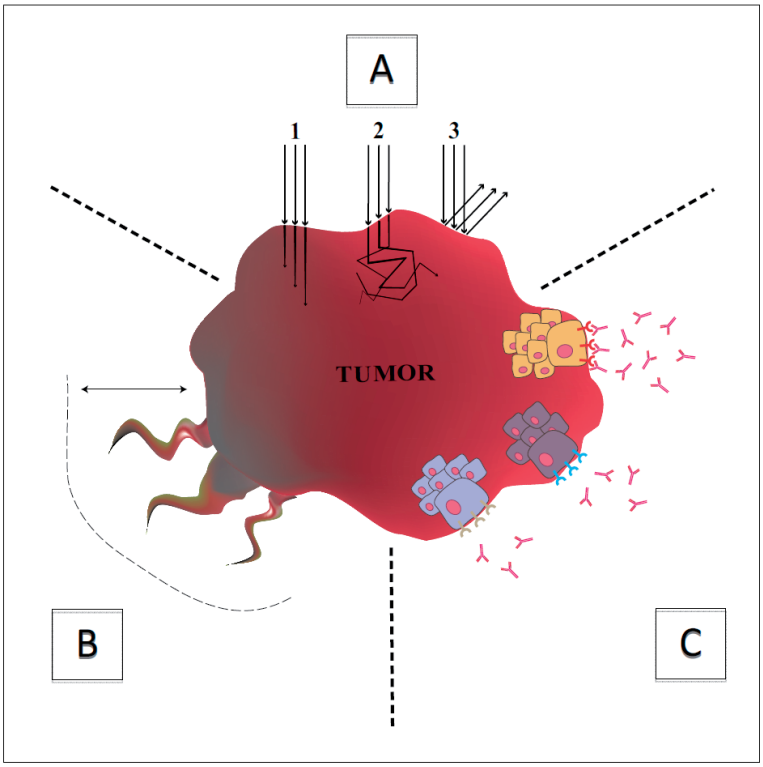


**Fig. 1.** Schematic illustration of the three fundamental problems in optical image-guided cancer surgery. A. How to deal with differences in optical properties that influence propagation of light in tissue (1-3): Absorption by tissue components that influences the optical pathlength (1); scattering by tissue components that influences the spatial distribution of light (2); and specular reflection at the tissue surface (3). B. How to obtain adequate resection margins that include invasive tumor strands that extend beyond the (visible) tumor border. C. How to cope with tumor heterogeneity that results in variability in expression of surface receptors, hampering target-specific imaging.

## Challenges of tumor-specific imaging

### *Tumor heterogeneity*

The first problem that is currently challenging tumor-specific imaging is tumor heterogeneity. Different populations of tumor cells within a tumor display variable phenotypes such as the ability to metastasize or to survive chemo- or radiotherapy. This intra-tumor phenotypic diversity results from genetic and epigenetic heterogeneity, a consequence of genomic instability combined with high cell turnover, as well as from differences in the tumor microenvironment[9]. Improved molecular understanding of cancers has resulted in identification of targets for diagnostic and therapeutic interventions. However, the concept of tumor heterogeneity explains why tumor-specific imaging based on these targets is limited in many cases[9-10].

### *Invasive tumor strands*

The second factor that fluorescence-guided tumor resection has to deal with is the problem how to include invasive tumor strands into the resection margin. Invasive tumor strands are crucial for development of regional and distant metastasis. Moreover, invasive strands are less sensitive to adjuvant therapy due to adaptive responses to different types of therapy-induced stress inducing tumor cell survival[2]. This reactive resistance to adjuvant therapy emphasizes the importance of radical surgical resection that includes invasive strands[2-3]. In addition, the pattern of tumor invasion at the invasive front may be indicative for tumor behavior[11]. However, it remains to be determined whether high-risk tumors require greater margin distances than low-risk tumors[12].

In conventional surgery, an extra resection margin around the tumor mass is removed in order to include potential invasive strands and to compensate for inaccurate determination of the tumor border. Because it is practically infeasible to objectively determine a consistent margin, for instance of 1 cm by use of a caliper in all dimensions around the tumor, the resection margin is subjectively assessed by the surgeon, resulting in intersurgeon variability.[13] This interferes with standardized oncologic care and hampers complete surgical resection in some cases.

Although optical imaging techniques can provide the surgeon with direct feedback on histopathological markers, it is impossible to image individual invasive strands under many circumstances. To detect invasive strands, fluorescent agents would require very high affinity for these thin layers of cancer cells. However, as will be explained below, the influence of differences in background optical properties of tissue and their spatial heterogeneity would regularly prevent detection or detailed imaging. The inability to identify individual invasive strands dictates a new approach to consistently include an objective resection margin into the surgical resection.



### *Optical tissue properties*

Finally, tumor-specific imaging and subsequent image-guided surgical resection is strongly influenced by the background tissue optical properties. The basic geometry of optical imaging requires excitation light from an external light source that travels through the imaged tissue and excites the fluorophore inside the tissues[5, 7]. After excitation, the fluorescent light travels back through the tissues and is detected outside the body by a dedicated camera system. The path that these photons travel is influenced by the optical properties of the tissues at the excitation and emission wavelength. Scattering can change the direction of part of the photons and multiple consecutive scatter events will result in diffuse light; a gradual randomization of the propagation direction[5, 7, 14-15]. Additionally, photons can be absorbed by various components in the tissue. Consequently, fluorescence images will display intensities that are strongly influenced by varying absorption properties of the tissue and the images may be blurred due to scattering of light. The problem with targeting invasive tumor strands could be as follows: invasive strands can be very thin, limiting the amount of tumor-specific fluorescent agent that is bound or activated. This results in a

relatively low amount of fluorescent photons that are subsequently influenced by scattering and absorption. Imaging of strands that are invading the surrounding tissues will result in blurry images with very low intensity.

Various groups have developed imaging systems that incorporate tissue attenuation correction algorithms that have been validated using phantoms.[16-18] Although improved margin delineation and quantification is reported, it is unlikely that such estimations or more sensitive detectors will be able to completely resolve the effects caused by optical properties and autofluorescence in vivo, because of the heterogeneous composition of the tissue and differences in autofluorescence intensity in location and over time.[7]

## Current strategies of tumor-specific imaging

### *The "classic approach" targeting of tumor-specific cell surface receptors*

The most often approach employed for tumor-specific targeting is to conjugate a fluorophore to a tumor-specific antibody or peptide targeting a receptor. The limitless replicative potential of tumor cells, a key feature of carcinogenesis, offers useful targets because it is facilitated by increased metabolism, high expression of growth-signalling receptors, and increased tumor angiogenesis to supply sufficient oxygen and nutrients[19]. Many of these hallmarks of cancer have been a target for antibody-derivatives, peptides or small molecules conjugated to a fluorophore.[20] For instance, promising results have been reported in preclinical experiments that target growth-signalling receptors[1, 21-23]. However, these preclinical models mostly include homogeneous tumors, and antibody-specific targeting is likely to be limited when tumors become increasingly heterogeneous. Moreover, these models are often formed using human xenografts that are targeted by human antibody derivatives, resulting in zero background signal.

Sustained angiogenesis has been imaged by targeting integrins; specific cell-surface markers of tumor angiogenesis[24-25], which results in imaging of tumor vasculature. Although this strategy could strongly reduce the problem of tumor heterogeneity, studies have shown that these agents are taken up by cancer cells in vitro, improving their tumor-specific fluorescence signal but increasing variability of this signal due to tumor heterogeneity[25]. Moreover, this targeting strategy does not include an objective standardized resection margin, which is required because targeting of angiogenesis will not image strands that are not (yet) supported by new sprouting vessels, such as solid strands that can be found in basal and squamous cell carcinomas[3].

### *Targeting tumor-associated pathophysiological processes*

To reduce the problem of tumor heterogeneity and find a more universal tumor-specific target, the approach changed from targeting cell surface receptors to targeting tumor-associated pathophysiological processes. The best-known example of such a process is the degradation of the extracellular matrix, which is required for tumor growth and metastasis. By targeting enzymes that are involved in these general processes, the tumor border is imaged, independent from the type of receptors that are expressed by the cancer cells[19,

21, 26-27]. Targeting of proteolytic enzymes results in imaging of the invasive tumor front where these enzymes are abundant. Therefore, surgical resection guided by the enzyme-specific fluorescence signal could be sufficient for radical resection including invasive tumor strands.

To further improve sensitivity, different tumor-specific characteristics have been targeted simultaneously. These different targets can be imaged at different wavelengths, allowing separate analysis of different cancer features[21]. The use of a "cocktail" of fluorescent agents that target different tumor markers could reduce the effect of tumor heterogeneity. Although this may seem a feasible approach, it is difficult to assess in advance what percentage of the tumor would be "covered" by this mixture of tumor targets. As an alternative, the biologic tumor markers for each individual tumor could be determined preoperatively, which would require representative samples and complex biochemical analyses. Both approaches will most likely not be cost-effective compared to the use of a single universal targeting agent.

Moreover, although targeting of cancer cell surface receptors, either or not in combination with simultaneous imaging of tumor-specific pathophysiological processes, seem to solve most of the aforementioned limitations while imaging with high specificity, a closer look into its basic principles reveal that fundamental limitations remain equally existent.



First, targeting tumor-associated pathophysiological processes goes at the expense of sensitivity and specificity of the imaging technique. Although imaging of tumor-associated pathophysiological processes is not affected by phenotypic heterogeneity of cell surface receptors, there is still heterogeneity in behavioural features of the tumor that influences the sensitivity. For example, proteolytic activity may be reduced at the invasive front in less invasive tumors with fewer tendencies towards metastasis, or in cases of encapsulated tumors, reducing the sensitivity of this target. On the other hand, specificity of the target is limited due to the regular expression of these enzymes in healthy tissues and increased expression in inflammatory tissues[26, 28].

Second, a resection margin as indicated by fluorescent agents that target tumor-associated pathophysiological processes would be inconsistent as a result of the variability of proteolytic activity due to phenotypic heterogeneity and regular expression in inflammatory tissues. Although it is expected that proteolytic activity would be increased in regions where invasive strands are found, this approach does not incorporate a standardized objective resection margin. Consequently, the resection margin could be too small in slow-growing tumors or too large in tumors that are surrounded by inflammatory tissue.

Third, with either of the 2 targeting strategies, it is even more important to consider the influence of the tissue optical properties (absorption and scattering) in the tumor margin which are themselves likely to be altered differently by the presence of an invasive front or at the boundary of an encapsulated tumor. Consequently, smaller lesions and invasive strands may be very difficult to detect, and a basic understanding of the optical physics is required for the surgeon to adequately interpret the acquired images.

## Shifting focus in optical image-guided therapy

To establish a definite role for optical image-guided therapy into clinical practice, it is necessary to be able to identify the tumor with high sensitivity and specificity, and to remove the complete tumor mass including invasive tumor strands. In the following section, we propose that a shift in focus is required to deal with the 3 challenges that were identified: tumor heterogeneity; obtaining adequate resection margins that include invasive tumor strands; and managing and ultimately correcting for the effects of tissue optical properties during the surgical resection.

### *Circumventing the problems of tumor heterogeneity*

Recently, a new potential target was identified with the finding of expression of FSHR in tumor blood vessels of a wide range of different cancer types[29]. Expression was found from 5 mm within the tumor to 9 mm outside of the tumor and was not located in healthy tissue more than 10 mm from the tumor (Fig. 2). Although the exact pathogenic mechanism of expression of FSHR is yet unknown, this finding introduces new opportunities for image-guided cancer surgery: resection of tumor margin guided by an FSHR-specific signal may prove to be sufficient to completely remove the tumor.

Because expression of the FSHR was found in a wide range of different cancer types that have different cell-surface receptors and variable malignant behaviour, sensitivity is not influenced by tumor phenotypic or behavioural heterogeneity. Moreover, expression of the FSHR was found in tumor blood vessels and not in cancer cells. The specificity of this target is very high, as the FSHR is expressed only in the granulosa cells of the ovary and the Sertoli cells of the testis in adult humans. Hence, targeting of the FSHR would result in very low non-specific binding.

Although the amount of FSHRs might be lower in smaller tumors, Radu et al. calculated that the volume that consists of blood vessels that have FSHR-expressing endothelial cells represents a substantial fraction of the tumor volume (e.g., in a tumor with a 2-cm diameter, a 3-mm-thick peripheral layer inside the tumor accounts for 66% of its volume).[29] This example excludes the additional number of FSHR-expressing vessels that co-exist up to 10 mm outside the tumor border. Expression has been described even in early T1 tumors and in tumor metastases, illustrating the full potential of this target for image-guided cancer therapy. Development of a fluorescently labeled FSHR target is currently still in the experimental phase and future studies on pharmacodynamics, pharmacokinetics and toxicity (including side effects on the reproductive system) are required for FDA approval.

A possible drawback of this target could be that identification of tumors by targeting the FSHR is only feasible after formation of tumor blood vessels. In the prevascular phase, tumor volume is limited to 2-3 $mm^3$, a size that is usually clinically undetectable[30]. After the angiogenic switch has occurred, neovascularisation permits tumors to grow and metastasize, which heralds the onset of symptoms[30-31]. Because surgery is performed only on clinically detectable lesions that have given symptoms in most cases, neovascularisation will always be present and expression of the FSHR can be used as an imaging target for

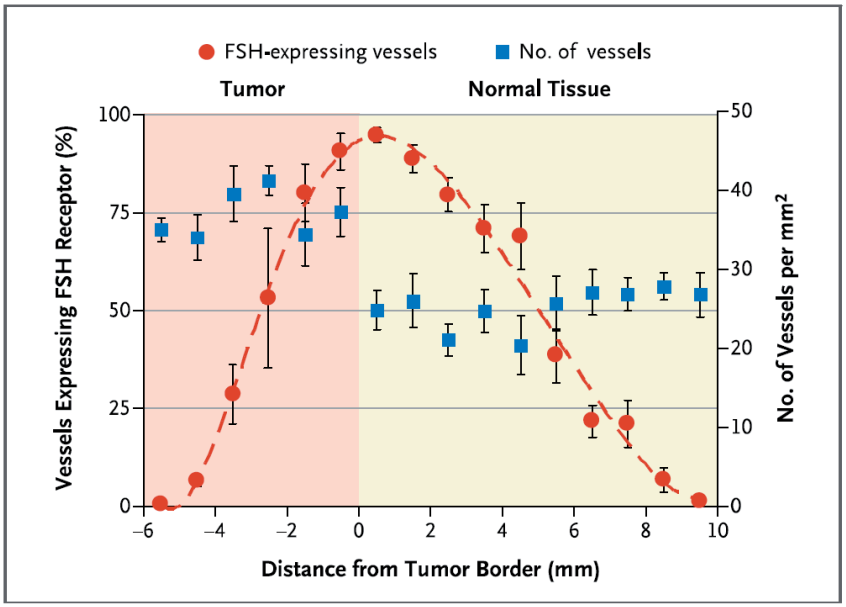


**Fig. 2.** FSH-receptor expression according to vessel location. The blood vessels were visualized with the use of anti–von Willebrand factor antibodies followed by Alexa-488 dye secondary antibodies, and FSH-receptor–stained vessels were visualized by the FSHR323 antibody followed by Alexa-555 dye–labeled secondary antibodies. The vessels were counted on 148 microscopical digital images of tumors obtained from five patients. Zero indicates the border of the tumor, the negative numbers indicate the interior of the tumor, and the positive numbers indicate the exterior of the tumor. The red circles and dashed line represent the percentage of FSH-receptor–expressing vessels. The blue squares indicate the total number of vessels per square millimeter; the mean number was higher in the interior of the tumor than in the exterior (37±2 vs. 25±1 vessels per square millimeter, P<0.001 with the use of a two-tailed t-test). I bars denote standard errors. (Reproduced with kind permission from Radu et al.,[29], Copyright Clearance Center Rightslink.)



optical image-guided surgery. In addition, most injectable agents have additional "tumor binding" through the non-specific effect of enhanced permeability and retention (EPR) that is present in many tumors.[32-33] Non-specific retention of the agent in the tumor (periphery) could have a positive effect by increasing the fluorescent signal, but on the other hand could reduce the exact specificity of margin delineation by the tumor-specific agent. Preclinical studies have demonstrated clear differences in tumor-specific binding localization[25] and intensity[17] between non-specific EPR and tumor-specific targeting.

Finally, similar to targeting of growth factor receptors, injection of contrast agents that target hormone receptors heralds a risk of potentially harmful effects such as tumor proliferation. In longitudinal animal studies on fluorescent agents targeting the epidermal growth factor receptor (EGFR) in prostate cancer, no tumor-promoting effects were found. [34] In contrast to prostate cancer cells that express EGFR, FSHR-expression was only found in the tumor vasculature and not in cancer cells,[29] but it is currently unknown

if stimulation of the FSHR has effects on tumor growth. As long as these agents are used solely for guidance of tumor resection, the agents would be injected preoperatively and such potentially proliferative effects would be limited to the tumor that is directly removed, provided that regional or distant metastasis are non-existent. Nevertheless, this aspect requires attention in the evaluation of the clinical feasibility of an FSHR-specific fluorescent agent.

### *Dealing with undetectable invasive tumor strands*

The high recurrence rates in many cancer types warrant a new approach to the inability to identify individual invasive tumor strands. Optical imaging would allow consistent inclusion of an objective resection margin into the surgical resection by targeting of the FSHR. Because FSHR expression was found up to 9 mm outside the tumor border, a resection guided by an FSHR-specific fluorescence signal would include a consistent resection margin and would theoretically include invasive tumor strands in the vast majority of resectable tumors.

Even with a highly specific targeting agent available, the fundamental problems associated with detecting weak fluorescence signals in an environment dominated by heterogeneous optical absorption may sometimes prevent undisputable identification of the border of the fluorescent resection margin[7-8, 15, 35]. Furthermore, high-risk pathological characteristics could imply that adjuvant therapy may still be required to completely treat the cancer[11]. In these selected cases, PDT may be very suitable for adjuvant therapy after optical image-guided cancer surgery for various important reasons.

In PDT, photosensitizers are used that produce cytotoxic reactive oxygen species after excitation by light with a specific wavelength. As a result, cancer cells are killed by apoptosis and/or necrosis, and tumor microvasculature is obliterated[36-37]. Specific damage of the tissue of interest is obtained by local illumination. Furthermore, the very short half-life of cytotoxic reactive oxygen species ensures that damage only occurs in the immediate vicinity of its formation. Although conventional adjuvant treatments (i.e., radiotherapy, chemotherapy, or a combination) can induce immunosuppression, PDT-induced immunogenic cell death induces a local inflammatory reaction and stimulates the host immune system[37]. In addition, formation of a tumor-specific immune response (e.g., production of tumor-specific cytotoxic T-cells) offers opportunities to treat distant metastases[37]. Preclinical studies showed possibilities of boosting the immune response by the adjuvant use of an oncolytic vaccine virus resulting in effective inhibition of distant metastatic spread[38]. Compared to other adjuvant therapeutic modalities, PDT has the potential to induce low toxicity in normal tissue, produce negligible systemic effects, and reduce acute and long-term morbidity[36]. Furthermore, PDT does not compromise future treatment options for patients with residual or recurrent disease and can be repeated with perpetual efficacy. However, due to limited light penetration depth (< 1 cm), PDT is only applicable for superficial lesions, unless the tumor is accessible for insertion of fibers into the tumor to deliver the light. In larger tumors that are inaccessible, debulking of the tumor mass is therefore preferred before adjuvant PDT could be performed[39].

Wavelength-specific excitation of photosensitizers could technically be performed using the same imaging systems as those used for optical image-guided surgery, emphasizing its practical advantages as an adjuvant therapeutic modality in the surgical theatre. In order to fully exploit the advantages of both modalities, a tumor-specific NIR fluorescent photosensitizer is required[40-41].

A tumor-specific photosensitizer has the potential to be much more efficient and cause less damage to surrounding normal tissue than a non-specific photosensitizer[40-41]. The increasing amount of photosensitizer that is expected to accumulate in the tissue of interest ensures that less light is required to induce a cytotoxic reaction. Consequently, even light that penetrates deeper into tissue (>1 cm) will result in specific damage of tumor cells that are deeper located. Moreover, such an agent could be used for both NIR fluorescence image-guided surgery and adjuvant PDT (i.e. a "theranostic"). Thereby, a targeting moiety and photosensitizer conjugate can be chosen that accumulates at a location in the cell that is favourable for eliciting a specific cellular or host response (e.g. apoptosis or an immune response)[36].

Recent studies report of tumor-specific PDT that could potentially be performed using heptamethine cyanine dyes that have been shown to specifically target cancer cells in vivo through internalization into the cell by the organic anion transporting polypeptide[42]. Because these agents have shown photosensitizing properties, they are nominated as promising theranostics for future NIR fluorescence image-guided surgery with adjuvant PDT[43]. A second approach could be to design a construct that is a combination of a fluorophore and photosensitizer conjugated with a tumor-specific target. The use of nanotechnology may circumvent some of the negative physio-chemical properties of photosensitiser conjugates [44] and a photosensitizer.



### *Managing and correcting for the effects of optical tissue properties*

As we have described above, a current approach to tumor specific imaging results in fluorescence signals that are strongly influenced by the background tissue optical properties of the tissue under investigation. Given the nature of the fluorescence signals, we propose a shift of focus in optical image-guided cancer therapy towards intraoperative quantitative intrinsic fluorescence measurements. While various groups have developed imaging systems that incorporate tissue attenuation correction algorithms,[16-18] other approaches are aimed at performing truly quantitative in vivo fluorescence measurements[45].

To perform truly quantitative intrinsic fluorescence measurements, the research field of biomedical optics has mainly focused on the use of optical techniques in which the path-length of light in tissue can be controlled. This generally involves placing a fiber optic probe on the surface of the tissue, through which light enters the tissue and is subsequently collected from a known distance inside the tissue. The use of a known distance between light source and light detection is important for two reasons. First, it determines the volume over which optical signals are averaged, which is an important consideration for the interrogation of tumor, tumor margin and the surrounding normal tissue. Second,

by using a known separation distance between the light source and the light detection, theoretical models can be built to describe the complex interaction of light with tissue over this distance. By applying these theoretical models to the light measured by the fiber optic probe, the tissue optical properties can be quantified.

The use of a fiber optic probe also facilitates the acquisition of spectrally resolved fluorescence with a high signal to background ratio. Spectral deconvolution allows intrinsic fluorophore fluorescence to be distinguished from the tissue autofluorescence and residual excitation light.

Recently, the use of a single fiber optic probe for the delivery and collection of light has been described; single fiber reflectance spectroscopy (SFR)[46]. Mathematical models have been developed to describe the underlying interaction of light with tissue[47-48]. The sampling volume can be tailored to a specific clinical application or suited to the intraoperative need by varying the diameter of the optical fiber(s) that are used [range in sampling depth 0.1 – 1 mm]. Using knowledge of the sampling volume, algorithms have been developed that can be used to perform quantitative reflectance and fluorescence spectroscopy[45, 49]. By utilizing two or more fiber diameters in a single fiber optic probe, SFR spectroscopy enables a complete determination of tissue optical properties[49-50]. This technique, termed multi-diameter single fiber reflectance spectroscopy (MDSFR), can then be used to recover a fully quantitative measure of intrinsic fluorescence[51]. In MDSFR spectroscopy, an overlap exists in delivery and collection of light, which provides information on the distribution of angles at which the light scatters[52-53]. Preclinical studies have suggested that measuring these types of scattering properties may have diagnostic value[54]. This approach yields the quantification of intrinsic fluorescence, given as the product of the tissue fluorophore absorption coefficient at the excitation wavelength. Recently, the first promising clinical results were reported in neurosurgical and gastrointestinal applications using similar approaches[55-56].

The use of a fiber optic probe has some disadvantages; the point measurement technique needs to be incorporated into the procedure of image-guided surgery and it is not ideal for covering a large proportion of the tumor margin. In addition, true real-time acquisition is not possible, because the measurements take a few seconds to produce at each measurement location. Future developments in the clinical implementation of MDSFR such as the use of lager coherent fiber bundles[57] could allow this fiber based technique to approach the resolution and speed of optical imaging. It is also important to consider how point spectroscopic information and optical imaging might be registered most optimally.

The acquisition of point measurements as an adjuvant intraoperative optical imaging technique to fluorescence-guided surgery is clearly not limited to the use of reflectance and fluorescence spectroscopy. Other spectroscopic approaches such as Raman spectroscopy have significant potential[58] but spectral analysis of a tumor margin during fluorescence-guided surgery may be hampered by the presence of the exogenous fluorophores. In addition, although these techniques are rapidly improving, the acquisition-time of a representative Raman spectrum is currently too long to be used intraoperatively.

Given the potential of the approaches that we have presented, we advocate the use of fluorescence-guided surgery for resection of the gross tumor mass, followed by point spectroscopic fluorescence measurements of suspect tumor margins.

### *The paradigm of field cancerization*

An interesting problem for optical image-guided cancer therapy is introduced with the concept of field cancerization that suggests that achieving histological adequate margins may not be sufficient in some cases[59]. Squamous cell carcinomas develop within preneoplastic fields of mucosal epithelium made up of genetically altered cells. However, these precursor changes in the mucosa may have a macroscopically normal appearance. Therefore, preneoplastic lesions can be found in parts of the surrounding mucosal epithelium[59] and can extend into the surgical margins when tumors are excised[60] causing local recurrences and second primary tumors. The relation between dysplastic changes surrounding tumors and the rate of local recurrences and multiple primary tumors in cancer has been reviewed extensively[59-60].

An important aspect of the genetic basis of multi-step progression from normal mucosa to squamous cell carcinoma is found in the role of p53[61] and loss of heterozygosity of specific chromosomes[59-60, 62]. Although the cancerization process can be clearly identified genetically, no specific targeting agents have thus far been found for identification of preneoplastic lesions. An important reason is that preneoplastic fields have much more biological similarities with normal mucosa than with tumor, making array and proteomic studies very difficult. The paradigm of field cancerization poses a problem for identification of tumor-free margins using optical imaging. Considering the surrounding preneoplastic lesions and their relevance for local recurrence rates, it might not be sufficient to completely remove the tumor at its borders. At present, no literature exists that is able to guide a surgeon towards adequate margins in the setting of field cancerization[12]. However, the potential extent of this problem emphasizes the necessity to include a consistent objective resection margin as would be indicated by targeting of the FSHR.



## Conclusion

Although the introduction of optical imaging techniques for intraoperative applications has great potential to improve assessment of tumor margins during surgery, optimizing sensitivity and specificity remain challenging because of tumor heterogeneity. In addition, results of optical image-guided surgery are potentially limited due to difficulty in including invasive tumor strands in the resection margin, and dealing with the influences that optical tissue properties have on the image.

We review 3 new concepts that could deal with these challenges. First, expression of the FSHR provides an ideal target for cancer imaging and could theoretically circumvent the problems of tumor heterogeneity. Next, the inability to identify individual invasive strands dictates a new approach to consistently include an objective resection margin into the surgical resection. The FSHR positive margin would provide such a consistent objective

resection margin. Extension of invasive strands beyond such a standardized resection margin could ideally be treated with adjuvant photodynamic therapy. And finally, the confounding effects of variable background tissue optical properties can be overcome by combining fluorescence-guided surgery with quantitative optical spectroscopy of the tumor margin. We anticipate that these promising concepts will play an elementary role in the next generation of optical image-guided cancer therapy.

## Acknowledgements

M.T.N. is gratefully acknowledged for his supporting contribution during the writing process.

## Conflict of interest

The authors declare that they have no conflict of interest.

## References

1. van Dam GM, Themelis G, Crane LM, et al. (2011) Intraoperative tumor-specific fluorescence imaging in ovarian cancer by folate receptor-alpha targeting: first in-human results. Nature medicine 17:1315-1319.
2. Alexander S, Friedl P (2012) Cancer invasion and resistance: interconnected processes of disease progression and therapy failure. Trends Mol Med 18:13-26.
3. Friedl P, Alexander S (2011) Cancer invasion and the microenvironment: plasticity and reciprocity. Cell 147:992-1009.
4. Hilderbrand SA, Weissleder R (2010) Near-infrared fluorescence: application to in vivo molecular imaging. Curr Opin Chem Biol 14:71-79.
5. Frangioni JV (2003) In vivo near-infrared fluorescence imaging. Curr Opin Chem Biol 7:626-634.
6. Gioux S, Choi HS, Frangioni JV (2010) Image-guided surgery using invisible near-infrared light: fundamentals of clinical translation. Mol Imaging 9:237-255.
7. Keereweer S, Van Driel PB, Snoeks TJ, et al. (2013) Optical Image-Guided Cancer Surgery: Challenges and Limitations. Clinical cancer research : an official journal of the American Association for Cancer Research.
8. Weissleder R, Pittet MJ (2008) Imaging in the era of molecular oncology. Nature 452:580-589.
9. Marusyk A, Almendro V, Polyak K (2012) Intra-tumour heterogeneity: a looking glass for cancer? Nat Rev Cancer 12:323-334.
10. Gerlinger M, Rowan AJ, Horswell S, et al. (2012) Intratumor heterogeneity and branched evolution revealed by multiregion sequencing. The New England journal of medicine 366:883-892.
11. Li Y, Bai S, Carroll W, et al. (2012) Validation of the Risk Model: High-Risk Classification and Tumor Pattern of Invasion Predict Outcome for Patients with Low-Stage Oral Cavity Squamous Cell Carcinoma. Head Neck Pathol.
12. Hinni ML, Ferlito A, Brandwein-Gensler MS, et al. (2012) Surgical margins in head and neck cancer: A contemporary review. Head & neck.
13. Martling A, Cedermark B, Johansson H, Rutqvist LE, Holm T (2002) The surgeon as a prognostic factor after the introduction of total mesorectal excision in the treatment of rectal cancer. Br J Surg 89:1008-1013.
14. Chance B (1998) Near-infrared images using continuous, phase-modulated, and pulsed light with quantitation of blood and blood oxygenation. Ann N Y Acad Sci 838:29-45.
15. Ntziachristos V (2010) Going deeper than microscopy: the optical imaging frontier in biology. Nat Methods 7:603-614.
16. Valdes PA, Leblond F, Jacobs VL, Wilson BC, Paulsen KD, Roberts DW (2012) Quantitative, spectrally-resolved intraoperative fluorescence imaging. Sci Rep 2:798.

17. Zhu B, Wu G, Robinson H, et al. (2013) Tumor Margin Detection Using Quantitative NIRF Molecular Imaging Targeting EpCAM Validated by Far Red Gene Reporter iRFP. Molecular imaging and biology : MIB : the official publication of the Academy of Molecular Imaging.
18. Themelis G, Yoo JS, Soh KS, Schulz R, Ntziachristos V (2009) Real-time intraoperative fluorescence imaging system using light-absorption correction. J Biomed Opt 14:064012.
19. Keereweer S, Kerrebijn JD, van Driel PB, et al. (2011) Optical image-guided surgery--where do we stand? Mol Imaging Biol 13:199-207.
20. Van Driel PBAA, Keereweer S, Snoeks TJA, Lowik CWGM (2013) Fluorescence-Guided Surgery: A Promising Approach for Future Oncologic Surgery. In Comprehensive Biomedical Physics. Elsevier.
21. Keereweer S, Mol IM, Vahrmeijer AL, et al. (2012) Dual wavelength tumor targeting for detection of hypopharyngeal cancer using near-infrared optical imaging in an animal model. Int J Cancer.
22. Mieog JS, Hutteman M, van der Vorst JR, et al. (2011) Image-guided tumor resection using real-time near-infrared fluorescence in a syngeneic rat model of primary breast cancer. Breast cancer research and treatment 128:679-689.
23. Kovar JL, Volcheck W, Sevick-Muraca E, Simpson MA, Olive DM (2009) Characterization and performance of a near-infrared 2-deoxyglucose optical imaging agent for mouse cancer models. Analytical biochemistry 384:254-262.
24. Kossodo S, Pickarski M, Lin SA, et al. (2010) Dual in vivo quantification of integrin-targeted and protease-activated agents in cancer using fluorescence molecular tomography (FMT). Molecular imaging and biology : MIB : the official publication of the Academy of Molecular Imaging 12:488-499.
25. Keereweer S, Mol IM, Kerrebijn JD, et al. (2011) Targeting integrins and enhanced permeability and retention (EPR) effect for optical imaging of oral cancer. J Surg Oncol.
26. Weissleder R, Tung CH, Mahmood U, Bogdanov A, Jr. (1999) In vivo imaging of tumors with protease-activated near-infrared fluorescent probes. Nat Biotechnol 17:375-378.
27. Blum G, von Degenfeld G, Merchant MJ, Blau HM, Bogyo M (2007) Noninvasive optical imaging of cysteine protease activity using fluorescently quenched activity-based probes. Nature chemical biology 3:668-677.
28. Keereweer S, Mieog JS, Mol IM, et al. (2011) Detection of oral squamous cell carcinoma and cervical lymph node metastasis using activatable near-infrared fluorescence agents. Arch Otolaryngol Head Neck Surg 137:609-615.
29. Radu A, Pichon C, Camparo P, et al. (2010) Expression of follicle-stimulating hormone receptor in tumor blood vessels. The New England journal of medicine 363:1621-1630.
30. Folkman J (1995) Angiogenesis in cancer, vascular, rheumatoid and other disease. Nature medicine 1:27-31.
31. Hanahan D, Folkman J (1996) Patterns and emerging mechanisms of the angiogenic switch during tumorigenesis. Cell 86:353-364.
32. Fang J, Nakamura H, Maeda H (2011) The EPR effect: Unique features of tumor blood vessels for drug delivery, factors involved, and limitations and augmentation of the effect. Adv Drug Deliv Rev 63:136-151.
33. Maeda H (2010) Tumor-selective delivery of macromolecular drugs via the EPR effect: background and future prospects. Bioconjugate chemistry 21:797-802.
34. Kovar JL, Johnson MA, Volcheck WM, Chen J, Simpson MA (2006) Hyaluronidase expression induces prostate tumor metastasis in an orthotopic mouse model. The American journal of pathology 169:1415-1426.
35. Chance B (1998) Near-infrared images using continuous, phase-modulated, and pulsed light with quantitation of blood and blood oxygenation. Annals of the New York Academy of Sciences 838:29-45.
36. Agostinis P, Berg K, Cengel KA, et al. (2011) Photodynamic therapy of cancer: an update. CA Cancer J Clin 61:250-281.
37. Castano AP, Mroz P, Hamblin MR (2006) Photodynamic therapy and anti-tumour immunity. Nat Rev Cancer 6:535-545.
38. Gil M, Bieniasz M, Seshadri M, et al. (2011) Photodynamic therapy augments the efficacy of oncolytic vaccinia virus against primary and metastatic tumours in mice. Br J Cancer 105:1512-1521.
39. Hendren SK, Hahn SM, Spitz FR, et al. (2001) Phase II trial of debulking surgery and photodynamic therapy for disseminated intraperitoneal tumors. Annals of surgical oncology 8:65-71.

40. Schmitt F, Juillerat-Jeanneret L (2012) Drug targeting strategies for photodynamic therapy. Anticancer Agents Med Chem 12:500-525.
41. Bugaj AM (2011) Targeted photodynamic therapy--a promising strategy of tumor treatment. Photochemical & photobiological sciences : Official journal of the European Photochemistry Association and the European Society for Photobiology 10:1097-1109.
42. Yang X, Shi C, Tong R, et al. (2010) Near IR heptamethine cyanine dye-mediated cancer imaging. Clinical cancer research : an official journal of the American Association for Cancer Research 16:2833-2844.
43. Tan X, Luo S, Wang D, Su Y, Cheng T, Shi C (2012) A NIR heptamethine dye with intrinsic cancer targeting, imaging and photosensitizing properties. Biomaterials 33:2230-2239.
44. Kepczynski M, Dzieciuch M, Nowakowska M (2012) Nanostructural hybrid sensitizers for photodynamic therapy. Curr Pharm Des 18:2607-2621.
45. Amelink A, Kruijt B, Robinson DJ, Sterenborg HJ (2008) Quantitative fluorescence spectroscopy in turbid media using fluorescence differential path length spectroscopy. Journal of biomedical optics 13:054051.
46. Kanick SC, Sterenborg HJ, Amelink A (2009) Empirical model of the photon path length for a single fiber reflectance spectroscopy device. Optics express 17:860-871.
47. Kanick SC, Sterenborg HJ, Amelink A (2008) Empirical model description of photon path length for differential path length spectroscopy: combined effect of scattering and absorption. Journal of biomedical optics 13:064042.
48. Kanick SC, Robinson DJ, Sterenborg HJ, Amelink A (2009) Monte Carlo analysis of single fiber reflectance spectroscopy: photon path length and sampling depth. Physics in medicine and biology 54:6991-7008.
49. Kanick SC, Robinson DJ, Sterenborg HJ, Amelink A (2011) Method to quantitate absorption coefficients from single fiber reflectance spectra without knowledge of the scattering properties. Optics letters 36:2791-2793.
50. Kanick SC, Gamm UA, Sterenborg HJ, Robinson DJ, Amelink A (2011) Method to quantitatively estimate wavelength-dependent scattering properties from multidiameter single fiber reflectance spectra measured in a turbid medium. Optics letters 36:2997-2999.
51. Kanick SC, Robinson DJ, Sterenborg HJ, Amelink A (2012) Extraction of intrinsic fluorescence from single fiber fluorescence measurements on a turbid medium. Optics letters 37:948-950.
52. Gamm UA, Kanick SC, Sterenborg HJ, Robinson DJ, Amelink A (2012) Quantification of the reduced scattering coefficient and phase-function-dependent parameter gamma of turbid media using multidiameter single fiber reflectance spectroscopy: experimental validation. Optics letters 37:1838-1840.
53. Kanick SC, Gamm UA, Schouten M, Sterenborg HJ, Robinson DJ, Amelink A (2011) Measurement of the reduced scattering coefficient of turbid media using single fiber reflectance spectroscopy: fiber diameter and phase function dependence. Biomed Opt Express 2:1687-1702.
54. van Leeuwen-van Zaane F, Gamm UA, van Driel PB, et al. (2013) In vivo quantification of the scattering properties of tissue using multi-diameter single fiber reflectance spectroscopy. Biomed Opt Express 4:696-708.
55. Valdes PA, Leblond F, Kim A, et al. (2011) Quantitative fluorescence in intracranial tumor: implications for ALA-induced PpIX as an intraoperative biomarker. J Neurosurg 115:11-17.
56. Roy HK, Backman V (2012) Spectroscopic applications in gastrointestinal endoscopy. Clin Gastroenterol Hepatol 10:1335-1341.
57. Nijssen A, Koljenovic S, Bakker Schut TC, Caspers PJ, Puppels GJ (2009) Towards oncological application of Raman spectroscopy. J Biophotonics 2:29-36.
58. Braakhuis BJ, Tabor MP, Kummer JA, Leemans CR, Brakenhoff RH (2003) A genetic explanation of Slaughter's concept of field cancerization: evidence and clinical implications. Cancer Res 63:1727-1730.
59. Graveland AP, Golusinski PJ, Buijze M, et al. (2011) Loss of heterozygosity at 9p and p53 immunopositivity in surgical margins predict local relapse in head and neck squamous cell carcinoma. Int J Cancer 128:1852-1859.
60. Califano J, van der Riet P, Westra W, et al. (1996) Genetic progression model for head and neck cancer: implications for field cancerization. Cancer Res 56:2488-2492.
61. Leemans CR, Braakhuis BJ, Brakenhoff RH (2011) The molecular biology of head and neck cancer. Nat Rev Cancer 11:9-22.

# & | Addendum

## Conclusion

NIR optical imaging is a new technique that can be used to discriminate between healthy and diseased tissues. Intraoperative application of NIR optical imaging has the potential to be of major benefit for the practice of surgical oncology. In case of head and neck squamous cell carcinoma (HNSCC), real-time intraoperative visualization of the primary tumor and cervical lymph node metastases can assist the surgeon in complete resection of the tumor, which could drastically improve patient outcome and survival.

This thesis focuses on current modalities and cancer targeting strategies of optical imaging. We have demonstrated that the tumor can be detected in animal models of HNSCC targeting various hallmarks of cancer. The invasive tumor front can be imaged using NIR fluorescence agents that become activated by specific enzymes that are involved in degradation of the extracellular matrix, a prerequisite for tumor invasion. Furthermore, tumor-specific targeting of HNSCC was demonstrated using NIR fluorescence agents that target receptors that are highly upregulated on the tumor cells to promote tumor growth (e.g. EGF receptor and the GLUT-1 receptor) or involved in cell migration, invasion and extravasation (e.g. integrin receptor). Non-targeted agents were also used to image the tumor by exploiting of the enhanced permeability and retention (EPR) effect: a process of leakage of agents out of tumor vasculature and into tumor interstitial tissue. Due to distorted lymphatic drainage, agents are retained in these regions. Dual wavelength imaging allows for simultaneous imaging of two different characteristics of the tumor. Using this principle of imaging at different wavelengths, both the primary tumor and the invasive tumor front can be imaged.

Overall, optical imaging using NIR fluorescence light is a new imaging modality that has recently emerged in the field of cancer imaging. The first steps of translation to the clinical practice are currently being made in non-invasive detection and classification of tumors, therapy monitoring, sentinel lymph node procedures, and image-guided cancer surgery. Although it is very likely that the technique will deliver an important contribution to surgical oncology, there are fundamental limitations to this approach that should not be overlooked in the process of implementation into clinical care. Optical imaging is based on detection of photons, but the path that photons travel through the imaged tissue is influenced by scattering and part of the photons are absorbed by tissue components. These features of tissue are called the optical tissue properties. In addition, it can be difficult to distinguish the photons of the fluorescent agent from photons coming from the tissue components itself, i.e. autofluorescence. These factors influence the image, and these effects become larger with increasing depth of the fluorophore within the tissue. Next to the fundamental principles, optical imaging is dependent on adequate efficacy and biodistribution of the fluorescent agent and accurate imaging systems. Although there are limitations to the intrinsic capacity of the technique, when practical and technical surgical issues are considered with care, optical imaging can be a very powerful intraoperative tool in guiding the future head and neck surgeon towards radical resection and optimal clinical results.

# English summary

Although imaging of tumors in the head and neck region has made great progress over the last decades, translation of these images to the operation field sometimes remains a challenge for the surgeon. The essence of oncologic surgery is to adequately discriminate tumor from normal tissue and consequently determine the tumor-free margin, which is essential for the prognosis of the patient. Currently, the only way to do this during surgery is by visual appearance and palpation, which might in part explain the suboptimal survival rates after head and neck surgery.

New intraoperative visualization techniques using near-infrared (NIR) fluorescence imaging are being developed that could help the surgeon to discriminate between healthy and cancer tissue. The concept of using NIR light has proven a crucial step towards the application in intraoperative image-guided surgery. Introduction of real-time imaging technologies into the operating room has the potential to improve resection of diseased tissue with optimal preservation of healthy tissue, resulting in image-guided surgery. Although a very promising technique, optical image-guided surgery has yet no place in head and neck oncology. The aim of this thesis was to explore the possibilities of image-guided head and neck cancer surgery within the relatively young revolutionary field of optical imaging.

In part I: Current modalities of optical image-guided surgery, the current modalities of optical imaging are introduced and reviewed. Chapter 2 focuses on the various techniques, contrast agents, and camera systems that are currently used for image-guided cancer surgery. Furthermore, an overview is provided of the wide range of molecular contrast agents that each target specific hallmarks of cancer, and the perspectives on its future use in cancer surgery is described.

In order to investigate the feasibility of these alternative optical imaging strategies for targeting of head and neck cancers, two different head and neck cancer animal models were introduced. Using these models, detection of head and neck cancer using optical imaging was performed *in vivo*, which is described in Part II: Optical imaging of head and neck cancer in animal models. The use of various NIR fluorescence agents was explored in this section.

In the first animal model, human oral cancer cells were inoculated submucosally into the distal end of the tongue of immunodeficient mice. These cells had been retrovirally infected with luciferase to allow bioluminescence imaging (BLI). Tumor growth was followed with BLI and visual inspection of the tongue. Next to orthotopical growth of the primary tumor, cervical lymph node metastases developed after two weeks, allowing assessment of detection of these metastases by optical imaging.

In Chapter 3, the use of activatable NIR fluorescence agents is described to detect head and neck cancer in this animal model. To gain optimal tumor-to-background ratios (TBR), new agents have been designed that contain a cleavage site specific to tumor specific enzymes. These agents are injected in a quenched (i.e., non-fluorescent) state, minimizing fluorescence at the time of administration. After cleavage by the specific enzyme, the agent becomes

dequenched (i.e., fluorescent) and emits a fluorescent signal of 700 nm. The capability to degrade the extracellular matrix (ECM) surrounding the tumor in order to access blood vessels and lymphatic vessels is a prerequisite for tumors to invade and metastasize. In this process, the same mechanisms that normal cells use for migrating through tissue barriers are exploited. Proteolytic enzymes, including matrix metalloproteinases (MMPs), and cathepsins (mostly cathepsin B) are involved in ECM degradation of head and neck cancer. We demonstrated that oral cancer and cervical lymph node metastases could be detected by targeting increased proteolytic activity at the tumor borders. To the best of our knowledge, this was the first study that described the use of activatable NIR fluorescence agents to detect head and neck cancer *in vivo*.

In Chapter 2, NIR fluorescence agents were described that target the various hallmarks of cancer. One of these hallmarks, limitless replicative potential of tumor cells, contains an essential feature of carcinogenesis and is facilitated in part by increased expression of growth signaling receptors. In the majority of head and neck cancers, increased expression of the epidermal growth factor (EGF) receptor is found, providing a useful target for tumor imaging. A second feature of tumor growth is exploited in positron emission tomography (PET) technology, by targeting the increased metabolism of cancer cells using the glucose-mimetic 2-deoxy-2-[18F]fluoro-D-glucose (18FDG). Increased EGF receptor expression and glucose uptake in tumors was targeted in Chapter 4 to detect oral cancer and cervical lymph node metastases in the aforementioned animal model. The fluorescence properties of agents that emit light in the 800 nm region resulted in sufficient TBRs, which is essential in intraoperative cancer detection.

Head and neck cancer is a collective noun for all cancers originating within the anatomical boundaries of the head and neck. For example, hypopharyngeal squamous cell carcinoma will have different molecular characteristics than oral squamous cell carcinoma. Therefore, a second head and neck cancer model was used to demonstrate the extensive applicability of the used agents. In this model, human hypopharyngeal cancer cells were used in immunodeficient mice. Similar to the first model, these cells had been retrovirally infected with the luciferase gene to allow tumor growth monitoring using BLI. Although an orthotopical tumor model is preferred in order to maintain optimal conditions of the natural surroundings of the tumor, the cells could not be inoculated into the hypopharynx due to a high risk of dyspnea or suffocation during the earliest stages of cancerogenesis. Therefore, similar to many other animal models, cells were inoculated subcutaneously.

In Chapter 3, NIR fluorescence agents were used that fluoresce at 700 nm. Subsequently, the use of agents that have emission peaks at 800 nm was described in Chapter 4. However, we hypothesized that tumor detection could be improved by targeting multiple tumor-specific characteristics simultaneously with fluorophores that emit light at different wavelengths. Therefore, in Chapter 5, dual wavelength targeting by NIR fluorescence technologies for *in vivo* cancer imaging was explored. In the 700 nm region, ProSense680 and MMPSense680 (PerkinElmer, Waltham, MA) were used that detect increased activity of cathepsins and MMPs, respectively. The use of these agents was combined with NIR fluorescence agents

that emit at 800 nm, including 2DG CW800 (LI-COR Biosciences), which detects increased glucose uptake, and EGF CW800 (LI-COR Biosciences), which is internalized by the EGF receptor of tumor cells. We demonstrated the feasibility of combined tumor detection using different targeting strategies simultaneously in an animal model of hypopharyngeal cancer. Dual wavelength targeting allowed for simultaneous imaging of different tumor characteristics.

The use of dual wavelength imaging was further exploited in Chapter 6, which focused on two important aspects of cancer: involvement of αvβ3 integrins[19] and the enhanced permeability and retention (EPR) effect. Integrins are transmembrane cell surface receptors that are involved in cell migration, invasion and extravasation, and specifically integrin αvβ3 is upregulated in activated endothelial cells as well as in head and neck cancer cells. The EPR effect results from abnormal architecture of newly formed bloof vessels and defective lymphatic drainage, which leads to leakage of tumor vessels with accumulation and retention of the agent in tumor interstitial tissues. Simultaneous, dual wavelength targeting of integrins and the EPR effect resulted in clear demarcation of head and neck cancer in an orthotopical mouse model.

After extensive preclinical research, the first steps of translation to the clinical practice are finally being made. In Part III: Current status of optical imaging in diagnosis and treatment of cancer (Chapter 7), the preclinical and clinical results are discussed of near-infrared optical imaging for non-invasive detection and classification of tumors, therapy monitoring, sentinel lymph node procedures, and image-guided cancer surgery. This chapter provides a clear overview of the future directions of optical imaging in clinical practice, and the broad field of preclinical studies that have preceded the current essential steps of translational medicine. Furthermore, it is stated that widespread availability of imaging systems and optical contrast agents will enable larger studies on their clinical benefit and can help establish a definitive role in clinical practice.

Although it is very likely that the technique will deliver an important contribution to surgical oncology, there are fundamental limitations to this approach that introduce uncertainties that should not be overlooked in the process of implementation into clinical care. Optical imaging is based on detection of photons, but the path that photons travel through the imaged tissue is influenced by scattering and part of the photons are absorbed by tissue components. These features of tissue are called the optical tissue properties. In addition, it can be difficult to distinguish the photons of the fluorescent agent from photons coming from the tissue components itself, i.e. autofluorescence. These factors influence the accuracy of the image, and the effects become larger with increasing depth of the fluorescent agent within the tissue. It is impossible to know all these factors in the inhomogeneous tissues of a patient and therefore a small level of uncertainty remains regarding the accuracy of the image. Next to the fundamental principles, optical imaging is dependent on adequate efficacy and biodistribution of the fluorescent agent and accurate imaging systems. The fundamental aspects of optical imaging, its limitations and the challenges that lie ahead are the focus of Part IV: General Discussion. When optical image-guided surgery is used for

radical removal of the tumor, it is essential to understand the advantages and limitations of the technique and to know how the expertise of a trained oncologic surgeon can improve the accuracy of the images. This is discussed in Chapter 8, where a clear overview is presented of the possibilities and limitations of optical image-guided cancer surgery. Next, a general discussion on the results of NIR fluorescence imaging of head and neck cancer in animal models is provided in Chapter 9. Several important aspects are discussed in this chapter that warrant future research, including the paradigm of field cancerization, prospects on the use of immunocompetent animal models and dual wavelength imaging, and future applications of mutimodal fluorescence agents. In Chapter 10, the future directions are discussed that are required to define the role of optical imaging as a powerful intraoperative tool in guiding the future oncologic surgeon towards radical resection with subsequent optimal clinical results, forming the foundation of tomorrow's medicine. Limitations of the "classic approach" of imaging tumor-specific targets or tumor-associated pathophysiological processes are pointed out and possible solutions are suggested.

In this thesis, we have set the first steps of detection of head and neck cancer within the relatively young revolutionary field of optical imaging. In the Conclusion, it is stated that although there are limitations to the intrinsic capacity of the technique, when practical and technical surgical issues are considered with care, optical imaging will introduce a new era of oncologic surgery and can be a very powerful intraoperative tool in guiding the future head and neck surgeon towards radical resection and optimal clinical results. All results are summarized in the English and Dutch Summary.

# Nederlandse samenvatting

De ontwikkeling van beeldvormende technieken heeft in de laatste decennia een grote vlucht genomen, met als resultaat een uitgebreid palet aan modaliteiten om een maligniteit in het hoofd-halsgebied in kaart te brengen. Eenmaal in de operatiekamer ontstaat echter een andere situatie. Waar vooraf de anatomische locatie van de tumor nauwkeurig kan worden bepaald met behulp van beeldvorming, is de hoofd-halschirurg tijdens de operatie aangewezen op zijn handen en ogen om palpatoire en visuele veranderingen van tumoreus veranderd weefsel te kunnen herkennen. Aangezien radicale resectie (dat wil zeggen: met tumorvrije marges) een van de belangrijkste prognostische factoren is van overleving, is het onderscheiden van gezond en maligne weefsel een essentieel aspect van oncologische chirurgie. In de huidige chirurgische praktijk worden tumoren helaas nog regelmatig irradicaal verwijderd.

Een techniek die beeldvorming direct onder de handen van de chirurg plaatst zou een zeer waardevolle bijdrage kunnen leveren aan het adequaat bepalen van de tumorvrije marge tijdens de operatie. Optische beeldvorming met behulp van nabij-infraroodfluorescentie zou hiervoor een bruikbare techniek kunnen zijn. Om de tumor zichtbaar te maken worden fluorescerende tumorspecifieke stoffen bij de patiënt ingespoten, die vervolgens met speciaal ontworpen camerasystemen worden gedetecteerd. De combinatie van geschikte camerasystemen en tumorspecifieke stoffen kan in de toekomst leiden tot fluorescentiegeleide chirurgie van hoofd-halstumoren. Deze veelbelovende techniek heeft momenteel nog geen plaats binnen de hoofd-hals chirurgie. In dit proefschrift worden de mogelijkheden verkend voor het verrichten van fluorescentiegeleide chirurgie binnen het revolutionaire jonge onderzoeksgebied van optische beeldvorming.

In Deel I: Huidige modaliteiten van optische beeldgeleide chirurgie, worden de bestaande mogelijkheden van optische beeldvorming beschreven. Hoofdstuk 2 behandelt de verschillende technieken, fluorescerende stoffen, en camerasystemen die momenteel worden gebruikt in optische beeldgeleide chirurgie. Samen met goede fluorescente eigenschappen van de stof is tumorspecificiteit van essentieel belang voor beeldgeleide chirurgie van tumoren. De laatste jaren zijn hiervoor vele strategieën ontwikkeld die alle aangrijpen op verschillende kenmerkende eigenschappen van tumorcellen. De toekomstige toepassing van deze stoffen voor oncologische chirurgie in het algemeen en voor hoofd-hals chirurgie in het bijzonder wordt besproken in dit hoofdstuk.

Om te kunnen testen of deze stoffen toepasbaar zouden kunnen zijn voor het detecteren van hoofd-hals tumoren werden twee verschillende proefdiermodellen van hoofd-hals kanker gebruikt. De resultaten van de studies waarbij de verschillende fluorescente stoffen werden getest zijn beschreven in Deel II: Optische beeldvorming van hoofd-hals tumoren in diermodellen. In het eerste proefdiermodel werden humane cellen van een mondholtetumor geïnoculeerd in de tong van immuundeficiënte muizen. De cellen waren verrijkt met luciferase om bioluminescente beeldvorming (BLI) mogelijk te maken waarmee de tumorgroei kon worden gevolgd. Na twee weken ontstonden naast groei van de primaire tumor ook lymfkliermetastasen in de hals waardoor ook beeldvorming van halskliermetastasering kon worden onderzocht.

In Hoofdstuk 3 werd gebruikgemaakt van fluorescente stoffen die 'activeerbaar' zijn, hetgeen betekent dat deze pas een fluorescent signaal geven na contact met de specifieke doeleiwitten. Op deze manier kan de ratio van de stof ten opzichte van onspecifiek achtergrondsignaal (signaal-ruis-verhouding) worden vergroot. Het vermogen van de tumor om de omliggende matrix af te breken en zodoende bloed- en lymfbanen te kunnen bereiken is een voorwaarde om voor invasie en uitzaaiing. Hierbij wordt gebruik gemaakt van dezelfde processen en enzymen die normale cellen gebruiken om door weefselbarrières te migreren. Met behulp van deze "activeerbare" stoffen werd dergelijke verhoogde enzymatische activiteit aan de (invasieve) rand afgebeeld van zowel de primaire tongtumor als ook in de halskliermetastasen. Voor zover bekend is dit de eerste studie die het gebruik van "activeerbare" stoffen beschrijft om een hoofd-hals tumor *in vivo* te detecteren.

In hoofdstuk 2 werden verschillende strategieën beschreven die aangrijpen op de verschillende kenmerkende eigenschappen van kanker. Een van deze eigenschappen is de onbeperkte mogelijkheid van kankercellen om zichzelf te vermenigvuldigen. Dit komt voor een deel door de verhoogde expressie van groeifactor-receptoren op kankercellen. In hoofd-hals tumoren is de expressie van epidermale groeifactor (EGF)-receptor sterk verhoogd. Een tweede eigenschap is het verhoogde metabolisme van kankercellen, hetgeen wordt gebruikt in de technologie van positron-emissie-tomografie (PET) door middel van het glucose-mimetic 2-deoxy-2-[18F]fluoro-D-glucose (18FDG). In Hoofdstuk 4 werden fluorescente stoffen gebruikt die specifiek binden aan de epidermale groeifactor (EGF)-receptor en die gericht zijn op de verhoogde opname van glucose in de kankercellen. Met deze stoffen werden de primaire tumor en halsmetastasen opgespoord in het bovenbeschreven proefdiermodel.

Aangezien tumoren die op verschillende locaties in het hoofd-hals gebied voorkomen ook moleculair van elkaar (kunnen) verschillen, werden de eerder genoemde stoffen ook getest in een ander proefdiermodel: dat van een hypofarynxcarcinoom. Ook hier werden de tumorcellen verrijkt met luciferase om tumorgroei middels BLI te vervolgen. Maar hoewel een tumor idealiter onderzocht wordt in zijn natuurlijke (orthotopische) omgeving is het risico te groot dat de proefdieren zouden stikken wanneer de cellen in de hypofarynx worden geïnoculeerd. Daarom werden deze tumoren in de flank geïnoculeerd, gelijk aan vele proefdiermodellen van andere vormen van kanker.

In hoofdstuk 3 werden fluorescente stoffen gebruikt die hun signaal geven op 700 nm golflengte. De stoffen die vervolgens in hoofdstuk 4 werden gebruikt geven hun signaal op 800 nm golflengte. Gelijktijdig gebruik van verschillende NIR-fluorescente stoffen zou de sensitiviteit van de techniek kunnen verhogen, omdat op die manier meer tumoreigenschappen tegelijk kunnen worden gedetecteerd. Door stoffen te gebruiken die op verschillende golflengtes fluorescent licht uitstralen, kunnen de signalen van deze stoffen bovendien apart worden onderscheiden en de tumorkenmerken worden bestudeerd. In Hoofdstuk 5 werden verschillende combinaties van de eerder genoemde fluorescente stoffen gebruikt om hypofarynxcarcinoom te detecteren. Hierbij werden gelijktijdig stoffen in beeld gebracht die fluoresceren door verhoogde activiteit van specifieke enzymen in de

(invasieve) tumorrand, gecombineerd met detectie van stoffen die specifiek gericht zijn op de tumorcellen zelf.

Het gecombineerd gebruik van verschillende golflengtes werd verder onderzocht in Hoofdstuk 6 waarbij toegenomen vaatnieuwvorming in de tumor werd gedetecteerd met stoffen die binden aan integrines. Integrines zijn stoffen die een essentiële rol spelen bij de verbinding van onderlinge cellen en vaatnieuwvorming. De tweede strategie om de tumor te detecteren was door gebruik te maken van de toegenomen permeabiliteit en retentie van stoffen in en rond de tumor. Het gelijktijdig in beeld brengen van deze stoffen zorgde voor een duidelijke demarcatie van tongtumor in een orthotopisch proefdiermodel.

Na uitgebreid preklinisch onderzoek worden de eerste translationele stappen naar in de kliniek inmiddels gezet. In Deel III: Huidige status van optische beeldvorming voor diagnose en behandeling van kanker (Hoofdstuk 7) worden de preklinische en klinische resultaten beschreven van nabij-infrarood optische beeldvorming voor non-invasieve detectie en classificatie van tumoren, monitoren van therapie, schildwachtklierprocedures, en beeldgeleide kankerchirurgie.

Gezien de grote vaart waarin de techniek zich momenteel wereldwijd ontwikkelt, lijkt introductie in de kliniek niet ver meer van ons af te staan. De vele preklinische onderzoeken geven een goed beeld van de potentiële verbetering die fluorescentiegeleide chirurgie in de oncologische chirurgie zou kunnen brengen. Toch zijn er belangrijke beperkingen die niet mogen worden onderschat in het proces van implementatie in de klinische praktijk. Optische beeldvorming is gebaseerd op detectie van fotonen, maar het pad dat de fotonen afleggen door weefsels wordt beïnvloed door verstrooiing en een deel van de fotonen wordt geabsorbeerd door componenten van het weefsel. Deze kenmerken worden de optische eigenschappen van het weefsel genoemd. Daarnaast kan het lastig zijn om de fotonen die afkomstig zijn van de fluorescente stoffen te onderscheiden van fotonen die van het weefsel zelf afkomstig zijn: de autofluorescentie. De invloed die deze factoren hebben op de afbeelding wordt bovendien groter naarmate de fluorescente stof zich dieper in het weefsel bevindt. Naast de fundamentele beperkingen van optische beeldvorming is de techniek ook afhankelijk van accurate binding van de stoffen, biodistributie, en adequate camerasystemen.

De fundamentele aspecten van optische beeldvorming, de beperkingen, en de uitdagingen die nog in het verschiet liggen zijn het onderwerp van Deel IV: Algehele discussie. Voor het gebruik van optische beeldgeleide chirurgie is het belangrijk dat de oncologisch chirurg op de hoogte is van de beperkingen en mogelijkheden om optimaal voordeel te kunnen behalen in de operatiekamer. Een helder overzicht van deze mogelijkheden en beperkingen wordt gepresenteerd in Hoofdstuk 8, gevolgd door een discussie in Hoofdstuk 9 over de resultaten van de studies die beschreven zijn in dit proefschrift. Enkele aspecten die nader onderzoek behoeven worden in dit hoofdstuk genoemd, zoals het probleem van "field cancerization", het gebruik van immuuncompetente diermodellen, en de toepassingen van beeldvorming op meerdere golflengtes of zelfs verschillende modaliteiten van beeldvorming tegelijk. Een toekomstperspectief wordt geschetst in Hoofdstuk 10 waarin aan bod komt wat er voor

nodig is om een definitieve rol te kunnen spelen als krachtig intraoperatief hulpstuk zodat de toekomstig oncologisch chirurg kan worden begeleid naar radicale resecties met de daarbij behorende optimale functionele en oncologische uitkomsten. Mogelijke beperkingen worden hierin genoemd van de "klassieke" benadering waarbij gebruik wordt gemaakt van tumor-specifieke antistoffen om de tumor in beeld te brengen, en verschillende suggesties worden gedaan om deze beperkingen te omzeilen.

In dit proefschrift werden de eerste stappen gezet op weg naar fluorescentiegeleide chirurgie van hoofd-hals tumoren. In de Conclusie wordt gesteld dat er beperkingen zijn aan de intrinsieke capaciteit van deze techniek. Wanneer echter rekening wordt gehouden met de praktische en chirurgisch-technische beperkingen kan optische beeldvorming wel degelijk een nieuw tijdperk van oncologische chirurgie inluiden. Het zal echter nog enkele jaren duren voordat kan worden bepaald of deze techniek daadwerkelijk leidt tot radicalere chirurgie van hoofd-halstumoren met betere overleving als resultaat. Desondanks is het helder dat de techniek een potentiële doorbraak kan betekenen voor oncologische hoofd-halschirurgie waarmee mogelijk een nieuwe basis wordt gelegd voor verbeterde oncologische zorg voor de volgende generaties patiënten. De inhoud van het proefschrift wordt samengevat in een Engelse en Nederlandse samenvatting.

## List of abbreviations

| | |
|---|---|
| 18FDG | 2-deoxy-2-[18F]fluoro-D-glucose |
| 2-DG | 2-deoxyglucose |
| 4NQO | 4-nitroquinoline-1-oxide |
| 5-ALA | 5-aminolevulinic acid |
| αvβ3 | alpha-v-beta-3 |
| BLI | bioluminescence imaging |
| cRGD | cyclic arginine-glycine-aspartate |
| CT | computed tomography |
| ECM | extracellular matrix |
| EGF | epidermal growth factor |
| EGFR | epidermal growth factor receptor |
| EPR | enhanced permeability and retention |
| FDA | food and drug administration |
| FLI | fluorescence imaging |
| FSH | follicle-stimulating hormone |
| GLUT | glucose transporters |
| HCC | hepatocellular carcinoma |
| HE | hematoxylin-eosin |
| HNSCC | head and neck squamous cell carcinoma |
| ICG | indocyanine green |
| MMP | matrix metalloproteinase |
| MRI | magnetic resonance imaging |
| NIR | near-infrared |
| NIRF | near-infrared fluorescence |
| OSCC | oral squamous cell carcinoma |
| PBS | phosphate buffered saline |
| PDT | photodynamic therapy |
| PET | positron emission tomography |
| SBR | signal-to-background ratio |
| SD | standard deviation |
| SLN | sentinel lymph node |
| SPECT | single-photon-emission computed tomography |
| TBR | tumor-to-background ratio |
| TfR | transferrin receptor |
| US | ultrasonography |
| VEGF | vascular endothelial growth factor |

## Glossary

### *Absorption*

The phenomenon that describes how the electromagnetic energy of a photon is taken up by matter, typically the electrons of an atom. Absorption decreases intensities.

### *Agent, Fluorescence*

Antibody or ligand conjugated to an optically active reporter that is designed to target a disease-specific biomarker.
(See also Probe, fluorescence.)

### *Autofluorescence*

Fluorescence of normal endogenous components of the tissue. In intrinsic fluorescence spectroscopy, the autofluorescence spectrum is measured to determine the biochemical tissue components.

### *Bioluminescence*

Bioluminescence is the process of light emission in living organisms. In contrast to fluorescence, bioluminescence does not require excitation by light, but is generated chemically. In bioluminescence imaging, the DNA of such an organism that encodes the luminescent protein is incorporated into a laboratory animal either via a viral vector or by creating a transgenic animal. Bioluminescence imaging is based on the detection of light produced during enzyme (luciferase)-mediated oxidation of a molecular substrate when the enzyme is expressed *in viv*o as a molecular reporter. The technique enables monitoring throughout the course of disease, allowing localization and serial quantification of biological processes without killing the laboratory animal.

### *Differential path length spectroscopy*

A form of scattering spectroscopy that uses two optical fibers that are in contact with the medium that is measured. One of the two fibers (dc) is used to deliver white light to the medium, both fibers (dc and c) collect light from the medium. Subtracting the c-spectrum from the dc-spectrum forms the differential path length spectrum. Photons traveling deep into the tissue have an equal chance of getting detected by either fiber and their contribution to the differential path length spectrum will be subtracted away. Photons that stay close to the dc fiber have a larger chance of getting detected by the dc-fiber than by the c-fiber. Hence the differential path length spectrum consists mainly of photons that never left the vicinity of the dc-fiber and hence have traveled only superficially through the medium. This specialized fiber geometry makes the photon path length insensitive to variations in tissue optical properties over a wide range of absorption and scattering coefficients. Thereby, it allows determination of fluorophore concentration based on the fluorescence intensity corrected for absorption.

### *Diffuse optical spectroscopy*

Measurement technique based on detection of diffusely scattered light. It is used to estimate the average optical properties of tissue at multiple wavelengths based on diffusion theory.

### *Diffuse optical tomography*

Imaging technique based on diffuse optical spectroscopy. Diffuse optical tomography assumes that light propagation is dominated by multiple scattering and is modeled as a diffusive process where photons behave as stochastic particles. Semi-quantitative tissue measurements can be obtained by separating light absorption from scattering using spatially- or temporally-modulated photon migration technologies. Tissue molecular composition, including the concentration oxy- and deoxy- hemoglobin, water, lipid, and exogenous probes; and tissue structure can be determined from quantitative absorption and scattering measurements, respectively.
(See also Diffuse optical spectroscopy.)

### *Diffuse reflectance spectroscopy*

Measurement technique based on detection of diffusely scattered light, specifically in reflection geometry. When incident light strikes a surface, the light that penetrates is reflected in all directions, a phenomenon that is called diffuse reflectance. Diffusely reflected white light enters the tissue and scatters multiple times before it is collected at the tissue surface and its intensities can be estimated based on diffusion theory.
(See also Diffuse optical spectroscopy.)

### *Emission light*

The light that is emitted by a fluorophore after it has been excited by the excitation signal. This is the signal that can be detected by the fluorescence camera system. The wavelengths generated by a fluorescent molecule are molecule specific.

### *Excitation light*

The light that is used to excite a fluorescent component. Once absorbed by the fluorophore there is a chance that it subsequently emits light with a lower energy and longer wavelength. The wavelengths suitable to excite a fluorescent molecule are molecule specific.

### *Fluorescence*

Light emitted from materials after absorption of excitation light. The excitation light has a shorter wavelength. Fluorescence excitation and emission spectra are molecule specific.

### *Fluorescence tomography*

Imaging technology that is capable of spatially resolving the concentration of fluorescent agents located deep in soft tissue *in vivo*. Because of the possibility of co-registration with other imaging modalities such as MRI, PET, SPECT, and CT, it determines the position and quantity of a fluorescent source in a three-dimensional image.

### *Intrinsic fluorescence spectroscopy*
See "Autofluorescence".

### *Optical imaging*
A general term for imaging techniques that uses the behaviour and properties of visible, ultraviolet, and infrared light, including its interactions with matter to create an image.

### *Lifetime imaging*
Imaging technique that distinguishes individual fluorophores by their specific temporal decay (i.e. time domain) after excitation.
(See also Stokes shift; Time domain imaging.)

### *Linear mixing*
The concept that is based on the assumption that the measured spectrum consists of the sum of the fluorescence spectra of all the components in the tissue. This theory is challenged by the observation that inhomogeneous tissues influence the path that photons travel through the imaged tissue. Therefore, optical tissue properties may put their own signatures on the fluorescence spectrum, and may do so in a non-linear way.

### *Multiplexed imaging*
Fluorescence imaging of multiple wavelengths, allowing for simultaneous analysis of different fluorophores that could have different targets.

### *Near-infrared spectroscopy*
Measurement technique based on detection of light with wavelengths ranging from 700-1100 nm.

### *Planar fluorescence imaging*
General term for the conventional imaging technique that uses illumination of tissues with a plane wave (i.e. an expanded light beam), with subsequent collection of fluorescence signals that are emitted toward the camera. This can be applied in epi-illumination (i.e. photographic or reflectance imaging) or transillumination (collection of data on the opposite side) mode.

### *Probe, Fluorescence*
Antibody or ligand conjugated to an optically active reporter that is designed to target a disease-specific biomarker.
(See also Agent, fluorescence.)

### *Photoacoustic imaging*
When a short laser pulse, typically in the nanosecond range, is used to irradiate tissue, it produces a temperature rise in the tissue in a short time frame. Even if this temperature rise is small, fast enough thermoelastic expansion causes emission of acoustic waves, referred to as

photoacoustic (also known as optoacoustic) waves, that can be measured by photoacoustic spectroscopy. The resolution in photoacoustic imaging is not limited by optical scattering but by the attenuation of acoustic frequencies by tissue (it is stronger for higher frequencies, which contribute to high spatial resolution). The resolution therefore also drops with depth, but at a slower rate compared to purely optical imaging methods. Light scattering, together with optical absorption, contributes to the overall light attenuation, which dictates the penetration depth of photoacoustic imaging.

### *Raman spectroscopy*

Imaging technology that is based on inelastic scattering of light. Inelastic scattering means that the frequency of the photons of the excitation light changes upon interaction with the medium (e.g. tissue). This frequency can be shifted up or down in comparison with the original frequency. This phenomenon was named after Sir Chandrasekhara Venkata Raman, a physicist who first described the effect and received the Nobel Prize of Physics for it. This shift provides information about vibrational, rotational and other low frequency transitions in molecules.
(See also Surface-enhanced Raman scattering.)

### *Real-time imaging*

Synchronous data capturing and processing that results in a direct presentation of the fluorescent images.



### *Reflection*

The change in direction of a light wave at the interface between two different media, so that the light beam returns into the medium from which it originated.
(See also Refraction.)

### *Refraction*

A change in direction of a wave at the surface between two different media. In optics, this describes the phenomenon that occurs when waves travel at an oblique angle to a medium with a different refractive index. At this surface, the wave's phase velocity is altered, causing a change in direction. As a result, its wavelength changes but the frequency remains constant.
(See also Reflection; Refractive index mismatch.)

### *Refractive index mismatch*

A mismatch between the indices of refraction (usually of tissue and air), causing a change in direction of the light wave. The index of refraction is defined as the speed of light in vacuum divided by the speed of light in the medium. How much the refracted ray bends can be calculated using Snell's law.
(See also Refraction.)

### *Scattering*

In a medium with a constant index of refraction, photons travel in a straight path. However, when photons contact particles or irregularities in the propagation medium, the path of photons can be deflected. This effect is called scattering.

### *Spectral unmixing*

The decomposition of the complete spectrum of a fluorescence signal into a collection of predefined spectra. This technique is used to determine the individual contribution of each fluorophore, i.e. linear unmixing.
(See also Linear mixing.)

### *Stokes shift*

The difference in wavelength between the absorption and emission spectra of a fluorophore. When a photon is absorbed by a fluorophore, the fluorophore molecule gains energy and enters an excited state. The electrons remain in this state for about $10^{-8}$ seconds depending on the molecule, which is called the lifetime of the fluorophore (See also Lifetime imaging). After this phase, the system returns to its ground state and emits the photon. The change in energy between the absorbed and the emitted photon results in a change in wavelength. This shift of shorter wavelengths (higher energy) of the absorption spectrum to longer wavelengths (lower energy) of the emitted fluorophores is called the Stokes shift, named after the physicist George G. Stokes.

### *Surface-enhanced Raman scattering*

A technique of Raman spectroscopy that exploits prior injection of tumor-specific nanobodies that are able to increase the intrinsically very low Raman effect, thereby improving detectability. It uses a plasmon resonance effect that is able to increase the Raman effect several orders of magnitude. This increase is caused by small molecules that are adsorbed onto a nano-roughened noble metal surface, resulting in an increase in the incident electromagnetic field. By injecting tumor-specific Raman active gold or silver nanoparticles, they can be used as molecular imaging contrast agents in conjunction with Raman spectroscopy.
(See also Raman spectroscopy.)

### *Time-domain imaging*

Imaging technique that distinguishes the contribution of individual fluorophores to the spectrum based on the specific temporal decay (ie time-domain, the lifetime) of a fluorophore. In time-domain imaging, their temporal response at which photons emerge from the tissue is measured.
(See also Lifetime imaging.)

### *Time-domain optical mammography*

Mammographic imaging technology based on time-domain optical imaging techniques.
(See also Lifetime imaging, Time-domain imaging.)

## Een woord van dank

Professor Löwik, beste Clemens,

*"The true sign of intelligence is not knowledge but imagination" – Albert Einstein.*
Jouw lef om buiten de begane paden te treden zal soms tot verbazing of zelfs hoon hebben geleid. Maar wat sommigen opportunisme zullen noemen zie ik als een unieke eigenschap waarmee jij je onderscheidt als wetenschapper. Je weet al dat ik je eindeloze enthousiasme enorm waardeer. Dat ik onze ontelbare onvergetelijke feestjes en congressen koester. En dat ik je dankbaar ben voor je onvoorwaardelijke steun en positiviteit die mij hebben gestimuleerd betrokken te blijven bij de volgende stappen van het onderzoek. Maar bovenal hebben de afgelopen jaren feilloos inzichtelijk gemaakt waar Steef zijn talent voor slechte grappen vandaan heeft. Dank voor alles.

Professor Baatenburg de Jong, beste Rob,

Je bood mij de mogelijkheid om anderhalf jaar lang, naast de diensten en wekelijkse polidag in het Erasmus MC, de overige tijd in Leiden door te brengen. Met dit gestelde vertrouwen legde je de basis om een unieke samenwerking op te bouwen tussen de afdelingen Keel-, Neus-, Oorheelkunde (Erasmus MC), Moleculaire Beeldvorming (LUMC), Heelkunde (LUMC) en Center for Optical Diagnostics and Therapy (Erasmus MC). Wie weet wat voor mooi vervolg deze samenwerking nog mag krijgen. Je bent een voorbeeld in hoe je iedereen uitdaagt niet te snel tevreden te zijn en zo het beste uit zichzelf te halen.

Jeroen Kerrebijn, beste Jeroen,

We begonnen onze samenwerking met retrospectieve onderzoeken naar functionele uitkomsten van verschillende hoofd-hals chirurgische ingrepen. In die tijd heb ik veel meer van je geleerd dan je zelf zal willen erkennen, zeker over het schrijven van een artikel. Een klinische vraag bracht ons uiteindelijk door een combinatie van toeval en opportunisme naar Leiden. Ik realiseer me dat die eerste stappen zonder jouw steun op de achtergrond waarschijnlijk niet hadden plaatsgevonden. Dank voor dit alles. En voor wat betreft de avonden zoals in San Francisco toen de Giants de Super Bowl wonnen, of zoals bij het Algonquin Park in Canada: ik kan me niet voorstellen dat we zo'n avond niet nog eens ergens dunnetjes zouden overdoen…

Professor Sterenborg, beste Dick,

*"In het land der blinden is eenoog koning. In het land der eenogen is hij koning die bereid is moeite te doen een tweede oog te openen."*
Woorden van deze strekking sprak jij op een van de middagen waarin ik met veel pijn en moeite probeerde de essenties en subtiliteiten van de optische fysica te begrijpen. Je geduld om aan een eenvoudige, weliswaar geïnteresseerde, arts met weinig talent voor natuurkunde deze lastige principes bij te brengen is bewonderenswaardig. Ik ben er van overtuigd dat jouw bijdrage aan ons project essentieel is geweest om de wetenschappelijke waarde ervan te verhogen en hoop dat deze vruchtbare samenwerking gevolg zal vinden bij eventuele aanvullende projecten.

Pieter van Driel, Pjotr!

Behalve collega en paranimf ben je natuurlijk bovenal een bijzonder goede vriend. Dat we onze promotieonderzoeken grotendeels samen hebben kunnen doen was een feest dat denk ik weinigen is gegeven. Inhoudelijke discussies werden meestal tijdens het sporten of in de kroeg gevoerd. De inmiddels befaamde pizza-met-bier avonden met Clemens en Thomas waren naast productief toch vooral ook hilarisch. Op wetenschappelijk gebied heb je enorm veel in je mars, op het moment dat ik dit schrijf ben je bij 11 verschillende projecten tegelijk betrokken. Zo'n inzet is alleen mogelijk door de gedrevenheid en onophoudelijke positiviteit die zo kenmerkend is voor jou, al wordt het langzamerhand de hoogste tijd om al die inspanning eens te gaan oogsten. Wat we allemaal op de congressen hebben uitgespookt kan de weerschijn van dit boekje niet verdragen. Het doet er ook niet toe, het was mooi!

Alexander Vahrmeijer, beste Lex,

Het is inspirerend om te zien hoe je het preklinische werk naar de kliniek hebt weten te brengen. Ik hoop dat je zal slagen om nu ook met tumor-specifieke stoffen de toonaangevende resultaten te boeken die het veld nodig heeft om daadwerkelijk zijn meerwaarde te kunnen gaan bewijzen voor de individuele oncologische patiënt. Dank je voor de goede samenwerking, in het bijzonder natuurlijk ook met de heren van het eerste uur: Sven en kort daarna Merlijn, gevolgd door Joost en Bob. Stuk voor stuk wetenschappers waar de heelkunde trots op mag zijn.

Isabel Mol, Molletje!

Ik heb het nooit onder stoelen of banken geschoven dat jij een heel belangrijke rol hebt gespeeld in de totstandkoming van dit proefschrift. Je hebt me enorm veel werk uit handen genomen, waarvoor ik je enorm dankbaar ben. Ik ben er van overtuigd dat het uitermate belangrijk is voor een onderzoeksgroep om een ervaren en goed opgeleide laborante in je midden te hebben. Ik wens je alle geluk bij de nieuw ingeslagen weg.

Geert Buijze, Gerrit!

Ik koester nog altijd onze tijd in Zuid-Afrika, waar wij de basis legden van ons beider wetenschappelijke carrières. We schreven onze eerste artikelen samen, en ik ben er trots op dat we nu ook elkaars paranimf zijn geweest. Dank voor je onvoorwaardelijke vriendschap.

Professor dr. Van der Lugt en Professor dr. Verhoef dank ik van harte voor hun bereidheid om de wetenschappelijke waarde en leesbaarheid van dit proefschrift te toetsen.

Verder dank ik alle vrienden (Baeszen en Snavels!) en collega's (de gewèldige arts-assistentengroep!) die op hun eigen manier bijdrage hebben geleverd aan de omstandigheden waarin dit proefschrift heeft kunnen uitgroeien tot wat het nu is. Zij die hiermee bedoeld worden hoeven hier niet met naam genoemd: zij weten exact wie dat zijn.

Mijn ouders,

Lieve Truus en Nico, ik ben geworden wie ik ben dankzij alle bagage die jullie mij in de loop der jaren hebben meegegeven. De bewondering en het respect daarvoor is alleen maar gegroeid sinds ik zelf vader ben geworden. Dank voor alles.

Lieve Rinske,

Licht van mijn leven, vuur van mijn lendenen! Ik dank jou voor wie je bent, meer woorden zijn hier niet nodig.

Lieve Melle,

"The greatest thing you'll ever learn
is just to love and be loved in return"
*Nature boy – eden ahbez*

Dank dat jij er bent.

## About the author

De auteur van dit proefschrift werd geboren op 10 februari 1982 in Hoorn. In 2000 behaalde hij het gymnasium diploma op het Atlas College, locatie OSG West-Friesland te Hoorn. Omdat hij werd uitgeloot voor de studie Geneeskunde kon hij een jaar lang full-time aan zijn grote passie besteden: jazz piano studeren aan het Conservatorium, Hoge School voor de Kunsten, te Utrecht. In 2001 startte hij de opleiding Geneeskunde aan de Universiteit van Leiden. Gedurende zijn opleiding werkte hij onder andere bij het Center for Human Drug Research (Leiden) en was hij zelfstandig hoofdexplanteur hartklepdonatie bij de Stichting Bio Implant Services (Leiden). Hij was enkele jaren lid van het Medisch Discussie Dispuut onder leiding van Prof. Dr. R.G.J. Westendorp (LUMC) waar de basis werd gelegd voor zijn interesse in wetenschappelijk onderzoek. Onderzoeksstages werden vervolgens gevolgd aan de Universiteit Stellenbosch, Kaapstad, Zuid-Afrika en het Daniel den Hoed Ziekenhuis, Erasmus Medisch Centrum, Rotterdam. In 2008 werd het artsexamen behaald waarna hij startte als ANIOS Keel-, Neus-, Oorheelkunde in het Daniel den Hoed Ziekenhuis. In 2010 zette hij een nieuwe samenwerking op tussen de afdelingen Keel-, Neus-, Oorheelkunde (Erasmus MC, Prof. Dr. R.J. Baatenburg de Jong) en Moleculaire Beeldvorming (LUMC, Prof. Dr. C.W.G.M. Löwik), hetgeen resulteerde in de studies die zijn beschreven in dit proefschrift. Sinds deze periode is hij lid van de Head and Neck Optical Diagnostics Society en European Society of Molecular Imaging. Sinds maart 2011 is hij in opleiding tot Keel-, Neus-, Oorarts in het Erasmus MC onder Prof. Dr. R.J. Baatenburg de Jong. De auteur is getrouwd met Rinske Thöne-Keereweer. Samen hebben zij een zoon Melle (2012) en wonen in Den Haag.

# List of publications

2014: Necrosis avid cyanines as new probes for diagnostic and therapeutic applications in cancer and ischemic diseases

Bangwen Xie, Marieke A. Stammes Inge A. Mulder, Pieter B.A.A. van Driel, Luis J. Cruz Ricondo, Vicky T. Knol-Blankevoort, Hans R.I.J. Feitsma, Laura Mezzanotte, Ivo Que, Alan Chan, Robert A Cortfunke, Marieke J.H. Wermer, Azusa Maeda, Ralph S DaCosta, Jeroen P.H.M. van den Wijngaard, Maria Siebes, Sven Gottschalk, Daniel Razansky, Stijn Keereweer, Mathias Hoehn, Eric L. Kaijzel, Ermond R. van Beek, Thomas J. A. Snoeks, Clemens W. G. M. Löwik

Nature Biotechnology, under review

2014: Characterization and Evaluation of the Artemis Camera for Near-Infrared Optical Image-Guided Cancer Surgery

P.B.A.A. van Driel, M. van de Giessen, M.C. Boonstra, T.J.A. Snoeks, S. Keereweer, S. Oliveira, C.J.H. van de Velde, B.P.F. Lelieveldt, A.L. Vahrmeijer, C.W.G.M. Löwik, J. Dijkstra

In preparation

2014: Intra-operatieve fluorescente beeldvorming: een nieuwe kijk op oncologische chirurgie

Stijn Keereweer, Clemens W.G.M. Löwik, Alexander L. Vahrmeijer, Robert J. Baatenburg de Jong

Nederlands Tijdschrift voor Oncologie, under review

2013: Towards a successful clinical implementation of fluorescence-guided surgery

Snoeks TJA, van Driel PBAA, Keereweer S, Aime S, Brindle KM, van Dam GM, Löwik CWGM, Vahrmeijer AL, Ntziachristos V.

Molecular Imaging & Biology, 2013, Nov 19

2013: Preclinical studies on tumor-specific fluorescent targeting agents: the need for gold standard of tumor localization

Stijn Keereweer, Pieter B.A.A. Van Driel, Clemens W.G.M. Löwik

Molecular Imaging & Biology, 2013 Aug 28. PMID: 23982796

2013: Laryngomalacie bij een jonge adolescent

Stijn Keereweer, Arwen J. Sprij, Henk M. Blom

Nederlands Tijdschrift voor Geneeskunde, (Dutch Medical Journal), under review

2013: Shifting Focus in Optical Image-Guided Cancer Therapy

Stijn Keereweer, Pieter B.A.A. Van Driel, Dominic R. Robinson, Clemens W.G.M. Löwik

Molecular Imaging & Biology, 2013 Sept 14. PMID: 24037176

2013: Aberrant verloop van de arteria carotis interna door het middenoor

Stijn Keereweer, Bas Pullens, Marc P. Van der Schroeff

Nederlands Tijdschrift voor Keel-, Neus-, Oorheelkunde, (Dutch Journal of Otorhinolaryngology), under review

2013: Traumatic Displacement of a Cochlear Implant Magnet

Stijn Keereweer, Marc P. Van der Schroeff, Bas Pullens

Annals of otolaryngology, in press

2013: Intraoperative fluorescence delineation of head and neck cancer with a fluorescent anti-epidermal growth factor receptor nanobody

P.B.A.A. van Driel, J.R. van der Vorst, F.P.R. Verbeek, S. Oliveira, T.J.A. Snoeks, S. Keereweer, J.V. Frangioni, P.M.P van Bergen en Henegouwen, A.L. Vahrmeijer, C.W.G.M. Lowik

International Journal of Cancer, 2013 Nov 13. doi: 10.1002/ijc.28601.

2013: Book Chapter 4.22: Fluorescence-guided surgery: a promising approach for future oncologic surgery

Pieter B.A.A. Van Driel, Stijn Keereweer, Thomas J.A. Snoeks, Clemens W.G.M. Löwik

Comprehensive Biomedical Physics, Elsevier. Volume IV: Optical Molecular Imaging, in press.

2012: Optical Image-Guided Cancer Surgery: Challenges and Limitations

Stijn Keereweer, Thomas J.A. Snoeks, Pieter B.A.A. Van Driel, Jeroen D. F. Kerrebijn, Robert J. Baatenburg de Jong, Alexander L. Vahrmeijer, Henricus J.C.M. Sterenborg, Clemens W.G.M. Löwik

Clinical Cancer Research, 2013 Jul 15;19(14):3745-54.

2012: Subglottic Stenosis In Shwachman-Diamond Syndrome - Is There A Link?

Stijn Keereweer, Inge M. Appel, Hans J. Hoeve

Internation Journal of Paediatric Otolaryngology, 2012 Oct;76(10):1531-2.

2012: Near-Infrared Fluorescence Sentinel Lymph Node Mapping of the Oral Cavity in Head and Neck Cancer Patients.

Joost R. van der Vorst, Boudewijn E. Schaafsma, Floris P.R. Verbeek, Stijn Keereweer, Jeroen C. Jansen, Lilly-Ann van der Velden, Antonius Langeveld, Merlijn Hutteman, Clemens Löwik, Cornelis J.H. van de Velde, M.D., John V. Frangioni, Alexander L. Vahrmeijer

Oral Oncology, 2013 Jan;49(1):15-9.

2012: Dual Wavelength Tumor Targeting for Detection of Hypopharyngeal Cancer Using Near-Infrared Optical Imaging in an Animal Model.

Stijn Keereweer, Isabel M. Mol, Alexander L. Vahrmeijer, Pieter B.A.A. van Driel, Robert J. Baatenburg de Jong, Jeroen D.F. Kerrebijn, Clemens W.G.M. Löwik.

International Journal of Cancer, 2012 Jan 10. doi: 10.1002/ijc.27430.

2012: Dual-wavelength imaging of tumor progression by activatable and targeting near-infrared fluorescent probes in a bioluminescent mouse model of breast cancer.

Bang-Wen Xie, Isabel M Mol, Stijn Keereweer, Ermond R van Beek, Ivo Que, Thomas J A Snoeks, Alan Chan, Eric L Kaijzel and Clemens W G M Löwik.

PLoS ONE, 2012;7(2):e31875. Epub 2012 Feb 13.

2012: Translational Optical Imaging in Diagnosis and Treatment of Cancer

Stijn Keereweer & Merlijn Hutteman, Jeroen D.F. Kerrebijn, Cornelis J.H. van de Velde, Alexander L. Vahrmeijer, Clemens W.G.M. Löwik

Current Pharmaceutical Biotechnology, 2012 Mar 1;13(4):498-503

2012: High Complication Risk of Salvage Surgery after Chemoradiation Failures

Aniel Sewnaik, Stijn Keereweer, Abrahim Al-Mamgani, Robert Jan Baatenburg de Jong, Marjan H. Wieringa, Cees A. Meeuwis, Jeroen D.F. Kerrebijn

Acta Otolaryngologica, 2012 Jan;132(1):96-100. Epub 2011 Oct 25.

2011: Chronic Serous Otitis Media as a Manifestation of Temporal Meningioma.

Stijn Keereweer, R.M. Metselaar, R. Dammers, J.A.U. Hardillo.

ORL J Otorhinolaryngol Relat Spec. 2011 Sep 1;73(5):287-290.

2011: Targeting Integrins and Enhanced Permeability and Retention (EPR) Effect for Optical Imaging of Oral Cancer.

Stijn Keereweer, Isabel M. Mol, Pieter B.A.A. van Driel, Alexander L. Vahrmeijer, Robert J. Baatenburg de Jong, Jeroen D.F. Kerrebijn, Clemens W.G.M. Löwik.

Journal of Surgical Oncology. 2011 Sep 27. doi: 10.1002/jso.22102. [Epub ahead of print]

2011: Fluorescentiegeleide chirurgie van hoofd-hals tumoren – een overzicht van de mogelijkheden.

Stijn Keereweer, Jeroen D.F. Kerrebijn, Alexander L. Vahrmeijer, Jeroen C. Jansen, Robert J. Baatenburg de Jong, Clemens W.G.M. Löwik.

Nederlands Tijdschrift voor Keel-, Neus-, Oorheelkunde, 2011, 17e jaargang, nr.4 (179-181)

2010: Chemoradiation for Advanced Hypopharyngeal Carcinoma – A Retrospective Study on Efficacy, Morbidity and Quality Of Life.

Stijn Keereweer, Jeroen D.F. Kerrebijn, Abrahim Al-Mamgani, Aniel Sewnaik, Robert J. Baatenburg de Jong, Esther van Meerten

European Archives of Oto-Rhino-Laryngology, 2011 Jul. 8

2010: Image-Guided Surgery Using Optical Imaging.

Stijn Keereweer, Jeroen D.F. Kerrebijn, Alexander L. Vahrmeijer, Clemens W.G.M. Löwik.

Magazine of International Hospital and Equipment. 2010 December

2010: Optical Imaging of Oral Squamous Cell Carcinoma and Cervical Lymph Node Metastasis

Stijn Keereweer, Jeroen D.F. Kerrebijn, Isabel M. Mol, J. Sven D. Mieog, Pieter B.A.A. van Driel, Robert J. Baatenburg de Jong, Alexander L. Vahrmeijer, Clemens W.G.M. Löwik.

Head Neck. 2011 Oct 10. doi: 10.1002/hed.21861. [Epub ahead of print]

2010: Detection of Oral Squamous Cell Carcinoma and Cervical Lymph Node Metastasis Using Activatable Near-Infrared Fluorescence Agents

Stijn Keereweer, J. Sven D. Mieog, Isabel M. Mol, Pieter B.A.A. van Driel, Thomas J.A. Snoeks, Robert J. Baatenburg de Jong, Alexander L. Vahrmeijer, Jeroen D.F. Kerrebijn, Clemens W.G.M. Löwik.

Archives of Otolaryngology Head Neck Surgery, 2011 Jun; 137(6):609-15.

2010: Detection of Oral Squamous Cell Carcinoma and Cervical Lymph Node Metastasis Using Activatable Near-Infrared Fluorescence Agents

Stijn Keereweer, J. Sven D. Mieog, Isabel M. Mol, Pieter B.A.A. van Driel, Thomas J.A. Snoeks, Robert J. Baatenburg de Jong, Alexander L. Vahrmeijer, Jeroen D.F. Kerrebijn, Clemens W.G.M. Löwik.

Abstract or oral presentation, Archives of Otolaryngology Head Neck Surgery, 2011

2010: Image-Guided Surgery in Head and Neck Cancer: Current Practice and Future Directions of Optical Imaging

S. Keereweer, H.J.C.M. Sterenborg, J.D.F. Kerrebijn, P.B.A.A. Van Driel, R.J. Baatenburg de Jong, C.W.G.M. Löwik.

Head Neck. 2011 Jan 31. doi: 10.1002/hed.21625.

2010: Optical Image-Guided Surgery – Where Do We Stand?

Stijn Keereweer, Jeroen D.F. Kerrebijn, Pieter B.A.A. van Driel, Bangwen Xie, Eric L. Kaijzel, Thomas J.A. Snoeks, Ivo Que, Merlijn Hutteman, Joost R. van der Vorst, J. Sven D. Mieog, Alexander L. Vahrmeijer, Cock J.H. van de Velde, Robert J. Baatenburg de Jong, Clemens W.G.M. Löwik.

Molecular Imaging Biology. 2011 Apr;13(2):199-207.

2010: Early and long-term morbidity after total laryngopharyngectomy

Stijn Keereweer, Johannes H de Wilt, Aniel Sewnaik, Cees A. Meeuwis, Hugo W. Tilanus, Jeroen D.F. Kerrebijn.

European Archives of Oto-Rhino-Laryngology. 2010 Sep;267(9):1437-44.

2009: Dysphagia after an L-shaped reconstruction technique of the free jejunum graft

Stijn Keereweer, Aniel Sewnaik, Jeroen D.F. Kerrebijn, Cees A. Meeuwis, Hugo W. Tilanus, Johannes H. De Wilt.

Journal of Plastic Reconstructive and Aesthetic Surgery. 2010 Nov;63(11):1820-4. Epub 2009 Dec 7.

2009: Salvage or what follows the failure of a free jejunum transfer for reconstruction of the hypopharynx?

Stijn Keereweer, Aniel Sewnaik, Jeroen D.F. Kerrebijn, Cees A. Meeuwis, Hugo W. Tilanus, Johannes H. de Wilt.

Journal of Plastic Reconstructive Aesthetic and Surgery. Jun;63(6):976-80. Epub 2009 Apr 10.

2007: Transfer of segmentally split pectoralis major for the treatment of irreparable rupture of the subscapularis tendon

Gavin J. Jennings, Stijn Keereweer, Geert A. Buijze, Willie Vorster, Don F. Du Toit

Journal of Shoulder and Elbow Surgery. 2007 Nov-Dec;16(6):837-42. Epub 2007 Nov 1.

2007: Musculotendinous transfer as a treatment option for irreparable rotator cuff tears: teres major or latissimus dorsi?

Geert A. Buijze, Stijn Keereweer, Gavin J. Jennings

Clinical Anatomy 2007 Nov;20(8):919-23.